THE UNIVERSITY
of EDINBURGH

THE UNIVERSITY *of* EDINBURGH

Carbon Allocation and Trait Optimality Drives Amazon Forest Response to Changing Water Availability

Sophie Flack-Prain

Thesis submitted for the degree of Doctor of Philosophy
School of Geosciences The University of Edinburgh

August 2018

Declaration

I declare that this thesis has been composed solely by myself and that it has not been submitted, either in whole or in part, in any previous application for a degree. The research chapters presented are intended for publication, as such I have written in the first person plural, in line with standard practice. I acknowledge the provision of field data from the Global Ecosystems Monitoring network, and the model I have used, developed by my supervisor Professor Mathew Williams. Except where otherwise stated, the work presented is entirely my own.

Sophie Flack-Prain

August 2018

Acknowledgements

Enormous appreciation and thanks is owed to my supervisor Professor Mathew Williams, for his invaluable guidance, support and encouragement throughout. In our first meeting he said by the end of this I'd be teaching him things. It might be that the biggest thing I've taught him is to understand a scouse accent, but that's an achievement not to be underestimated. Thanks to my second supervisor Professor Patrick Meir, who has always been a great source of advice and kind words. I could not have completed this research without the wealth of data provided by Professor Yadvinder Malhi and his team, and I thank all who were involved in its collection. I would also like to thank my research group, for their sharing of ideas, insights and wheels (lest they never be reinvented). Special thanks is due to Luke Smallman, whose speedy reply to 'help' emails never went unappreciated. Thanks to the school of Geosciences and the Natural Environment Research Council (NERC) for supporting and funding this PhD.

I owe huge thanks to my husband Richie, first and foremost for his superb cups of tea, but also for the wonderful support he has given me, and for keeping me laughing these past 4 years. I would like to thank my dad, Gary, for his amazing example of sheer determination and hard work, and that a little kindness goes a long way. Thanks to my beautiful mum, Sue, for her cutting wit, helping me keep everything in perspective and always knowing whether I need a hug or a kick up the backside. I thank my sister Laura for her surprise visits and whenever I needed to vent, always agreeing that I am in the right no matter what the circumstances. Thanks to my sister Katie, for her overall loveliness and always maintaining that Flack sisters can achieve anything. I would like to thank my other, other half, the Castle of 'Flack and Castle' just because. And lastly, to the honourable members of the Bay Whiskey Society (Rose Pritchard, Kathleen Allen and Yaqing Gou), I couldn't imagine having done this PhD without the Spice Girl esque help from these fabulous ladies.

I am the daughter of Earth and Water,
And the nursling of the Sky;
I pass through the pores of the ocean and shores;
I change, but I cannot die.
For after the rain when with never a stain
The pavilion of Heaven is bare,
And the winds and sunbeams with their convex gleams
Build up the blue dome of air,
I silently laugh at my own cenotaph,
And out of the caverns of rain,
Like a child from the womb, like a ghost from the tomb,
I arise and un-build it again.

Shelley

Abstract

Climate change induced shifts in precipitation threaten the future carbon balance of Amazon rainforests. Our understanding of water constraints to photosynthesis is largely limited to physiology-climate effects. Less is known about the effects of carbon allocation and trait shifts in response to water availability. Mechanisms linking carbon allocation and trait responses are not well represented in current ecosystem models, causing uncertainty in predicted carbon dynamics under future climates. We ask

(i) What drives the coupling between photosynthesis and precipitation is it canopy structure (leaf area index; LAI), leaf traits, or solely a physiology-climate response?

(ii) Why do LAI and leaf traits vary with precipitation?

(iii) What is the role of water availability and plant traits in driving carbon allocation between leaves and roots?

Process based modelling allows the links between photosynthesis, water availability, carbon allocation and traits to be quantified explicitly, exploring interaction space not available to in-situ experiments. We calibrated the Soil Plant Atmosphere model (SPA) to eight permanent sample plots across an Amazon mean annual precipitation gradient (1400-2800mm), as part of the Global Ecosystems Monitoring network. The model's representation of local carbon fluxes was evaluated against biometric estimates. We then conducted a series of model experiments to quantify the principal drivers of photosynthesis across the precipitation gradient and explore mechanisms of LAI, leaf trait and carbon allocation responses to water availability.

LAI increased with precipitation (R^2=0.42, p=0.08), and was the principal driver of differences in photosynthesis across the gradient, accounting for 36% of observed variation. Differences in leaf traits accounted for 20% of variance and physiology-climate interactions accounted for a further 12%.

Spatial variance in LAI was underpinned by carbon economics, and best predicted by an optimality approach that maximised net canopy carbon export (R^2=0.87, p<0.001). Across the precipitation gradient, leaf trait strategies shifted from fast to slow as water availability

increased (where fast leaf traits are a cohort of high photosynthetic capacitance, high metabolic rate, high nitrogen content, low LMA and short lifespan and vice versa for slow leaf traits). Leaf traits had a determinate effect on LAI optimality, and higher leaf areas at wet plots were supported by longer leaf lifespans rather than an increase in leaf net primary production (NPP). At dry plots, short leaf lifespans, inherent of fast leaf trait cohorts, effected lower LAI. However, fast leaf trait strategies did prove optimal at dry plots, as carbon losses during the dry season were minimised, whilst photosynthesis during the wet season was maximised.

Field estimates showed that leaf NPP was highest at dry plots and declined with increasing precipitation, whilst root NPP was highest at wet plots, converse to optimal partitioning theory, which suggests prioritisation of roots under moisture stress and leaves under light limitation. Yet model results show that leaf:root NPP across the precipitation gradient was optimal, and was similarly best predicted by the maximisation of net canopy carbon export (R^2=0.60, p=0.02). Optimality was supported by concurrent shifts in leaf and root traits, which together accounted for 63% of variation in optimal leaf:root NPP.

Our findings demonstrate that optimality approaches can be used to successfully predict spatial variation in LAI, leaf:root NPP and leaf traits across an Amazon precipitation gradient. Leaf traits fundamentally shaped modelled optimal responses, ultimately determining carbon assimilation. The response of Amazon forests to increased moisture stress is therefore dependent on the current spatial distribution of leaf traits, their plasticity and the likelihood of future shifts in floristic and functional trait composition. Future work should expand on the findings presented by exploring the responses of carbon allocation and traits to water availability over different timescales.

Lay Summary

Increasing atmospheric carbon dioxide concentrations are a major contributor to global climate change. Across the Amazon rainforest, trees take in carbon dioxide through photosynthesis. However, photosynthesis across Amazon forests is threatened by predicted shifts in rainfall patterns, as a result of climate change. At the leaf level, short-term changes in water availability limit photosynthesis. To cope with prolonged changes in rainfall, forests adapt their leaf properties (such as leaf lifespan and the rate at which leaves photosynthesise) and overall structure (including the leaf surface area, and rooting depth to increase water uptake). However, it is difficult to separate the direct impact of rainfall on photosynthesis from the indirect effects through changes in leaf properties and forest structure. To unpick how changes in rainfall affect photosynthesis, we use a model which combines climate data with our knowledge around photosynthesis and other plant processes. We focus on plots along an Amazon rainfall gradient with detailed field measurements of forest processes. By using an existing rainfall gradient, we aim to understand the long-term effects of changes in water availability on photosynthesis.

We find that the biggest factors controlling photosynthesis along the gradient were differences in leaf surface area and leaf properties (the indirect effects of rainfall), whilst direct effects on stomata proved less important. We show that underpinning the changes in leaf surface area along the rainfall gradient, is a leaf economy, where carbon investment into the growth of leaves was optimised against the photosynthesis returns, taking into account local water availability. Leaf properties were central to shaping this leaf economy. Leaves at drier plots had shorter lifespans but a higher rate of photosynthesis; as such they were able to maximise photosynthesis during wetter periods, and shed leaves during dry periods to reduce losses. We further show that forests trade-off how much carbon they invest into growing leaves and roots to balance light capture and water uptake. The relative growth of leaves versus roots was also related to the lifespan of the leaf or root, whereby the shorter the leaf or root lifespans the more investment into growth was needed. As a result, despite higher leaf growth and lower root growth, forests in the lowest rainfall zones still supported more roots and less leaves than forests in higher rainfall zones.

The results presented in this thesis can be used to improve predictions on the effect changes in rainfall will have on photosynthesis across Amazon forests in future. The research provides a basis for models to use an optimal growth approach, and highlights the importance of leaf properties in shaping the response of Amazon forests to changes in rainfall. We identify key focal areas for future research, including continued efforts to collect data on leaf surface area and leaf properties, exciting opportunities for which are offered by new satellite missions. Our findings uncover a new key question around how growth trade-offs and leaf and root properties interact to optimise water uptake and photosynthesis.

Contents

List of Figures

allow clarity around the distribution of error bars for plots at the same location. Values presented are averages from the years 2009-2010. Error bars represent standard error. (R^2=0.42, p=0.08, RMSE=0.87).

Figure 4.2. A schematic of the physiological and structural responses (grey dashed boxes) of forests to precipitation and the pathways through which responses impact GPP. An influence of one process, variable, stock or flux on another is shown by directional arrows. Two-way arrows represent a trade-off between the two variables. Boxes represent fluxes or processes (modelled), triangles are stocks (SPA state variables) and circles are leaf traits (SPA parameters). Grey boxes indicate fluxes that are not integral to the processes discussed. Bold text indicate that the value of the variable, stock or flux was known in this study, derived from biometric data. Blue shading shows the pathway of direct physiological impacts of meteorology on GPP, whilst green shading shows the principal pathway for plant structural impacts on GPP. Net primary productivity and fraction of NPP are separated by component; leaf (NPP_{leaf}; $frac_{leaf}$), wood (NPP_{wood}; $frac_{wood}$), course roots ($NPP_{course\ root}$; $frac_{course\ root}$) and fine roots ($NPP_{fine\ root}$; $frac_{fine\ root}$). Gross Primary Productivity (GPP), total Net Primary Productivity (NPP), Net Canopy carbon Export (NCE), Leaf Area Index (LAI), leaf growth respiration ($R_{g\ leaf}$), leaf maintenance respiration ($R_{m\ leaf}$), leaf turnover ($turnover_{leaf}$), Leaf Mass per unit Area (LMA) and leaf nitrogen content (leaf N) are denoted respectively. 124

Figure 4.3. Contour plot of model simulated net canopy carbon export (NCE) across an Amazon mean annual precipitation gradient, under a range of simulated LAI strategies. NCE values are SPA estimates derived from LAI time-series alternated at each plot, whilst maintaining the observed meteorology, soil, vegetation structure and leaf traits. Contours represent interpolated NCE estimates (n=192). Points are the observed mean annual LAI of each plot, whilst error bars represent standard error. Estimates of LAI, precipitation and simulated NCE are mean annual values for 2009-2010. The corresponding precipitation value to LAI observations are marginally offset around the true value to allow clarity around the distribution of error bars for plots at the same 127

location. The shaded area represents the smoothed interaction between observed precipitation and LAI values.

Figure 4.4. Comparison of SPA simulated NCE under local conditions, GEM field estimated NCE and maximum simulated NCE under LAI alternations for eight permanent sample plots across an Amazon precipitation gradient. Maximum NCE values are derived from interpolated SPA estimates whereby LAI time-series were alternated at each plot, whilst maintaining the observed meteorology, soil, vegetation structure and leaf traits. SPA error bars represent simulated NCE under field measured LAI standard error. GEM error bars represent propagated error for summed field estimates of fine root, coarse root and woody NPP and respiration. The dashed line is the 1:1 and the solid line is the linear regression between NCE estimates (a) R^2= 0.87, p<0.001, RMSE= 150.6, (b) R^2=0.68, p=0.01, 279.5 and (c) R^2=0.68 p=0.01, RMSE=236.5. 129

Figure 4.5. Model simulated net canopy carbon export (NCE), leaf specific conductance (LSC), and root carbon stocks in the presence, and absence of carbon cycle feedbacks, for a typical core (CAX04) and transitional forest (TAN05), under a range of simulated LAI strategies. Dashed lines represent SPA estimates of NCE and LSC where carbon cycle feedbacks were enabled, whilst dotted lines represent estimates where feedbacks were absent. Solid lines represent root carbon stocks in the presence of carbon cycle feedbacks, as in their absence, stocks were held constant at observed levels. Carbon stock and carbon and water flux values are SPA estimates derived from LAI time-series alternated at each plot, whilst maintaining the observed meteorology, soil and vegetation structure and leaf traits (n=24 for each plot). The shaded area represents the standard error of local observed mean annual LAI. Data points are estimated NCE (summed fine root, coarse root and wood NPP and respiration) and root carbon stock derived from field measurements, together with error bars showing propagated NCE error and LAI standard error. Field estimates of root stocks at TAN05 were absent. 130

List of Tables

Table 5.4. The percentage of variation in optimal leaf:root NPP allocation (maximised NCE) across eight GEM lowland Amazonian permanent sample plots explained by sampling multiply individual drivers and driver combinations in SPA. Optimal leaf:root NPP was obtained from simulations under which leaf traits, root traits and precipitation were varied at each plot. Proportion of variance explained was calculated as Condition Sum of squares/Total Sum of Squares. Drivers listed are model inputs and are either fixed values or time series. Values in bold indicate a significant interaction ($p<0.05$) (n=350). 172

Table 1. A list of acronyms and symbols used in the presented thesis. A brief description is given within the text when used for the first time in each chapter.

Acronyms and Symbol	Definition
GPP	Gross Primary Productivity
NPP	Net Primary Productivity
NCE	Net canopy Carbon Export
LAI	Leaf Area Index
MAP	Mean Annual Precipitation
GEM	Global Ecosystems Monitoring Network
SPA	Soil Plant Atmosphere model
NSC	Non-structural carbon
R_a	Autotrophic Respiration
V_{cmax}	maximum rate of carboxylation
J_{max}	maximum rate of electron transport
κ_c	maximum rate of carboxylation normalised by leaf nitrogen content
κ_j	maximum rate of electron transport normalised by leaf nitrogen content
LMA	Leaf Mass per unit Area
WQ	temperature during the warmest quarter
b	nitrogen scalar
N_{leaf}	leaf nitrogen content
Rr_{leaf}	leaf respiration rate
T	temperature
Rt_{leaf}	temperature adjusted leaf respiration rate
Rs_{leaf}	total leaf respiration
M_{leaf}	foliar biomass
SST	sea surface temperature
ENSO	El Nino Southern Oscillation
AMO	Atlantic Multi-decadal Oscillation

1. Introduction

1.1 Motivation

The Amazon basin is home to the largest rainforest on Earth (Hansen *et al.*, 2010). Covering around 5.3 million km^2, Amazon forests account for 40% of the global tropical forest area (Aragao *et al*., 2014; Soares-Filho *et al*., 2006). The basin is a major carbon sink, storing an estimated 120 Pg of carbon, and contributing ~14% of global total terrestrial photosynthesis (Field *et al*., 1998; Malhi and Grace, 2000; Malhi *et al*., 2006; Pan *et al*., 2011; Zhao and Running, 2010). Amazon forests also provide other important ecosystem services, such as biodiversity, hydrology and climate regulation, as well as supporting the livelihoods of millions of people (FAO, 2001; Gloor *et al*., 2013; Nasi *et al*., 2011). The Amazon is a hotspot for biodiversity and hosts around a quarter of the world's terrestrial species (Dirzo and Raven, 2003; Ter Steege *et al*., 2006). Across the basin, precipitation is recirculated through evaporation, cycling an estimated eight trillion tons of water each year (IPCC, 2007). Resultant increases in latent heat and cloud cover modulate temperature across the region (Feddema *et al*., 2005), whilst water not evaporated is discharged into rivers, accounting for ~17% of global freshwater inflow to oceans (Callede *et al*., 2002). Given the role of the Amazon in Earth system functioning, small changes in forest dynamics could have global consequences.

Amazonia faces an unprecedented suite of threats from deforestation, degradation, increased risk of fire, and anthropogenic climate change (Coe *et al*., 2013; Malhi *et al*., 2008). Towards the end of the twentieth and into the twenty first century, deforestation rates in the Brazilian Amazon averaged 18,100 $km^2\ yr^{-1}$, and it is estimated that only 62% of the original extent remains (Malhi *et al*., 2008). The expansion of cattle and soybean production has led to forest clearances, concentrated in an 'arc of deforestation' across the southern and eastern margins. Forest degradation through selective logging is reported to account for 15-19% higher carbon emissions than clear cutting alone (for the years 1999-2002), reducing carbon sequestered and assimilation potential (Huang and Asner, 2010). Whilst deforestation rates have slowed in recent years (Nepstad *et al*., 2014), past activity has left forests vulnerable to drought and fire. Deforestation rates are closely linked to annual fire incidences (Aragao *et al*., 2008), with

carbon emissions from forest fires totalling ~270 Tg C yr^{-1} (Aragão *et al.*, 2018). Furthermore, drought feedbacks increase the risk of fire induced tree mortality (Brando *et al.*, 2014). Since the 1980s, warming across the Amazon region has averaged 0.13°C $decade^{-1}$, rising to 0.22-0.33°C $decade^{-1}$ for the period 2000-2012 (Jiménez-Muñoz *et al.*, 2013; Malhi and Wright, 2004). By 2100 warming across the Amazon is projected to reach 4-6°C (Marengo *et al.*, 2012). Predicted shifts in precipitation patterns as a result of anthropogenic climate change remain uncertain (Hawkins and Sutton, 2011), largely due to disparate assumptions around rainfall formation (Li *et al.*, 2006). Understanding global hydrological cycling is therefore critical to discerning the impact of precipitation change on Amazon forests.

Amazon precipitation is sensitive to variation in sea surface temperatures (SST) of the tropical Atlantic and Pacific (Liebmann and Marengo, 2001; Marengo, 2004). Drought events across the basin have long been associated with El Nino Southern Oscillation (ENSO) anomalies (Marengo, 1992, 2004; Uvo *et al.*, 1998). Variation in Pacific SST, dominated by El Niño events, supress convection in northern and eastern Amazonia, causing reduced rainfall during the wet season. However, more recent Amazon drought events (2005 and 2010) have been linked to Atlantic Multi-decadal Oscillation (AMO) anomalies *(*Li *et al.*, 2006; Marengo *et al.*, 2008; Marengo *et al.*, 2011). Strengthening of the tropical Atlantic north-south SST gradient, shifts the intertropical convergence zone further northward, intensifying the Hadley cell circulation. As a result, AMO anomalies suppress rainfall in southern and western Amazonia (Zeng *et al.*, 2008). Predicted rapid warming of Pacific regions and slower warming of the North Atlantic (Yoon and Zeng, 2010) suggest that whilst annual precipitation is set to increase in the western Amazon, decreases are expected in eastern regions (Duffy *et al.*, 2015). Longer and more intense dry seasons are also predicted, together with an increase in drought events (Boisier *et al.*, 2015; Joetzjer *et al.*, 2013). Drying has already been reported in some Amazon regions (Fu *et al.*, 2013; Hilker *et al.*, 2014; Li *et al.*, 2008). Across the southern Amazon, precipitation is decreasing by an average of 0.32% $decade^{-1}$ (Li *et al.*, 2008). In contrast, increased rainfall is reported over the Northern Amazon (Rao *et al.*, 2016), and Gloor *et al.*, (2013) argue that basin-wide precipitation has increased since 1990, driven by higher tropical Atlantic SST. Trends in seasonality are more disparate, as for parts of Amazonia, decreases in annual precipitation have led to reduced seasonality (Feng *et al.*, 2013). 2005, 2010 and 2015 saw some Amazon regions experience the most intense droughts on record. The 2005 drought was focused around the southwest Amazon, whilst the 2010 event was more widespread (Asner and Alencar, 2010; Xu *et al.*, 2011). The 2015 drought affected more than 80% of the Amazon

basin, almost double that of the 2005 event (Marengo *et al*., 2008; Panisset *et al*., 2018). As a result of both emerging and predicted shifts in precipitation across the basin, Amazon forests are vulnerable to increased moisture stress (Aragao *et al*., 2014; Beer *et al*., 2010; Malhi *et al*., 2008; Meir and Woodward, 2010; Phillips *et al*., 2009; Schuur, 2003; Wagner *et al*., 2012).

The impact of water limitation on forest functioning has consequently been the subject of much research (Doughty *et al*., 2014; Doughty *et al*., 2015; Gatti *et al*., 2014; Metcalfe *et al*., 2010; Phillips *et al*., 2010; Saatchi *et al*., 2013). To investigate the response of forests to water limitation, researchers have used a combination of field measurements, artificial drought experiments, flux towers, remote sensing and modelling approaches. Across the RAINFOR network (a collation of pan-tropical permanent sample plot inventory data), Phillips *et al*. (2009) report carbon losses of between 1.2-1.6 Pg as a result of the 2005 Amazon drought. Permanent sample plots have also enabled investigation into the effects of water limitation on more detailed carbon dynamics, reporting both shifts in NPP allocation and respiration in response to the 2010 drought (Doughty *et al*., 2015). Artificial drought experiments are able to capture the impact of long-term reductions in precipitation. Throughfall exclusion at Caxiuaña and the Tapajós National Forest resulted in increased stem mortality, lower net primary productivity, and differential effects on autotrophic respiration (da Costa *et al*., 2010; da Costa *et al*., 2014; Nepstad *et al*., 2002; Nepstad *et al*., 2007). However, a number of challenges are associated with the measurement and scaling of biometric carbon estimates causing uncertainty in results (Malhi *et al.*, 2014). Flux towers have offered new insights into the effect of seasonal water limitation on biosphere-atmosphere exchanges, but have largely been absent from studies investigating Amazon responses to drought, due to coincidences of tower operations with drought event timing and location (Huete *et al*., 2006; Restrepo-Coupe *et al*., 2013; Saleska *et al*., 2009). The interpretation of forest responses to drought through remote sensing approaches have perhaps caused the most controversy (Asner and Alencar, 2010; Saleska *et al*., 2007; Samanta *et al*., 2010). However recent advances in atmospheric correction, cloud detection and normalised angles have shown a decline in greenness during drought years (Bi *et al*., 2016). Model simulations of drought effects on forest functioning have had varied success (Fisher *et al*., 2007; Powell *et al*., 2013), highlighting areas of limited understanding, which require further work to reduce uncertainty in predicted responses to climate change.

GEM network is particularly suited to the investigation of precipitation effects on plant functioning, given the spatial and temporal span of the database, which is basin-wide and includes data from as early as 2005 (Malhi *et al*., 2004; Malhi *et al*., 2015; Malhi *et al*., 2017). However, the GEM approach does have some disadvantages, including the underlying assumption that permanent sample plots are in steady state, which remains unresolved (Rocha *et al*., 2014). As a result, the steady state assumption causes uncertainty in GPP estimates, which are the sum of NPP and respiration measurements, assuming C assimilated into the plant equates to C out (Araujo-Murakami *et al*., 2014; Malhi *et al*., 2014b). Furthermore, uncertainty exists around both the measurements of component NPP and respiration, and the scaling of measurements to the plot level (Araujo-Murakami *et al*., 2014; Doughty *et al*., 2014; Malhi *et al*., 2015; Malhi *et al*., 2014b). However, despite the uncertainty around C flux estimates from the GEM network, the data produced have nonetheless continued to provide valuable insights into the functioning of Amazon forests (Doughty *et al*., 2015a; Doughty *et al*., 2015b; Malhi *et al*., 2015).

1.2 Knowledge Gaps

Direct physiological responses to climate effect photosynthesis via a number of pathways including (i) the temperature sensitivity of V_{cmax} and J_{max} (Hikosaka *et al*., 2005; Medlyn *et al*., 2002), (ii) the effect of shortwave radiation on electron transport (Farquhar and Von Caemmerer, 1982; Farquhar *et al*., 1980), and (iii) the effect of water availability on stomatal conductance (Farquhar and Sharkey, 1982; Wong *et al*., 1979) (Figure 1.1). The influence of water limitation on stomata is exerted externally, via atmospheric vapour pressure deficit, and internally, via gradients in the soil-plant hydraulic continuum, ultimately constraining carbon assimilation and transpiration. Stomatal responses to water availability are important in driving the photosynthesis-precipitation interaction across Amazon forests, with Amazon throughfall exclusion experiments reporting a drop in stomatal conductance, and consequently photosynthesis, with exclusion onset (Fisher *et al*., 2007). Research efforts have put a deservedly large focus on direct physiological responses to climate, resulting in an increasingly accurate representation in ecosystem models (Bonan *et al*., 2014; Smith *et al*., 2016). However, the interaction between climate, forest structure and traits have received less attention, despite increasing evidence suggesting that such 'indirect' effects of climate determine ecosystem productivity (Fyllas *et al*., 2017; Hui *et al*., 2003; Richardson *et al*., 2007).

Across the tropics, indirect responses to climate through shifts in forest structure and plant traits have been reported under both short and long term changes in precipitation. Here we define forest structural responses as emergent canopy and root properties such as LAI, root biomass and root depth. Artificial drought experiments report a decline in canopy leaf area in response to throughfall exclusion onset (Brando *et al*., 2008; Fisher *et al*., 2007; Meir *et al*., 2008), with reduced leaf area index (LAI) linked to lower leaf production rather than increases in leaf shedding (Nepstad *et al*., 2002). Yet, model comparison studies highlight a disparity between simulated LAI under climate change projections (Rowland *et al*., 2015). The poor representation of canopy dynamics in response to water limitation has been identified as a key cause of differences in model estimates (Powell *et al*., 2013; Restrepo-Coupe *et al*., 2017). Rooting depth is also expected to play an important role in shaping the response of Amazon forests to precipitation change, whereby access to deep soil water and hydraulic lift allows plants to maintain photosynthesis when water is limited (Baker *et al*., 2008; Harper *et al*., 2010; Oliveira *et al*., 2005). However, the role of forest structural responses in shaping the photosynthesis-precipitation interaction remains unclear.

Indirect responses to climate through plant traits are effected through shifts across the fast (acquisitive) to slow (conservative) trait spectrum. In the presented thesis we focus on plant traits such as photosynthetic capacity, metabolic rate, leaf mass per area (LMA) and leaf lifespan, however, these are a subset of traits likely to be important in the photosynthesis-precipitation interaction. Fast traits include high photosynthetic capacitance, high metabolic rate, low LMA, and short leaf lifespan, and vice versa for slow traits. Traits operate across an 'economic spectrum' whereby trade-offs constrain trait combinations (Wright *et al*., 2004). Long term drying is reported to induce shifts in plant traits and community composition (Fauset *et al*., 2012), ultimately driving the directional distribution of plant traits across tropical precipitation gradients (Santiago *et al*., 2004). Whilst we expect that shifts in forest structure and plant traits in response to water limitation are important, our ability to represent the integrated effect of indirect responses to climate remains limited, causing uncertainty in predicted carbon dynamics. Furthermore, we are yet to quantify the feedback effect of forest structure and plant traits on photosynthesis across the Amazon basin.

The integration of 'Optimal Functioning' into ecosystem models has been proposed as a potential solution to capture forest structure and plant trait responses to climate (Dewar *et al*., 2009; Franklin *et al*., 2012; Mäkelä, 2012; McMurtrie and Dewar, 2013; Meir *et al*., 2015).

The approach works on the basis that plants aim to maximise fitness, which they achieve by optimising forest structure and trait composition. Plant fitness is modelled by way of a fitness proxy, however the proxy used varies between studies. Gross primary productivity (GPP), net canopy carbon export (NCE; photosynthesis minus the C cost of leaf growth and respiration), net primary productivity (NPP) and wood NPP, have all been used as fitness proxies to test the applicability of optimality theory (Dewar *et al*., 2009; Mäkelä *et al*., 2008; McMurtrie and Dewar, 2011; McMurtrie and Dewar, 2013). However, an in depth comparison of fitness proxy performance is currently limited, as is the application of optimality theory to mixed forests, across larger spatial gradients. Further investigation is therefore required to test the suitability of optimality theory as a tool to improve modelled forest structure and plant trait responses to resource availability.

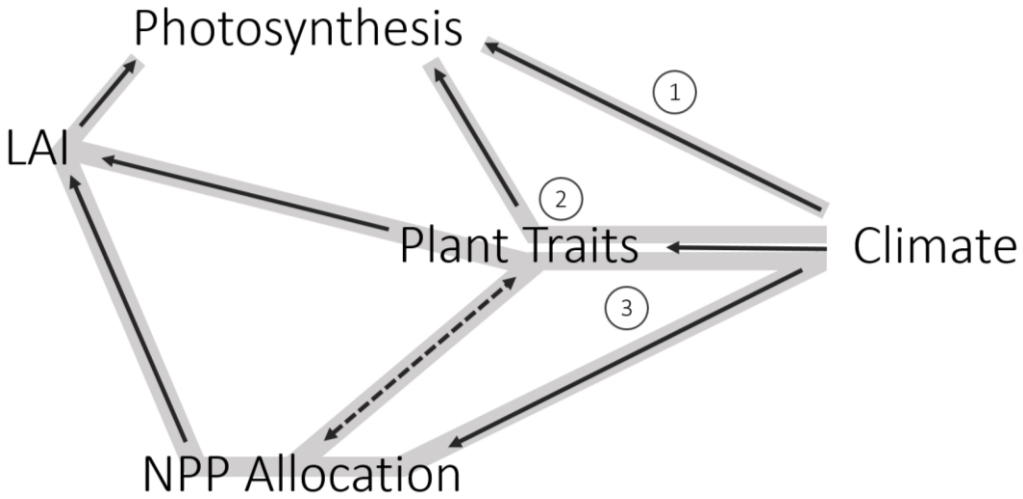

Figure 1.1 The direct and indirect effects of climate on photosynthesis. Direct (1) and indirect (2 and 3) pathways are highlighted in grey. Interactions where it is unclear which is the dependent and which is the independent variable are denoted by a dashed double headed arrow. 'Plant traits' include photosynthetic capacity, LMA and leaf lifespan. We hypothesise that indirect climate effect pathways (2 & 3) will prove more important in driving variation in photosynthesis across Amazon forests.

1.3 Research Questions

Photosynthesis increases with precipitation across Amazon forests (Malhi *et al*., 2015), yet little is known about how direct (physiology-climate interactions) and indirect (forest structure and plant traits) responses to climate shape productivity. Whilst direct physiology-climate interactions constrain photosynthesis via stomatal conductance, indirect responses via LAI

and leaf traits determine the surface area for potential photosynthesis and carbon assimilation rate. Current evidence suggests that indirect effects could prove more important than direct effects in determining photosynthesis (Fyllas *et al*., 2017; Hui *et al*., 2003; Richardson *et al*., 2007). We ask:

> *What drives the coupling between photosynthesis and precipitation; is it canopy structure (leaf area index; LAI), leaf traits, or solely a physiology-climate response?*

We quantify the effects of physiology-climate interactions, LAI and leaf traits on spatial variation in photosynthesis. We explore the sensitivity of annual and sub-annual photosynthesis to physiology-climate interactions, LAI, and leaf traits (across annual timescales only), and assess how water availability shapes responses. We hypothesise that LAI will be the principal driver of spatial co-variation between photosynthesis and precipitation, and that leaf traits will also prove important. On an annual timescale, we predict that for forests experiencing high mean annual precipitation (MAP), photosynthesis will be more sensitive to differences in LAI and photosynthetic capacity, whilst low MAP forests will be most sensitive to differences in soil and rooting properties, reflecting differences in resource limitation. Across sub-annual timescales, we predict the role of physiology-climate interactions will prove more important than indirect responses (Figure 1.2). A detailed understanding of how direct and indirect effects of climate drive photosynthesis across Amazon forests, allows us to focus our attention on key mechanisms most important to modelling forest responses to climate change. We focus on mean annual precipitation rather than a water deficit metric to avoid the introduction of known uncertainty through a fixed estimate of monthly evapotranspiration (~100mm mon^{-1}; Aragao *et al*., 2007) typically used in their calculation. Furthermore, mean annual precipitation is reported to successfully capture variation in tropical photosynthetic seasonality independently, without the need to account for wet and dry season differences (Guan *et al*., 2015).

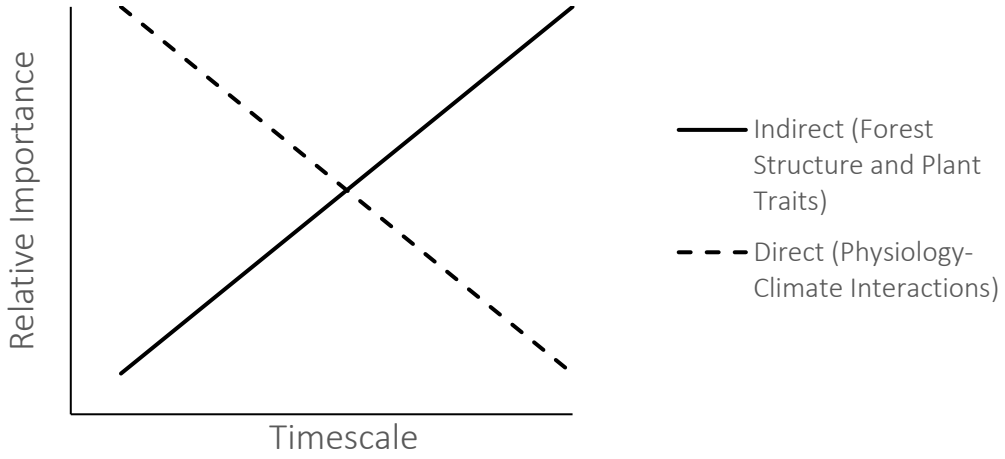

Figure 1.2 The hypothesised relative importance of direct (physiology-climate interactions) and indirect (forest structure and plant traits) drivers of photosynthesis in explaining variation with precipitation across timescales in Amazon forests. Direct responses to water availability via stomatal conductance are expected to be more important across shorter timescales, whilst indirect responses via LAI, photosynthetic capacity and rooting properties are expected to be more important across longer timescales.

Under the assumption that LAI is the principal driver of photosynthesis across Amazon forest, the mechanism coupling LAI with precipitation (Bradley *et al*., 2011), is central to understanding forest responses to future climate change. We ask:

> *What drives co-variance between LAI and precipitation and how do carbon cycle feedbacks and leaf traits shape the interaction?*

In line with current evidence (Franklin, 2007; McMurtrie and Dewar, 2011; McMurtrie *et al*., 2008), we hypothesise that LAI is shaped by carbon economics via maximisation of net canopy carbon export (NCE; photosynthesis minus the carbon cost of leaf construction and maintenance). We predict that for low MAP forests, as investment into the canopy increases, marginal returns are limited by stomatal conductance. As a result, higher LAI would be deleterious for low MAP forests, and NCE is maximised by lower LAI. Conversely, we predict that for high MAP forests, increased LAI is remunerative due to higher water availability (Figure 1.3). We further hypothesise that carbon cycle feedbacks will strengthen the LAI-precipitation interaction, as reduced NCE causes lower fine root growth, reducing water acquisition, and further constraining photosynthesis via limits to stomatal conductance. Given the role of traits in determining the cost of leaf growth, maintenance, and carbon assimilation rate, we hypothesise that covariation between leaf traits and precipitation will also shape LAI dynamics. Fast leaf traits typical of low MAP forests are predicted to maximise productivity during dry

periods, whilst in high MAP forests slow leaf traits are predicted to minimise leaf maintenance costs throughout the year (Figure 1.4). An improved understanding of how LAI responds to climate would help to reduce uncertainty around carbon flux predictions (Powell *et al*., 2013; Restrepo-Coupe *et al*., 2017), by addressing a key challenge for ecosystem models, which are typically poor at representing tropical phenology (De Weirdt *et al*., 2012; Kim *et al*., 2012).

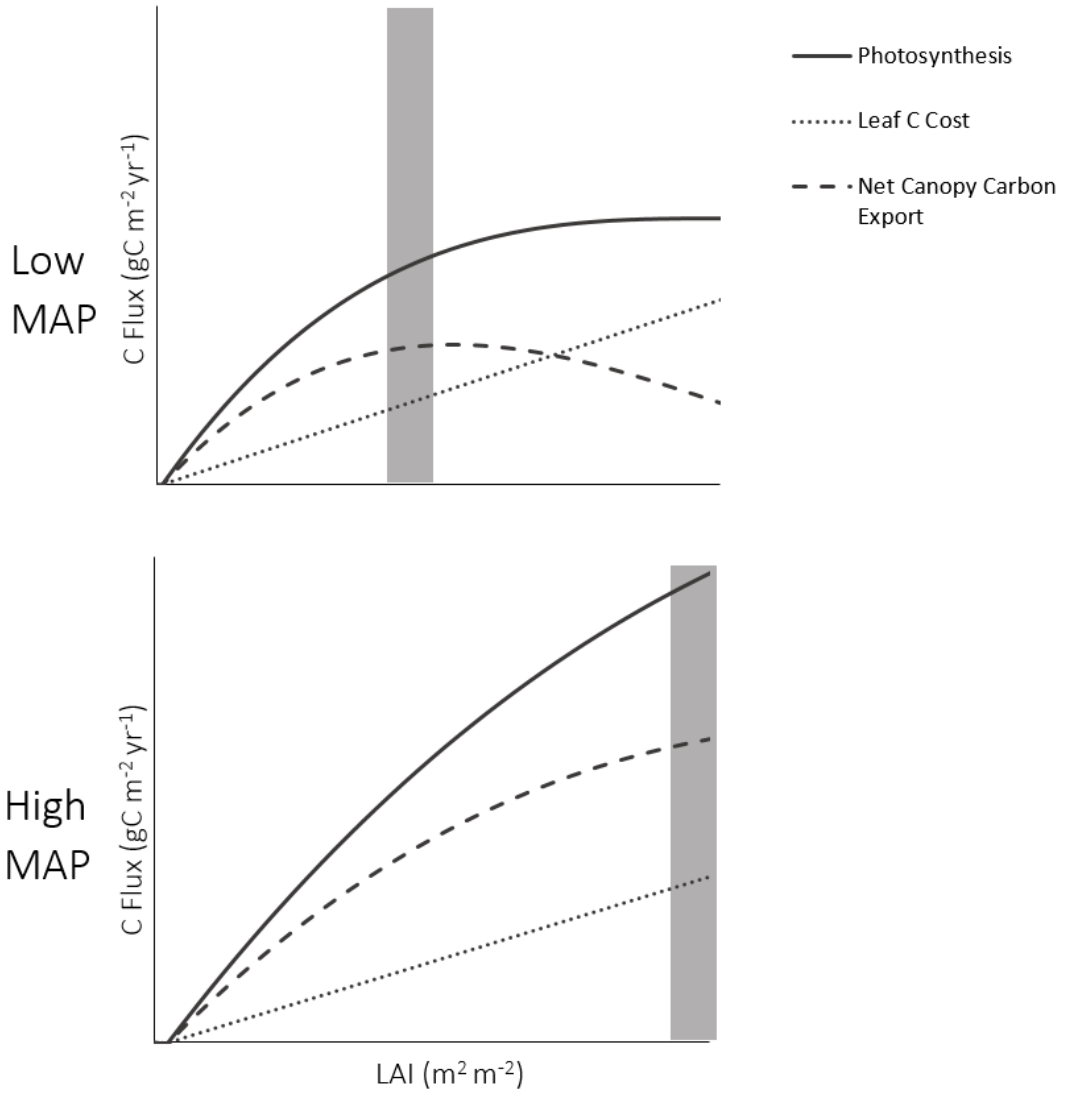

Figure 1.3 Hypothesised photosynthesis, net canopy carbon export and leaf growth and maintenance costs across an LAI gradient for a typical high and low MAP forest plot. Grey bars show optimal LAI under respective plot conditions. Optimal LAI is lower for low MAP plots due the effect of water limitation on stomatal conducatance, and consequently photosynthesis, limiting net canopy carbon export at higher leaf area. Photosynthesis and net canopy carbon export increase with LAI (across the observed range) for high MAP forests as water constraints to stomatal conductance are lower.

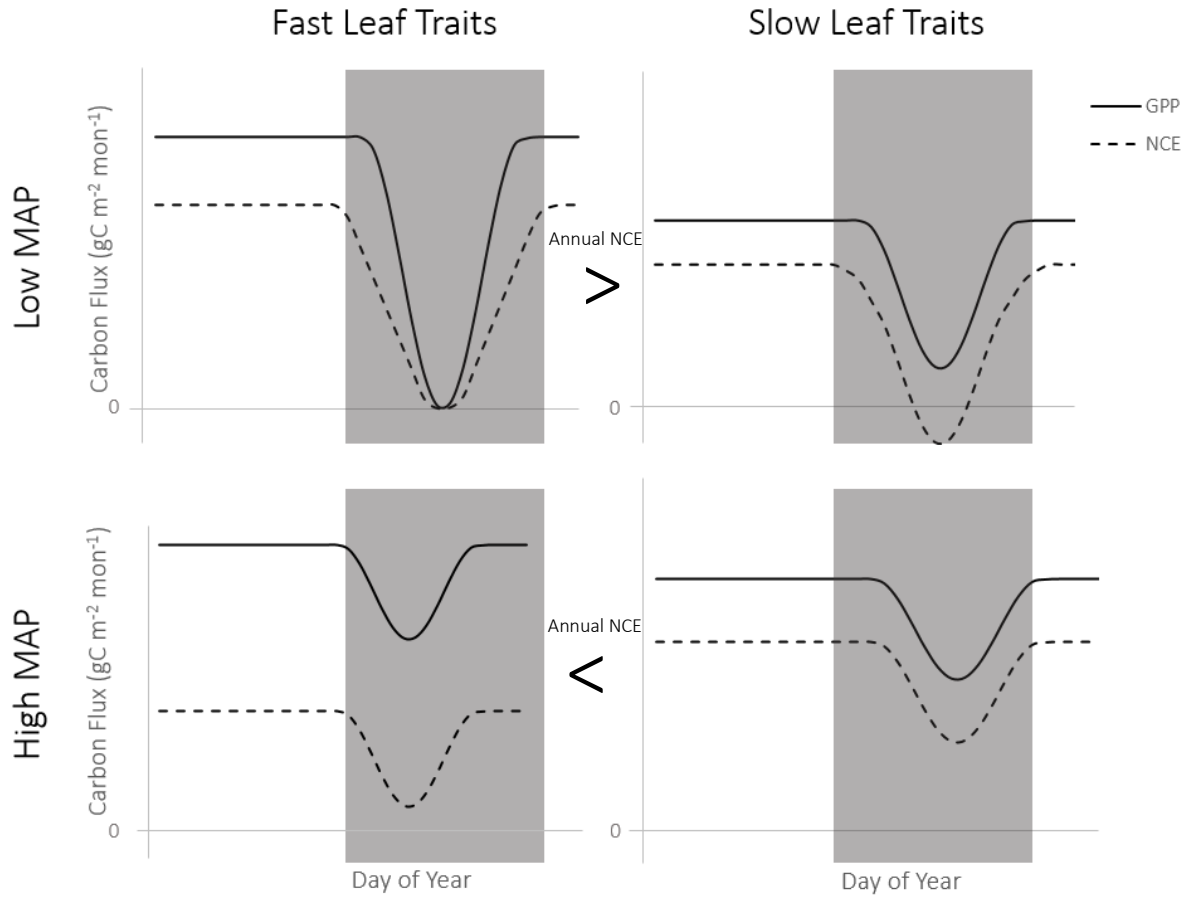

Figure 1.4 The hypothesised effect of fast and slow leaf traits on gross primary productivity (GPP) and net canopy carbon export (NCE) throughout the year for a typical high and low MAP Amazon forest. Grey bars denote dry season timing. For low MAP forests, GPP and NCE is predicted to be higher under fast leaf traits due to the maximisation of photosynthesis during the wet season, and minimisation of leaf growth and maintenance carbon costs (the difference between GPP and NCE) during the dry season. For high MAP forests, despite higher GPP under fast leaf traits, we predict lower leaf growth and maintenance costs under slow leaf traits will drive higher annual NCE.

The coupling between leaf (and root) biomass with precipitation is underpinned by shifts in NPP allocation and plant traits. We expect that NPP allocation is driven by optimal partitioning to maximise uptake of the most limiting resource. However, we remain unable to accurately predict the ratio of NPP allocated to leaves versus roots. Evidence from field studies presents a divergent picture, with some reporting allocation ratios reflecting optimal partitioning, whilst others are unclear (Aragão *et al*., 2009; Hertel *et al.*, 2013; Jiménez *et al*., 2009; Lima *et al*., 2010; Malhi *et al*., 2011; Moore *et al*., 2017). The disparity between findings highlights uncertainty in our understanding of NPP allocation. It has been suggested that plant traits may play an important role in optimal partitioning to drive resultant biomass ratios, through determination of organ lifespan (Aragão *et al*., 2009; Moore *et al*., 2017). However, empirical studies alone are unable to quantify the effects of NPP allocation ratios and traits on forest functioning. We ask

> *Is leaf:root NPP allocation optimal across Amazon forests, and what role do trait distributions play in determining leaf:root NPP in response to water availability?*

We hypothesise that leaf:root NPP allocation is optimal across Amazon forests, and that leaf and root traits have a determinate effect, whereby slow leaf traits with long lifespans support low leaf:root NPP, and fast leaf traits with short lifespans support high leaf:root NPP, with the opposite true for roots (Figure 1.5). We further predict that the covariation of leaf and root traits with precipitation reflects optimal strategies that maximise productivity. Understanding the effect of resource availability on NPP allocation is critical to discerning the impact of climate change on carbon cycle dynamics, and an explanation of trends in leaf:root NPP, and leaf and root traits in response to water availability using an optimality approach could be used to inform ecosystem models.

We predict that our results will show (i) photosynthesis across the Amazon is principally determined by LAI, (ii) LAI is in turn shaped by carbon economics in response to water availability, and that (iii) underlying changes in leaf area with precipitation, is the optimal partitioning of NPP allocation and optimal leaf and root trait distributions (Figure 1.1). We predict that indirect effects of climate, through forest structure and plant traits, will prove more important than direct physiology-climate interactions in shaping forest functioning. We expect optimal responses to water availability to explain variation in biomass, NPP allocation and traits. The aim of this research is to improve understanding around the effects of climate on photosynthesis, LAI, NPP allocation and traits across the Amazon basin. Our findings will

contribute towards reducing uncertainty around modelled responses to shifts in precipitation across Amazon forests as a result of anthropogenic climate change. We aim to offer an evidence base for adopting different modelling approaches. Furthermore, the findings presented will highlight new gaps in our understanding, which can be used to inform future data collection campaigns.

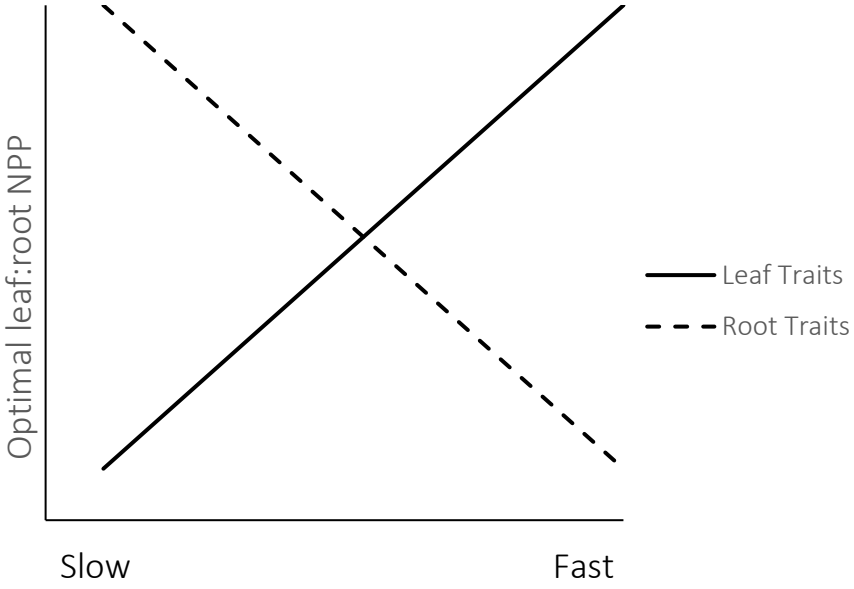

Figure 1.5 The hypothesised interaction between observed fast and slow, leaf and root traits and optimal leaf:root NPP allocation across forest plots. Leaf traits shift from fast to slow, and root traits shift from slow to fast, with increasing precipitation. Slow leaf traits coupled with fast root traits drive low leaf:root NPP allocation as reported for high MAP Amazon forests. Conversely, fast leaf traits coupled with slow root traits drive high leaf:root NPP allocation as reported for low MAP Amazon forests.

1.4 Summary of Methods

We use a model-data approach, focusing on permanent sample plots across an Amazon precipitation gradient, to answer a series of questions around forest functioning in response to water availability. Plots used were part of the Global Ecosystems Monitoring network, and have detailed measurements of carbon fluxes, traits, metoerology, soil properties, and LAI (Doughty *et al.*, 2015; Malhi *et al.*, 2015). We use the Soil Plant atmosphere model (SPA; (Williams *et al.*, 1998; Williams *et al.*, 1996), which has been proven to successfully simulate carbon and water fluxes in tropical forests (Fisher *et al.*, 2007). Modelling approaches offer a valuable tool to develop our understanding of forest functioning in response to climate

change. By using a modelling approach we are able to explore the interaction between climate, forest structure and traits, and their feedback effects, which would be unachievable in a field or lab setting due to cost, practicality and the physical limitations of experimental methods. SPA was calibrated and validated for each plot using biometric data, before undertaking a series of model experiments. We use model parameter alternations to separate direct effects of LAI, plant traits, climate and NPP allocation on productivity, and explore carbon cycle feedbacks. Much of this work adopts an 'optimality' approach to ecosystem functioning and the use of different fitness proxies is discussed where relevant. The results from each chapter will then be collated to discuss the impact of direct and indirect climate effects on forest functioning, the applicability of optimality approaches to predict carbon dynamics under changes in resource availability, and how plant traits capture the effects of climate on ecosystem functioning across Amazon forests.

1.5 Key Results

LAI was the principal driver of photosynthesis across the Amazon precipitation gradient, accounting for 36% of observed variation, leaf traits which included photosynthetic capacity accounted for 20%, and physiology-climate interactions accounted for a further 12%. Carbon economics underpinned spatial variance in LAI, which was sucessfully predicted by an optimality approach that maximised net canopy carbon export (R^2=0.87, p<0.001). Leaf trait distributions across the precipitation gradient were optimal and shaped the interaction between canopy dynamics and water availability. Leaf:root NPP across the precipitation gradient was also optimal, and was similarly best predicted by NCE maximisation (R^2=0.60, p=0.02). The partitioning of NPP to maximise NCE was supported by concurrent shifts in leaf and root traits, which together accounted for 63% of variation in optimal leaf:root NPP. The indirect effects of climate, through forest structure and plant traits, proved more important than direct physiology-climate interactions in shaping forest functioning. Optimal responses to water availability explained variation in LAI, leaf:root NPP and leaf traits across the precipitation gradient.

1.6 References

Aragao, L. E., Poulter, B., Barlow, J. B., Anderson, L. O., Malhi, Y., Saatchi, S., Phillips, O. L., & Gloor, E. (2014). Environmental change and the carbon balance of Amazonian forests. Biol Rev Camb Philos Soc, 89(4), 913-931.

Aragao, L. E. O. C., Anderson, L. O., Fonseca, M. G., Rosan, T. M., Vedovato, L. B., Wagner, F. H., Silva, C. V. J., Silva, C. H. L., Arai, E., Aguiar, A. P., Barlow, J., Berenguer, E., Deeter, M. N., Domingues, L. G., Gatti, L., Gloor, M., Malhi, Y., Marengo, J. A., Miller, J. B., Phillips, O. L., & Saatchi, S. (2018). 21st Century drought-related fires counteract the decline of Amazon deforestation carbon emissions. Nature Communications, 9(1), 536.

Aragao, L. E. O. C., Malhi, Y., Barbier, N., Lima, A., Shimabukuro, Y., Anderson, L., & Saatchi, S. (2008). Interactions between rainfall, deforestation and fires during recent years in the Brazilian Amazonia. Philosophical Transactions of the Royal Society B-Biological Sciences, 363(1498), 1779-1785.

Aragao, L. E. O. C., Malhi, Y., Metcalfe, D. B., Silva-Espejo, J. E., Jimenez, E., Navarrete, D., Almeida, S., Costa, A. C. L., Salinas, N., Phillips, O. L., Anderson, L. O., Alvarez, E., Baker, T. R., Goncalvez, P. H., Huaman-Ovalle, J., Mamani-Solorzano, M., Meir, P., Monteagudo, A., Patino, S., Penuela, M. C., Prieto, A., Quesada, C. A., Rozas-Davila, A., Rudas, A., Silva, J. A., & Vasquez, R. (2009). Above- and below-ground net primary productivity across ten Amazonian forests on contrasting soils. Biogeosciences, 6(12), 2759-2778.

Aragao, L. E. O. C., Malhi, Y., Roman-Cuesta, R. M., Saatchi, S., Anderson, L. O., & Shimabukuro, Y. E. (2007). Spatial patterns and fire response of recent Amazonian droughts. Geophysical Research Letters, 34(7).

Araujo-Murakami, A., Doughty, C. E., Metcalfe, D. B., Silva-Espejo, J. E., Arroyo, L., Heredia, J. P., Flores, M., Sibler, R., Mendizabal, L. M., Pardo-Toledo, E., Vega, M., Moreno, L., Rojas-Landivar, V. D., Halladay, K., Girardin, C. A. J., Killeen, T. J., & Malhi, Y. (2014). The productivity, allocation and cycling of carbon in forests at the dry margin of the Amazon forest in Bolivia. Plant Ecology & Diversity, 7(1-2), 55-69.

Asner, G. P., & Alencar, A. (2010). Drought impacts on the Amazon forest: the remote sensing perspective. New Phytol, 187(3), 569-578.

Baker, I. T., Prihodko, L., Denning, A. S., Goulden, M., Miller, S., & da Rocha, H. R. (2008). Seasonal drought stress in the Amazon: Reconciling models and observations. Journal of Geophysical Research-Biogeosciences, 113(G1).

Beer, C., Reichstein, M., Tomelleri, E., Ciais, P., Jung, M., Carvalhais, N., Rodenbeck, C., Arain, M. A., Baldocchi, D., Bonan, G. B., Bondeau, A., Cescatti, A., Lasslop, G., Lindroth, A., Lomas, M., Luyssaert, S., Margolis, H., Oleson, K. W., Roupsard, O., Veenendaal, E., Viovy, N., Williams, C., Woodward, F. I., & Papale, D. (2010). Terrestrial gross carbon dioxide uptake: global distribution and covariation with climate. Science, 329(5993), 834-838.

Bi, J., Myneni, R., Lyapustin, A., Wang, Y., Park, T., Chi, C., Yan, K., & Knyazikhin, Y. (2016). Amazon forests' response to droughts: A perspective from the MAIAC product. Remote Sensing, 8(4), 356.

Boisier, J. P., Ciais, P., Ducharne, A., & Guimberteau, M. (2015). Projected strengthening of Amazonian dry season by constrained climate model simulations. Nature Climate Change, 5(7), 656-660.

Bonan, G. B., Williams, M., Fisher, R. A., & Oleson, K. W. (2014). Modeling stomatal conductance in the earth system: linking leaf water-use efficiency and water transport along the soil–plant–atmosphere continuum. Geoscientific Model Development, 7(5), 2193-2222.

Bradley, A. V., Gerard, F. F., Barbier, N., Weedon, G. P., Anderson, L. O., Huntingford, C., Aragão, L. E. O. C., Zelazowski, P., & Arai, E. (2011). Relationships between phenology, radiation and precipitation in the Amazon region. Global Change Biology, 17(6), 2245-2260.

Brando, P. M., Balch, J. K., Nepstad, D. C., Morton, D. C., Putz, F. E., Coe, M. T., Silvério, D., Macedo, M. N., Davidson, E. A., & Nóbrega, C. C. (2014). Abrupt increases in Amazonian tree mortality due to drought–fire interactions. Proceedings of the National Academy of Sciences, 111(17), 6347-6352.

Brando, P. M., Nepstad, D. C., Davidson, E. A., Trumbore, S. E., Ray, D., & Camargo, P. (2008). Drought effects on litterfall, wood production and belowground carbon cycling in an Amazon forest: results of a throughfall reduction experiment. Philos Trans R Soc Lond B Biol Sci, 363(1498), 1839-1848.

Callede, J., Guyot, J. L., Ronchail, J., Molinier, M., & De Oliveira, E. (2002). L'Amazone à Obidos (Brésil): étude statistique des débits et bilan hydrologique. Hydrological Sciences Journal, 47(2), 321-333.

Coe, M. T., Marthews, T. R., Costa, M. H., Galbraith, D. R., Greenglass, N. L., Imbuzeiro, H. M. A., Levine, N. M., Malhi, Y., Moorcroft, P. R., & Muza, M. N. (2013). Deforestation and climate feedbacks threaten the ecological integrity of south–southeastern Amazonia. Phil. Trans. R. Soc. B, 368(1619), 20120155.

da Costa, A. C. L., Galbraith, D., Almeida, S., Portela, B. T. T., da Costa, M., de Athaydes Silva Junior, J., Braga, A. P., de Gonçalves, P. H. L., de Oliveira, A. A. R., & Fisher, R. (2010). Effect of 7 yr of experimental drought on vegetation dynamics and biomass storage of an eastern Amazonian rainforest. New Phytologist, 187(3), 579-591.

da Costa, A. C. L., Metcalfe, D. B., Doughty, C. E., de Oliveira, A. A. R., Neto, G. F. C., da Costa, M. C., Silva Junior, J. d. A., Aragão, L. E. O. C., Almeida, S., & Galbraith, D. R. (2014). Ecosystem respiration and net primary productivity after 8–10 years of experimental through-fall reduction in an eastern Amazon forest. Plant Ecology & Diversity, 7(1-2), 7-24.

De Weirdt, M., Verbeeck, H., Maignan, F., Peylin, P., Poulter, B., Bonal, D., Ciais, P., & Steppe, K. (2012). Seasonal leaf dynamics for tropical evergreen forests in a process-based global ecosystem model. Geoscientific Model Development, 5(5), 1091-1108.

Dewar, R. C., Franklin, O., Mäkelä, A., McMurtrie, R. E., & Valentine, H. T. (2009). Optimal function explains forest responses to global change. Bioscience, 59(2), 127-139.

Dirzo, R., & Raven, P. H. (2003). Global state of biodiversity and loss. Annual Review of Environment and Resources, 28(1), 137-167.

Doughty, C. E., Malhi, Y., Araujo-Murakami, A., Metcalfe, D. B., Silva-Espejo, J. E., Arroyo, L., Heredia, J. P., Pardo-Toledo, E., Mendizabal, L. M., & Rojas-Landivar, V. D. (2014). Allocation trade-offs dominate the response of tropical forest growth to seasonal and interannual drought. Ecology, 95(8), 2192-2201.

Doughty, C. E., Metcalfe, D. B., Girardin, C. A., Amezquita, F. F., Cabrera, D. G., Huasco, W. H., Silva-Espejo, J. E., Araujo-Murakami, A., da Costa, M. C., Rocha, W., Feldpausch, T. R., Mendoza, A. L., da Costa, A. C., Meir, P., Phillips, O. L., & Malhi, Y. (2015). Drought impact on forest carbon dynamics and fluxes in Amazonia. Nature, 519(7541), 78-82.

Doughty, C. E., Metcalfe, D. B., Girardin, C. A. J., Amezquita, F. F., Durand, L., Huasco, W. H., Silva-Espejo, J. E., Araujo-Murakami, A., da Costa, M. C., da Costa, A. C. L., Rocha, W., Meir, P., Galbraith, D., & Malhi, Y. (2015). Source and sink carbon dynamics and carbon allocation in the Amazon basin. Global Biogeochemical Cycles, 29(5), 645-655.

Duffy, P. B., Brando, P., Asner, G. P., & Field, C. B. (2015). Projections of future meteorological drought and wet periods in the Amazon. Proc Natl Acad Sci U S A, 112(43), 13172-13177.

FAO. (2001). Global Forest Resources Assessment. FAO Forestry Paper 140.

Farquhar, G. D., & Sharkey, T. D. (1982). Stomatal conductance and photosynthesis. Annual review of plant physiology, 33(1), 317-345.

Farquhar, G. D., & Von Caemmerer, S. (1982). Modelling of photosynthetic response to environmental conditions Physiological plant ecology II (pp. 549-587): Springer.

Farquhar, G. D. v., von Caemmerer, S. v., & Berry, J. A. (1980). A biochemical model of photosynthetic CO2 assimilation in leaves of C3 species. Planta, 149(1), 78-90.

Fauset, S., Baker, T. R., Lewis, S. L., Feldpausch, T. R., Affum-Baffoe, K., Foli, E. G., Hamer, K. C., & Swaine, M. D. (2012). Drought-induced shifts in the floristic and functional composition of tropical forests in Ghana. Ecol Lett, 15(10), 1120-1129.

Feddema, J. J., Oleson, K. W., Bonan, G. B., Mearns, L. O., Buja, L. E., Meehl, G. A., & Washington, W. M. (2005). The importance of land-cover change in simulating future climates. Science, 310(5754), 1674-1678.

Feng, X., Porporato, A., & Rodriguez-Iturbe, I. (2013). Changes in rainfall seasonality in the tropics. Nature Climate Change, 3, 811.

Field, C. B., Behrenfeld, M. J., Randerson, J. T., & Falkowski, P. (1998). Primary production of the biosphere: integrating terrestrial and oceanic components. Science, 281(5374), 237-240.

Fisher, R. A., Williams, M., Da Costa, A. L., Malhi, Y., Da Costa, R. F., Almeida, S., & Meir, P. (2007). The response of an Eastern Amazonian rain forest to drought stress: results and modelling analyses from a throughfall exclusion experiment. Global Change Biology, 13(11), 2361-2378.

Franklin, O. (2007). Optimal nitrogen allocation controls tree responses to elevated CO2. New Phytologist, 174(4), 811-822.

Franklin, O., Johansson, J., Dewar, R. C., Dieckmann, U., McMurtrie, R. E., Brännström, Å., & Dybzinski, R. (2012). Modeling carbon allocation in trees: a search for principles. Tree Physiology, 32(6), 648-666.

Fu, R., Yin, L., Li, W., Arias, P. A., Dickinson, R. E., Huang, L., Chakraborty, S., Fernandes, K., Liebmann, B., & Fisher, R. (2013). Increased dry-season length over southern Amazonia in recent decades and its implication for future climate projection. Proceedings of the National Academy of Sciences, 110(45), 18110-18115.

Fyllas, N. M., Bentley, L. P., Shenkin, A., Asner, G. P., Atkin, O. K., Diaz, S., Enquist, B. J., Farfan-Rios, W., Gloor, E., Guerrieri, R., Huasco, W. H., Ishida, Y., Martin, R. E., Meir, P., Phillips, O., Salinas, N., Silman, M., Weerasinghe, L. K., Zaragoza-Castells, J., & Malhi, Y. (2017). Solar radiation and functional traits explain the decline of forest primary productivity along a tropical elevation gradient. Ecol Lett, 20(6), 730-740.

Gatti, L. V., Gloor, M., Miller, J. B., Doughty, C. E., Malhi, Y., Domingues, L. G., Basso, L. S., Martinewski, A., Correia, C. S. C., & Borges, V. F. (2014). Drought sensitivity of Amazonian carbon balance revealed by atmospheric measurements. Nature, 506(7486), 76.

Gloor, M., Brienen, R. J. W., Galbraith, D., Feldpausch, T. R., Schöngart, J., Guyot, J. L., Espinoza, J. C., Lloyd, J., & Phillips, O. L. (2013). Intensification of the Amazon hydrological cycle over the last two decades. Geophysical Research Letters, 40(9), 1729-1733.

Guan, K. Y., Pan, M., Li, H. B., Wolf, A., Wu, J., Medvigy, D., Caylor, K. K., Sheffield, J., Wood, E. F., Malhi, Y., Liang, M. L., Kimball, J. S., Saleska, S. R., Berry, J., Joiner, J., & Lyapustin, A. I. (2015). Photosynthetic seasonality of global tropical forests constrained by hydroclimate. Nature Geoscience, 8(4), 284-289.

Hansen, M. C., Stehman, S. V., & Potapov, P. V. (2010). Quantification of global gross forest cover loss. Proceedings of the National Academy of Sciences, 107(19), 8650-8655.

Harper, B. A., Denning, A. S., Baker Ian, T., Branson Mark, D., Prihodko, L., & Randall David, A. (2010). Role of deep soil moisture in modulating climate in the Amazon rainforest. Geophysical Research Letters, 37(5).

Hawkins, E., & Sutton, R. (2011). The potential to narrow uncertainty in projections of regional precipitation change. Climate Dynamics, 37(1-2), 407-418.

Hertel, D., Strecker, T., Müller-Haubold, H., & Leuschner, C. (2013). Fine root biomass and dynamics in beech forests across a precipitation gradient–is optimal resource partitioning theory applicable to water-limited mature trees? Journal of ecology, 101(5), 1183-1200.

Hikosaka, K., Ishikawa, K., Borjigidai, A., Muller, O., & Onoda, Y. (2005). Temperature acclimation of photosynthesis: mechanisms involved in the changes in temperature dependence of photosynthetic rate. Journal of experimental botany, 57(2), 291-302.

Hilker, T., Lyapustin, A. I., Tucker, C. J., Hall, F. G., Myneni, R. B., Wang, Y., Bi, J., Mendes de Moura, Y., & Sellers, P. J. (2014). Vegetation dynamics and rainfall sensitivity of the Amazon. Proc Natl Acad Sci U S A, 111(45), 16041-16046.

Huang, M., & Asner, G. P. (2010). Long-term carbon loss and recovery following selective logging in Amazon forests. Global Biogeochemical Cycles, 24(3).

Huete, A. R., Didan, K., Shimabukuro, Y. E., Ratana, P., Saleska, S. R., Hutyra, L. R., Yang, W., Nemani, R. R., & Myneni, R. (2006). Amazon rainforests green-up with sunlight in dry season. Geophysical Research Letters, 33(6).

Hui, D., Luo, Y., & Katul, G. (2003). Partitioning interannual variability in net ecosystem exchange between climatic variability and functional change. Tree Physiology, 23(7), 433-442.

IPCC. (2007). The Physical Science Basis. Contribution of Working Group I to the Fourth Assessment Report of the IPCC. Published by the Intergovernmental Panel on Climate Change: by S. Solomon, D. Qin, M. Manning, et al.(Cambridge University Press, Cambridge, United Kingdom and New York, NY, USA, 2007).

Jiménez, E. M., Moreno, F. H., Peñuel, M. C., Patino, S., & Lloyd, J. (2009). Fine root dynamics for forests on contrasting soils in the Colombian Amazon. Biogeosciences, 6, 2809-2827.

Jiménez-Muñoz, J. C., Sobrino, J. A., Mattar, C., & Malhi, Y. (2013). Spatial and temporal patterns of the recent warming of the Amazon forest. Journal of Geophysical Research: Atmospheres, 118(11), 5204-5215.

Joetzjer, E., Douville, H., Delire, C., & Ciais, P. (2013). Present-day and future Amazonian precipitation in global climate models: CMIP5 versus CMIP3. Climate Dynamics, 41(11-12), 2921-2936.

Kim, Y., Knox, R. G., Longo, M., Medvigy, D., Hutyra, L. R., Pyle, E. H., Wofsy, S. C., Bras, R. L., & Moorcroft, P. R. (2012). Seasonal carbon dynamics and water fluxes in an Amazon rainforest. Global Change Biology, 18(4), 1322-1334.

Li, W., Fu, R., & Dickinson, R. E. (2006). Rainfall and its seasonality over the Amazon in the 21st century as assessed by the coupled models for the IPCC AR4. Journal of Geophysical Research: Atmospheres, 111(D2).

Li, W., Fu, R., Juarez, R. I. N., & Fernandes, K. (2008). Observed change of the standardized precipitation index, its potential cause and implications to future climate change in the Amazon region. Philosophical Transactions of the Royal Society of London B: Biological Sciences, 363(1498), 1767-1772.

Liebmann, B., & Marengo, J. (2001). Interannual variability of the rainy season and rainfall in the Brazilian Amazon Basin. Journal of Climate, 14(22), 4308-4318.

Lima, T. T. S., Miranda, I. S., & Vasconcelos, S. S. (2010). Effects of water and nutrient availability on fine root growth in eastern Amazonian forest regrowth, Brazil. New Phytologist, 187(3), 622-630.

Mäkelä, A. (2012). On guiding principles for carbon allocation in eco-physiological growth models. Tree Physiology, 32(6), 644-647.

Mäkelä, A., Valentine, H. T., & Helmisaari, H. S. (2008). Optimal co-allocation of carbon and nitrogen in a forest stand at steady state. New Phytologist, 180(1), 114-123.

Malhi, Y., Amezquita, F. F., Doughty, C. E., Silva-Espejo, J. E., Girardin, C. A. J., Metcalfe, D. B., Aragao, L. E. O. C., Huaraca-Quispe, L. P., Alzamora-Taype, I., Eguiluz-Mora, L., Marthews, T. R., Halladay, K., Quesada, C. A., Robertson, A. L., Fisher, J. B., Zaragoza-Castells, J., Rojas-Villagra, C. M., Pelaez-Tapia, Y., Salinas, N., Meir, P., & Phillips, O. L. (2014). The productivity, metabolism and carbon cycle of two lowland tropical forest plots in south-western Amazonia, Peru. Plant Ecology & Diversity, 7(1-2), 85-105.

Malhi, Y., Baker, T. R., Phillips, O. L., Almeida, S., Alvarez, E., Arroyo, L., Chave, J., Czimczik, C. I., Fiore, A. D., & Higuchi, N. (2004). The above-ground coarse wood productivity of 104 Neotropical forest plots. Global Change Biology, 10(5), 563-591.

Malhi, Y., Doughty, C., & Galbraith, D. (2011). The allocation of ecosystem net primary productivity in tropical forests. Phil. Trans. R. Soc. B, 366(1582), 3225-3245.

Malhi, Y., Doughty, C. E., Goldsmith, G. R., Metcalfe, D. B., Girardin, C. A. J., Marthews, T. R., del Aguila-Pasquel, J., Aragao, L. E. O. C., Araujo-Murakami, A., Brando, P., da Costa, A. C. L., Silva-Espejo, J. E., Amezquita, F. F., Galbraith, D. R., Quesada, C. A., Rocha, W., Salinas-Revilla, N., Silverio, D., Meir, P., & Phillips, O. L. (2015). The linkages between photosynthesis, productivity, growth and biomass in lowland Amazonian forests. Global Change Biology, 21(6), 2283-2295.

Malhi, Y., Girardin, C. A. J., Goldsmith, G. R., Doughty, C. E., Salinas, N., Metcalfe, D. B., Huasco, W. H., Silva-Espejo, J. E., del Aguilla-Pasquell, J., & Amézquita, F. F. (2017). The variation of productivity and its allocation along a tropical elevation gradient: a whole carbon budget perspective. New Phytologist, 214(3), 1019-1032.

Malhi, Y., & Grace, J. (2000). Tropical forests and atmospheric carbon dioxide. Trends in ecology & evolution, 15(8), 332-337.

Malhi, Y., Roberts, J. T., Betts, R. A., Killeen, T. J., Li, W., & Nobre, C. A. (2008). Climate change, deforestation, and the fate of the Amazon. Science, 319(5860), 169-172.

Malhi, Y., Wood, D., Baker, T. R., Wright, J., Phillips, O. L., Cochrane, T., Meir, P., Chave, J., Almeida, S., & Arroyo, L. (2006). The regional variation of aboveground live biomass in old-growth Amazonian forests. Global Change Biology, 12(7), 1107-1138.

Malhi, Y., & Wright, J. (2004). Spatial patterns and recent trends in the climate of tropical rainforest regions. Philosophical Transactions of the Royal Society B: Biological Sciences, 359(1443), 311-329.

Marengo, J. A. (1992). Interannual variability of surface climate in the Amazon basin. International journal of climatology, 12(8), 853-863.

Marengo, J. A. (2004). Interdecadal variability and trends of rainfall across the Amazon basin. Theoretical and applied climatology, 78(1-3), 79-96.

Marengo, J. A., Chou, S. C., Kay, G., Alves, L. M., Pesquero, J. F., Soares, W. R., Santos, D. C., Lyra, A. A., Sueiro, G., & Betts, R. (2012). Development of regional future climate change scenarios in South America using the Eta CPTEC/HadCM3 climate change projections: climatology and regional analyses for the Amazon, São Francisco and the Paraná River basins. Climate Dynamics, 38(9-10), 1829-1848.

Marengo, J. A., Nobre, C. A., Tomasella, J., Oyama, M. D., Sampaio de Oliveira, G., De Oliveira, R., Camargo, H., Alves, L. M., & Brown, I. F. (2008). The drought of Amazonia in 2005. Journal of Climate, 21(3), 495-516.

Marengo, J. A., Tomasella, J., Alves, L. M., Soares, W. R., & Rodriguez, D. A. (2011). The drought of 2010 in the context of historical droughts in the Amazon region. Geophysical Research Letters, 38(12).

McMurtrie, R. E., & Dewar, R. C. (2011). Leaf-trait variation explained by the hypothesis that plants maximize their canopy carbon export over the lifespan of leaves. Tree Physiology, 31(9), 1007-1023.

McMurtrie, R. E., & Dewar, R. C. (2013). New insights into carbon allocation by trees from the hypothesis that annual wood production is maximized. New Phytologist, 199(4), 981-990.

McMurtrie, R. E., Norby, R. J., Medlyn, B. E., Dewar, R. C., Pepper, D. A., Reich, P. B., & Barton, C. V. M. (2008). Why is plant-growth response to elevated CO2 amplified when water is limiting, but reduced when nitrogen is limiting? A growth-optimisation hypothesis. Functional Plant Biology, 35(6), 521-534.

Medlyn, B. E., Dreyer, E., Ellsworth, D., Forstreuter, M., Harley, P. C., Kirschbaum, M. U. F., Le Roux, X., Montpied, P., Strassemeyer, J., & Walcroft, A. (2002). Temperature response of parameters of a biochemically based model of photosynthesis. II. A review of experimental data. Plant, Cell & Environment, 25(9), 1167-1179.

Meir, P., Mencuccini, M., & Dewar, R. C. (2015). Drought-related tree mortality: addressing the gaps in understanding and prediction. New Phytol, 207(1), 28-33.

Meir, P., Metcalfe, D. B., Costa, A. C. L., & Fisher, R. A. (2008). The fate of assimilated carbon during drought: impacts on respiration in Amazon rainforests. Philosophical Transactions of the Royal Society of London B: Biological Sciences, 363(1498), 1849-1855.

Meir, P., & Woodward, F. I. (2010). Amazonian rain forests and drought: response and vulnerability. New Phytol, 187(3), 553-557.

Metcalfe, D. B., Meir, P., Aragão, L. E. O. C., Lobo-do-Vale, R., Galbraith, D., Fisher, R. A., Chaves, M. M., Maroco, J. P., da Costa, A. C. L., & de Almeida, S. S. (2010). Shifts in plant respiration and carbon use efficiency at a large-scale drought experiment in the eastern Amazon. New Phytologist, 187(3), 608-621.

Moore, S., Adu-Bredu, S., Duah-Gyamfi, A., Addo-Danso, S. D., Ibrahim, F., Mbou, A. T., Grandcourt, A., Valentini, R., Nicolini, G., & Djagbletey, G. (2017). Forest biomass, productivity and carbon cycling along a rainfall gradient in West Africa. Global Change Biology.

Nasi, R., Taber, A., & Vliet, N. V. (2011). Empty forests, empty stomachs? Bushmeat and livelihoods in the Congo and Amazon Basins. International Forestry Review, 13(3), 355-368.

Nepstad, D., McGrath, D., Stickler, C., Alencar, A., Azevedo, A., Swette, B., Bezerra, T., DiGiano, M., Shimada, J., & da Motta, R. S. (2014). Slowing Amazon deforestation through public policy and interventions in beef and soy supply chains. Science, 344(6188), 1118-1123.

Nepstad, D. C., Moutinho, P., Dias, M. B., Davidson, E., Cardinot, G., Markewitz, D., Figueiredo, R., Vianna, N., Chambers, J., Ray, D., Guerreiros, J. B., Lefebvre, P., Sternberg, L., Moreira, M., Barros, L., Ishida, F. Y., Tohlver, I., Belk, E., Kalif, K., & Schwalbe, K. (2002). The effects of partial throughfall exclusion on canopy processes, aboveground production, and biogeochemistry of an Amazon forest. Journal of Geophysical Research-Atmospheres, 107(D20).

Nepstad, D. C., Tohver, I. M., Ray, D., Moutinho, P., & Cardinot, G. (2007). Mortality of large trees and lianas following experimental drought in an Amazon forest. Ecology, 88(9), 2259-2269.

Oliveira, R. S., Dawson, T. E., Burgess, S. S. O., & Nepstad, D. C. (2005). Hydraulic redistribution in three Amazonian trees. Oecologia, 145(3), 354-363.

Pan, Y., Birdsey, R. A., Fang, J., Houghton, R., Kauppi, P. E., Kurz, W. A., Phillips, O. L., Shvidenko, A., Lewis, S. L., & Canadell, J. G. (2011). A large and persistent carbon sink in the world's forests. Science, 333(6045), 988-993.

Panisset, J. S., Libonati, R., Gouveia, C. M. P., Machado-Silva, F., França, D. A., França, J. R. A., & Peres, L. F. (2018). Contrasting patterns of the extreme drought episodes of 2005, 2010 and 2015 in the Amazon Basin. International journal of climatology, 38(2), 1096-1104.

Phillips, O. L., Aragao, L. E., Lewis, S. L., Fisher, J. B., Lloyd, J., Lopez-Gonzalez, G., Malhi, Y., Monteagudo, A., Peacock, J., Quesada, C. A., van der Heijden, G., Almeida, S., Amaral, I., Arroyo, L., Aymard, G., Baker, T. R., Banki, O., Blanc, L., Bonal, D., Brando, P., Chave, J., de Oliveira, A. C., Cardozo, N. D., Czimczik, C. I., Feldpausch, T. R., Freitas, M. A., Gloor, E., Higuchi, N., Jimenez, E., Lloyd, G., Meir, P., Mendoza, C., Morel, A., Neill, D. A., Nepstad, D., Patino, S., Penuela, M. C., Prieto, A., Ramirez, F., Schwarz, M., Silva, J., Silveira, M., Thomas, A. S., Steege, H. T., Stropp, J., Vasquez, R., Zelazowski, P., Alvarez Davila, E., Andelman, S., Andrade, A., Chao, K. J., Erwin, T., Di Fiore, A., Honorio, C. E., Keeling, H., Killeen, T. J., Laurance, W. F., Pena Cruz, A., Pitman, N. C., Nunez Vargas, P., Ramirez-Angulo, H., Rudas, A., Salamao, R., Silva, N., Terborgh, J., & Torres-Lezama, A. (2009). Drought sensitivity of the Amazon rainforest. Science, 323(5919), 1344-1347.

Phillips, O. L., Van Der Heijden, G., Lewis, S. L., López-González, G., Aragão, L. E. O. C., Lloyd, J., Malhi, Y., Monteagudo, A., Almeida, S., & Dávila, E. A. (2010). Drought–mortality relationships for tropical forests. New Phytologist, 187(3), 631-646.

Powell, T. L., Galbraith, D. R., Christoffersen, B. O., Harper, A., Imbuzeiro, H. M., Rowland, L., Almeida, S., Brando, P. M., da Costa, A. C., Costa, M. H., Levine, N. M., Malhi, Y., Saleska, S. R., Sotta, E., Williams, M., Meir, P., & Moorcroft, P. R. (2013). Confronting model predictions of carbon fluxes with measurements of Amazon forests subjected to experimental drought. New Phytol, 200(2), 350-365.

Restrepo-Coupe, N., da Rocha, H. R., Hutyra, L. R., da Araujo, A. C., Borma, L. S., Christoffersen, B., Cabral, O. M. R., de Camargo, P. B., Cardoso, F. L., & da Costa, A. C. L. (2013). What drives the seasonality of photosynthesis across the Amazon basin? A cross-site analysis of eddy flux tower measurements from the Brasil flux network. Agricultural and Forest Meteorology, 182, 128-144.

Restrepo-Coupe, N., Levine, N. M., Christoffersen, B. O., Albert, L. P., Wu, J., Costa, M. H., Galbraith, D., Imbuzeiro, H., Martins, G., & Araujo, A. C. (2017). Do dynamic global vegetation models capture the seasonality of carbon fluxes in the Amazon basin? A data-model intercomparison. Global Change Biology, 23(1), 191-208.

Richardson, A. D., Hollinger, D. Y., Aber, J. D., Ollinger, S. V., & Braswell, B. H. (2007). Environmental variation is directly responsible for short-but not long-term variation in forest-atmosphere carbon exchange. Global Change Biology, 13(4), 788-803.

Rocha, W., Metcalfe, D. B., Doughty, C. E., Brando, P., Silverio, D., Halladay, K., Nepstad, D. C., Balch, J. K., & Malhi, Y. (2014). Ecosystem productivity and carbon cycling in intact and annually burnt forest at the dry southern limit of the Amazon rainforest (Mato Grosso, Brazil). Plant Ecology & Diversity, 7(1-2), 25-40.

Rowland, L., Harper, A., Christoffersen, B. O., Galbraith, D. R., Imbuzeiro, H. M. A., Powell, T. L., Doughty, C., Levine, N. M., Malhi, Y., Saleska, S. R., Moorcroft, P. R., Meir, P., & Williams, M. (2015). Modelling climate change responses in tropical forests: similar productivity estimates across five models, but different mechanisms and responses. Geoscientific Model Development, 8(4), 1097-1110.

Saatchi, S., Asefi-Najafabady, S., Malhi, Y., Aragão, L. E. O. C., Anderson, L. O., Myneni, R. B., & Nemani, R. (2013). Persistent effects of a severe drought on Amazonian forest canopy. Proceedings of the National Academy of Sciences, 110(2), 565-570.

Saleska, S., Da Rocha, H., Kruijt, B., & Nobre, A. (2009). Ecosystem carbon fluxes and Amazonian forest metabolism. Amazonia and Global Change, 389-407.

Saleska, S. R., Didan, K., Huete, A. R., & da Rocha, H. R. (2007). Amazon forests green-up during 2005 drought. Science, 318(5850), 612.

Samanta, A., Ganguly, S., Hashimoto, H., Devadiga, S., Vermote, E., Knyazikhin, Y., Nemani, R. R., & Myneni, R. B. (2010). Amazon forests did not green-up during the 2005 drought. Geophysical Research Letters, 37(5).

Santiago, L. S., Kitajima, K., Wright, S. J., & Mulkey, S. S. (2004). Coordinated changes in photosynthesis, water relations and leaf nutritional traits of canopy trees along a precipitation gradient in lowland tropical forest. Oecologia, 139(4), 495-502.

Schuur, E. A. G. (2003). Productivity and global climate revisited: the sensitivity of tropical forest growth to precipitation. Ecology, 84(5), 1165-1170.

Smith, N. G., Malyshev, S. L., Shevliakova, E., Kattge, J., & Dukes, J. S. (2016). Foliar temperature acclimation reduces simulated carbon sensitivity to climate. Nature Climate Change, 6(4), 407.

Soares-Filho, B. S., Nepstad, D. C., Curran, L. M., Cerqueira, G. C., Garcia, R. A., Ramos, C. A., Voll, E., McDonald, A., Lefebvre, P., & Schlesinger, P. (2006). Modelling conservation in the Amazon basin. Nature, 440(7083), 520.

Ter Steege, H., Pitman, N. C. A., Phillips, O. L., Chave, J., Sabatier, D., Duque, A., Molino, J.-F., Prévost, M.-F., Spichiger, R., & Castellanos, H. (2006). Continental-scale patterns of canopy tree composition and function across Amazonia. Nature, 443(7110), 444-447.

Uvo, C. B., Repelli, C. A., Zebiak, S. E., & Kushnir, Y. (1998). The relationships between tropical Pacific and Atlantic SST and northeast Brazil monthly precipitation. Journal of Climate, 11(4), 551-562.

Wagner, F., Rossi, V., Stahl, C., Bonal, D., & Herault, B. (2012). Water availability is the main climate driver of neotropical tree growth. PloS one, 7(4), e34074.

Williams, M., Malhi, Y., Nobre, A. D., Rastetter, E. B., Grace, J., & Pereira, M. G. P. (1998). Seasonal variation in net carbon exchange and evapotranspiration in a Brazilian rain forest: a modelling analysis. Plant Cell and Environment, 21(10), 953-968.

Williams, M., Rastetter, E. B., Fernandes, D. N., Goulden, M. L., Wofsy, S. C., Shaver, G. R., Melillo, J. M., Munger, J. W., Fan, S. M., & Nadelhoffer, K. J. (1996). Modelling the soil-plant-atmosphere continuum in a Quercus–Acer stand at Harvard Forest: the regulation of stomatal conductance by light, nitrogen and soil/plant hydraulic properties. Plant, Cell & Environment, 19(8), 911-927.

Wong, S. C., Cowan, I. R., & Farquhar, G. D. (1979). Stomatal conductance correlates with photosynthetic capacity. Nature, 282(5737), 424.

Wright, I. J., Reich, P. B., Westoby, M., Ackerly, D. D., Baruch, Z., Bongers, F., Cavender-Bares, J., Chapin, T., Cornelissen, J. H., Diemer, M., Flexas, J., Garnier, E., Groom, P. K., Gulias, J., Hikosaka, K., Lamont, B. B., Lee, T., Lee, W., Lusk, C., Midgley, J. J., Navas, M. L., Niinemets, U., Oleksyn, J., Osada, N., Poorter, H., Poot, P., Prior, L., Pyankov, V. I., Roumet, C., Thomas, S. C., Tjoelker, M. G., Veneklaas, E. J., & Villar, R. (2004). The worldwide leaf economics spectrum. Nature, 428(6985), 821-827.

Xu, L., Samanta, A., Costa, M. H., Ganguly, S., Nemani, R. R., & Myneni, R. B. (2011). Widespread decline in greenness of Amazonian vegetation due to the 2010 drought. Geophysical Research Letters, 38(7).

Yoon, J.-H., & Zeng, N. (2010). An Atlantic influence on Amazon rainfall. Climate Dynamics, 34(2-3), 249-264.

Zeng, N., Yoon, J.-H., Marengo, J. A., Subramaniam, A., Nobre, C. A., Mariotti, A., & Neelin, J. D. (2008). Causes and impacts of the 2005 Amazon drought. Environmental Research Letters, 3(1), 014002.

Zhao, M., & Running, S. W. (2010). Drought-induced reduction in global terrestrial net primary production from 2000 through 2009. Science, 329(5994), 940-943.

2. Methods Overview

We apply the Soil Plant Atmosphere (SPA) model to forests with detailed measurements of carbon fluxes, carbon stocks and leaf traits, across an Amazon precipitation gradient to answer a series of questions around the drivers of photosynthesis, LAI, NPP allocation and trait distributions. Here we describe the site characteristics, field data used, the SPA model, and model development, which formed the basis of experiments presented in Chapters 3-5.

2.1 Site Characteristics

The research presented in this thesis focuses on forest plots across an Amazon mean annual precipitation gradient (MAP; 1400 to 2800 mm yr^{-1}) (Figure 2.1). Data from the Global Ecosystem Monitoring (GEM) network were utilised from eight one-hectare permanent sample plots at four locations across the east and west Amazon (Table 2.1). Differences between plot soil and species composition at each location were deemed sufficient to avoid pseuodoreplication (Malhi *et al*., 2015). Soil physical and chemical properties varied across plots. Notably, western Amazon plots were more fertile but weaker in structure (limited rooting depth, low drainage capacity, low water holding capacity and the presence of hardpans) than their eastern counterparts (Quesada *et al*., 2012). There was little evidence of an anthropogenic impact on forest community structure, excluding the effects of fire at the south eastern plot TAN06.

The two north eastern plots (CAX04 and CAX06) were located in the humid Caxiuanã National Forest in Para State, Brazil. The infertile, slow-growing but high biomass plots are typical of the eastern Amazon. CAX04 (-1.7160 °N, -51.4570 °E) is located on sandy loam, vetic acrisol soil, whereas CAX06 (-1.7369 °N, -51.46194 °E) occupies clay rich, ferralsol soil, causing species composition to differ between plots (Malhi *et al*., 2015; Metcalfe *et al*., 2010). The south western Peruvian plots (TAM05 and TAM06) of the Tambopata Biological Reserve in the Madre de Dios region are subject to a moderate dry season (Malhi *et al*., 2014). The regions geomorphology is a result of it being situated on old floodplains of the Tambopata River (Doughty *et al*., 2015). TAM05 (-12.8309°N, -69.2705°E) is located on a Pleistocene terrace (Doughty *et al*., 2015), whilst the palm rich forest of TAM06 (-12.8385 °N, -69.2960°E) is

located on a Holocene floodplain (Malhi *et al*., 2014). Soils at TAM05 are relatively infertile cambisols compared to the more fertile alisols found at TAM06 (Aragão *et al*., 2009). Bolivian plots (KEN01 and KEN02) located in the Hacienda Kenia in Guarayos Province, Santa Cruz (-16.0158°N, -62.7301°E), experience a strong dry season and occupy the transition zone between humid Amazonian forests and chiquitano dry forests (Araujo-Murakami *et al*., 2014). Both plots are situated on sandy loam, cambisol soils (Malhi *et al*., 2015), though soil depth varies, with KEN01 positioned on deeper soil in a slight topographic depression, whilst KEN02 occupies more shallow soil over Precambrian rock (Doughty *et al*., 2015), leading to a difference in species composition between plots (Araujo-Murakami *et al*., 2014). The south eastern plots (TAN05 and TAN06) of the Fazenda Tanguro, Mato Grosso State (-13.0765°N, -52.3858°E) are subject to an intense dry season. The dry old growth forest plots sit close to the dry forest- savannah transition zone (Malhi *et al*., 2015). Both plots occupy relatively infertile sandy ferralsol soils (Doughty *et al*., 2015). Whilst species composition is relatively similar between plots, there is a difference in fire history, with TAN06 having experienced more frequent burning (Rocha *et al*., 2014). We recognise that the history of disturbance at TAN06 introduces uncertainty into our findings which typically assume ecosystems are in steady state. Caxiuanã and Tambopata plots are more typical Amazon terra-firme or 'core forests', whilst Kenia and Tanguro are 'transitional forests' at the extreme fringes of the biome.

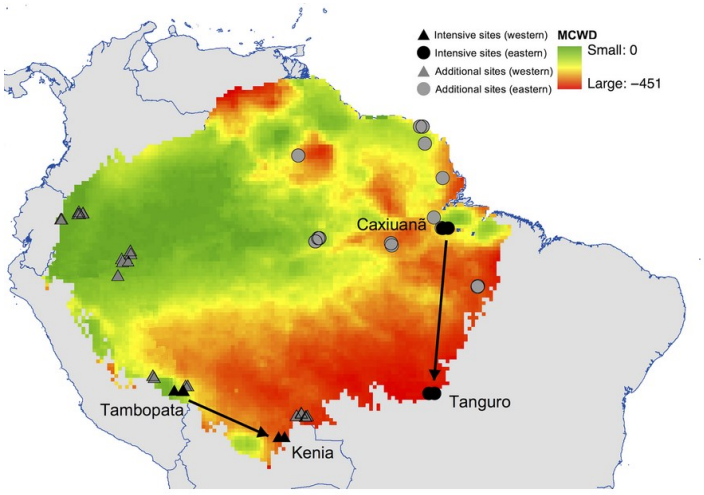

Figure 2.1. From Malhi *et al*. (2015). Location of GEM network permanent sample plots, along eastern and western latitudinal gradients as a function of mean maximum climatological water deficit (MCWD). Two 1ha permanent sample plots situated at each of the four locations, were used in SPA model calibration, validation and experiments.

Table 2.1. Location and climate characteristics of GEM network Amazon permanent sample plots across the precipitation gradient. Meteorological data is from local weather stations, gap filled with ERA interim data for the years 2009-2010 (Dee *et al.*, 2011).

Plot name	Caxiuanã Control	Caxiuanã Tower	Tambopata V	Tambopata VI	Kenia Wet	Kenia Dry	Tanguro Control	Tanguro Burn
RAINFOR site code	CAX04	CAX06	TAM05	TAM06	KEN01	KEN02	---	---
Latitude	-1.716	-1.737	-12.831	-12.839	-16.016	-16.016	-13.077	-13.077
Longitude	-51.457	-51.462	-69.271	-69.296	-62.73	-62.73	52.386	52.386
Elevation (m.a.s.l)	47		223		384		385	
Mean Annual Precipitation (mm yr^{-1})	2810 (± 193)		1800 (± 253)		1710 (±189)		1409 (±90)	
Maximum Climatological Water Deficit (mm)	-85		-265		-342		-452	
Mean annual air temperature (^{0}C)	26.1		24.6		23.4		25.4	

2.2 Field Data

We use field data from the Global Ecosystems Monitoring (GEM) network to calibrate and validate SPA prior to model experiments. The GEM network carried out intensive field campaigns on the focal permanent sample plots, in which data on meteorology, soil properties, carbon stocks, net primary productivity (NPP), respiration, litterfall, leaf area index (LAI), leaf traits and root properties were collected.

Hourly meteorological data was retrieved from local weather stations for the period 2009-2011. Small gaps in air temperature, wind speed, shortwave radiation and vapour pressure deficit estimates (<6 hours), were filled by interpolating between existing data, accounting for diurnal cycles. Where local meteorological data was unavailable for longer period of time, or for gaps in precipitation estimates, hourly-interpolated ERA-Interim data was used to fill (Dee *et al*., 2011). It is noteworthy that the use of ERA-interim data at Caxiuanã yielded precipitation estimates higher than previously reported mean annual values (ERA-interim estimate ~2800 mm yr^{-1}; typically reported as ~2300 mm yr^{-1}) (Fisher *et al*., 2007; Malhi *et al*., 2015). The disparity was largely driven by higher precipitation estimates in 2010. Consistent with ERA interim trends, Lewis *et al*. (2011) similarly report regionally high rainfall anomalies in 2010. However, we continue to recognise uncertainty caused by the use of satellite products.

For each permanent sample plot, soil physical and chemical properties were measured, together with soil carbon and water dynamics. Soil texture (clay, sand and silt content) and depth are reported for plots across the precipitation gradient (Quesada *et al*., 2010; Quesada *et al*., 2012). Soil carbon stocks were also assessed, and estimates of soil moisture (typically between 5-30cm depth) were collected on a monthly timescale throughout the study period (Malhi *et al*., 2015).

Aboveground wood carbon stocks were estimated using forest inventory data and an allometric relationship between tree height and diameter (Chave and Sabatier, 2005; Malhi *et al*., 2015). Coarse root carbon stocks were estimated using a root:shoot ratio of 0.21 ± 0.3, reflecting values reported by Jackson *et al*. (1996). Fine root carbon stock estimates for each forest plot were either published values (Aragão *et al*., 2009; Araujo-Murakami *et al*., 2014; Fisher *et al*., 2007), or communicated directly from the GEM network, and were estimated using ingrowth cores. The only location without fine root carbon stock estimates was Tanguro,

which was assumed equal to the mean of KEN01 and KEN02, Kenia being closest in forest structure and precipitation regime.

LAI was estimated for each plot on a monthly timescale using hemispherical photographs. The resultant images were analysed using CAN-EYE software. Together with estimates of community weighted mean leaf mass per area (LMA), we were able to estimate foliar carbon stocks from LAI measurements. Monthly litter was estimated using litterfall traps ($0.25m^2$) placed 1m above the forest floor at the centre of each permanent sample plot. The contents of the traps were then sorted between leaf, fruit, flower and wood, before weighing.

Leaf NPP was estimated using monthly leaf litterfall and the change in LAI, accounting for differences in LMA. Monthly aboveground wood NPP was estimated using incremental growth measurements from forest inventory data, together with the allometric relationship used in total wood carbon stock estimates (Chave and Sabatier, 2005; Malhi *et al*., 2015). Fine root NPP was also estimated on a monthly timescale, using root ingrowth cores and rhizotron screens.

Leaf respiration rate was estimated using an IRGA and specialised cuvette for around 20 trees. For each tree a sunlit and shaded branch were randomly selected. Branches were then re-cut under water to restore hydraulic connectivity. For each plot, a measurement of leaf respiration rate was made during the wet season and the dry season. Leaf respiration was then scaled to the canopy level using LAI estimates and the season-specific rate. Wood respiration rate was measured using an IRGA and stem collar at 1.3m height, for around 25 trees distributed evenly throughout the plot. Measurements were taken every 1-2 months and wood respiration rate was scaled to the plot level using wood surface area estimates. Belowground respiration measurements were taken from the corner of plots each month, using a closed dynamic chamber with the IRGA and soil respiration chamber sealed to a permanent collar in the soil (Doughty *et al*., 2015; Malhi *et al*., 2015). Fluxes were separated into rhizosphere respiration and heterotrophic soil respiration measurements using collars with differing permeability.

Community weighted mean leaf nitrogen content and LMA were estimated for Caxiuanã and Tambopata plots as detailed in (Fyllas *et al*., 2009). Leaf nitrogen content for Kenia and Tanguro plots were estimated using data from the TRY trait database, weighted by plot species composition (Kattge, *et al*., 2011). Species-specific estimates from Poorter & Bongers (2006) were used to derive KEN01 and KEN02 LMA, as local data was unavailable. Field estimates of

LMA were used for TAN05 and TAN06 (P.Brando pcom). Photosynthetic capacity (κ_c, V_{cmax} normalised by leaf N, and κ_j, J_{max} normalised by leaf N) estimates were derived from field measurements (Caxiuanã), or from leaf nitrogen content, using equations presented in Walker *et al*. (2014).

Estimates of root depth and distribution for each plot were derived from published values or estimated given the depth of soil hardpan layers (Araujo-Murakami *et al*., 2014; Fisher *et al*., 2007; Malhi *et al*., 2014; Quesada *et al*., 2011; Quesada *et al*., 2010; Quesada *et al*., 2012; Sotta *et al*., 2007). Where rooting depth estimates were absent (Tanguro), we assumed no obstruction to root growth above 10m (Rocha *et al*., 2014).

2.3 The Soil Plant Atmosphere model (SPA)

The Soil-Plant-Atmosphere model (SPA) is a hydrodynamic terrestrial ecosystem model, which has been calibrated and evaluated for moist tropical forests in Manaus and Caxiuanã (Fisher *et al*., 2007; Williams *et al*., 1998; Williams *et al*., 1996). In SPA, carbon and water fluxes are estimated through process-based modelling of radiative transfer, boundary layer and stomatal conductance, plant and leaf ecophysiology and soil-plant energy and water balance (Bonan *et al*., 2014). Plant physiological responses to precipitation are well represented in SPA due to the stomatal conductance algorithm being coupled directly to plant water use (Fisher *et al*., 2006).

Canopy layers in SPA are partitioned between sunlit and shaded fractions. A radiative transfer scheme determines the transmittance, reflectance and absorption of long wave, near infra-red and direct and diffuse photosynthetically active radiation (PAR) for each canopy layer (determined by Beer-Lambert's Law) and the soil surface. Boundary layer characteristics of leaves within the canopy are estimated at different heights using an exponential wind relationship (Cionco, 1985). At the leaf level, the Farquhar model is used to determine photosynthesis (Farquhar and Von Caemmerer, 1982), whilst the Penman-Monteith equation is used to estimate transpiration.

SPA employs a novel stomatal conductance model, which links leaf gas exchange, plant hydraulics and the soil-plant-atmosphere continuum. The representation of stomatal conductance within SPA optimises leaf carbon gain per unit nitrogen and limits stomatal

opening to prevent leaf water potential dropping below a critical value. The difference between soil water potential and minimum sustainable leaf water potential, together with the hydraulic resistance of the soil-to-leaf pathway determine maximum hydraulic supply. Simulated stomatal conductance minimises the risk of cavitation, whilst balancing evaporative losses with the maximum flux rate of water, thereby combining water use efficiency and hydraulic safety.

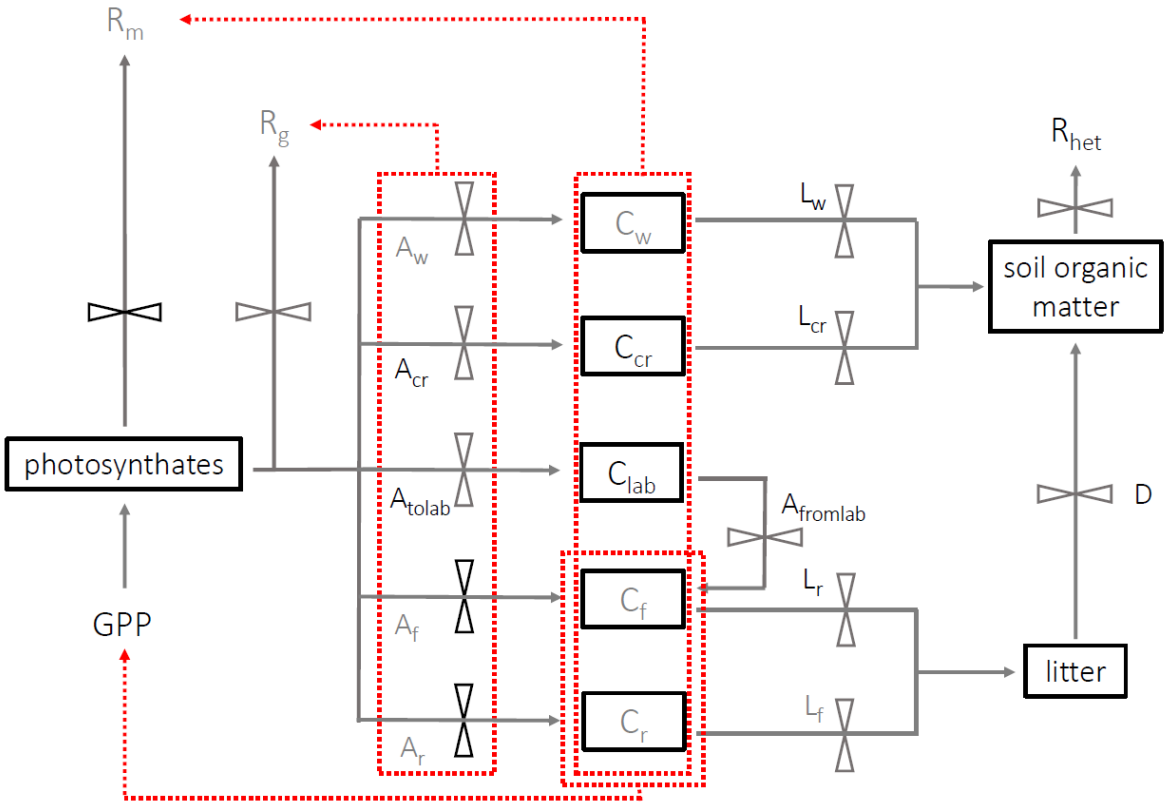

Figure 2.2. A schematic of DALEC2, the carbon allocation sub-model integrated within the soil-plant-atmosphere model. Carbon moves between pools (boxes) via fluxes (solid arrows). An effect of carbon pools or fluxes on plant processes is shown by a red dashed arrow, whereby red dashed boxes indicate a collective impact of the contained carbon pools or fluxes. Grey text indicates that biometric data contributed to calibration of the carbon pool or flux. Black flux bars indicate that the carbon pathway is prioritised within the model above pathways from the same nodule. Carbon pools (C), allocation (A) and litterfall (L) are separated by component: w = wood, cr = coarse roots, r = fine roots, f = foliage, lab = labile (or non-structural carbon), with to and from used for labile carbon

Energy and water balances are simulated for 10 soil layers of varying thickness accounting for differences in organic matter content, mineral fraction and water content. Incoming radiation at the soil surface is used to solve the surface energy balance, estimating sensible, latent and

ground heat fluxes, together with soil surface temperature. Ground heat flux estimates are then used to simulate energy transfer through the soil profile. Water inputs to the soil via precipitation are calculated using local meteorology, taking into account canopy interception, evaporation from the canopy, and drainage. Soil water retention curves then relate soil texture to water transfer for each layer (Saxton *et al.*, 1986).

Within SPA, carbon allocation between structural tissue and the non-structural carbon (NSC; or labile C) pool is executed via the sub model DALEC2 (Bloom and Williams, 2015) (Figure 2.2). Using carbon inputs from photosynthesis (GPP), DALEC2 allocates carbon first to an independently calculated autotrophic respiration term, then to NPP (growth of leaf, stems and roots) and the NSC pool. The fraction of NPP allocated to leaves, stems, roots and the NSC pool together with the turnover rate of leaves, stems and roots are determined by model input parameters which are fixed throughout each simulation. Carbon from the NSC pool is transferred to leaves when leaf growth demand exceeds total NPP. Under the assumption that allocation to NSC is an active process and that the pool serves functions additional to the seasonal redistribution of carbon (Dietze *et al.*, 2014), depletions in the NSC pool induce redirection of a fraction of NPP towards NSC storage to maintain a stable NSC pool.

2.4 Model Development

Within SPA autotrophic respiration was estimated as a fixed fraction of GPP. To improve the functionality of SPA in the context of the posed experiments, an independent respiration term was calculated. Maintenance respiration was calculated as a function of plant traits and plant biomass, whilst growth respiration was calculated as fixed fraction of NPP (0.28) (Waring and Schlesinger, 1985). Leaf maintenance respiration was estimated using leaf nitrogen content as detailed in Reich *et al*. (2008), adjusted for temperature. Leaf respiration is calculated as follows:

$$b = 1.025 - 0.036\,WQ$$

$$Rr_{leaf} = 10^{\,b}\, N_{leaf}^{\,1.411}$$

$$Rt_{leaf} = 2.0^{\,0.1\,(T-20)}\, Rr_{leaf}$$

$$Rs_{leaf} = M_{leaf} * Rt_{leaf}$$

Where

WQ is the temperature during the warmest quarter (^{o}C)

b is a nitrogen scalar to account for differences in WQ

N_{leaf} is the nitrogen content of the leaf (mmol g^{-1})

Rr_{leaf} is the leaf respiration rate (nmol g biomass^{-1} s^{-1})

T is temperature (^{o}C)

Rt_{leaf} is the temperature adjusted respiration rate (nmol g biomass^{-1} s^{-1})

M_{leaf} is the leaf biomass (gC m^{-2})

Rs_{leaf} is the total leaf respiration (nmol m^{-2} s^{-1})

Wood and fine root maintenance respiration were estimated using empirical models derived from GEM respiration estimates. The model used a plot specific respiration coefficient as a function of component carbon stock.

2.5 References

Aragao, L. E. O. C., Malhi, Y., Metcalfe, D. B., Silva-Espejo, J. E., Jimenez, E., Navarrete, D., Almeida, S., Costa, A. C. L., Salinas, N., Phillips, O. L., Anderson, L. O., Alvarez, E., Baker, T. R., Goncalvez, P. H., Huaman-Ovalle, J., Mamani-Solorzano, M., Meir, P., Monteagudo, A., Patino, S., Penuela, M. C., Prieto, A., Quesada, C. A., Rozas-Davila, A., Rudas, A., Silva, J. A., & Vasquez, R. (2009). Above- and below-ground net primary productivity across ten Amazonian forests on contrasting soils. Biogeosciences, 6(12), 2759-2778.

Araujo-Murakami, A., Doughty, C. E., Metcalfe, D. B., Silva-Espejo, J. E., Arroyo, L., Heredia, J. P., Flores, M., Sibler, R., Mendizabal, L. M., Pardo-Toledo, E., Vega, M., Moreno, L., Rojas-Landivar, V. D., Halladay, K., Girardin, C. A. J., Killeen, T. J., & Malhi, Y. (2014). The productivity, allocation and cycling of carbon in forests at the dry margin of the Amazon forest in Bolivia. Plant Ecology & Diversity, 7(1-2), 55-69.

Bloom, A. A., & Williams, M. (2015). Constraining ecosystem carbon dynamics in a data-limited world: integrating ecological "common sense" in a model-data fusion framework. Biogeosciences, 12(5), 1299-1315.

Bonan, G. B., Williams, M., Fisher, R. A., & Oleson, K. W. (2014). Modeling stomatal conductance in the earth system: linking leaf water-use efficiency and water transport along the soil–plant–atmosphere continuum. Geoscientific Model Development, 7(5), 2193-2222.

Chave, J., & Sabatier, U. P. (2005). Measuring tree height for tropical forest trees. PAN-AMAZONIA Field Manual.

Cionco, R. M. (1985). Modeling windfields and surface layer wind profiles over complex terrain and within vegetative canopies The forest-atmosphere interaction (pp. 501-520): Springer.

Dee, D. P., Uppala, S. M., Simmons, A. J., Berrisford, P., Poli, P., Kobayashi, S., Andrae, U., Balmaseda, M. A., Balsamo, G., & Bauer, P. (2011). The ERA-Interim reanalysis: Configuration and performance of the data assimilation system. Quarterly Journal of the royal meteorological society, 137(656), 553-597.

Dietze, M. C., Sala, A., Carbone, M. S., Czimczik, C. I., Mantooth, J. A., Richardson, A. D., & Vargas, R. (2014). Nonstructural carbon in woody plants. Annu Rev Plant Biol, 65, 667-687.

Doughty, C. E., Metcalfe, D. B., Girardin, C. A. J., Amezquita, F. F., Durand, L., Huasco, W. H., Silva-Espejo, J. E., Araujo-Murakami, A., da Costa, M. C., da Costa, A. C. L., Rocha, W., Meir, P., Galbraith, D., & Malhi, Y. (2015). Source and sink carbon dynamics and carbon allocation in the Amazon basin. Global Biogeochemical Cycles, 29(5), 645-655.

Farquhar, G. D., & Von Caemmerer, S. (1982). Modelling of photosynthetic response to environmental conditions Physiological plant ecology II (pp. 549-587): Springer.

Fisher, R. A., Williams, M., Da Costa, A. L., Malhi, Y., Da Costa, R. F., Almeida, S., & Meir, P. (2007). The response of an Eastern Amazonian rain forest to drought stress: results and modelling analyses from a throughfall exclusion experiment. Global Change Biology, 13(11), 2361-2378.

Fisher, R. A., Williams, M., Do Vale, R. L., Da Costa, A. L., & Meir, P. (2006). Evidence from Amazonian forests is consistent with isohydric control of leaf water potential. Plant Cell and Environment, 29(2), 151-165.

Fyllas, N. M., Patino, S., Baker, T. R., Nardoto, G. B., Martinelli, L. A., Quesada, C. A., Paiva, R., Schwarz, M., Horna, V., Mercado, L. M., Santos, A., Arroyo, L., Jimenez, E. M., Luizao, F. J., Neill, D. A., Silva, N., Prieto, A., Rudas, A., Silviera, M., Vieira, I. C. G., Lopez-Gonzalez, G., Malhi, Y., Phillips, O. L., & Lloyd, J. (2009). Basin-wide variations in foliar properties of Amazonian forest: phylogeny, soils and climate. Biogeosciences, 6(11), 2677-2708.

Jackson, R. B., Canadell, J., Ehleringer, J. R., Mooney, H. A., Sala, O. E., & Schulze, E. D. (1996). A global analysis of root distributions for terrestrial biomes. Oecologia, 108(3), 389-411.

Kattge, J., Knorr, W., Raddatz, T., & Wirth, C. (2009). Quantifying photosynthetic capacity and its relationship to leaf nitrogen content for global-scale terrestrial biosphere models. Global Change Biology, 15(4), 976-991.

Lewis, S. L., Brando, P. M., Phillips, O. L., van der Heijden, G. M. F., & Nepstad, D. (2011). The 2010 amazon drought. Science, 331(6017), 554-554.

Malhi, Y., Amezquita, F. F., Doughty, C. E., Silva-Espejo, J. E., Girardin, C. A. J., Metcalfe, D. B., Aragao, L. E. O. C., Huaraca-Quispe, L. P., Alzamora-Taype, I., Eguiluz-Mora, L., Marthews, T. R., Halladay, K., Quesada, C. A., Robertson, A. L., Fisher, J. B., Zaragoza-Castells, J., Rojas-Villagra, C. M., Pelaez-Tapia, Y., Salinas, N., Meir, P., & Phillips, O. L. (2014). The productivity,

metabolism and carbon cycle of two lowland tropical forest plots in south-western Amazonia, Peru. Plant Ecology & Diversity, 7(1-2), 85-105.

Malhi, Y., Doughty, C. E., Goldsmith, G. R., Metcalfe, D. B., Girardin, C. A. J., Marthews, T. R., del Aguila-Pasquel, J., Aragao, L. E. O. C., Araujo-Murakami, A., Brando, P., da Costa, A. C. L., Silva-Espejo, J. E., Amezquita, F. F., Galbraith, D. R., Quesada, C. A., Rocha, W., Salinas-Revilla, N., Silverio, D., Meir, P., & Phillips, O. L. (2015). The linkages between photosynthesis, productivity, growth and biomass in lowland Amazonian forests. Global Change Biology, 21(6), 2283-2295.

Metcalfe, D. B., Meir, P., Aragão, L. E. O. C., Lobo-do-Vale, R., Galbraith, D., Fisher, R. A., Chaves, M. M., Maroco, J. P., da Costa, A. C. L., & de Almeida, S. S. (2010). Shifts in plant respiration and carbon use efficiency at a large-scale drought experiment in the eastern Amazon. New Phytologist, 187(3), 608-621.

Poorter, L., & Bongers, F. (2006). Leaf traits are good predictors of plant performance across 53 rain forest species. Ecology, 87(7), 1733-1743.

Quesada, C. A., Lloyd, J., Anderson, L. O., Fyllas, N. M., Schwarz, M., & Czimczik, C. I. (2011). Soils of Amazonia with particular reference to the RAINFOR sites. Biogeosciences, 8(6), 1415-1440.

Quesada, C. A., Lloyd, J., Schwarz, M., Patino, S., Baker, T. R., Czimczik, C., Fyllas, N. M., Martinelli, L., Nardoto, G. B., Schmerler, J., Santos, A. J. B., Hodnett, M. G., Herrera, R., Luizao, F. J., Arneth, A., Lloyd, G., Dezzeo, N., Hilke, I., Kuhlmann, I., Raessler, M., Brand, W. A., Geilmann, H., Moraes, J. O., Carvalho, F. P., Araujo, R. N., Chaves, J. E., Cruz, O. F., Pimentel, T. P., & Paiva, R. (2010). Variations in chemical and physical properties of Amazon forest soils in relation to their genesis. Biogeosciences, 7(5), 1515-1541.

Quesada, C. A., Phillips, O. L., Schwarz, M., Czimczik, C. I., Baker, T. R., Patino, S., Fyllas, N. M., Hodnett, M. G., Herrera, R., Almeida, S., Davila, E. A., Arneth, A., Arroyo, L., Chao, K. J., Dezzeo, N., Erwin, T., di Fiore, A., Higuchi, N., Coronado, E. H., Jimenez, E. M., Killeen, T., Lezama, A. T., Lloyd, G., Lopez-Gonzalez, G., Luizao, F. J., Malhi, Y., Monteagudo, A., Neill, D. A., Vargas, P. N., Paiva, R., Peacock, J., Penuela, M. C., Cruz, A. P., Pitman, N., Priante, N., Prieto, A., Ramirez, H., Rudas, A., Salomao, R., Santos, A. J. B., Schmerler, J., Silva, N., Silveira, M., Vasquez, R., Vieira, I., Terborgh, J., & Lloyd, J. (2012). Basin-wide variations in Amazon

forest structure and function are mediated by both soils and climate. Biogeosciences, 9(6), 2203-2246.

Reich, P. B., Tjoelker, M. G., Pregitzer, K. S., Wright, I. J., Oleksyn, J., & Machado, J. L. (2008). Scaling of respiration to nitrogen in leaves, stems and roots of higher land plants. Ecol Lett, 11(8), 793-801.

Rocha, W., Metcalfe, D. B., Doughty, C. E., Brando, P., Silverio, D., Halladay, K., Nepstad, D. C., Balch, J. K., & Malhi, Y. (2014). Ecosystem productivity and carbon cycling in intact and annually burnt forest at the dry southern limit of the Amazon rainforest (Mato Grosso, Brazil). Plant Ecology & Diversity, 7(1-2), 25-40.

Saxton, K. E., Rawls, W. J., Romberger, J. S., & Papendick, R. I. (1986). Estimating generalized soil-water characteristics from texture 1. Soil Science Society of America Journal, 50(4), 1031-1036.

Sotta, E. D., Veldkamp, E., Schwendenmann, L., Guimaraes, B. R., Paixao, R. K., Ruivo, M. D. L. P., da Costa, L., Carlos, A., & Meir, P. (2007). Effects of an induced drought on soil carbon dioxide (CO2) efflux and soil CO2 production in an Eastern Amazonian rainforest, Brazil. Global Change Biology, 13(10), 2218-2229.

Walker, A. P., Beckerman, A. P., Gu, L., Kattge, J., Cernusak, L. A., Domingues, T. F., Scales, J. C., Wohlfahrt, G., Wullschleger, S. D., & Woodward, F. I. (2014). The relationship of leaf photosynthetic traits–Vcmax and Jmax–to leaf nitrogen, leaf phosphorus, and specific leaf area: a meta-analysis and modeling study. Ecology and evolution, 4(16), 3218-3235.

Waring, R. H., & Schlesinger, W. H. (1985). Forest ecosystems. Concepts and management: Academic Press.

Williams, M., Malhi, Y., Nobre, A. D., Rastetter, E. B., Grace, J., & Pereira, M. G. P. (1998). Seasonal variation in net carbon exchange and evapotranspiration in a Brazilian rain forest: a modelling analysis. Plant Cell and Environment, 21(10), 953-968.

Williams, M., Rastetter, E. B., Fernandes, D. N., Goulden, M. L., Wofsy, S. C., Shaver, G. R., Melillo, J. M., Munger, J. W., Fan, S. M., & Nadelhoffer, K. J. (1996). Modelling the soil-plant-atmosphere continuum in a Quercus–Acer stand at Harvard Forest: the regulation of stomatal conductance by light, nitrogen and soil/plant hydraulic properties. Plant, Cell & Environment, 19(8), 911-927.

3. Leaf area index drives the interaction between canopy photosynthesis and precipitation across Amazon forests

3.1 Abstract

The Amazon rainforest is an integral part of the terrestrial carbon cycle, but its capacity to sequester C is deemed vulnerable to increased moisture stress as a result of anthropogenic climate change. Whilst the direct physiological (stomatal) response of plants to water availability has been of much recent interest, indirect constraints to photosynthesis through structural and trait responses (via LAI, rooting properties and leaf traits) have received less attention. We used the Soil Plant Atmosphere model to investigate the role of direct and indirect responses to water availability in driving photosynthesis across Amazon forests. We calibrated and evaluated the model's representation of carbon cycling at plots along a precipitation gradient with detailed time series data. We used the model to; (i) apportion spatial variation in photosynthesis to physiological, structural and trait responses to precipitation, (ii) compare the sensitivity of photosynthesis to variations in climate, LAI, rooting depth and leaf traits and (iii) quantify the importance of phenology against climate in driving sub-annual photosynthesis. Model analyses showed that LAI (ranging from 2.2 - 5.2 m^2m^{-2} across plots) was the principal driver of differences in photosynthesis across the precipitation gradient, accounting for 36% of observed variation. Differences in photosynthetic capacity accounted for 20% of variance and physiology-climate interactions accounted for a further 12%. Photosynthesis was most sensitive to LAI and leaf traits for forests with high rainfall. Shallow rooting depth coupled with high LAI resulted in a heightened sensitivity of forest photosynthesis to differences in climate. Likewise, high LAI relative to precipitation caused increased sensitivity to rooting depth. On monthly timescales, the importance of solar radiation in driving photosynthesis increased with mean annual

precipitation (R^2 = 0.64, p=0.017), whilst the importance of VPD and LAI decreased (R^2= 0.32, p=0.14; R^2=0.56, p=0.033). Given the role of LAI in driving photosynthesis across the Amazon precipitation gradient, improved mapping of canopy dynamics is critical, opportunities for which are offered by new satellite-based remote sensing missions such as GEDI, Sentinel and FLEX.

3.2 Introduction

Photosynthesis is the entry point for carbon into the terrestrial biosphere, playing a central role in the global carbon cycle. Tropical rainforests alone account for one third of total terrestrial photosynthesis and assimilate 40.8 Pg of carbon each year (Beer et al., 2010). Carbon fluxes across the tropics are tightly coupled to climate, and precipitation is a principal driver of spatial and temporal variation in photosynthesis (Beer et al., 2010b; Fisher et al., 2007; Guan et al., 2015; Malhi et al., 2015; Von Randow et al., 2013). Across Amazon forests, there exists a positive linear relationship between photosynthesis, or gross primary productivity (GPP), and mean annual precipitation (Malhi *et al*., 2015). Shifts in precipitation patterns as a result of anthropogenic climate change are predicted to have a major impact on Amazon photosynthesis (Malhi *et al*., 2008; Meir and Woodward, 2010; Phillips *et al*., 2009; Zhang *et al*., 2015). Given the global importance of Amazon forests, understanding the mechanisms through which forests respond to water availability is critical to predicting carbon cycling under current and future climates.

Ecosystem models and DGVMs disagree on the effects of projected precipitation change on Amazon carbon dynamics. Galbraith *et al*. (2010) found that for two of the three models tested, future shifts in precipitation patterns had surprisingly little effect on model estimates of biomass change, reflecting poorly the observed sensitivity of Amazon forests to water availability illustrated by through-fall exclusion experiments and natural drought events (Nepstad *et al*., 2007; Phillips *et al*., 2009; Rowland *et al*., 2015a). Whilst able to accurately simulate physiological (stomatal) responses to water availability (Fisher *et al*., 2007), models fail to represent forest structure and trait responses (leaf area index LAI, stem demography, rooting properties and leaf traits). Model-data comparison studies have identified the poor representation of phenological responses to water availability as a likely cause of the disparity between field observations and model predictions (Powell *et al*., 2013; Restrepo-Coupe *et al*.,

2017). Changes in rooting depth and root traits are unaccounted for, but could influence modelled carbon assimilation via water uptake *(*Metcalfe *et al*., 2008). Changes in leaf trait composition in response to water availability are similarly absent from most modelling approaches, despite having a major impact on simulated photosynthesis (Fauset *et al*., 2012; Sakschewski *et al*., 2016). In order to improve model predictions, a better understanding of structural and trait responses underlying the precipitation-photosynthesis interaction is needed (Meir *et al*., 2015b).

Precipitation is linked to photosynthesis directly via stomatal conductance, and indirectly via induced changes in forest structure and or leaf traits (see Chapter 1, Figure 1.1). Stomatal conductance is constrained by water availability and atmospheric demand, with the resultant changes in CO_2 supply coupling photosynthesis with precipitation. However, under the assumption that plants operate in accordance with their hydraulic environment (Katul *et al*., 2003; Tyree and Sperry, 1988), stomatal conductance is more likely a short, rather than long-term response to water availability (Sperry *et al*., 2002). Structural and trait responses to climate forcings are expected to be more longstanding (Meir *et al*., 2015a). Deep roots support hydraulic conductance during dry periods, and together with root surface area, and root biomass, may play an important role in alleviating water constraints to photosynthesis (Metcalfe *et al*., 2008; Nepstad *et al*., 1994). Extensive evidence links spatial and temporal variation in precipitation with LAI (Barbosa and Asner, 2017; Brando *et al*., 2008; Grier and Running, 1977; Hilker *et al*., 2014; Iio *et al*., 2014; Meir *et al*., 2015b; Schleppi *et al*., 2011; Wright *et al*., 2013; Zhou *et al*., 2014). LAI determines the surface area for photosynthesis. To support higher LAI, the carbon gain, constrained by stomatal conductance, must outweigh the cost of leaf growth and maintenance (Caldararu *et al*., 2012). The co-variation of leaf traits with precipitation (Santiago *et al*., 2004; Wright *et al*., 2004) could also prove important in shaping the response of photosynthesis to water availability. Leaf traits effect photosynthesis directly via photosynthetic capacity, and indirectly through their influence on canopy carbon economics, via leaf growth and maintenance costs. Yet, the role of forest structure and trait responses in determining photosynthesis remain largely unexplored in data-constrained analysis.

Spatial variation in photosynthesis across the Amazon basin has previously been associated with a variety of factors. Mercado *et al*. (2011) suggested links between leaf traits and soil nutrient status, though other drivers such as changes in leaf area were not quantified. Whilst

current evidence supports climate as a key determinate (Beer et al., 2010b; Malhi et al., 2015), analyses do not separate the role of direct and indirect responses. Furthermore, how the relative importance of drivers differ across forests remains unclear. Inter-annual variation in photosynthesis has been linked to canopy photosynthetic light-use efficiency (associated with phenology) (Wu *et al.*, 2017). Similarly, on a sub-annual timescale a number of studies point towards phenology and photosynthetic capacity as the dominant controls over photosynthesis (Goulden *et al.*, 2004; Hutyra *et al.*, 2007; Restrepo-Coupe *et al.*, 2013; Wagner *et al.*, 2017; Wu *et al.*, 2017). Yet, the evidence is not universal and Rowland *et al.* (2014) report that for an eastern amazon forest, LAI was relatively invariant, and solar radiation was the principal driver of photosynthetic seasonality. In order to inform model predictions and reduce uncertainty, we undertake an in-depth assessment of the relative effects physiological, structural and trait responses to water availability have on photosynthesis across monthly to annual timescales.

We apply an ecosystem model to plots across the Amazon, spanning a precipitation gradient. Process modelling allows the links between climate, forest structure (LAI, root depth and biomass) and leaf traits to be quantified explicitly, and separated, across time scales. The soil plant atmosphere model (SPA) (Fisher *et al.*, 2007; Fisher *et al.*, 2006; Rowland *et al.*, 2015b; Williams *et al.*, 1998; Williams *et al.*, 1996) is well suited to this investigation given its proven ability in accurately simulating carbon and water fluxes in Amazon tropical forests. We link the modelling to data gathered over multiple years on permanent sample plots from the Global Ecosystems Monitoring (GEM) network (Doughty *et al.*, 2015; Malhi *et al.*, 2015). The plots have detailed measurements of carbon fluxes, carbon stocks and leaf traits, which were available to constrain the model. We compare the covariation of observed leaf traits (LMA, photosynthetic capacity and leaf N content) and those derived from model calibrations (leaf lifespan) along the precipitation gradient. We use SPA to address the following questions:

1. Is spatial variation in photosynthesis across the precipitation gradient driven by physiological responses to water availability (via the effect of climate and soils on hydraulic transport and stomatal conductance) or structural and trait responses (via shifts in LAI, rooting properties and leaf traits)?

2. Does the sensitivity of photosynthesis to differences in climate, LAI, leaf traits (photosynthetic capacity) and rooting depth vary across the precipitation gradient?

3. What drives sub-annual variation in photosynthesis across Amazon forests?

We hypothesise that structural and trait responses to water availability are more important than physiological responses in explaining spatial variation in photosynthesis across the precipitation gradient. We further posit that LAI is the principal driver of differences in photosynthesis between Amazon forests, effected through the observed increase in leaf area with mean annual precipitation (MAP).

Within the bounds of observations across the precipitation gradient, we predict that core forests (which experience higher MAP) will be most sensitive to differences in LAI, leaf traits (photosynthetic capacity) and climate, whilst transitional forests (which experience lower MAP) will be more sensitive to differences in root properties. Water constraints to photosynthesis are expected to underpin the response to differences in LAI and photosynthetic capacity. We predict the covariation of precipitation and LAI will drive the response to differences in climate, as LAI determines evaporative demand. The importance of water retention and acquisition to support photosynthetic processes is dependent on precipitation. Consequently, the response to differences in rooting properties is similarly expected to be driven by water availability.

We hypothesise that on monthly timescales, the role of phenology in driving photosynthesis will be less than that across spatial scales, whilst climate will be more important. Across the precipitation gradient, we expect that solar radiation will be relatively more important during the wet season, whilst VPD will be more important during the dry season, reflecting seasonal shifts in light and water availability. Due to differences in dry season length, we predict that for core forests solar radiation will be most important in driving sub-annual variation in photosynthesis, whilst for transitional forests VPD will be the dominant driver.

In light of projected changes in rainfall patterns across the Amazon basin, accurately capturing the nature of the precipitation-photosynthesis interaction is critical to predicting future carbon dynamics. The aim of this research is to reduce current uncertainty around climate-vegetation feedbacks, by better understanding the relative importance of physiological, structural and trait responses to water availability. Our findings offer new and important

insights, by explicitly quantifying the direct and indirect effects of climate on ecosystem functioning, which has not previously been estimated across large tropical spatial gradients.

3.3 Methods

We calibrated and validated the ecosystem model SPA to permanent sample plots across an Amazon mean annual precipitation gradient (located at Caxiuanã, Tambopata, Kenia and Tanguro). We calibrated the simulations for each plot to track the observed time series of LAI, leaf litterfall and soil moisture; and tested the resulting simulations of the C cycle against plot measurements of photosynthesis, respiration and NPP. We then undertook a series of model experiments to: (i) apportion spatial variation in photosynthesis to drivers (climate, soils, LAI, leaf traits, and root properties), (ii) investigate how the sensitivity of photosynthesis to differences in drivers varies across the precipitation gradient, and (iii) quantify the importance of LAI, VPD, solar radiation, precipitation and air temperature in driving sub-annual variation in photosynthesis using the random forest technique. Plot characteristics, the SPA model, and data used in model calibration and validation are detailed in Chapter 2.

3.3.1 Model Calibration and Validation

Following data collation to parameterise SPA, the model was calibrated and validated for each plot prior to conducting model experiments. Measurements used to parameterise SPA include: soil texture, soil C stock, leaf N content, LMA, photosynthetic capacity, the fraction of NPP allocated to fine roots and wood, root depth, and foliar, wood and fine root C stocks (Table 3.1 and 3.2). Soil, wood and fine root C stocks (single point measurements, not time series) were initial model inputs and allowed to vary thereafter dependent on simulated C dynamics. Wood and root respiration measurements were used together with component C stocks to estimate plot specific wood and root respiration coefficients.

The model was driven using hourly meteorological data, retrieved from local weather stations. Short gaps in air temperature, wind speed, shortwave radiation and vapour pressure deficit measurements (<6 hours), were filled by spline interpolation between existing data. Where local meteorological data was unavailable for a longer period of time, or for gaps in precipitation measurements, hourly spline-interpolated ERA-Interim data was used (Dee *et al.*, 2011). The interpolation of solar radiation estimates accounted for the solar zenith angle.

The simulation of soil water drainage in SPA was calibrated against time series of field measurements of soil moisture. Initial investigations comparing modelled soil moisture to monthly field data highlighted an overestimation by SPA. The empirical model used in SPA to relate soil texture to water retention (Saxton *et al*., 1986, eqn. 10) was then calibrated by adjusting the slope of the interaction to better represent soil moisture across tropical soils (to within standard error estimates of mean annual soil moisture).

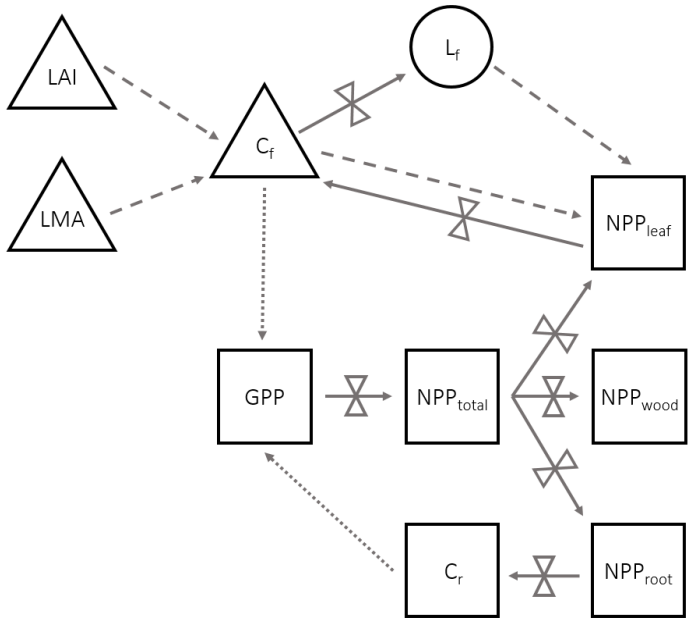

Figure 3.1. A schematic of model-data constraints in the version of SPA used in the presented calibration, validation and experiments. Squares identify SPA simulated fluxes and carbon pools, circles denote SPA fluxes calibrated against field estimates, whilst triangles represent field-derived estimates used to constrain SPA simulations. Solid lines denote a carbon flux, dotted lines identify the effect of a carbon pool on a SPA process based carbon flux estimate, and dashed lines represent field estimate constraints to a SPA carbon pool or flux. SPA fluxes, carbon stocks and parameters are denoted as follows; GPP = gross primary productivity, NPP_{total}= total net primary productivity, NPP_{leaf} = foliar net primary productivity, NPP_{wood} = wood net primary productivity, NPP_{root} = root net primary productivity, LAI = leaf area index, LMA = leaf mass per unit area, C_f = foliar carbon stock, L_f = leaf litterfall

Leaf litterfall parameters (day of peak leaf fall, leaf fall period and leaf lifespan) were calibrated against field data to accurately simulate litterfall period and amplitude (within standard error estimates of annual litterfall). Wood and fine root biomass turnover rates were estimated assuming each forest ecosystem was at steady state given the maturity of stands and their disturbance history:

$$turnover\ rate \propto \frac{NPP}{C\ stock}$$

Where turnover rate, NPP and C stock are specific to wood or roots.

Local LAI estimates derived from hemispherical photographs were used to constrain simulated LAI. Leaf NPP was calculated as the difference between the foliar C stock of the previous timestep and that which would equate to field measured LAI. Leaf NPP was allocated prior to other plant components, and if the leaf NPP requirement exceeded total NPP for the given timestep, the non-structural C pool was drawn upon (where total NPP was calculated as the difference between simulated GPP and autotrophic respiration; Figure 3.1). Under the assumption that allocation to NSC is an active process and that the pool serves functions additional to the seasonal redistribution of C (Dietze *et al*., 2014), depletions in the NSC pool induce redirection of a fraction of NPP towards NSC storage to maintain a stable NSC pool. Root and wood NPP was calculated as a fraction of total NPP minus leaf NPP.

For each plot, SPA calibrations were constrained by the upper and lower sample error of LAI measurements to produce an estimate of model uncertainty. However, we recognise that the error associated with model estimates was underestimated. Observation constrained SPA simulations were then validated against biometric field measurements of C fluxes (i.e. from infra-red gas analysers, dendrometers, root ingrowth cores litterfall traps etc.). Linear regression models were constructed to compare modelled estimates and field measurements of GPP, autotrophic respiration and total NPP. A comprehensive comparison of model estimates and field measurements of component NPP and respiration was also made. Validation of the SPA model against biometric data lent confidence to subsequent analyses, where the model was used to explore C fluxes under non-observed conditions.

Table 3.1. Summary of the relationship between model variable and field data. Values are either a SPA model driver (input) or output. Model drivers may be initial conditions subsequently allowed to fluctuate, a fixed parameter value, or a time-series, whereby the parameter value at each time point is prescribed to the model. Model outputs are generated on either an hourly or daily time-step and are presented in the text as the mean annual sum (2009-2010), unless otherwise stated. Model outputs are calibrated or evaluated using field data. Values are specific to each of the eight GEM Amazonian permanent sample plots.

Value	Model Driver or Output	Source of Value or Calibration Data
LMA	driver (single fixed)	GEM plot measured value or literature based estimate from plot species list
κ_c	driver (single fixed)	(estimate from) GEM plot measured value or TRY database estimate from plot species list
κ_j	driver (single fixed)	(estimate from) GEM plot measured value or TRY database estimate from plot species list
Leaf N content	driver (single fixed)	GEM plot measured value or TRY database estimate from plot species list
LAI	driver (time-series fixed)	GEM monthly plot measured value
Leaf NPP	output	model calibration to GEM plot measured leaf litterfall and LAI
Wood NPP	output	model estimate using GEM calculated wood NPP fraction (single fixed driver)
Root NPP	output	model estimate using GEM calculated root NPP fraction (single fixed driver)
Leaf turnover	driver (single fixed; function of three individual fixed parameters relating to the leaf litterfall cycle)	model calibration to GEM plot measured leaf litterfall
Root turnover	driver (single fixed)	model calibration using GEM root NPP assuming steady state conditions
Wood turnover	driver (single fixed)	model calibration using GEM wood NPP assuming steady state conditions
Foliar C stock	driver (time-series fixed)	product of LAI and LMA
Wood C stock	driver (initial) and output (varies thereafter)	initial C stock estimate from GEM plot measured DBH values converted to C stock using allometric

		equation (driver); thereafter calculated in SPA as Wood C stock + NPP – turnover (output)
Root C stock	driver (initial) and output (varies thereafter)	initial C stock estimate from GEM plot measured root stock values or literature based estimate (driver); thereafter calculated in SPA as Root C stock + NPP – turnover (output)
Leaf respiration	output	sum of leaf maintenance and growth respiration; maintenance respiration generated using measured leaf N content, foliar C stock and the Reich *et al*., (2008) leaf respiration model, validated against GEM estimates; growth respiration calculated in SPA as leaf NPP × 0.28
Wood respiration	output	sum of wood maintenance and growth respiration; maintenance respiration calculated using an empirical model of measured wood C stock, calibrated against GEM estimates; growth respiration calculated in SPA as wood NPP × 0.28
Root respiration	output	sum of root maintenance and growth respiration; maintenance respiration calculated using an empirical model of measured root C stock, calibrated against GEM estimates; growth respiration calculated in SPA as root NPP × 0.28
Respiration	output	sum of SPA leaf, wood and root respiration
GPP	output	generated through SPA process based modelling of photosynthesis using detailed parameters, evaluated against GEM data
NPP	output	calculated in SPA as GPP minus autotrophic respiration, evaluated against GEM data

Table 3.2. Field estimated mean annual leaf area index (LAI) and community weighted mean leaf traits for Amazon permanent sample plots along a precipitation gradient. LAI estimates were derived from monthly hemispherical photographs. LAI and leaf trait estimates were used to constrain SPA model runs. Standard errors are presented in brackets.

	LAI (m^2 m^{-2})	LMA (g m^{-2})	leaf N content (g m^{-2})
CAX04	4.99 (± 1.07)	93 (± 17)	1.82 (± 0.43)
CAX06	5.23 (± 0.92)	87 (± 54)	2.12 (± 0.7)
TAM05	4.85 (± 0.81)	101 (± 24)	2.38 (± 0.56)
TAM06	4.64 (± 0.77)	96 (± 21)	2.51 (± 0.64)
KEN01	2.77 (± 0.17)	53 (± 13)	2.12 (± 0.25)
KEN02	2.22 (± 0.14)	42 (± 13)	2.31 (± 0.31)
TAN05	4.13 (± 1.01)	64 (± 13)	2.01 (± 0.52)
TAN06	2.62 (± 1.05)	61 (± 10)	2.01 (± 0.52)

3.3.2 Model Carbon Cycle Feedbacks

In order to isolate the direct and indirect effects of climate on simulated photosynthesis (and avoid capturing feedback effects of changes in forest structure i.e. leaf and root carbon stocks, as a result of changing photosynthate quantities), model experiments were conducted in the absence of carbon cycle feedbacks. Within model experiments, carbon stocks for each component (leaves, wood, fine root, coarse root) were constrained to calibration estimates unless otherwise stated (i.e. during driver alternations). Carbon cycle feedbacks within SPA were enabled during model calibration and uncertainty calculation (see Chapter 2, Figure 2.2).

3.3.3 Model Experiments

Drivers of Spatial Variation in Photosynthesis

SPA was used to apportion variation in photosynthesis across the precipitation gradient to that driven by physiological, and that driven by structural and trait responses to water availability. Through a series of model input alternations, we quantified the effects of physiological responses to water availability driven by (i) climate and (ii) soil properties, and structural and trait responses including (iii) LAI, (iv) photosynthetic capacity, (v) root biomass and (vi) rooting depth. Model inputs for each potential driver of variation in photosynthesis were alternated at each plot, to that of all other plots, and annual GPP values for each year retrieved. SPA simulated GPP values for each alternation (5 drivers × 8 plots × 7 alternations × 2 years, plus for climate, 1 driver× 8 plots × 3 alternations × 2 years) were combined with annual GPP estimates from calibration (control) runs (8 plots × 2 years). A factorial ANOVA was applied to

the difference between GPP from each model run and its control simulation (n=624)(Galbraith *et al*., 2010). The proportion of variation in GPP explained by climate, soil properties, LAI, photosynthetic capacity, root biomass and rooting depth, was then calculated as the conditional sum of square divided by the total sum of squares.

Within-Forest Sensitivity to Drivers of Photosynthesis

We investigated within-forest sensitivity of photosynthesis to differences in LAI, climate, photosynthetic capacity and rooting depth, within the bounds of observations across the precipitation gradient, using model outputs from the aforementioned driver alternations. Root biomass and soil properties were not included as previous analyses showed them to have little effect on variation in photosynthesis. The sensitivity of photosynthesis to drivers at each plot was calculated as the absolute range in simulated GPP values under named driver alternations. The mean sensitivity of plot GPP at each location was retrieved to assess how differences in sensitivity to LAI, climate, photosynthetic capacity and rooting depth vary across the precipitation gradient. Findings from the analysis also prompted us to calculate the ratio of LAI:MAP as an explanatory variable of GPP sensitivity.

Drivers of Sub-Annual Variation in Photosynthesis

We used the random forest technique to compute the relative importance of LAI, VPD, solar radiation, precipitation and air temperature driving variation in monthly GPP (n=192; 8 plots × 24 months), where GPP estimates were derived from SPA simulations. The random forest machine learning technique was applied by means of the Python Scikit-Learn module (Breiman, 2001; Pedregosa *et al*., 2011) to quantify the effects of LAI and climate variables on monthly GPP. The random forest approach uses a subset of the data (n) as a training set. Samples of the training set are taken at random, but with replacement, to build a prediction tree. Assuming the number of explanatory variables equals M, m is specified (where m<M) such that at each node m variables are selected at random from M. At the node the data is split or regressed by a function which minimising error across the two branches. Each tree is grown to the largest extent possible. New data is then predicted by averaging the predictions of n trees. The approach has an advantage over simple regression models as it allows for more complicated interactions across non-linear relationships. An importance value between 0 to 1 was assigned to each explanatory variable (driver) based on a tree wise comparison of explanatory power (López-Blanco *et al*., 2017; Moore *et al*., 2018). We calculated the average relative importance of drivers at each plot, and investigated the seasonality of driver

importance. We further considered the potential impact of seasonal shifts in mean canopy leaf age. Mean canopy leaf age was calculated in SPA using the timings of leaf growth and litterfall to generate a dynamic leaf age estimate. However, changes in photosynthetic capacity were not linked with leaf age within SPA due to a lack of data available to constrain the model.

3.4 Results

3.4.1 Model Calibration and Validation

Following model calibration to accurately simulate local soil moisture and leaf litterfall, SPA was successfully validated against field estimates of GPP, NPP and Respiration. Given the importance of water availability to the posed experiments, an accurate representation of local soil moisture was important. Calibrated SPA soil water content corresponded well to field measurements from the GEM network (Figure 3.2). Simulated mean annual soil moisture estimates were within standard error estimates for all plots, and seasonality was well captured (soil moisture range of GEM measurements and SPA simulations R^2=0.44, p=0.10, RMSE=5.1 %; timing of soil moisture peak R^2=0.97, p<0.001, RMSE=1.2 months). However, for some plots such as Kenia, the magnitude of seasonal peak soil water fluxes were not captured by SPA simulations, whilst for Tanguro, peak soil water lasted for longer periods in SPA simulations than was measured in the field.

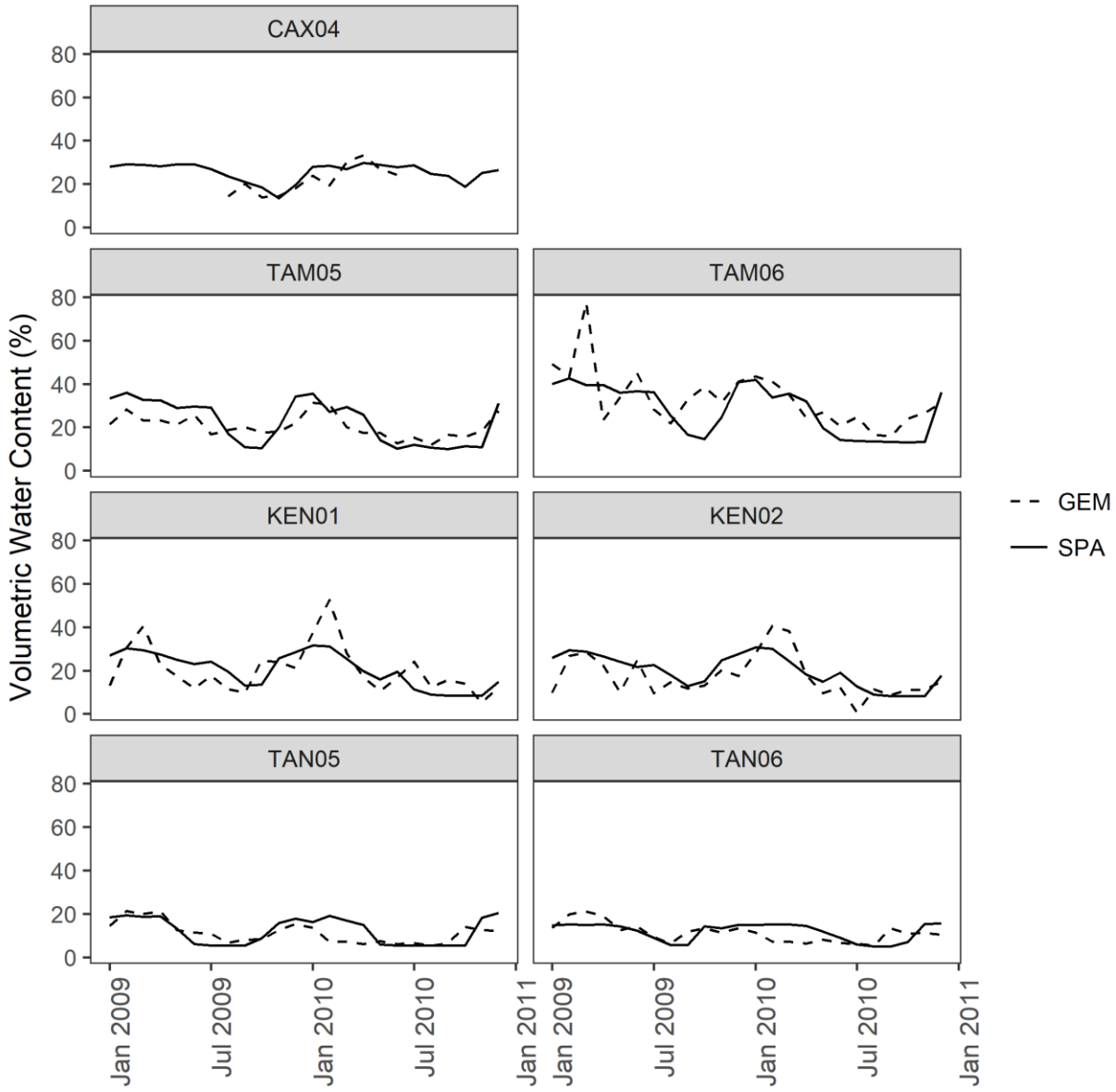

Figure 3.2. SPA estimated soil volumetric water content at 30cm depth compared to GEM measured values for seven of the eight sample plots at four locations across the Amazon basin. Data presented is for the time period 2009-2010. Field data for CAX04 was limited to a shorter time period and for CAX06 was unavailable.

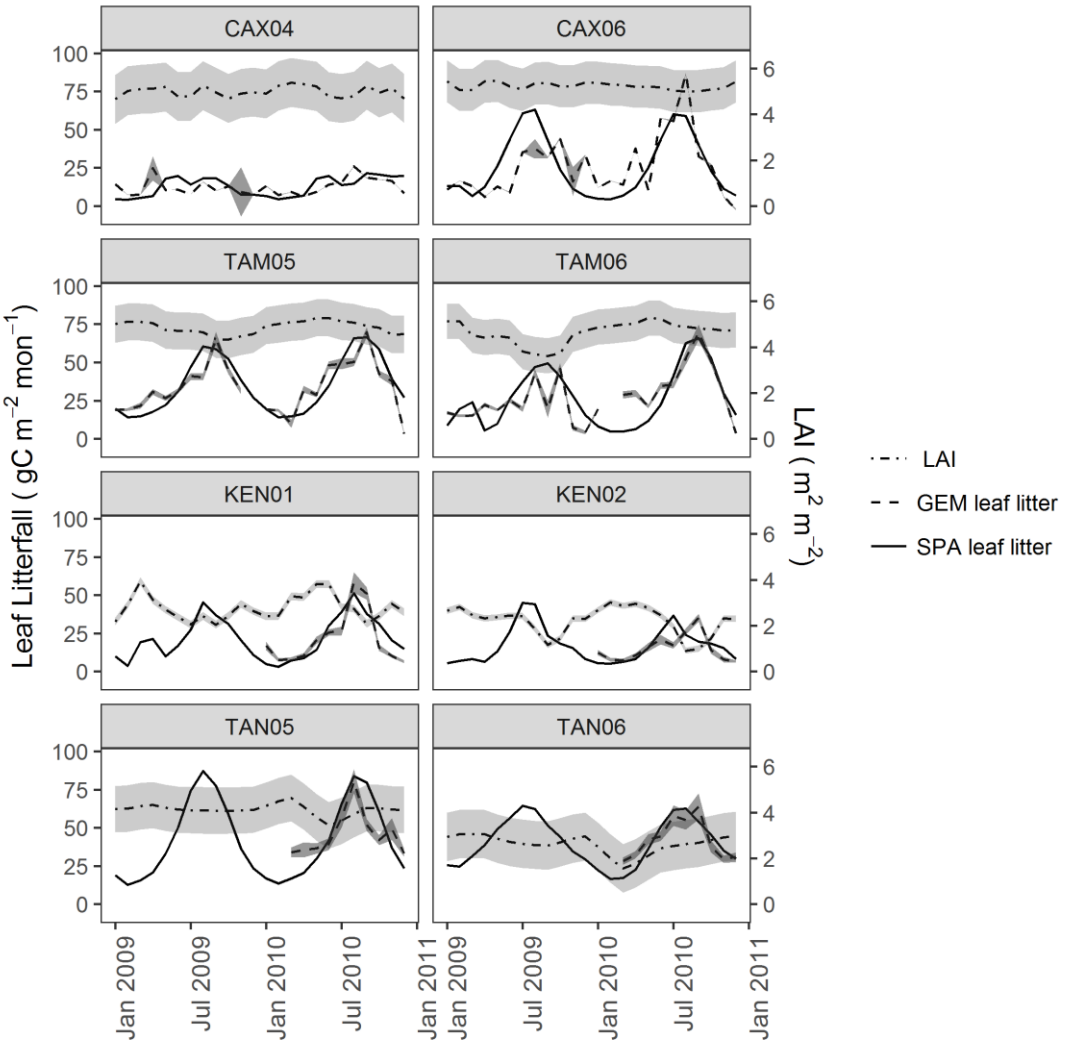

Figure 3.3. Field estimated monthly LAI, leaf litterfall (GEM), and standard error, compared with SPA simulated leaf litterfall for eight plots at four locations across the Amazon basin. SPA leaf litterfall was calibrated against GEM estimates to derive three fixed model drivers relating to the leaf cycle (leaf out timing, leaf out period and leaf lifespan). GEM leaf litterfall data was available for 2009-2010 for CAX04, CAX06, TAM05, TAM06 and for 2010 only for KEN01, KEN02, TAN05, TAN06.

SPA leaf litterfall was successfully calibrated to each of the permanent sample plots across the precipitation gradient. The calibration of leaf fall cycle parameters in SPA using GEM leaf litterfall time-series (Table 3.3), resulted in the magnitude and timing of leaf litterfall being well captured by the model for all plots (monthly leaf litterfall range of GEM measurements and SPA simulations R^2=0.53, p=0.007, RMSE= 10.9 gC m^{-2} yr^{-1}; timing of leaf litterfall peak R^2=0.97, p<0.001, RMSE=1.1 months) (Figure 3.3). SPA simulated annual leaf litterfall correlated significantly with GEM estimates (R^2=0.99, p=<0.001, RMSE=9.6 gC m^{-2} yr^{-1}).

Furthermore, calibrated leaf lifespan correlated significantly with mean annual precipitation (R^2=0.59, p=0.03, coeff=0.9). A significant positive correlation existed between model calibrated leaf lifespan and field estimated LMA (R^2=0.68 p=0.01). Field estimated LMA also correlated negatively with photosynthetic capacity estimates derived from measured leaf N content (R^2=0.74 p=0.006).

Table 3.3. SPA calibrated leaf litterfall parameters for plots across an Amazon precipitation gradient. Leaf fall day is the day of year leaf fall is initiated, leaf lifespan reflects potential lifespan of leaves and leaf fall period is the number of days over which leaf fall occurs. Leaf litterfall parameters were calibrated against GEM field estimates of leaf litterfall and timing.

	Leaf Fall Day (day of year)	Leaf Lifespan (years)	Leaf Fall Period (days)
CAX04	210	3	150
CAX06	190	1.45	100
TAM05	220	1.3	130
TAM06	230	1.42	100
KEN01	200	1.05	100
KEN02	180	1.01	100
TAN05	180	1.04	120
TAN06	120	1.005	160

Estimates of carbon fluxes from SPA model runs were validated against biometrically derived estimates from the GEM network. SPA and GEM GPP estimates were significantly correlated (R^2=0.48, p=0.05, RMSE=339.07 gC m^{-2} yr^{-1}) (Figure 3.4a). Error bars overlap between estimates for all plots except KEN01 and TAM06, though marginally (KEN01 115 gC m^{-2} yr^{-1}, TAM06 50 gC m^{-2} yr^{-1}) (where GEM error bars are field estimate standard error, and SPA error bars represent simulated GPP variance under LAI standard error). The correlation between GPP and MAP was similar for SPA (R^2=0.56, p=0.03, coeff=0.62) and GEM estimates (R^2=0.57, p=0.03, coeff=0.60). SPA NPP estimates (the sum of model simulated root and wood NPP and data constrained leaf NPP) were also correlated with GEM estimates across plots, though not significantly due to differences for Kenia plots (R^2=0.35, p= 0.12, RMSE=145.60 gC m^{-2} yr^{-1}; on exclusion of Kenia plots R^2=0.79, p= 0.02, RMSE=94.65 gC m^{-2} yr^{-1}) (Figure 3.4b). Model estimates of mean annual autotrophic respiration (the summation of predicted leaf respiration and calibrated root and wood respiration) were significantly correlated with biometric estimates across plots (R^2= 0.65, p= 0.02, RMSE =260.09 gC m^{-2} yr^{-1}) (Figure 3.4c).

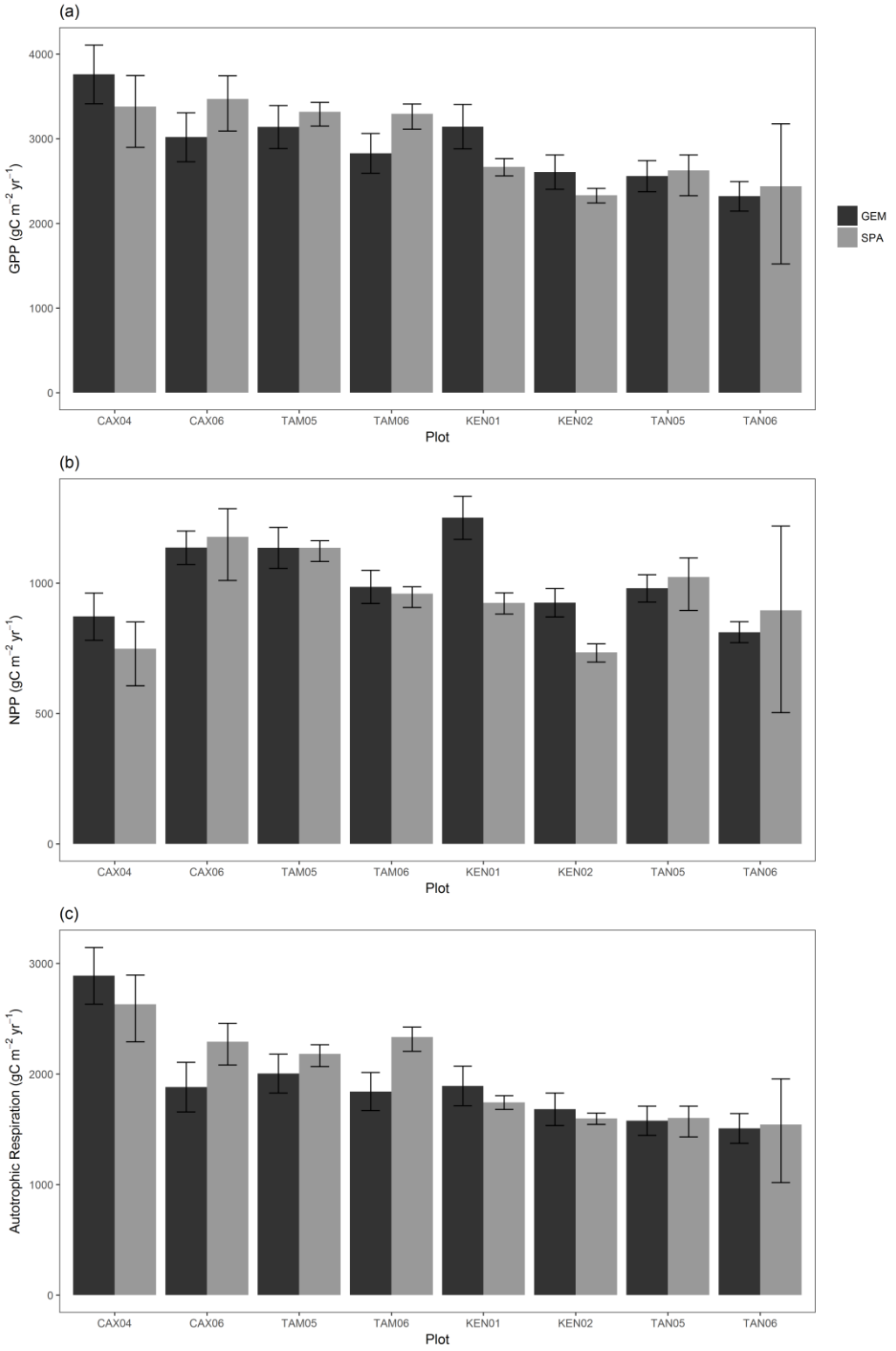

Figure 3.4. Carbon flux estimates (gC m^{-2} yr^{-1}) of (a) GPP, (b) NPP and (c) autotrophic respiration, derived from process based modelling (SPA) and biometric methods (GEM) for eight permanent sample plots at four locations across the Amazon basin. Estimates are mean annual values representative of the years 2009-2010. GEM error bars represent standard error from field carbon flux measurements.

Leaf respiration simulated using leaf nitrogen content correlated with field estimates though not significantly (R^2=0.46, p=0.07, RMSE=88.0 gC m^{-2} yr^{-1}). Wood and fine root respiration coefficients simulated values correlated significantly with field estimates (fine roots R^2=0.92, p<0.001, RMSE=69.4 gC m^{-2} yr^{-1}; wood R^2=0.79, p=0.03, RMSE=94.5 gC m^{-2} yr^{-1}). SPA simulated fine root NPP correlated significantly with GEM estimates (R^2=0.78, p=0.004, RMSE=47.8 gC m^{-2} yr^{-1}), simulated wood NPP also correlated though not significantly (R^2=0.21, p=0.24, RMSE=23.8 gC m^{-2} yr^{-1}) due to underestimation at KEN01 (on exclusion R^2=0.77, p=0.01, RMSE=7.1 gC m^{-2} yr^{-1}). Further comparisons of SPA and GEM estimates of component NPP and respiration are presented in Table 3.4.

Table 3.4. Summary of the range in GEM biometrically derived estimates and the difference between GEM and SPA process-based modelling estimates of component autotrophic respiration and NPP across eight sample plots at four locations across the Amazon basin. Estimates are mean annual values from 2009-2010. The standard deviation of the difference across plots is shown in brackets.

Component	Range in Field Estimates (gC m^{-2} yr^{-1})	Mean Difference between SPA and GEM site Estimates (gC m^{-2} yr^{-1})
Respiration		
Foliage	454-830	12.1 (±104.5)
Wood	411-1054	38.3 (±101.1)
Fine Root	232-1041	28.9 (±76.0)
NPP		
Foliage	150-491	-115.2 (±95.4)
Wood	189-292	23.7 (±43.0)
Fine Root	97-418	23.0 (±54.3)

3.4.2 Model Experiments

Drivers of Spatial Variation in Photosynthesis

Biotic responses to water availability explained more variation in photosynthesis across the precipitation gradient than did physiology-climate interactions. LAI accounted for the largest proportion of variance in mean annual GPP across plots (35.7%), whilst 19.8% was explained by differences in photosynthetic capacity (Table 3.5). Photosynthetic capacity was highest at dry plots; this relationship reduced the increase in photosynthesis with precipitation. The direct effects of climate on stomata accounted for 11.5% of plot variation in mean annual GPP. Rooting depth did not vary directionally with precipitation and consequently only had a small determinate effect on GPP (5.8%). Soil properties and root biomass accounted for even less (<3%).

Table 3.5. The proportion of variation in GPP across eight GEM Amazonian permanent sample plots explained by photosynthetic drivers in SPA. Proportion of variance explained was calculated as conditional sum of squares divided by the total sum of squares (n=624; where the conditions were LAI, photosynthetic capacity, rooting depth, root biomass, climate and soil). Drivers accounting for less than 5% of variation are not presented.

Driver	Percentage of Variation Explained (%)
LAI	35.7
Photosynthetic capacity	19.8
Climate/Stomata	11.5
Rooting depth	5.8

Within-Forest Sensitivity to Drivers of Photosynthesis

The sensitivity of forest photosynthesis to differences in LAI was dependent on local water constraints and rooting depth. Plots located at Caxiuaña experienced the highest MAP and as such were not water limited. A lack of water constraint shifted resource limitation towards light acquisition, causing plot photosynthesis to be more sensitive to changes in LAI (Figure 3.5) (Caxiuaña LAI sensitivity Δ 1616 gC m^{-2} yr^{-1}, mean LAI sensitivity Δ 1216 gC m^{-2} yr^{-1}). However, the increase in GPP sensitivity to LAI was non-linear across the precipitation gradient, and was marginally higher at Tanguro than at Kenia and Tambopata (Tanguro LAI sensitivity Δ 1147 gC m^{-2} yr^{-1}, Kenia LAI sensitivity Δ 1039 gC m^{-2} yr^{-1}, Tambopata LAI sensitivity Δ 1064 gC m^{-2} yr^{-1}). Comparatively higher rooting depths at Tanguro plots alleviated water constraints to photosynthesis driving elevated sensitivity to LAI change. The sensitivity of GPP to differences in photosynthetic capacity was also highest at Caxiuaña, again due to higher plant available water, but also due to the effect of higher LAI (Caxiuaña photosynthetic capacity sensitivity Δ 1130 gC m^{-2} yr^{-1}, mean photosynthetic capacity sensitivity Δ 838 gC m^{-2} yr^{-1}). Reflecting LAI trends, sensitivity to differences in photosynthetic capacity was not linear across the precipitation gradient and varied little between Tambopata, Kenia and Tanguro plots (Tambopata photosynthetic capacity sensitivity Δ 763 gC m^{-2} yr^{-1}, Kenia photosynthetic capacity sensitivity Δ 750 gC m^{-2} yr^{-1}, Tanguro photosynthetic capacity sensitivity Δ 709 gC m^{-2} yr^{-1}). The sensitivity of GPP to differences in climate and rooting properties was governed by the balance between evaporative demand and supply. Tambopata plots and TAN05 were the most sensitive to differences in climate, though the response of Tanguro was dampened by averaging with TAN06 (Tambopata climate sensitivity Δ 1417 gC m^{-2} yr^{-1}, TAN05 climate sensitivity Δ 1143 gC m^{-2} yr^{-1}, mean climate sensitivity Δ 912 gC m^{-2} yr^{-1}).

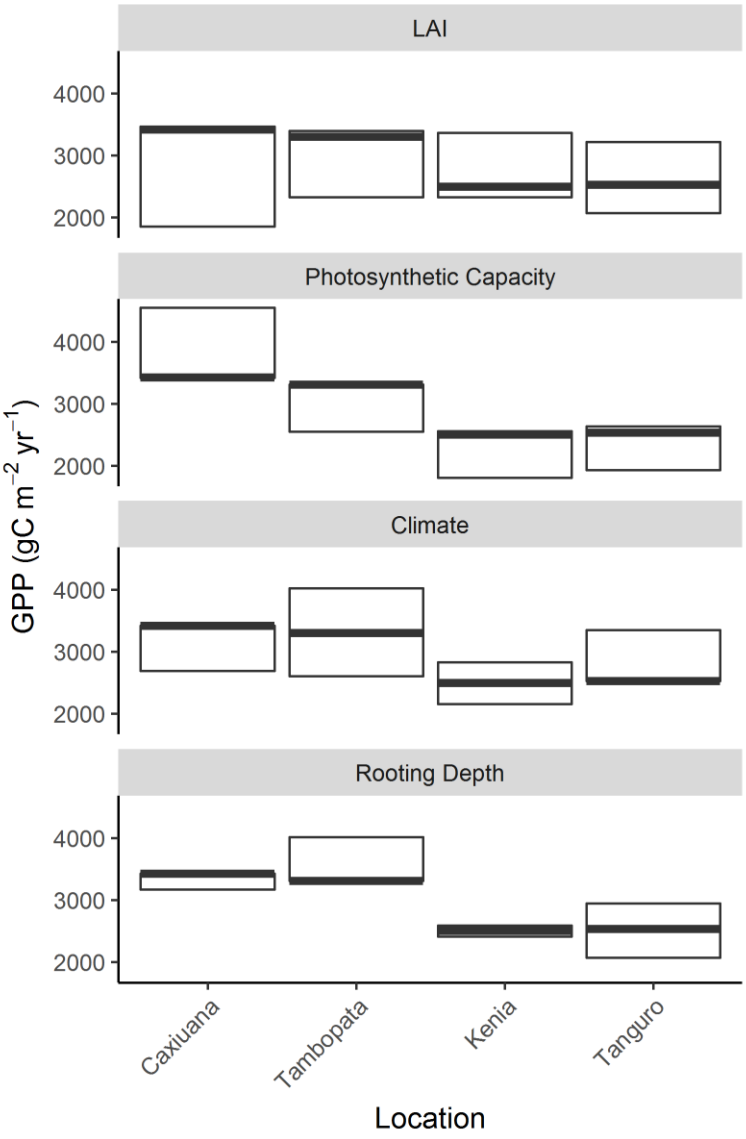

Figure 3.5. The sensitivity of location GPP to model driver alternations in SPA. Model drivers LAI, climate, photosynthetic capacity and rooting depth, derived from field observations, were alternated individually at each plot to that of all other plots, the resultant GPP retrieved, and location mean calculated. Boxes represent the total range of SPA simulated values under the named driver alternations, whilst the central bar represents the simulated value under observed conditions. Climate and LAI were input to the model as time-series, whilst photosynthetic capacity and rooting depth were fixed values. Plots are ordered to reflect mean annual precipitation which declined from Caxiuaña >Tambopata>Kenia>Tanguro.

High LAI at Tambopata and TAN05 enabled elevated photosynthesis when water availability was sufficient, but shallower rooting constrained GPP at low rainfall. Photosynthesis at Caxiuaña plots was less sensitive to reduced precipitation (Caxiuaña climate sensitivity Δ 734 gC m^{-2} yr^{-1}) due to higher rooting depths, which alleviated water limitation. Low LAI at Kenia

and TAN06 reduced the sensitivity of GPP to climate (Kenia climate sensitivity Δ 677 gC m^{-2} yr^{-1}, TAN06 climate sensitivity Δ 494 gC m^{-2} yr^{-1}). Similarly, the sensitivity of GPP to differences in rooting depth was also higher at Tambopata and TAN05 (Tambopata rooting depth sensitivity Δ 713 gC m^{-2} yr^{-1}, TAN05 rooting depth sensitivity Δ 1028 gC m^{-2} yr^{-1}), and lower at Caxiuaña, Kenia and TAN06 (Caxiuaña rooting depth sensitivity Δ 256 gC m^{-2} yr^{-1}, Kenia rooting depth sensitivity Δ 179 gC m^{-2} yr^{-1}, TAN06 rooting depth sensitivity Δ 716 gC m^{-2} yr^{-1},) (Figure 3.5), due to a high LAI:MAP ratio at Tambopata and TAN05 (Table 3.6), relatively lower LAI at Kenia and TAN06, and high MAP at Caxiuaña. We can therefore conclude that whilst photosynthesis is most sensitive to differences in light harvesting (LAI and photosynthetic capacity) for core forests, forests with a high evaporative demand relative to water supply (transitional forests) are most sensitive to differences in water availability and acquisition capabilities (climate and rooting depth).

Table 3.6. The ratio of mean annual LAI (m^2 m^{-2}) to mean annual precipitation (m). LAI estimates are field measurements, whilst precipitation estimate are derived from local meteorological data, gap filled with ERA interim data (Dee *et al.*, 2011), for eight permanent sample plots at four locations across the Amazon basin.

	LAI:MAP ratio
CAX04	1.78
CAX06	1.86
TAM05	2.70
TAM06	2.58
KEN01	1.62
KEN02	1.29
TAN05	2.93
TAN06	1.85

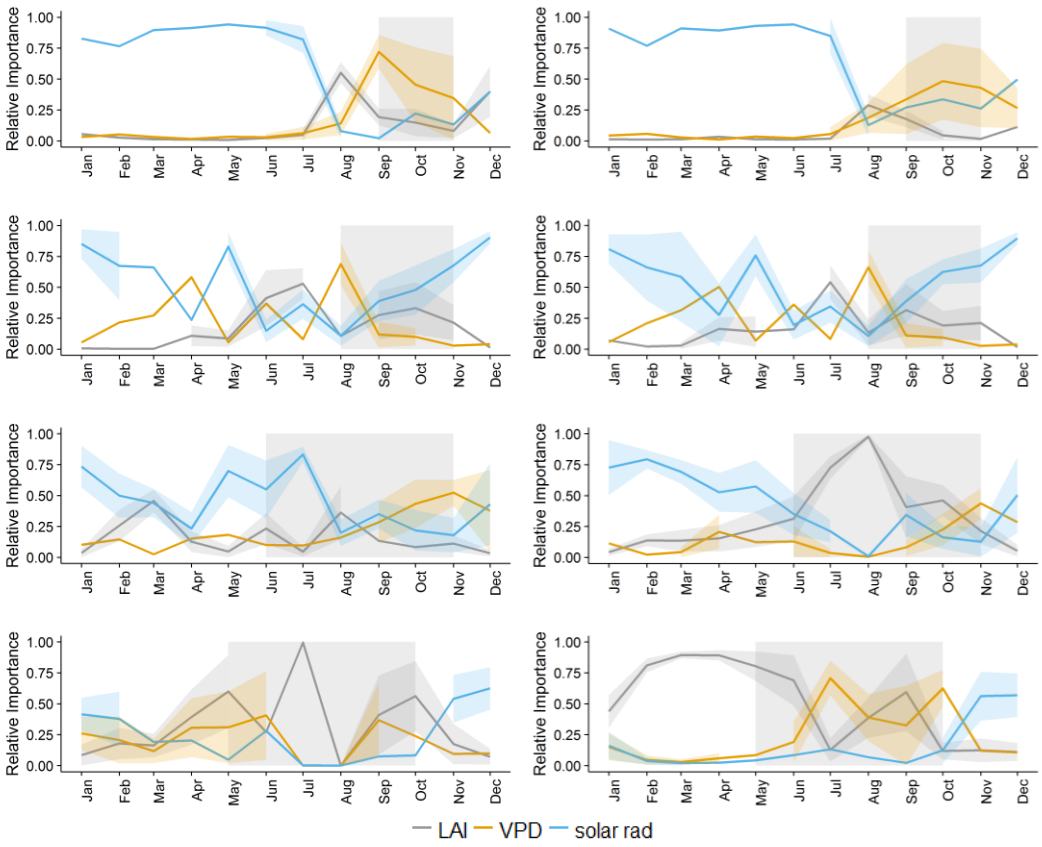

Figure 3.6. The relative importance of LAI, vapour pressure deficit (VPD) and solar radiation (solar rad) in driving SPA estimated monthly photosynthesis at permanent sample plots across an Amazon precipitation gradient. Relative importance was calculated using random forest machine learning. Shaded regions represent the dry season, where monthly precipitation was below 100mm. Plots are ordered to reflect mean annual precipitation which declined from Caxiuaña> Tambopata> Kenia> Tanguro.

Drivers of Sub-Annual Variation in Photosynthesis

In contrast to drivers of spatial variation in photosynthesis, on a sub-annual timescale LAI had less explanatory power than climate (Tables 3.5 and 3.7). The relative importance of solar radiation in driving monthly GPP increased significantly with precipitation (R^2 = 0.64, p=0.017, coeff=0.24), whilst the relative importance of VPD and LAI declined (VPD R^2= 0.32, p=0.14, coeff=-0.03; LAI R^2=0.56, p=0.033, coeff=-0.19). Both precipitation and air temperature had little effect on monthly GPP and as such, seasonal changes in their relative importance were not investigated further. The relative importance of LAI, VPD and solar radiation shifted seasonally, reflecting changes in the availability of light and water. Solar radiation was typically the most important driver of monthly GPP during the wet season, whilst VPD was more important during the dry season (Figure 3.6). The relative importance of LAI forcings peaked before dry season onset for core forests (Caxiuaña and Tambopata), and during the dry season

for transitional forests (Kenia and Tanguro). A notable exception is TAN06, where LAI was most important during the wet season. The key difference between TAN06 and other permanent sample plots is its history of burning. LAI was also more important during the dry season at KEN02, which occupies shallow soil in comparison to KEN01. Disturbance history and soil properties could therefore be linked to differences in the relative importance of sub-annual drivers of photosynthesis. Furthermore, these results did not take into account the effect of changes in photosynthetic capacity with leaf age. Leaf age typically co-varied with LAI, and for core forests was peaked during the wet season, whilst for transitional forests it was highest during dry season onset (Figure 3.7).

Table 3.7. The relative importance of LAI, VPD, solar radiation, precipitation and air temperature (T_{air}) in driving monthly variation in GPP. Monthly GPP estimates are derived from calibrated SPA simulations for eight permanent sample plots across an Amazon mean annual precipitation gradient. LAI estimates are derived from monthly field measurements. Local meteorological data was gap filled with ERA interim values (*Dee et al*., 2011) for the years 2009-2010 to obtain climate forcings. Relative importance values were derived from analyses using the random forest technique (n=192).

Plot	LAI	VPD	Solar Radiation	Precipitation	T_{air}
CAX04	0.13	0.17	0.58	0.08	0.05
CAX06	0.06	0.16	0.64	0.08	0.05
TAM05	0.17	0.22	0.53	0.03	0.05
TAM06	0.17	0.21	0.53	0.03	0.07
KEN01	0.16	0.21	0.45	0.10	0.08
KEN02	0.32	0.14	0.42	0.04	0.08
TAN05	0.33	0.20	0.24	0.06	0.10
TAN06	0.50	0.24	0.15	0.05	0.06

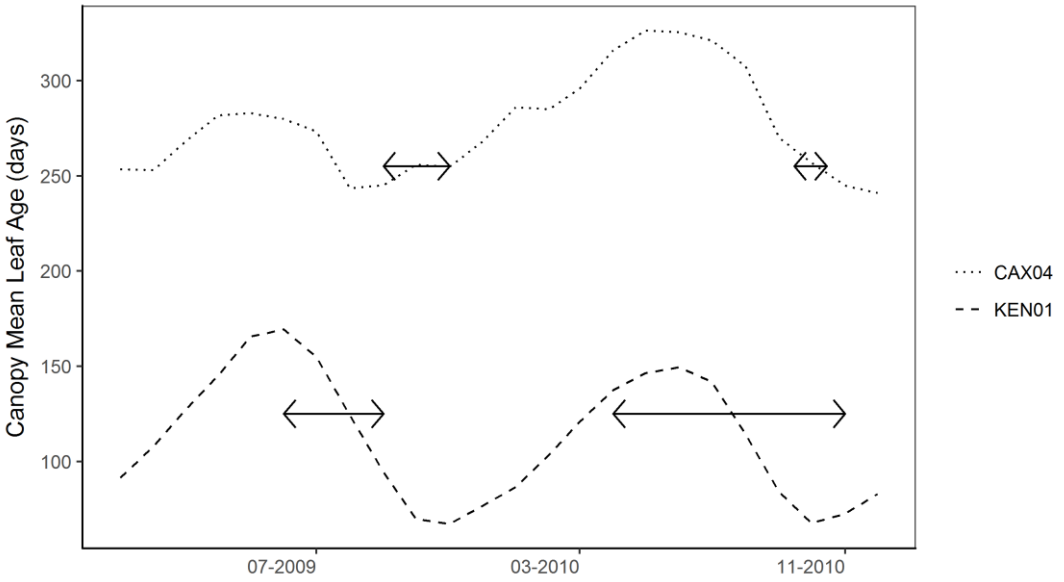

Figure 3.7. Intra-annual variation in SPA estimated leaf age for a typical core (CAX04) and transitional (KEN01) Amazon permanent sample plot, representative of the years 2009-2010. Arrows represent the dry season, where monthly precipitation was below 100mm. Leaf age estimates were derived from SPA simulated leaf NPP, field measurements of LAI, and leaf litterfall calibrations.

3.5 Discussion

Our aim was to better understand the coupling between photosynthesis and precipitation across Amazon forests. We (i) quantified the role of direct and indirect responses to water availability in driving photosynthesis trends across an Amazon precipitation gradient, (ii) investigated the relative sensitivity of forests to changes in climate, LAI, rooting depth and leaf traits and, (iii) explored the importance of phenology and climate forcings in driving sub-annual photosynthesis. Leaf traits (both modelled and observed) co-varied along the precipitation gradient. We found that LAI was the principal driver of spatial variation in photosynthesis, followed by photosynthetic capacity. Forests occupying the highest rainfall zone were most sensitive to differences in LAI and photosynthetic capacity, whilst forests with a bigger evaporative demand (high LAI) relative to water supply were most sensitive to differences in climate and rooting depth. Solar radiation was a key driver of sub-annual variation in GPP, the relative effect of which increased with mean annual precipitation, coincident with declines in the relative importance of VPD and LAI.

3.5.1 Observed and Model Calibrated Leaf Trait Distributions

Leaf trait parameters retrieved from SPA litterfall calibrations suggest a wide range of community weighted mean leaf lifespan across the precipitation gradient, and are in accordance with estimates for Amazon tree species, reported by Reich *et al*. (1991) of between two months and four years. Furthermore, calibrated leaf lifespan estimates correlated significantly with field LMA estimates, in line with leaf economic theory (Wright *et al*., 2004). The interaction between community weighted mean leaf traits reflects reported species specific interactions (Reich *et al*. (1991) species specific equation, log(specific leaf area) = 2.37 - 0.33 log(leaf lifespan), R^2=0.78, p<0.001; SPA calibration derived community weighted mean leaf lifespan equation, log(specific leaf area) =-1.79 - 0.56 log(leaf lifespan), R^2=0.41 p=0.085). The co-variation of leaf traits along the precipitation gradient shapes both the rate of carbon assimilation (photosynthetic capacity), and the carbon economics of canopy dynamics.

3.5.2 Drivers of Spatial Variation in Photosynthesis

Indirect responses to water availability (forest structure and traits) accounted for 62.1% of variation in photosynthesis across the precipitation gradient. The direct effect of physiology-climate interactions accounted for only 11.5% of observed variance. LAI was the principal cause of spatial variation in photosynthesis, followed by photosynthetic capacity (LAI accounted for 35.7% of variation, photosynthetic capacity accounted for 19.8%). Root and soil properties had little explanatory power. Our approach utilised field measurements of LAI from hemispherical photographs to constrain model simulations. The accuracy and spatial validity of indirect estimates has been questioned at higher leaf areas (Bréda, 2003; Jonckheere *et al*., 2004; Weiss *et al*., 2004). However, our highest estimates of LAI align with destructive sampling measurements from a terra-firme Amazon forest (Caxiuaña 5.11 ± 1.41 m^2m^{-2}, McWilliam *et al*. (1993) 5.7 ± 0.5 m^2m^{-2}). Furthermore, a comparison of LAI measurement approaches suggested that indirect methods were appropriate for broadleaved forests, and presented no statistical difference between destructive harvesting and indirect methods (Asner *et al*., 2003).

Evidence of LAI as a structural response to precipitation has been presented across alternate ecosystems and across time (Dobbertin *et al*., 2010; Grier and Running, 1977; Iio *et al*., 2014; Schleppi *et al*., 2011; Wright *et al*., 2013). Amazonian throughfall exclusion experiments identified a decline in LAI with the onset of reduced soil water (Brando *et al*., 2008; Fisher *et*

al., 2007; Meir *et al*., 2008), with Meir *et al*. (2009) observing a 20-30% reduction compared to the control stands over a 4-year period. After 15 years, leaf litterfall remained consistently lower under throughfall exclusion (Rowland *et al*., 2018). Investigations show that declines in LAI are not caused by increased leaf turnover due to water stress, but instead are the result of lower leaf production, suggesting a forest driven response to water availability (Nepstad *et al*., 2002; Schuldt *et al*., 2011). Reported trends in canopy dynamics are therefore in accordance with our findings and indicate that LAI is a key pathway of plant response to precipitation regime. However, whilst other studies such as da Costa *et al*. (2018) have similarly pointed towards structural responses as the dominant control over photosynthesis, they identify changes in sapwood area as the principal driver, rather than LAI. We argue that whilst sapwood area may be more important in shaping the response to changes in precipitation, for forests at steady state emergent canopy properties (LAI) drive photosynthesis trends.

Photosynthetic capacity also proved an important driver of spatial variation in photosynthesis across the precipitation gradient. Our results are consistent with a number of Amazon based studies linking leaf traits to productivity (Aragao *et al*., 2009; Castanho *et al*., 2013; Cleveland *et al*., 2011). We show that the directional variation of photosynthetic capacity actually lessens the interaction between photosynthesis and precipitation. However, as we have focused on the role of leaf traits in the absence of carbon cycle feedbacks, we do not take into account the effects of LMA and leaf lifespan, which together shape canopy carbon economics (McMurtrie and Dewar, 2011; Osnas *et al*., 2013; Wright *et al*., 2004). Furthermore, it is unclear whether the decrease in photosynthetic capacity with increasing water availability is in response to precipitation or to soil nutrient status (Maire *et al*., 2015; Malhi *et al*., 2015). As nutrient dynamics are not accounted for in SPA, we are unable to quantify the impact of soil nutrients on the photosynthesis-precipitation interaction, beyond its manifestation in leaf traits. Nevertheless, the interaction between photosynthetic capacity and LAI is important in driving photosynthesis across the precipitation gradient. Consistent with the results of Fyllas *et al*. (2017), our results also show that the effect of environmental forcings on carbon fluxes can be successfully captured through spatial variation in canopy dynamics and leaf traits.

Root depth, root biomass and soil properties demonstrated little effect on spatial variation in photosynthesis. Whilst we recognise the difficulty of measuring root depth and biomass (Metcalfe *et al*., 2007) adds uncertainty to our results, the findings presented do not reflect

the importance of belowground functioning highlighted by other studies (Baker *et al*., 2008; Fisher *et al*., 2007; Ichii *et al*., 2007; Metcalfe *et al*., 2008; Phillips *et al*., 2009). Notably, a number of plots had hard pan layers (Quesada *et al*., 2012) and so may be acclimated to operate in shallow rooting zones, and are then not necessarily representative of other Amazon forests under the same precipitation regime. However, it is likely that given these drivers are largely associated with the acquisition of water, rather than carbon, if feedbacks were enabled within analyses, root and soil properties would prove to have a more determinant effect.

3.5.3 Within-Forest Sensitivity to Drivers of Photosynthesis

Water availability, demand and acquisition potential shaped the sensitivity of photosynthesis to differences in LAI, climate, photosynthetic capacity and rooting depth across the precipitation gradient. As the experiment was conducted in the absence of carbon cycle feedbacks, sensitivities reflect short rather than long term effects of changes in forcings. The sensitivity of photosynthesis to differences in LAI and photosynthetic capacity was greatest for forests occupying the highest precipitation zone. Our results are in line with findings from Wright *et al*. (2013), who reported that plots with higher available water were most sensitive to decreases in leaf area. Heightened sensitivity at the highest MAP plots was a result of those plots not being water limited, and so were able to maximise the potential of increased photosynthetic surface area and capacity. However, the effect was not linear across the precipitation gradient as responses were constrained by shallow rooting.

Forests with a high LAI but relatively shallow rooting depth were most sensitive to differences in climate, whilst forests with a high LAI relative to MAP were most sensitive to differences in rooting depth. The effect was driven by a high evaporative demand coupled with relatively lower water uptake. Our results indicate that where rooting depth is relatively shallow, and unable to ameliorate the effects of water stress as seen elsewhere (Malhi *et al*., 2009; Nepstad *et al*., 2007), forests with a high LAI are likely to be more vulnerable to reduced precipitation, both due to constraints to photosynthesis and due to narrow hydraulic safety margins (Choat *et al*., 2012). Forests with a high evaporative demand relative to water uptake capacity should therefore be an important focus for studies assessing the sensitivity of Amazon forests to future shifts in rainfall across the basin (Asner and Alencar, 2010; Malhi *et al*., 2009).

3.5.4 Drivers of Sub-Annual Variation in Photosynthesis

The effects of climate and LAI on monthly photosynthesis shifted across the precipitation gradient. Shortwave radiation was the dominant driver of sub-annual variation in GPP, and its relative effects increased with precipitation. The importance of LAI and VPD was highest for transitional forests. In accordance with our findings, a number of studies report that for Amazon forests subject to lower annual rainfall, GPP declines parallel to increased VPD, whilst in high rainfall zones GPP increases in line with solar radiation (Carswell *et al*., 2002; Goulden *et al*., 2004; Hutyra *et al*., 2007; Rowland *et al*., 2014; Saleska *et al*., 2003; Von Randow *et al*., 2013). Our results suggest that LAI is not the principal driver of sub-annual variance in photosynthesis, in contrast to its role driving spatial variation across the precipitation gradient. Whilst the current literature largely agrees that leaf area alone does not drive seasonal GPP, we fail to account for the role of concurrent shifts in photosynthetic capacity, pointed towards by many studies as a key factor driving sub-annual photosynthesis (Bi *et al*., 2015; Brando *et al*., 2010; Restrepo-Coupe *et al*., 2013; Wu *et al*., 2016; Wu *et al*., 2017). The coordination of leaf flushing and new leaf emergence with environmental drivers such as solar radiation is thought to exceed the effects of LAI in non-water limited forests (Myneni *et al*., 2007). However, the effect of leaf age on photosynthetic capacity is not accounted for in SPA. We therefore do not capture the interaction between temporal changes in photosynthetic capacity and water availability in our analysis, nor do we account for resultant shifts in GPP. Simulated dynamics suggest that if leaf age effects were included, GPP seasonality would be amplified.

3.5.5 Explaining Spatial Variation in Photosynthesis across the Amazon Basin

Our results have demonstrated the role of LAI and leaf traits in shaping photosynthesis across an Amazon precipitation gradient, however, they cannot be extrapolated to explain basin-wide variation in photosynthesis. Principal constraints to photosynthesis likely vary across lowland Amazon forests, spanning both climatic and edaphic controls (Malhi *et al*., 2015; Malhi and Wright, 2004; Quesada *et al*., 2009). Beer *et al*., (2010) report that for tropical forests, 29% of variation in GPP was associated with precipitation, whilst 39% was associated with temperature. Other studies have presented nutrient availability as a key driver of Amazon forest photosynthesis. Mercado *et al*. (2011) found that leaf nutrient content, assumed to be linked to soil nutrient status, exerted a strong effect on productivity across the Amazon basin. Soil chemical and physical properties together with disturbance history co-vary across the

Amazon basin (Quesada *et al.*, 2012), making it difficult to isolate discrete effects. In order to provide a full assessment of the principal drivers of basin-wide photosynthesis, a land surface model approach is required, as using only biometric and eddy flux data biases the result towards the key drivers of the individual plot, which are often strategically chosen locations across environmental gradients.

3.5.6 Informing Projections of Future Carbon Dynamics

The work presented has important implications for carbon cycling under future climates. Our findings suggest that LAI and photosynthetic capacity could play a key role in the response of Amazon forests to changes in precipitation. However, we note that the transitional forests used in this study are not predominant across the Amazon, limiting our ability to determine the principal cause of basin-wide variation in photosynthesis. The importance of LAI in driving photosynthetic responses to precipitation, identifies a need for improved understanding of leaf dynamics. An increase in canopy mapping through satellite missions will therefore be instrumental to efforts aiming to constrain carbon flux estimates across the basin. FLEX, GEDI and Sentinel will offer opportunity for new insights into changes in leaves in-situ, vertical canopy structure, and temporal variability via repeat measurements (Drusch *et al.*, 2017; Morton, 2016; Pettorelli *et al.*, 2018). We also found that forests with a high LAI to precipitation ratio were most sensitive to changes in climate. Studies investigating climate change resilience could usefully focus on these more vulnerable forests. Whilst we have highlighted principal covariates of photosynthetic seasonality, further work is needed to integrate leaf age effects in order to infer potential implications under future climate change scenarios. However, under projected strengthening of the dry season in some Amazon regions (Boisier *et al.*, 2015), we might expect monthly GPP to become more sensitive to VPD and LAI.

3.6 Conclusion

Our results show that structural and trait responses to precipitation drive spatial variation in photosynthesis across an Amazon precipitation gradient. We found that LAI was the principal driver of spatial variance in GPP followed by photosynthetic capacity. Furthermore, the relative sensitivity of photosynthesis to changes in direct and indirect forcings shifted across the precipitation gradient and was dependent on water availability, demand and acquisition potential. This research improves our understanding of the role of physiological, structural and

trait responses to water availability in driving the coupling between photosynthesis and precipitation across Amazon forests. In light of projected changes in rainfall patterns as a result of anthropogenic climate change, our findings can help reduce uncertainty and inform model predictions of the future Amazon carbon balance. We identify a need for improved understanding of canopy dynamics and further research should build on the findings presented, with a focus on exploring carbon cycle feedbacks under LAI changes, and the role of traits in shaping leaf carbon economics.

3.7 References

Aragao, L. E. O. C., Malhi, Y., Metcalfe, D. B., Silva-Espejo, J. E., Jimenez, E., Navarrete, D., Almeida, S., Costa, A. C. L., Salinas, N., Phillips, O. L., Anderson, L. O., Alvarez, E., Baker, T. R., Goncalvez, P. H., Huaman-Ovalle, J., Mamani-Solorzano, M., Meir, P., Monteagudo, A., Patino, S., Penuela, M. C., Prieto, A., Quesada, C. A., Rozas-Davila, A., Rudas, A., Silva, J. A., & Vasquez, R. (2009). Above- and below-ground net primary productivity across ten Amazonian forests on contrasting soils. Biogeosciences, 6(12), 2759-2778.

Asner, G. P., & Alencar, A. (2010). Drought impacts on the Amazon forest: the remote sensing perspective. New Phytol, 187(3), 569-578.

Asner, G. P., Scurlock, J. M. O., & Hicke, J. A. (2003). Global synthesis of leaf area index observations: implications for ecological and remote sensing studies. Global Ecology and Biogeography, 12(3), 191-205.

Baker, I. T., Prihodko, L., Denning, A. S., Goulden, M., Miller, S., & da Rocha, H. R. (2008). Seasonal drought stress in the Amazon: Reconciling models and observations. Journal of Geophysical Research-Biogeosciences, 113(G1).

Barbosa, J. M., & Asner, G. P. (2017). Prioritizing landscapes for restoration based on spatial patterns of ecosystem controls and plant–plant interactions. Journal of Applied Ecology, 54(5), 1459-1468.

Beer, C., Reichstein, M., Tomelleri, E., Ciais, P., Jung, M., Carvalhais, N., Rödenbeck, C., Arain, M. A., Baldocchi, D., & Bonan, G. B. (2010). Terrestrial gross carbon dioxide uptake: global distribution and covariation with climate. Science, 329(5993), 834-838.

Beer, C., Reichstein, M., Tomelleri, E., Ciais, P., Jung, M., Carvalhais, N., Rodenbeck, C., Arain, M. A., Baldocchi, D., Bonan, G. B., Bondeau, A., Cescatti, A., Lasslop, G., Lindroth, A., Lomas, M., Luyssaert, S., Margolis, H., Oleson, K. W., Roupsard, O., Veenendaal, E., Viovy, N., Williams, C., Woodward, F. I., & Papale, D. (2010). Terrestrial gross carbon dioxide uptake: global distribution and covariation with climate. Science, 329(5993), 834-838.

Bi, J., Knyazikhin, Y., Choi, S. H., Park, T., Barichivich, J., Ciais, P., Fu, R., Ganguly, S., Hall, F., Hilker, T., Huete, A., Jones, M., Kimball, J., Lyapustin, A. I., Mottus, M., Nemani, R. R., Piao, S. L., Poulter, B., Saleska, S. R., Saatchi, S. S., Xu, L., Zhou, L. M., & Myneni, R. B. (2015). Sunlight

mediated seasonality in canopy structure and photosynthetic activity of Amazonian rainforests. Environmental Research Letters, 10(6), 064014.

Boisier, J. P., Ciais, P., Ducharne, A., & Guimberteau, M. (2015). Projected strengthening of Amazonian dry season by constrained climate model simulations. Nature Climate Change, 5(7), 656-660.

Brando, P. M., Goetz, S. J., Baccini, A., Nepstad, D. C., Beck, P. S., & Christman, M. C. (2010). Seasonal and interannual variability of climate and vegetation indices across the Amazon. Proc Natl Acad Sci U S A, 107(33), 14685-14690.

Brando, P. M., Nepstad, D. C., Davidson, E. A., Trumbore, S. E., Ray, D., & Camargo, P. (2008). Drought effects on litterfall, wood production and belowground carbon cycling in an Amazon forest: results of a throughfall reduction experiment. Philos Trans R Soc Lond B Biol Sci, 363(1498), 1839-1848.

Brando, P. M., Nepstad, D. C., Davidson, E. A., Trumbore, S. E., Ray, D., & Camargo, P. (2008). Drought effects on litterfall, wood production and belowground carbon cycling in an Amazon forest: results of a throughfall reduction experiment. Philos Trans R Soc Lond B Biol Sci, 363(1498), 1839-1848.

Bréda, N. J. J. (2003). Ground-based measurements of leaf area index: a review of methods, instruments and current controversies. Journal of experimental botany, 54(392), 2403-2417.

Breiman, L. (2001). Random forests. Machine learning, 45(1), 5-32.

Caldararu, S., Palmer, P. I., & Purves, D. W. (2012). Inferring Amazon leaf demography from satellite observations of leaf area index. Biogeosciences, 9(4), 1389-1404.

Carswell, F. E., Costa, A. L., Palheta, M., Malhi, Y., Meir, P., Costa, J. D. R., Ruivo, M. D., Leal, L. D. M., Costa, J. M. N., Clement, R. J., & Grace, J. (2002). Seasonality in CO2 and H2O flux at an eastern Amazonian rain forest. Journal of Geophysical Research-Atmospheres, 107(D20).

Castanho, A. D. A., Coe, M. T., Costa, M. H., Malhi, Y., Galbraith, D., & Quesada, C. A. (2013). Improving simulated Amazon forest biomass and productivity by including spatial variation in biophysical parameters. Biogeosciences, 10(4), 2255-2272.

Choat, B., Jansen, S., Brodribb, T. J., Cochard, H., Delzon, S., Bhaskar, R., Bucci, S. J., Feild, T. S., Gleason, S. M., Hacke, U. G., Jacobsen, A. L., Lens, F., Maherali, H., Martinez-Vilalta, J.,

Mayr, S., Mencuccini, M., Mitchell, P. J., Nardini, A., Pittermann, J., Pratt, R. B., Sperry, J. S., Westoby, M., Wright, I. J., & Zanne, A. E. (2012). Global convergence in the vulnerability of forests to drought. Nature, 491(7426), 752-755.

Cleveland, C. C., Townsend, A. R., Taylor, P., Alvarez-Clare, S., Bustamante, M. M. C., Chuyong, G., Dobrowski, S. Z., Grierson, P., Harms, K. E., & Houlton, B. Z. (2011). Relationships among net primary productivity, nutrients and climate in tropical rain forest: a pan-tropical analysis. Ecology letters, 14(9), 939-947.

da Costa, A. C. L., Rowland, L., Oliveira, R. S., Oliveira, A. A. R., Binks, O. J., Salmon, Y., Vasconcelos, S. S., Junior, J. A. S., Ferreira, L. V., Poyatos, R., Mencuccini, M., & Meir, P. (2018). Stand dynamics modulate water cycling and mortality risk in droughted tropical forest. Glob Chang Biol, 24(1), 249-258.

Dee, D. P., Uppala, S. M., Simmons, A. J., Berrisford, P., Poli, P., Kobayashi, S., Andrae, U., Balmaseda, M. A., Balsamo, G., & Bauer, P. (2011). The ERA-Interim reanalysis: Configuration and performance of the data assimilation system. Quarterly Journal of the royal meteorological society, 137(656), 553-597.

Dietze, M. C., Sala, A., Carbone, M. S., Czimczik, C. I., Mantooth, J. A., Richardson, A. D., & Vargas, R. (2014). Nonstructural carbon in woody plants. Annu Rev Plant Biol, 65, 667-687.

Dobbertin, M., Eilmann, B., Bleuler, P., Giuggiola, A., Graf Pannatier, E., Landolt, W., Schleppi, P., & Rigling, A. (2010). Effect of irrigation on needle morphology, shoot and stem growth in a drought-exposed Pinus sylvestris forest. Tree Physiol, 30(3), 346-360.

Doughty, C. E., Metcalfe, D. B., Girardin, C. A., Amezquita, F. F., Cabrera, D. G., Huasco, W. H., Silva-Espejo, J. E., Araujo-Murakami, A., da Costa, M. C., Rocha, W., Feldpausch, T. R., Mendoza, A. L., da Costa, A. C., Meir, P., Phillips, O. L., & Malhi, Y. (2015). Drought impact on forest carbon dynamics and fluxes in Amazonia. Nature, 519(7541), 78-82.

Drusch, M., Moreno, J., Del Bello, U., Franco, R., Goulas, Y., Huth, A., Kraft, S., Middleton, E. M., Miglietta, F., & Mohammed, G. (2017). The FLuorescence EXplorer Mission Concept—ESA's Earth Explorer 8. IEEE Transactions on Geoscience and Remote Sensing, 55(3), 1273-1284.

Fauset, S., Baker, T. R., Lewis, S. L., Feldpausch, T. R., Affum-Baffoe, K., Foli, E. G., Hamer, K. C., & Swaine, M. D. (2012). Drought-induced shifts in the floristic and functional composition of tropical forests in Ghana. Ecol Lett, 15(10), 1120-1129.

Fisher, R. A., Williams, M., Da Costa, A. L., Malhi, Y., Da Costa, R. F., Almeida, S., & Meir, P. (2007). The response of an Eastern Amazonian rain forest to drought stress: results and modelling analyses from a throughfall exclusion experiment. Global Change Biology, 13(11), 2361-2378.

Fisher, R. A., Williams, M., Do Vale, R. L., Da Costa, A. L., & Meir, P. (2006). Evidence from Amazonian forests is consistent with isohydric control of leaf water potential. Plant Cell and Environment, 29(2), 151-165.

Fyllas, N. M., Bentley, L. P., Shenkin, A., Asner, G. P., Atkin, O. K., Diaz, S., Enquist, B. J., Farfan-Rios, W., Gloor, E., Guerrieri, R., Huasco, W. H., Ishida, Y., Martin, R. E., Meir, P., Phillips, O., Salinas, N., Silman, M., Weerasinghe, L. K., Zaragoza-Castells, J., & Malhi, Y. (2017). Solar radiation and functional traits explain the decline of forest primary productivity along a tropical elevation gradient. Ecol Lett, 20(6), 730-740.

Galbraith, D., Levy, P. E., Sitch, S., Huntingford, C., Cox, P., Williams, M., & Meir, P. (2010). Multiple mechanisms of Amazonian forest biomass losses in three dynamic global vegetation models under climate change. New Phytol, 187(3), 647-665.

Goulden, M. L., Miller, S. D., da Rocha, H. R., Menton, M. C., de Freitas, H. C., Figueira, A. M. E. S., & de Sousa, C. A. D. (2004). Diel and seasonal patterns of tropical forest CO2 exchange. Ecological Applications, 14(4), S42-S54.

Grier, C. C., & Running, S. W. (1977). Leaf Area of Mature Northwestern Coniferous Forests - Relation to Site Water-Balance. Ecology, 58(4), 893-899.

Guan, K. Y., Pan, M., Li, H. B., Wolf, A., Wu, J., Medvigy, D., Caylor, K. K., Sheffield, J., Wood, E. F., Malhi, Y., Liang, M. L., Kimball, J. S., Saleska, S. R., Berry, J., Joiner, J., & Lyapustin, A. I. (2015). Photosynthetic seasonality of global tropical forests constrained by hydroclimate. Nature Geoscience, 8(4), 284-289.

Hilker, T., Lyapustin, A. I., Tucker, C. J., Hall, F. G., Myneni, R. B., Wang, Y., Bi, J., Mendes de Moura, Y., & Sellers, P. J. (2014). Vegetation dynamics and rainfall sensitivity of the Amazon. Proc Natl Acad Sci U S A, 111(45), 16041-16046.

Hutyra, L. R., Munger, J. W., Saleska, S. R., Gottlieb, E., Daube, B. C., Dunn, A. L., Amaral, D. F., De Camargo, P. B., & Wofsy, S. C. (2007). Seasonal controls on the exchange of carbon and water in an Amazonian rain forest. Journal of Geophysical Research: Biogeosciences, 112(G3).

Ichii, K., Hashimoto, H., White, M. A., Potters, C., Hutyra, L. R., Huete, A. R., Myneni, R. B., & Nemanis, R. R. (2007). Constraining rooting depths in tropical rainforests using satellite data and ecosystem modeling for accurate simulation of gross primary production seasonality. Global Change Biology, 13(1), 67-77.

Iio, A., Hikosaka, K., Anten, N. P. R., Nakagawa, Y., & Ito, A. (2014). Global dependence of field-observed leaf area index in woody species on climate: a systematic review. Global Ecology and Biogeography, 23(3), 274-285.

Jonckheere, I., Fleck, S., Nackaerts, K., Muys, B., Coppin, P., Weiss, M., & Baret, F. (2004). Review of methods for in situ leaf area index determination - Part I. Theories, sensors and hemispherical photography. Agricultural and Forest Meteorology, 121(1-2), 19-35.

Katul, G., Leuning, R., & Oren, R. (2003). Relationship between plant hydraulic and biochemical properties derived from a steady-state coupled water and carbon transport model. Plant, Cell & Environment, 26(3), 339-350.

López-Blanco, E., Lund, M., Williams, M., Tamstorf, M. P., Westergaard-Nielsen, A., Exbrayat, J.-F., Hansen, B. U., & Christensen, T. R. (2017). Exchange of CO 2 in Arctic tundra: impacts of meteorological variations and biological disturbance. Biogeosciences, 14(19), 4467-4483.

Maire, V., Wright, I. J., Prentice, I. C., Batjes, N. H., Bhaskar, R., van Bodegom, P. M., Cornwell, W. K., Ellsworth, D., Niinemets, Ü., & Ordonez, A. (2015). Global effects of soil and climate on leaf photosynthetic traits and rates. Global Ecology and Biogeography, 24(6), 706-717.

Malhi, Y., Aragao, L. E., Galbraith, D., Huntingford, C., Fisher, R., Zelazowski, P., Sitch, S., McSweeney, C., & Meir, P. (2009). Exploring the likelihood and mechanism of a climate-change-induced dieback of the Amazon rainforest. Proc Natl Acad Sci U S A, 106(49), 20610-20615.

Malhi, Y., Doughty, C. E., Goldsmith, G. R., Metcalfe, D. B., Girardin, C. A. J., Marthews, T. R., del Aguila-Pasquel, J., Aragao, L. E. O. C., Araujo-Murakami, A., Brando, P., da Costa, A. C. L.,

Silva-Espejo, J. E., Amezquita, F. F., Galbraith, D. R., Quesada, C. A., Rocha, W., Salinas-Revilla, N., Silverio, D., Meir, P., & Phillips, O. L. (2015). The linkages between photosynthesis, productivity, growth and biomass in lowland Amazonian forests. Global Change Biology, 21(6), 2283-2295.

Malhi, Y., Doughty, C. E., Goldsmith, G. R., Metcalfe, D. B., Girardin, C. A. J., Marthews, T. R., del Aguila-Pasquel, J., Aragao, L. E. O. C., Araujo-Murakami, A., Brando, P., da Costa, A. C. L., Silva-Espejo, J. E., Amezquita, F. F., Galbraith, D. R., Quesada, C. A., Rocha, W., Salinas-Revilla, N., Silverio, D., Meir, P., & Phillips, O. L. (2015). The linkages between photosynthesis, productivity, growth and biomass in lowland Amazonian forests. Global Change Biology, 21(6), 2283-2295.

Malhi, Y., Roberts, J. T., Betts, R. A., Killeen, T. J., Li, W., & Nobre, C. A. (2008). Climate change, deforestation, and the fate of the Amazon. Science, 319(5860), 169-172.

Malhi, Y., & Wright, J. (2004). Spatial patterns and recent trends in the climate of tropical rainforest regions. Philosophical Transactions of the Royal Society B: Biological Sciences, 359(1443), 311-329.

McMurtrie, R. E., & Dewar, R. C. (2011). Leaf-trait variation explained by the hypothesis that plants maximize their canopy carbon export over the lifespan of leaves. Tree Physiology, 31(9), 1007-1023.

McWilliam, A. L., Roberts, J. M., Cabral, O. M. R., Leitao, M., De Costa, A. C. L., Maitelli, G. T., & Zamparoni, C. (1993). Leaf area index and above-ground biomass of terra firme rain forest and adjacent clearings in Amazonia. Functional ecology, 310-317.

Meir, P., Brando, P. M., Nepstad, D., Vasconcelos, S., Costa, A. C. L., Davidson, E., Almeida, S., Fisher, R. A., Sotta, E. D., & Zarin, D. (2009). The effects of drought on Amazonian rain forests. Amazonia and Global Change, 429-449.

Meir, P., Mencuccini, M., & Dewar, R. C. (2015). Drought-related tree mortality: addressing the gaps in understanding and prediction. New Phytol, 207(1), 28-33.

Meir, P., Metcalfe, D. B., Costa, A. C., & Fisher, R. A. (2008). The fate of assimilated carbon during drought: impacts on respiration in Amazon rainforests. Philos Trans R Soc Lond B Biol Sci, 363(1498), 1849-1855.

Meir, P., Wood, T. E., Galbraith, D. R., Brando, P. M., Da Costa, A. C., Rowland, L., & Ferreira, L. V. (2015). Threshold Responses to Soil Moisture Deficit by Trees and Soil in Tropical Rain Forests: Insights from Field Experiments. Bioscience, 65(9), 882-892.

Meir, P., & Woodward, F. I. (2010). Amazonian rain forests and drought: response and vulnerability. New Phytol, 187(3), 553-557.

Mercado, L. M., Patino, S., Domingues, T. F., Fyllas, N. M., Weedon, G. P., Sitch, S., Quesada, C. A., Phillips, O. L., Aragao, L. E., Malhi, Y., Dolman, A. J., Restrepo-Coupe, N., Saleska, S. R., Baker, T. R., Almeida, S., Higuchi, N., & Lloyd, J. (2011). Variations in Amazon forest productivity correlated with foliar nutrients and modelled rates of photosynthetic carbon supply. Philos Trans R Soc Lond B Biol Sci, 366(1582), 3316-3329.

Metcalfe, D. B., Meir, P., Aragao, L., Malhi, Y., Da Costa, A. C. L., Braga, A., Gonçalves, P. H. L., de Athaydes, J., De Almeida, S. S., & Williams, M. (2007). Factors controlling spatio-temporal variation in carbon dioxide efflux from surface litter, roots, and soil organic matter at four rain forest sites in the eastern Amazon. Journal of Geophysical Research: Biogeosciences, 112(G4).

Metcalfe, D. B., Meir, P., Aragao, L. E. O. C., da Costa, A. C. L., Braga, A. P., Goncalves, P. H. L., Silva, J. D., de Almeida, S. S., Dawson, L. A., Malhi, Y., & Williams, M. (2008). The effects of water availability on root growth and morphology in an Amazon rainforest. Plant and Soil, 311(1-2), 189-199.

Moore, C. E., Beringer, J., Donohue, R. J., Evans, B., Exbrayat, J. F., Hutley, L. B., & Tapper, N. J. (2018). Seasonal, interannual and decadal drivers of tree and grass productivity in an Australian tropical savanna. Glob Chang Biol, 24(6), 2530-2544.

Morton, D. C. (2016). FOREST CARBON FLUXES A satellite perspective. Nature Climate Change, 6(4), 346-348.

Myneni, R. B., Yang, W., Nemani, R. R., Huete, A. R., Dickinson, R. E., Knyazikhin, Y., Didan, K., Fu, R., Negron Juarez, R. I., Saatchi, S. S., Hashimoto, H., Ichii, K., Shabanov, N. V., Tan, B., Ratana, P., Privette, J. L., Morisette, J. T., Vermote, E. F., Roy, D. P., Wolfe, R. E., Friedl, M. A., Running, S. W., Votava, P., El-Saleous, N., Devadiga, S., Su, Y., & Salomonson, V. V. (2007). Large seasonal swings in leaf area of Amazon rainforests. Proc Natl Acad Sci U S A, 104(12), 4820-4823.

Nepstad, D. C., Decarvalho, C. R., Davidson, E. A., Jipp, P. H., Lefebvre, P. A., Negreiros, G. H., Dasilva, E. D., Stone, T. A., Trumbore, S. E., & Vieira, S. (1994). The Role of Deep Roots in the Hydrological and Carbon Cycles of Amazonian Forests and Pastures. Nature, 372(6507), 666-669.

Nepstad, D. C., Moutinho, P., Dias, M. B., Davidson, E., Cardinot, G., Markewitz, D., Figueiredo, R., Vianna, N., Chambers, J., Ray, D., Guerreiros, J. B., Lefebvre, P., Sternberg, L., Moreira, M., Barros, L., Ishida, F. Y., Tohlver, I., Belk, E., Kalif, K., & Schwalbe, K. (2002). The effects of partial throughfall exclusion on canopy processes, aboveground production, and biogeochemistry of an Amazon forest. Journal of Geophysical Research-Atmospheres, 107(D20).

Nepstad, D. C., Tohver, I. M., Ray, D., Moutinho, P., & Cardinot, G. (2007). Mortality of large trees and lianas following experimental drought in an Amazon forest. Ecology, 88(9), 2259-2269.

Nepstad, D. C., Tohver, I. M., Ray, D., Moutinho, P., & Cardinot, G. (2007). Mortality of large trees and lianas following experimental drought in an Amazon forest. Ecology, 88(9), 2259-2269.

Osnas, J. L., Lichstein, J. W., Reich, P. B., & Pacala, S. W. (2013). Global leaf trait relationships: mass, area, and the leaf economics spectrum. Science, 340(6133), 741-744.

Pedregosa, F., Varoquaux, G., Gramfort, A., Michel, V., Thirion, B., Grisel, O., Blondel, M., Prettenhofer, P., Weiss, R., Dubourg, V., Vanderplas, J., Passos, A., Cournapeau, D., Brucher, M., Perrot, M., & Duchesnay, E. (2011). Scikit-learn: Machine Learning in Python. Journal of machine learning research, 12(Oct), 2825-2830.

Pettorelli, N., Buhne, H. S. T., Tulloch, A., Dubois, G., Macinnis-Ng, C., Queiros, A. M., Keith, D. A., Wegmann, M., Schrodt, F., Stellmes, M., Sonnenschein, R., Geller, G. N., Roy, S., Somers, B., Murray, N., Bland, L., Geijzendorffer, I., Kerr, J. T., Broszeit, S., Leitao, P. J., Duncan, C., El Serafy, G., He, K. S., Blanchard, J. L., Lucas, R., Mairota, P., Webb, T. J., & Nicholson, E. (2018). Satellite remote sensing of ecosystem functions: opportunities, challenges and way forward. Remote Sensing in Ecology and Conservation, 4(2), 71-93.

Phillips, O. L., Aragao, L. E., Lewis, S. L., Fisher, J. B., Lloyd, J., Lopez-Gonzalez, G., Malhi, Y., Monteagudo, A., Peacock, J., Quesada, C. A., van der Heijden, G., Almeida, S., Amaral, I.,

Arroyo, L., Aymard, G., Baker, T. R., Banki, O., Blanc, L., Bonal, D., Brando, P., Chave, J., de Oliveira, A. C., Cardozo, N. D., Czimczik, C. I., Feldpausch, T. R., Freitas, M. A., Gloor, E., Higuchi, N., Jimenez, E., Lloyd, G., Meir, P., Mendoza, C., Morel, A., Neill, D. A., Nepstad, D., Patino, S., Penuela, M. C., Prieto, A., Ramirez, F., Schwarz, M., Silva, J., Silveira, M., Thomas, A. S., Steege, H. T., Stropp, J., Vasquez, R., Zelazowski, P., Alvarez Davila, E., Andelman, S., Andrade, A., Chao, K. J., Erwin, T., Di Fiore, A., Honorio, C. E., Keeling, H., Killeen, T. J., Laurance, W. F., Pena Cruz, A., Pitman, N. C., Nunez Vargas, P., Ramirez-Angulo, H., Rudas, A., Salamao, R., Silva, N., Terborgh, J., & Torres-Lezama, A. (2009). Drought sensitivity of the Amazon rainforest. Science, 323(5919), 1344-1347.

Phillips, O. L., Aragao, L. E., Lewis, S. L., Fisher, J. B., Lloyd, J., Lopez-Gonzalez, G., Malhi, Y., Monteagudo, A., Peacock, J., Quesada, C. A., van der Heijden, G., Almeida, S., Amaral, I., Arroyo, L., Aymard, G., Baker, T. R., Banki, O., Blanc, L., Bonal, D., Brando, P., Chave, J., de Oliveira, A. C., Cardozo, N. D., Czimczik, C. I., Feldpausch, T. R., Freitas, M. A., Gloor, E., Higuchi, N., Jimenez, E., Lloyd, G., Meir, P., Mendoza, C., Morel, A., Neill, D. A., Nepstad, D., Patino, S., Penuela, M. C., Prieto, A., Ramirez, F., Schwarz, M., Silva, J., Silveira, M., Thomas, A. S., Steege, H. T., Stropp, J., Vasquez, R., Zelazowski, P., Alvarez Davila, E., Andelman, S., Andrade, A., Chao, K. J., Erwin, T., Di Fiore, A., Honorio, C. E., Keeling, H., Killeen, T. J., Laurance, W. F., Pena Cruz, A., Pitman, N. C., Nunez Vargas, P., Ramirez-Angulo, H., Rudas, A., Salamao, R., Silva, N., Terborgh, J., & Torres-Lezama, A. (2009). Drought sensitivity of the Amazon rainforest. Science, 323(5919), 1344-1347.

Powell, T. L., Galbraith, D. R., Christoffersen, B. O., Harper, A., Imbuzeiro, H. M., Rowland, L., Almeida, S., Brando, P. M., da Costa, A. C., Costa, M. H., Levine, N. M., Malhi, Y., Saleska, S. R., Sotta, E., Williams, M., Meir, P., & Moorcroft, P. R. (2013). Confronting model predictions of carbon fluxes with measurements of Amazon forests subjected to experimental drought. New Phytol, 200(2), 350-365.

Quesada, C. A., Lloyd, J., Schwarz, M., Baker, T. R., Phillips, O. L., Patiño, S., Czimczik, C., Hodnett, M. G., Herrera, R., & Arneth, A. (2009). Regional and large-scale patterns in Amazon forest structure and function are mediated by variations in soil physical and chemical properties. Biogeosciences Discussion, 6, 3993-4057.

Quesada, C. A., Phillips, O. L., Schwarz, M., Czimczik, C. I., Baker, T. R., Patino, S., Fyllas, N. M., Hodnett, M. G., Herrera, R., Almeida, S., Davila, E. A., Arneth, A., Arroyo, L., Chao, K. J., Dezzeo, N., Erwin, T., di Fiore, A., Higuchi, N., Coronado, E. H., Jimenez, E. M., Killeen, T.,

Lezama, A. T., Lloyd, G., Lopez-Gonzalez, G., Luizao, F. J., Malhi, Y., Monteagudo, A., Neill, D. A., Vargas, P. N., Paiva, R., Peacock, J., Penuela, M. C., Cruz, A. P., Pitman, N., Priante, N., Prieto, A., Ramirez, H., Rudas, A., Salomao, R., Santos, A. J. B., Schmerler, J., Silva, N., Silveira, M., Vasquez, R., Vieira, I., Terborgh, J., & Lloyd, J. (2012). Basin-wide variations in Amazon forest structure and function are mediated by both soils and climate. Biogeosciences, 9(6), 2203-2246.

Reich, P. B., Uhl, C., Walters, M. B., & Ellsworth, D. S. (1991). Leaf lifespan as a determinant of leaf structure and function among 23 Amazonian tree species. Oecologia, 86(1), 16-24.

Restrepo-Coupe, N., da Rocha, H. R., Hutyra, L. R., da Araujo, A. C., Borma, L. S., Christoffersen, B., Cabral, O. M. R., de Camargo, P. B., Cardoso, F. L., & da Costa, A. C. L. (2013). What drives the seasonality of photosynthesis across the Amazon basin? A cross-site analysis of eddy flux tower measurements from the Brasil flux network. Agricultural and Forest Meteorology, 182, 128-144.

Restrepo-Coupe, N., Levine, N. M., Christoffersen, B. O., Albert, L. P., Wu, J., Costa, M. H., Galbraith, D., Imbuzeiro, H., Martins, G., & Araujo, A. C. (2017). Do dynamic global vegetation models capture the seasonality of carbon fluxes in the Amazon basin? A data-model intercomparison. Global Change Biology, 23(1), 191-208.

Rowland, L., Da Costa, A. C. L., Galbraith, D. R., Oliveira, R. S., Binks, O. J., Oliveira, A. A. R., Pullen, A. M., Doughty, C. E., Metcalfe, D. B., & Vasconcelos, S. S. (2015). Death from drought in tropical forests is triggered by hydraulics not carbon starvation. Nature, 528(7580), 119-122.

Rowland, L., da Costa, A. C. L., Oliveira, A. A. R., Almeida, S. S., Ferreira, L. V., Malhi, Y., Metcalfe, D. B., Mencuccini, M., Grace, J., & Meir, P. (2018). Shock and stabilisation following long-term drought in tropical forest from 15 years of litterfall dynamics. Journal of ecology, 106(4), 1673-1682.

Rowland, L., Harper, A., Christoffersen, B. O., Galbraith, D. R., Imbuzeiro, H. M. A., Powell, T. L., Doughty, C., Levine, N. M., Malhi, Y., Saleska, S. R., Moorcroft, P. R., Meir, P., & Williams, M. (2015). Modelling climate change responses in tropical forests: similar productivity estimates across five models, but different mechanisms and responses. Geoscientific Model Development, 8(4), 1097-1110.

Rowland, L., Hill, T. C., Stahl, C., Siebicke, L., Burban, B., Zaragoza-Castells, J., Ponton, S., Bonal, D., Meir, P., & Williams, M. (2014). Evidence for strong seasonality in the carbon storage and carbon use efficiency of an Amazonian forest. Global Change Biology, 20(3), 979-991.

Sakschewski, B., von Bloh, W., Boit, A., Poorter, L., Pena-Claros, M., Heinke, J., Joshi, J., & Thonicke, K. (2016). Resilience of Amazon forests emerges from plant trait diversity. Nature Climate Change, 6(11), 1032-+.

Saleska, S. R., Miller, S. D., Matross, D. M., Goulden, M. L., Wofsy, S. C., da Rocha, H. R., de Camargo, P. B., Crill, P., Daube, B. C., de Freitas, H. C., Hutyra, L., Keller, M., Kirchhoff, V., Menton, M., Munger, J. W., Pyle, E. H., Rice, A. H., & Silva, H. (2003). Carbon in Amazon forests: unexpected seasonal fluxes and disturbance-induced losses. Science, 302(5650), 1554-1557.

Santiago, L. S., Kitajima, K., Wright, S. J., & Mulkey, S. S. (2004). Coordinated changes in photosynthesis, water relations and leaf nutritional traits of canopy trees along a precipitation gradient in lowland tropical forest. Oecologia, 139(4), 495-502.

Saxton, K. E., Rawls, W. J., Romberger, J. S., & Papendick, R. I. (1986). Estimating generalized soil-water characteristics from texture 1. Soil Science Society of America Journal, 50(4), 1031-1036.

Schleppi, P., Thimonier, A., & Walthert, L. (2011). Estimating leaf area index of mature temperate forests using regressions on site and vegetation data. Forest Ecology and Management, 261(3), 601-610.

Schuldt, B., Leuschner, C., Horna, V., Moser, G., Koler, M., van Straaten, O., & Barus, H. (2011). Change in hydraulic properties and leaf traits in a tall rainforest tree species subjected to long-term throughfall exclusion in the perhumid tropics. Biogeosciences, 8(8), 2179-2194.

Sperry, J. S., Hacke, U. G., Oren, R., & Comstock, J. P. (2002). Water deficits and hydraulic limits to leaf water supply. Plant Cell and Environment, 25(2), 251-263.

Tyree, M. T., & Sperry, J. S. (1988). Do woody plants operate near the point of catastrophic xylem dysfunction caused by dynamic water stress? Answers from a model. Plant physiology, 88(3), 574-580.

Von Randow, C., Zeri, M., Restrepo-Coupe, N., Muza, M. N., de Gonçalves, L. G. G., Costa, M. H., Araujo, A. C., Manzi, A. O., da Rocha, H. R., & Saleska, S. R. (2013). Inter-annual variability of carbon and water fluxes in Amazonian forest, Cerrado and pasture sites, as simulated by terrestrial biosphere models. Agricultural and Forest Meteorology, 182, 145-155.

Wagner, F. H., Herault, B., Rossi, V., Hilker, T., Maeda, E. E., Sanchez, A., Lyapustin, A. I., Galvao, L. S., Wang, Y., & Aragao, L. (2017). Climate drivers of the Amazon forest greening. PloS one, 12(7), e0180932.

Weiss, M., Baret, F., Smith, G. J., Jonckheere, I., & Coppin, P. (2004). Review of methods for in situ leaf area index (LAI) determination Part II. Estimation of LAI, errors and sampling. Agricultural and Forest Meteorology, 121(1-2), 37-53.

Williams, M., Malhi, Y., Nobre, A. D., Rastetter, E. B., Grace, J., & Pereira, M. G. P. (1998). Seasonal variation in net carbon exchange and evapotranspiration in a Brazilian rain forest: a modelling analysis. Plant Cell and Environment, 21(10), 953-968.

Williams, M., Rastetter, E. B., Fernandes, D. N., Goulden, M. L., Wofsy, S. C., Shaver, G. R., Melillo, J. M., Munger, J. W., Fan, S. M., & Nadelhoffer, K. J. (1996). Modelling the soil-plant-atmosphere continuum in a Quercus–Acer stand at Harvard Forest: the regulation of stomatal conductance by light, nitrogen and soil/plant hydraulic properties. Plant, Cell & Environment, 19(8), 911-927.

Wright, I. J., Reich, P. B., Westoby, M., Ackerly, D. D., Baruch, Z., Bongers, F., Cavender-Bares, J., Chapin, T., Cornelissen, J. H., Diemer, M., Flexas, J., Garnier, E., Groom, P. K., Gulias, J., Hikosaka, K., Lamont, B. B., Lee, T., Lee, W., Lusk, C., Midgley, J. J., Navas, M. L., Niinemets, U., Oleksyn, J., Osada, N., Poorter, H., Poot, P., Prior, L., Pyankov, V. I., Roumet, C., Thomas, S. C., Tjoelker, M. G., Veneklaas, E. J., & Villar, R. (2004). The worldwide leaf economics spectrum. Nature, 428(6985), 821-827.

Wright, I. J., Reich, P. B., Westoby, M., Ackerly, D. D., Baruch, Z., Bongers, F., Cavender-Bares, J., Chapin, T., Cornelissen, J. H., Diemer, M., Flexas, J., Garnier, E., Groom, P. K., Gulias, J., Hikosaka, K., Lamont, B. B., Lee, T., Lee, W., Lusk, C., Midgley, J. J., Navas, M. L., Niinemets, U., Oleksyn, J., Osada, N., Poorter, H., Poot, P., Prior, L., Pyankov, V. I., Roumet, C., Thomas, S. C., Tjoelker, M. G., Veneklaas, E. J., & Villar, R. (2004). The worldwide leaf economics spectrum. Nature, 428(6985), 821-827.

Wright, J. K., Williams, M., Starr, G., McGee, J., & Mitchell, R. J. (2013). Measured and modelled leaf and stand-scale productivity across a soil moisture gradient and a severe drought. Plant Cell and Environment, 36(2), 467-483.

Wright, J. K., Williams, M., Starr, G., McGee, J., & Mitchell, R. J. (2013). Measured and modelled leaf and stand-scale productivity across a soil moisture gradient and a severe drought. Plant Cell and Environment, 36(2), 467-483.

Wu, J., Albert, L. P., Lopes, A. P., Restrepo-Coupe, N., Hayek, M., Wiedemann, K. T., Guan, K., Stark, S. C., Christoffersen, B., Prohaska, N., Tavares, J. V., Marostica, S., Kobayashi, H., Ferreira, M. L., Campos, K. S., da Silva, R., Brando, P. M., Dye, D. G., Huxman, T. E., Huete, A. R., Nelson, B. W., & Saleska, S. R. (2016). Leaf development and demography explain photosynthetic seasonality in Amazon evergreen forests. Science, 351(6276), 972-976.

Wu, J., Guan, K. Y., Hayek, M., Restrepo-Coupe, N., Wiedemann, K. T., Xu, X. T., Wehr, R., Christoffersen, B. O., Miao, G. F., da Silva, R., de Araujo, A. C., Oliviera, R. C., Camargo, P. B., Monson, R. K., Huete, A. R., & Saleska, S. R. (2017). Partitioning controls on Amazon forest photosynthesis between environmental and biotic factors at hourly to interannual timescales. Global Change Biology, 23(3), 1240-1257.

Zhang, K., Castanho, A. D. D., Galbraith, D. R., Moghim, S., Levine, N. M., Bras, R. L., Coe, M. T., Costa, M. H., Malhi, Y., Longo, M., Knox, R. G., McKnight, S., Wang, J. F., & Moorcroft, P. R. (2015). The fate of Amazonian ecosystems over the coming century arising from changes in climate, atmospheric CO2, and land use. Global Change Biology, 21(7), 2569-2587.

Zhou, L., Tian, Y., Myneni, R. B., Ciais, P., Saatchi, S., Liu, Y. Y., Piao, S., Chen, H., Vermote, E. F., Song, C., & Hwang, T. (2014). Widespread decline of Congo rainforest greenness in the past decade. Nature, 509(7498), 86-90.

4. Maximisation of Net Canopy Carbon Export Explains LAI across an Amazon Rainfall Gradient

4.1 Abstract

Canopy leaf area underpins ecosystem functioning, yet the mechanisms coupling LAI and climate remain unclear. For example, LAI increases with precipitation across Amazon forests. Here we ask why LAI increases with water availability, and how carbon cycle feedbacks and leaf traits shape the interaction? We calibrated and applied the Soil Plant Atmosphere model to plots with detailed measurements of carbon fluxes, leaf traits and LAI across an Amazon precipitation gradient, to determine nominal site C budgets. For each study site, we then compared the nominal carbon budgets to alternative, experimental budgets derived using LAI time-series of all other sites, keeping meteorology, soil, vegetation structure and leaf traits unchanged. We found that the increase in LAI with precipitation was best explained by maximisation of net canopy carbon export (NCE, photosynthesis minus the cost of leaf growth and maintenance). For core forests, increased foliar carbon costs were remunerative and simulated photosynthesis was maximised by high LAI. In contrast, higher LAI strategies were deleterious for transitional forests, as the carbon cost of leaf construction and maintenance was disproportional to photosynthesis achieved. Lower NCE resulted in a decrease in simulated NPP allocated to fine roots and wood, constraining water acquisition and consequently photosynthesis through carbon cycle feedbacks. Leaf traits also had a determinate effect on the interaction between LAI and NCE, shifting total NCE and the LAI at which NCE was maximised. Across the gradient, observed leaf trait strategies underwent a shift from fast to slow (where fast leaf traits are a cohort of high photosynthetic capacitance, high metabolic rate, high nitrogen content, low LMA and short lifespan and vice versa for slow leaf traits) as precipitation increased. Our modelling showed that for transitional forests, fast leaf traits allowed forests to maximise photosynthesis during the wet season, and minimise carbon losses during dry periods. Conversely, for core forests there was no significant

difference between modelled NCE under fast and slow leaf trait strategies. We demonstrate that spatial trends in LAI can be successfully predicted using an optimality approach on NCE, and highlight how leaf trait distributions fundamentally shape plant and canopy responses to climate.

4.2 Introduction

Leaf area index (LAI, the total leaf area per unit ground area) determines light interception and the surface area for potential photosynthesis, driving significant spatial and temporal variability in carbon assimilation (Caldararu *et al*., 2012; Muraoka *et al*., 2010; Street *et al*., 2007; Xu and Baldocchi, 2004). Through its role in governing plant productivity, LAI has a major impact on nutrient cycling and trophic interactions (Pettorelli *et al*., 2011). Variation in LAI also has cascading consequences for water cycling and heat transfer, via the efflux of water vapour through stomates, and the absorption of solar radiation and emission of long wave radiation, which together promote climate feedbacks (Bonan, 2008; Granier *et al*., 2000; Kergoat *et al*., 2002; Mu *et al*., 2007; Watson *et al*., 1999; Williams *et al*., 1998; Wilson and Baldocchi, 2000). Accordingly, LAI is a key property in the investigation of global biogeochemical cycles by both field and modelling studies (Baldocchi *et al*., 1996; Carswell *et al*., 2002; Sellers *et al*., 1997).

Understanding variation in LAI across Amazonian forests, and how it might change in the future, is of critical importance. The Amazon basin is a key component of the global carbon cycle (Malhi *et al*., 2008; Pan *et al*., 2011), supports biodiversity en masse (Dirzo and Raven, 2003; Mittermeier *et al*., 1998; Rull, 2011), and has a regulatory effect over its own climate system (Costa and Foley, 2000; Dickinson and Kennedy, 1992; Fu and Li, 2004; Shukla *et al*., 1990). Previous work investigating photosynthetic drivers across lowland Amazonia, found that LAI varied directionally with mean annual precipitation (R^2=0.42, p=0.08, RMSE=0.87, Figure 4.1), and accounted for 36% of variation in photosynthesis across the study sites (Chapter 3). Evidence linking precipitation regime and LAI (Grier and Running, 1977; Iio *et al*., 2014; Schleppi *et al*., 2011; Wright *et al*., 2013) suggests this interaction transcends ecosystem type, and plays a pivotal role in shaping forests' response to water availability.

Temporal shifts in precipitation have been reported to induce LAI change. A decline in annual precipitation has already led to a reported reduction in vegetation greenness (associated with leaf area) across large parts of Amazonia (Hilker *et al*., 2014). Similar responses to drying have been reported in Hawaiian and Congolese tropical forests (Barbosa *et al*., 2017; Zhou *et al*.,

2014), suggesting the interaction is pan-tropical. Across shorter time scales, Saatchi *et al*. (2013) documented a decline in canopy structure for western Amazon forests in response to the 2005 drought. Analogously, throughfall exclusion experiments report a drop in LAI under reduced water availability (Brando *et al*., 2008; Meir *et al*., 2015b), as a result of lower leaf production (Nepstad *et al*., 2002; Schuldt *et al*., 2011). Transitions in vegetation type are likely determined by the relationship between leaf area and precipitation, with declines below critical rainfall thresholds leading to increased mortality and replacement by new more drought-tolerant vegetation (Meir *et al*., 2015a). Despite evidence of spatial and temporal LAI responses to precipitation, the mechanism underlying the interaction remains unclear.

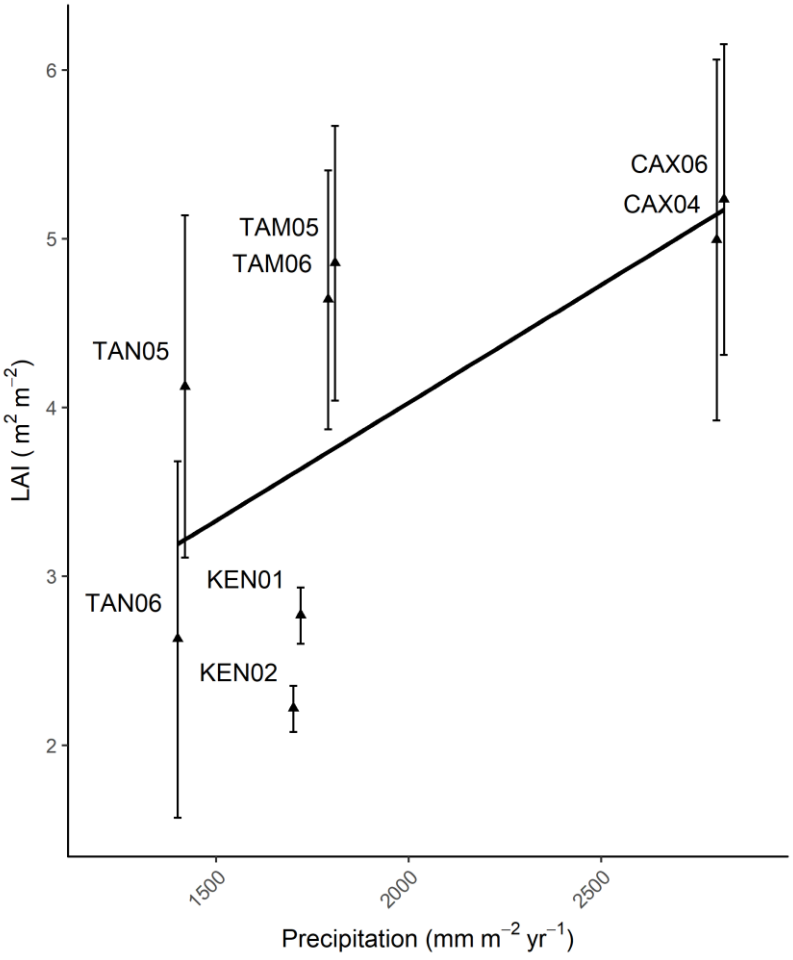

Figure 4.1. Field estimated mean annual LAI relative to mean annual precipitation for Global Ecosystems Monitoring network permanent sample plots. Two 1ha permanent sample plots are situated at each of the four locations. Precipitation values are marginally offset around the true value to allow clarity around the distribution of error bars for plots at the same location. Values presented are averages from the years 2009-2010. Error bars represent standard error. (R^2=0.42, p=0.08, RMSE=0.87).

Current theory suggests that LAI expression can be understood through plant economics (Franklin, 2007; McMurtrie *et al*., 2008), but direct application with appropriate data constraint is missing. Fundamental information on C uptake, allocation, metabolism and plant traits is lacking. As a result, modelling the economics of tropical leaf area remains a key challenge (De Weirdt *et al*., 2012; Kim *et al*., 2012). Poorly represented canopy dynamics continue to cause disparity between simulated and measured carbon fluxes (Powell *et al*., 2013; Restrepo-Coupe *et al*., 2017; Verbeeck *et al*., 2011). Forest canopies are expected to adapt to local climatic conditions and maximise light capture, whilst avoiding severe soil water depletion in line with hydrological equilibrium theory (Kergoat, 1998). To support a canopy at a given LAI the carbon gain via photosynthesis must outweigh the cost of growth and maintenance respiration over the lifetime of the leaf (McMurtrie and Dewar, 2011). Simple leaf phenology models testing this hypothesis against remote sensing data have had success at a coarse scale (Caldararu *et al*., 2012; Caldararu *et al*., 2014; Caldararu *et al*., 2016). However, the interaction between LAI and water availability is likely dependent on a number of key factors not yet taken into account, such as carbon cycle feedbacks and the spatial distribution of co-varying leaf traits (McMurtrie and Dewar, 2011; Poorter and Bongers, 2006; Reich *et al*., 1999; Wright *et al*., 2004).

C allocation feedbacks could drive optimisation of LAI across the precipitation gradient (Figure 4.2). Net canopy carbon export (NCE), defined here as photosynthesis minus the costs of leaf growth and maintenance, determines the amount of photosynthates available for net primary production, and consequently shapes resource acquisition, future assimilation and NCE potential (Bloom *et al*., 1985; Lacointe, 2000). If changes in NPP allocated to the canopy are not remunerative, a decline in root and wood growth could be induced. A consequent reduction in wood biomass could limit competitiveness for light (Coomes *et al*., 2011). Reduced root biomass could restrict water acquisition (Jackson *et al*., 2000), constraining stomatal conductance and photosynthetic activity, further reinforcing feedbacks. McMurtrie and Dewar (2011) propose that NCE maximisation therefore governs canopy optimisation. Yet the relative effect of carbon cycle feedbacks on the LAI-precipitation interaction remains unclear, the quantification of which requires detailed model-data coupling.

Leaf traits shape carbon economics through their effect on carbon assimilation rate and the carbon cost of leaf growth and maintenance. Across the Amazon basin, leaf mass per area (LMA) varies near nine fold, whilst leaf nitrogen content, associated with photosynthetic

capacity, varies near six fold (Fyllas *et al*., 2009). Leaf lifespan can range from less than two months to over four years (Reich *et al*., 1991). Evergreen species with longer-lived leaves typically dominate as precipitation increases (notwithstanding the effects of temperature seasonality), whilst more deciduous species with short-lived leaves prosper in drier forests. Concurrently, photosynthetic capacity, metabolic rate and leaf nitrogen content decline, and LMA increases, as precipitation increases across tropical forests (Atkin *et al*., 2015; Givnish, 2002; Kikuzawa, 1991; Maire *et al*., 2015; Santiago and Mulkey, 2005). Greater deciduousness in dry forests is thought to allow the maximisation of photosynthesis during the wet season when water limitation is low (Santiago *et al*., 2004), whilst simultaneous higher leaf nitrogen content is thought to promote increased water use efficiency (Wright *et al*., 2001; Wright and Westoby, 2002). It is therefore critical to account for directional variation in leaf traits when investigating the interaction between LAI and precipitation across Amazon forests.

To investigate carbon dynamics underpinning the LAI-precipitation interaction, we apply the soil plant atmosphere model (SPA) to analyse the C cycle and its optimisation for forest plots across an Amazonian rainfall gradient (1400-2800mm yr^{-1}). Permanent sample plots used are part of the global ecosystems monitoring network (GEM) and provide unprecedented, detailed measurements of carbon fluxes, LAI, and leaf traits (Doughty *et al*., 2015; Malhi *et al*., 2015). Previous work calibrating SPA to plots across the precipitation gradient, has shown that modelled carbon dynamics are consistent with field estimates (Chapter 3), and therefore provide a basis for model experimentation of C economics.

To develop our understanding of the mechanisms driving LAI trends we ask the following:

1. Why does LAI spatially co-vary with precipitation across Amazon forests?

2. Do carbon-cycle feedbacks have a determinate role in driving the LAI-precipitation interaction?

3. How do leaf traits shape the interaction between LAI and precipitation?

We hypothesise that the increase in LAI with precipitation across Amazon forests is explained by the maximisation of net canopy carbon export (NCE). As precipitation declines, investment of carbon into the canopy is less remunerative. Physiological constraints reduce photosynthetic returns, whilst leaf growth and respiratory costs are maintained, resulting in overall lower NCE. Leaf area is then regulated by carbon economics towards lower values, in

accordance with the local hydraulic environment, to maximise NCE, and thereby explaining observed spatial trends in LAI.

We predict that carbon cycle feedbacks will have a determinate effect on the LAI-precipitation interaction. The allocation of photosynthates between above and belowground components determines the relative acquisition of water and light (we do not take nutrient cycling into account in this analysis). If photosynthates available for growth are reduced (due to lower NCE), root growth and consequently water acquisition is constrained. Lower water acquisition further restricts stomatal conductance and photosynthesis, reinforcing lowered NCE through a positive feedback. We therefore hypothesise that a structural response pathway (Figure 4.2), strengthens the interaction between LAI, NCE and precipitation, via changes in root mass and water acquisition.

We hypothesise that leaf traits will shape the LAI-precipitation interaction, via a determinate effect on the LAI at which NCE is maximised. Leaf traits regulate carbon assimilation rate via photosynthetic capacity, and the carbon costs of leaf construction and maintenance respiration, LMA and leaf lifespan, thereby fixing carbon economic thresholds. Across the precipitation gradient, leaf traits shift from a 'fast' trait cohort (high photosynthetic capacity, high respiration rate, low LMA and low leaf lifespan) to a 'slow' trait cohort (low photosynthetic capacity, low respiration rate, high LMA and high leaf lifespan) (Table 4.1). We expect that low LAI coupled with fast leaf traits typical of transitional forests, enables maximal assimilation during the shorter growing season, thereby increasing realised NCE. For core forests, we predict that high LAI and typical slow leaf traits allow forests to maximise NCE throughout the year by minimising maintenance costs.

The aim of this research is to improve understanding of the C economics of LAI-precipitation interactions. Projected changes in rainfall across the Amazon basin and a poor understanding of leaf area drivers, causes uncertainty in model estimates of the future carbon balance. Our goal is to reduce uncertainty by testing the value in applying optimal response analyses.

Table 4.1. Mean annual LAI (LAI strategy) and leaf traits (leaf N content, photosynthetic capacity and LMA) used to parameterise SPA (and their sources), and SPA calibrated leaf litterfall parameters (leaf fall day, leaf lifespan and leaf fall period) for Amazon permanent sample plots across a mean annual precipitation gradient. Leaf fall day is the day of year leaf fall is initiated, leaf lifespan reflects potential lifespan of leaves and leaf fall period is the number of days over which leaf fall occurs. Leaf litterfall parameters were calibrated against GEM field estimates.

	Mean annual LAI (m^2 m^{-2})	Leaf N content (g m^{-2})	κ_c (µmol C gN^{-1} s^{-1})	κ_J (µmol C gN^{-1} s^{-1})	LMA (g m^{-2})	Sources	Leaf Fall Day (day of year)	Leaf Lifespan (years)	Leaf Fall Period (days)
CAX04	4.99	1.82	15.4	27.7	93.0	Fyllas *et al.*, 2009	210	3	150
CAX06	5.23	2.12	13.2	23.8	87.4	Kattge, *et al.*, 2011; Fyllas *et al.*, 2009	190	1.45	100
TAM05	4.86	2.42	28.9	49.9	101.0	Fyllas *et al.*, 2009	220	1.3	130
TAM06	4.64	2.38	29.0	50.3	96.0	Fyllas *et al.*, 2009	230	1.42	100
KEN01	2.77	2.12	29.3	51.6	52.5	Kattge, *et al.*, 2011; Poorter & Bongos 2006	200	1.05	100
KEN02	2.21	2.31	28.9	50.3	41.8	Kattge, *et al.*, 2011; Poorter & Bongos 2006	180	1.01	100
TAN05	4.13	2.01	30.0	53.1	64.4	Kattge, *et al.*, 2011; P.Brando pcom	180	1.04	120
TAN06	2.62	2.01	29.9	52.8	60.5	Kattge, *et al.*, 2011; P.Brando pcom	120	1.005	160

4.3 Methods

The Soil Plant Atmosphere model (SPA) was calibrated and validated using field data from eight permanent sample plots across the Amazon basin (located at Caxiuanã, Tambopata, Kenia and Tanguro), experiencing a gradient in mean annual precipitation of 1400 to 2800mm yr^{-1}. We then undertook a series of model experiments to explore: (i) the interaction between LAI, precipitation and net canopy carbon export (NCE), (ii) the effect of carbon cycle feedbacks on the LAI-NCE interaction across the precipitation gradient, and (iii) the role of leaf traits in shaping LAI optimality and total NCE. Plot characteristics, the SPA model, and data used in model calibration and validation are described in detail in Chapter 2. Here, we give a brief review of model-data constraints, model calibration and validation (presented in full in Chapter 3), highlighting key information relevant to the posed experiments, before detailing model experiments conducted.

4.3.1 Model-Data Constraints

Field estimated monthly LAI time-series were used to constrain SPA simulated foliar carbon stocks. Following leaf litterfall at each timestep, leaf NPP was calculated as the difference between observed (LAI × leaf carbon mass per area) and SPA simulated foliar carbon stocks. NPP was allocated to leaves before wood, coarse roots and fine roots. If leaf NPP requirements exceeded total NPP (day^{-1}), carbon from the non-structural carbon pool was redirected to foliar stocks. Constraining modelled LAI to field estimates allowed us to accurately quantify the effect of differences in leaf area on carbon dynamics through subsequent model experiments.

4.3.2 Model Calibration and Validation

We calibrated and validated SPA for each permanent sample plot using field data from the Global Ecosystems monitoring network. SPA was parameterised using local estimates of leaf traits, the fraction of NPP allocated to leaves, fine roots, coarse roots and wood, and their carbon stocks, soil properties, root properties, and wood and root respiration coefficients. The model was constrained by LAI time-series, and ran using local hourly meteorological data. Leaf traits used in the parameterisation of SPA include leaf nitrogen content, LMA and photosynthetic capacity (κ_c, V_{cmax} normalised by leaf N, and κ_j, J_{max} normalised by leaf N) (Table 4.1). Field estimates of leaf N content and LMA are presented in Fyllas *et al.* (2009), or where absent are derived from trait databases using plot species composition (Kattge *et al*., 2011;

Poorter and Bongers, 2006). Photosynthetic capacity estimates (κ_C and κ_J) were field measurements (Caxiuanã only) or derived from leaf N content (Walker *et al*., 2014). Monthly LAI estimates used to constrain SPA simulations were derived from hemispherical photographs.

SPA simulated soil moisture, leaf litterfall, wood turnover and fine root turnover were calibrated against field estimates. The equation in SPA relating soil texture to water retention was calibrated to better represent tropical soils by adjusting the slope of the interaction (Saxton *et al*., 1986) (eqn. 10). Modelled leaf litterfall was calibrated against field estimates to retrieve parameters on leaf fall timing, duration and leaf lifespan (see Chapter 3, Table 3.4). SPA estimates of wood and fine root turnover rates were calibrated assuming steady state conditions (i.e. turnover rate was proportional to component NPP and carbon stock). Following model calibration, uncertainty estimates were calculated by simulating SPA at each plot under the upper and lower standard error of field LAI measurements. SPA calibrations were validated against field estimates of photosynthesis, respiration and NPP using linear regression models and comprehensive component specific comparisons.

4.3.3 Model Experiments

The Interaction between LAI, Precipitation and Net Canopy Carbon Export

We explored the interaction between LAI and NCE across the precipitation gradient. For each forest plot, keeping meteorology, soil, vegetation structure and leaf traits at nominal values (Table 4.1), the carbon budget was quantified iteratively under the field measured LAI time-series of all other plots (LAI strategy) (n=192; 8 plots × 8 LAI time-series, repeated for upper and lower standard error). We generated model simulations on an hourly timescale, allowing sufficient iterations for feedbacks on component carbon pools to stabilise (300 years). Model predictions of NCE as a function of LAI and precipitation were interpolated to generate a contour graph. At each plot, local LAI was then compared to that under maximum interpolated NCE. We further compare SPA simulated maximum predicted NCE (n=192), to model estimated NCE under local conditions, and field estimated NCE, calculated as the sum of fine root, coarse root and woody NPP and respiration (field estimated NCE error was the propagated standard error of components). Linear regression models were constructed, and the slope of the interactions assessed. Within analyses plot are characterised by their mean annual precipitation.

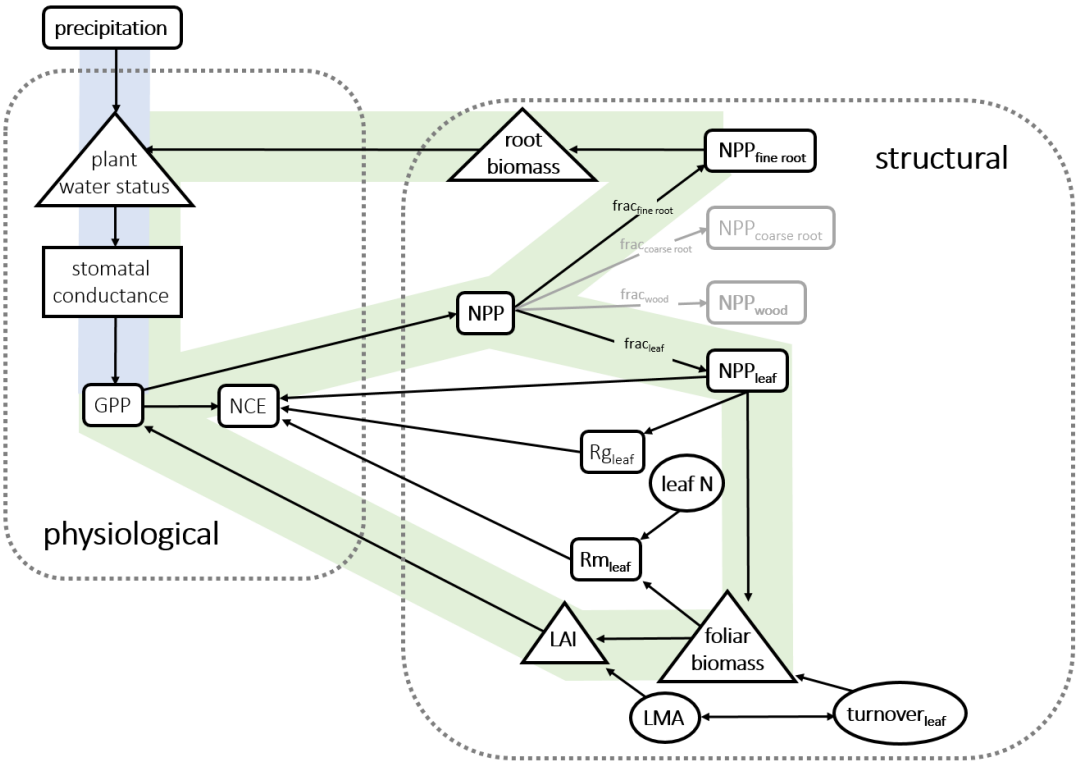

Figure 4.2. A schematic of the physiological and structural responses (grey dashed boxes) of forests to precipitation and the pathways through which responses impact GPP. An influence of one process, variable, stock or flux on another is shown by directional arrows. Two-way arrows represent a trade-off between the two variables. Boxes represent fluxes or processes (modelled), triangles are stocks (SPA state variables) and circles are leaf traits (SPA parameters). Grey boxes indicate fluxes that are not integral to the processes discussed. Bold text indicate that the value of the variable, stock or flux was known in this study, derived from biometric data. Blue shading shows the pathway of direct physiological impacts of meteorology on GPP, whilst green shading shows the principal pathway for plant structural impacts on GPP. Net primary productivity and fraction of NPP are separated by component; leaf (NPP_{leaf}; $frac_{leaf}$), wood (NPP_{wood}; $frac_{wood}$), course roots ($NPP_{course\ root}$; $frac_{course\ root}$) and fine roots ($NPP_{fine\ root}$; $frac_{fine\ root}$). Gross Primary Productivity (GPP), total Net Primary Productivity (NPP), Net Canopy carbon Export (NCE), Leaf Area Index (LAI), leaf growth respiration ($R_{g\ leaf}$), leaf maintenance respiration ($R_{m\ leaf}$), leaf turnover ($turnover_{leaf}$), Leaf Mass per unit Area (LMA) and leaf nitrogen content (leaf N) are denoted respectively.

The Effect of Carbon Cycle Feedbacks on the LAI-NCE Interaction

In order to separate the direct effects of LAI on NCE from feedback effects via structural pathways (Figure 4.2), the carbon budget was quantified iteratively under the field measured LAI time-series of all other plots in the absence of model carbon cycle feedbacks. Wood, coarse root and fine root carbon pools were held constant at nominal values, whilst foliar carbon stocks were constrained by LAI time-series alternations. We then compared the interaction between LAI and simulated NCE in the presence (Experiment 1) and absence of carbon cycle

feedbacks (n=384; 8 plots × 8 LAI time-series, repeated for upper and lower standard error in the presence and absence of model carbon cycle feedbacks). To understand the effect of carbon cycle feedbacks (i.e. changes in plant component biomass via an increase or decrease in C assimilated) on resource acquisition, and ultimately NCE, we also compared simulated leaf specific conductance (LSC, a measure of stem hydraulic capacity to supply leaves with water, it is the ratio of stem conductivity to leaf area) and root carbon stocks. We focused on a typical core and transitional forest, and compared the relative change in NCE, LSC and root carbon stocks in the presence and absence of carbon cycle feedbacks.

The Role of Leaf Traits in Shaping LAI Optimality and Total NCE

To explore the role of leaf traits in shaping the NCE-LAI interaction, we focus on a typical core forest with slow leaf traits (CAX04) and a transitional forest with fast leaf traits (KEN02). We define fast leaf traits as the coupling of high photosynthetic capacity, metabolic rate and leaf nitrogen with low LMA and a short leaf lifespan, with the opposite true for slow leaf traits (Table 4.1). We simulated carbon fluxes under fast and slow leaf traits for CAX04 and KEN02 under the LAI strategy of all other plots (n=96, 2 plots x 2 leaf trait strategies x 8 LAI strategies, repeated for upper and lower standard error). We then compared the interaction between simulated NCE, GPP and LAI under the different leaf trait strategies. We also explore the effect of fast and slow leaf traits on sub-annual GPP and NCE, under local LAI.

4.4 Results

4.4.1 Model Calibration and Validation

Here we highlight key model calibration and validation results relevant to the experiments presented (detailed in full in Chapter 3). Model performance gives confidence to further investigations, using SPA to explore carbon dynamics under non-observed LAI. Model calibration results demonstrate an accurate representation of soil water retention in relation to soil texture when compared to field measurements from the GEM network (see Chapter 3, Figure 3.2). SPA simulations captured soil water content seasonality and timing (soil moisture range of GEM measurements and SPA simulations R^2=0.44, p=0.10, RMSE=5.1 %; timing of soil moisture peak R^2=0.97, p<0.001, RMSE=1.2 months). Leaf litterfall in SPA was also successfully calibrated against GEM field estimates (Table 4.2; see Chapter 3, Figure 3.3). The magnitude and timing of leaf litterfall was captured by SPA for all plots (monthly leaf litterfall range of

GEM measurements and SPA simulations R^2=0.53, p<0.01, RMSE= 10.9 gC m^{-2} yr^{-1}; timing of leaf litterfall peak R^2=0.97, p<0.001, RMSE=1.1 months). The parameters retrieved from leaf litterfall calibration correlated with field derived leaf trait estimates (Table 4.1). Calibrated leaf lifespan correlated significantly with mean annual precipitation (R^2=0.59, p=0.03) and LMA (R^2=0.68 p=0.01). Field estimates of LMA, and photosynthetic capacity estimates derived from measured leaf N content, were negatively correlated (R^2=0.74 p<0.01). Model validation results show SPA simulated carbon fluxes corresponded well to biometric estimates measured by the GEM network (see Chapter 3, Figure 3.4). SPA and GEM GPP and autotrophic respiration estimates were significantly correlated (Table 4.2). NPP estimates were also correlated, and the interaction was significant on removal of Kenia plots (Table 4.2; on exclusion of Kenia plots R^2=0.79, p= 0.02, RMSE=94.65).

Table 4.2. Model calibration and validation performance for permanent sample plots across an Amazon precipitation gradient. SPA was calibrated against GEM estimates of leaf litterfall and soil moisture, and validated against estimates of NPP, GPP and autotrophic respiration. We compare modelled values to field estimates of carbon fluxes to derive the coefficient of determination, p value and root mean square error.

	R^2	p	RMSE
Validation			
GPP (gC m^{-2} yr^{-1})	0.48	0.05	339.07
R_a (gC m^{-2} yr^{-1})	0.65	0.02	260.09
NPP (gC m^{-2} yr^{-1})	0.35	0.12	145.6
Calibration			
Leaf Litterfall (gC m^{-2} yr^{-1})	0.99	<0.001	9.6
Litterfall Range (gC m^{-2} yr^{-1})	0.53	<0.01	10.9
Litterfall Peak Timing (months)	0.97	<0.001	1.1
Soil Moisture Range(%)	0.44	0.10	5.1
Soil Moisture Peak Timing (months)	0.97	<0.001	1.2

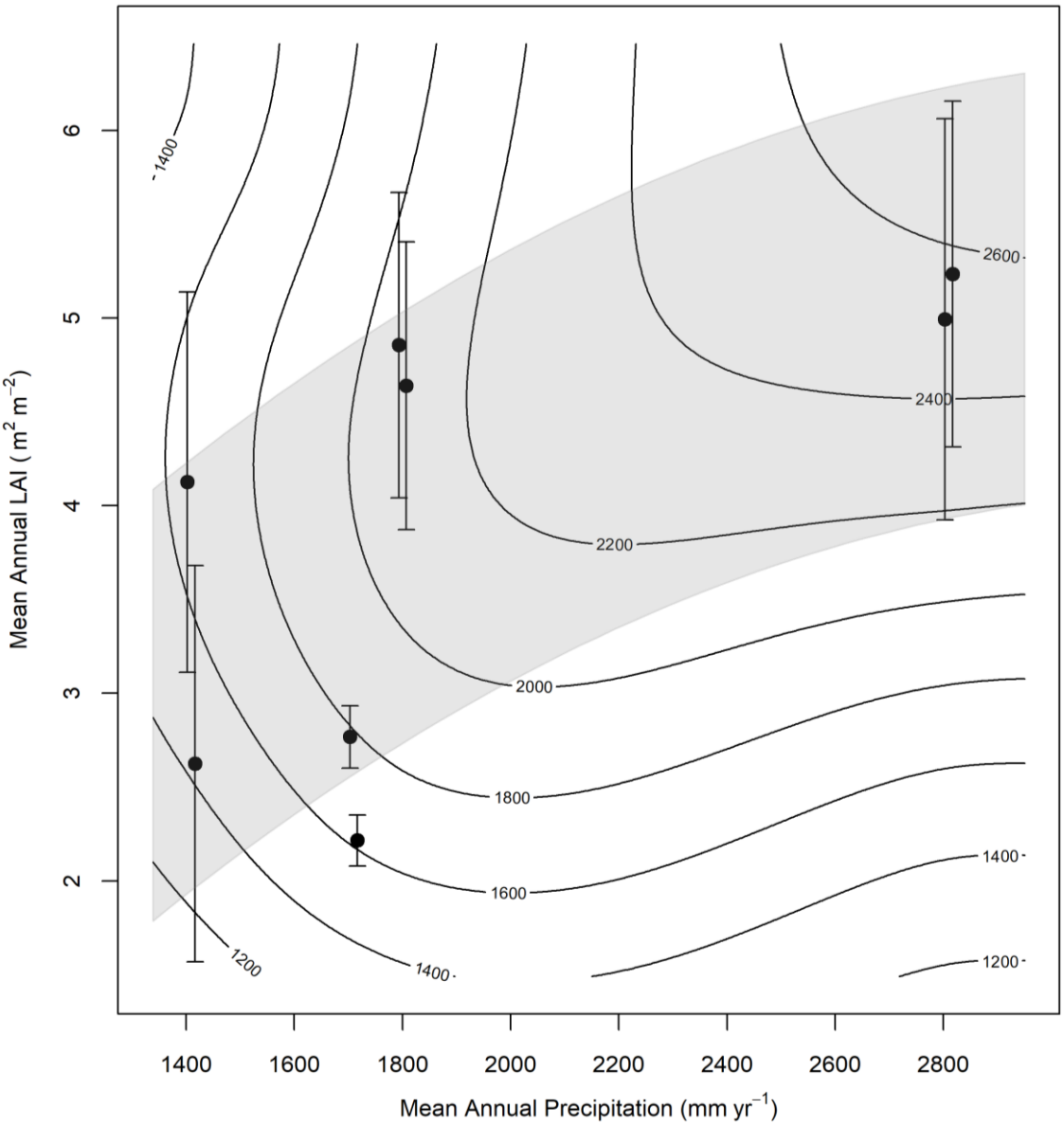

Figure 4.3. Contour plot of model simulated net canopy carbon export (NCE gC m^{-2} yr^{-1}) across an Amazon mean annual precipitation gradient, under a range of simulated LAI strategies. NCE values are SPA estimates derived from LAI time-series alternated at each plot, whilst maintaining the observed meteorology, soil, vegetation structure and leaf traits. Contours represent interpolated NCE estimates (n=192). Points are the observed mean annual LAI of each plot, whilst error bars represent standard error. Estimates of LAI, precipitation and simulated NCE are mean annual values for 2009-2010. The corresponding precipitation value to LAI observations are marginally offset around the true value to allow clarity around the distribution of error bars for plots at the same location. The shaded area represents the smoothed interaction between observed precipitation and LAI values.

4.4.2 Model Experiments

The Interaction between LAI, Precipitation and Net Canopy Carbon Export

The observed spatial variation in LAI across the precipitation gradient was consistent with simulated maximisation of net canopy carbon export (NCE). The LAI that maximised NCE increased with precipitation (Figure 4.3), according to the modelling of climate-carbon interactions. Field LAI estimates corresponded well with that for predicted NCE maxima (R^2=0.39, p=0.099, RMSE=0.88 m^2m^{-2}), but were typically 17.2% lower. For transitional forests, simulated NCE was reduced at high LAI. Underlying the decline in NCE was a disproportional increase in the carbon cost of leaf construction and maintenance relative to photosynthetic gains. For forests occupying high rainfall zones, sufficient water availability allowed simulated increases in LAI to be remunerative. Maximum predicted NCE was significantly correlated with SPA NCE estimates under local LAI, and GEM NCE estimates (Figure 4.4) (SPA R^2= 0.87, p<0.001, RMSE= 150.6 gC m^{-2} yr^{-1}; GEM R^2=0.68, p=0.01, RMSE=279.5 gC m^{-2} yr^{-1}). SPA NCE estimates under local LAI were 5.8% lower on average than maximum predicted NCE whilst GEM NCE estimates were 12.2% lower. SPA NCE estimates under local LAI were also correlated with GEM NCE estimates (R^2=0.68 p=0.01, RMSE=236.5 gC m^{-2} yr^{-1}). GEM NCE estimates were typically 6.6% lower than SPA NCE estimates under local LAI. Our results show that whilst SPA captures variation in NCE across the precipitation gradient, and NCE maximisation explains LAI trends, a gap exists between observations and simulated canopy dynamics which maximise NCE.

The Effect of Carbon Cycle Feedbacks on the LAI-NCE Interaction

Carbon cycle feedbacks had a limited effect on the LAI-precipitation interaction. By comparing the difference in SPA simulated NCE in the presence and absence of modelled carbon cycle feedbacks (Figure 4.5), we see for transitional forests, feedbacks promote a decline in NCE as LAI increases, but that for plots occupying high precipitation zones, feedbacks have little effect on NCE. For transitional forests, NCE was reduced at high LAI under carbon cycle feedbacks. The decline in NCE as LAI increased under carbon cycle feedbacks, caused a reduction in simulated total NPP and consequently reduced root biomass. Lower water uptake capacity resulted in reduced leaf specific conductance (LSC, LSC was 2% or 0.01mmol m^{-2} s^{-1} MPa lower under carbon cycle feedbacks), thereby constraining photosynthesis. Similarly, for core forests, LSC was reduced at low LAI when feedbacks were enabled (LSC was on average 3% or

0.019 mmol m^{-2} s^{-1} MPa lower under carbon cycle feedbacks), due to less root biomass supporting water acquisition.

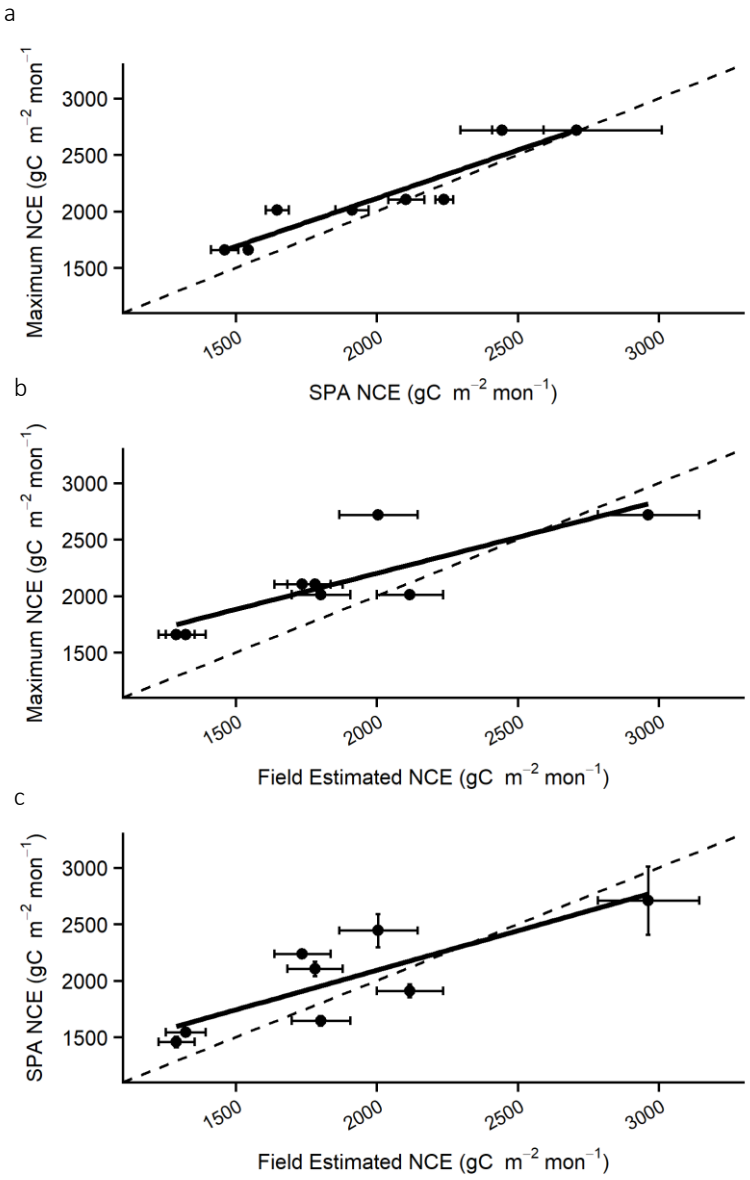

Figure 4.4. Comparison of SPA simulated NCE under local conditions, GEM field estimated NCE and maximum simulated NCE under LAI alternations for eight permanent sample plots across an Amazon precipitation gradient. Maximum NCE values are derived from interpolated SPA estimates whereby LAI time-series were alternated at each plot, whilst maintaining the observed meteorology, soil, vegetation structure and leaf traits. SPA error bars represent simulated NCE under field measured LAI standard error. GEM error bars represent propagated error for summed field estimates of fine root, coarse root and woody NPP and respiration. The dashed line is the 1:1 and the solid line is the linear regression between NCE estimates (a) R^2= 0.87, p<0.001, RMSE= 150.6, (b) R^2=0.68, p=0.01, 279.5 and (c) R^2=0.68 p=0.01, RMSE=236.5.

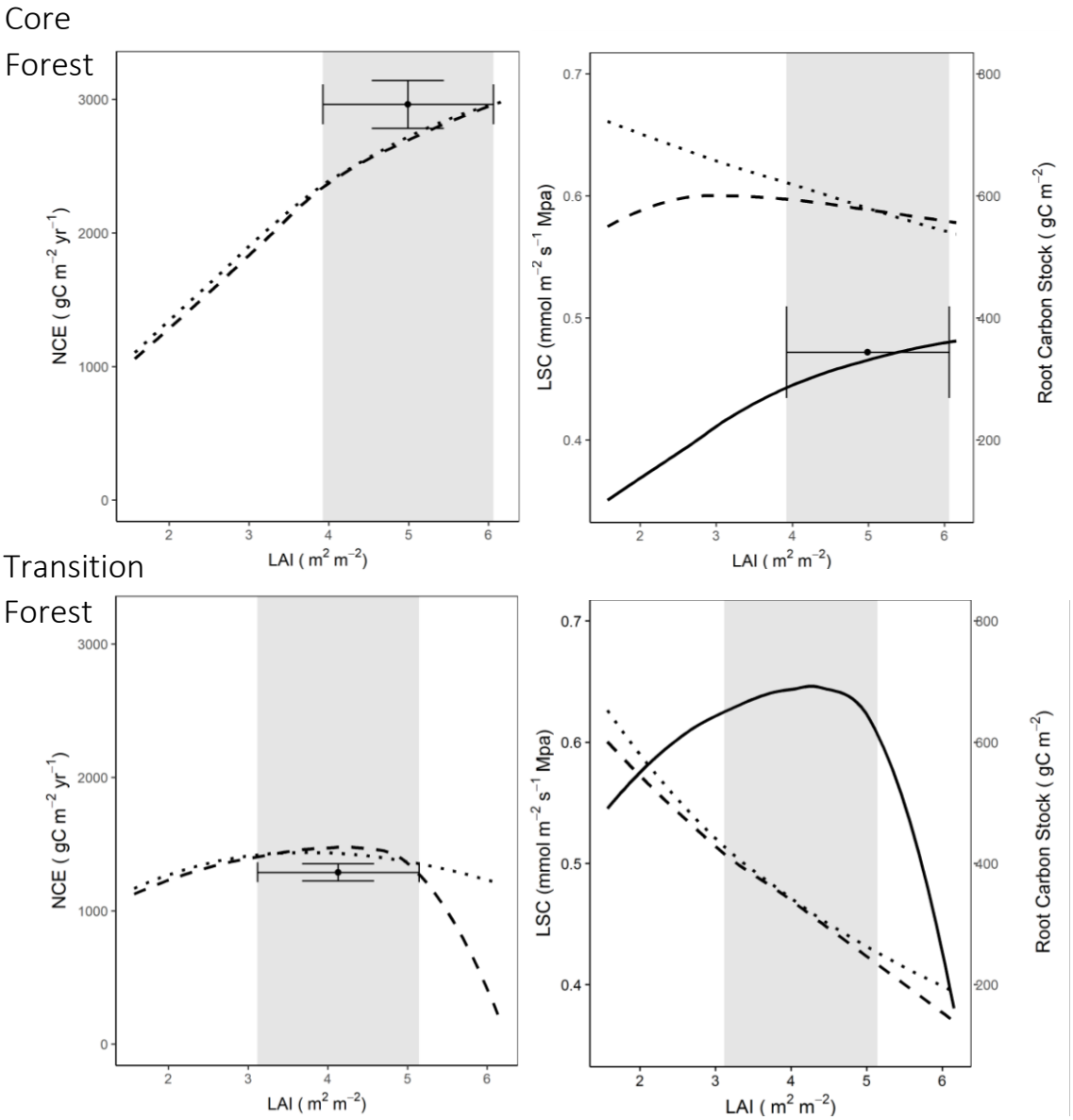

Figure 4.5. Model simulated net canopy carbon export (NCE), leaf specific conductance (LSC), and root carbon stocks in the presence, and absence of carbon cycle feedbacks, for a typical core (CAX04) and transitional forest (TAN05), under a range of simulated LAI strategies. Dashed lines represent SPA estimates of NCE and LSC where carbon cycle feedbacks were enabled, whilst dotted lines represent estimates where feedbacks were absent. Solid lines represent root carbon stocks in the presence of carbon cycle feedbacks, as in their absence, stocks were held constant at observed levels. Carbon stock and carbon and water flux values are SPA estimates derived from LAI time-series alternated at each plot, whilst maintaining the observed meteorology, soil and vegetation structure and leaf traits (n=24 for each plot). The shaded area represents the standard error of local observed mean annual LAI. Data points are estimated NCE (summed fine root, coarse root and wood NPP and respiration) and root carbon stock derived from field measurements, together with error bars showing propagated NCE error and LAI standard error. Field estimates of root stocks at TAN05 were absent.

However, as water availability was sufficient at core forest plots so as not to limit photosynthesis, relatively lower LSC had little feedback effect on NCE and photosynthate allocation to roots (NCE was on average 1.9% or 35.9 gC m^{-2} yr^{-1} lower under carbon cycle feedbacks). Therefore, whilst carbon cycle feedbacks had an effect on the LAI-precipitation interaction (Figure 4.2), it was largely confined to transitional forests, where photosynthesis was most sensitive to changes in water acquisition.

The Role of Leaf Traits in Shaping LAI Optimality and Total NCE

Leaf traits shape the interaction between LAI and NCE to determine optimal leaf area. The LAI at which NCE was maximised and total NCE differed between leaf traits strategies for forests occupying both low and high rainfall zones (transitional forest Δ LAI at maximum NCE 3.04 m^2 m^{-2}, Δ maximum NCE 168 gC m^{-2} yr^{-1}; core forest Δ LAI at maximum NCE 0.92 m^2 m^{-2}, Δ maximum NCE 155 gC m^{-2} yr^{-1}), (Figure 4.6). For transitional forests, under local LAI, simulated NCE was higher under fast (nominal) leaf traits (high photosynthetic capacity, high leaf nitrogen, low LMA and low lifespan) than under slow leaf traits (NCE under fast (nominal) leaf traits 1647±41 gC m^{-2} mon^{-1}; NCE under slow leaf traits 1239±57 gC m^{-2} mon^{-1}). As LAI increased, simulated NCE under fast leaf traits declined, whilst NCE under slow leaf traits increased. For the core forests, there was no significant difference in predicted NCE under local LAI for slow and fast leaf traits (NCE under slow (nominal) leaf traits 2710±301 gC m^{-2} mon^{-1}; NCE under fast leaf traits 2846±73 gC m^{-2} mon^{-1}). The difference in NCE under fast and slow leaf traits was greatest at low LAI, where fast traits maximised NCE, but declined with increasing LAI. Nominal fast leaf traits maximised predicted photosynthesis under local LAI during the wet season, compared to slow leaf traits (Figure 4.7). Whilst nominal slow leaf traits drive lower predicted photosynthesis throughout the year, reduced maintenance costs lessened the difference in NCE between trait strategies. Given the leaf trait distribution across the precipitation gradient, whereby fast leaf traits are typically associated with low rainfall, transitional forests and slow with high rainfall, core forests, we show that local leaf traits maximise NCE and shape LAI optimality.

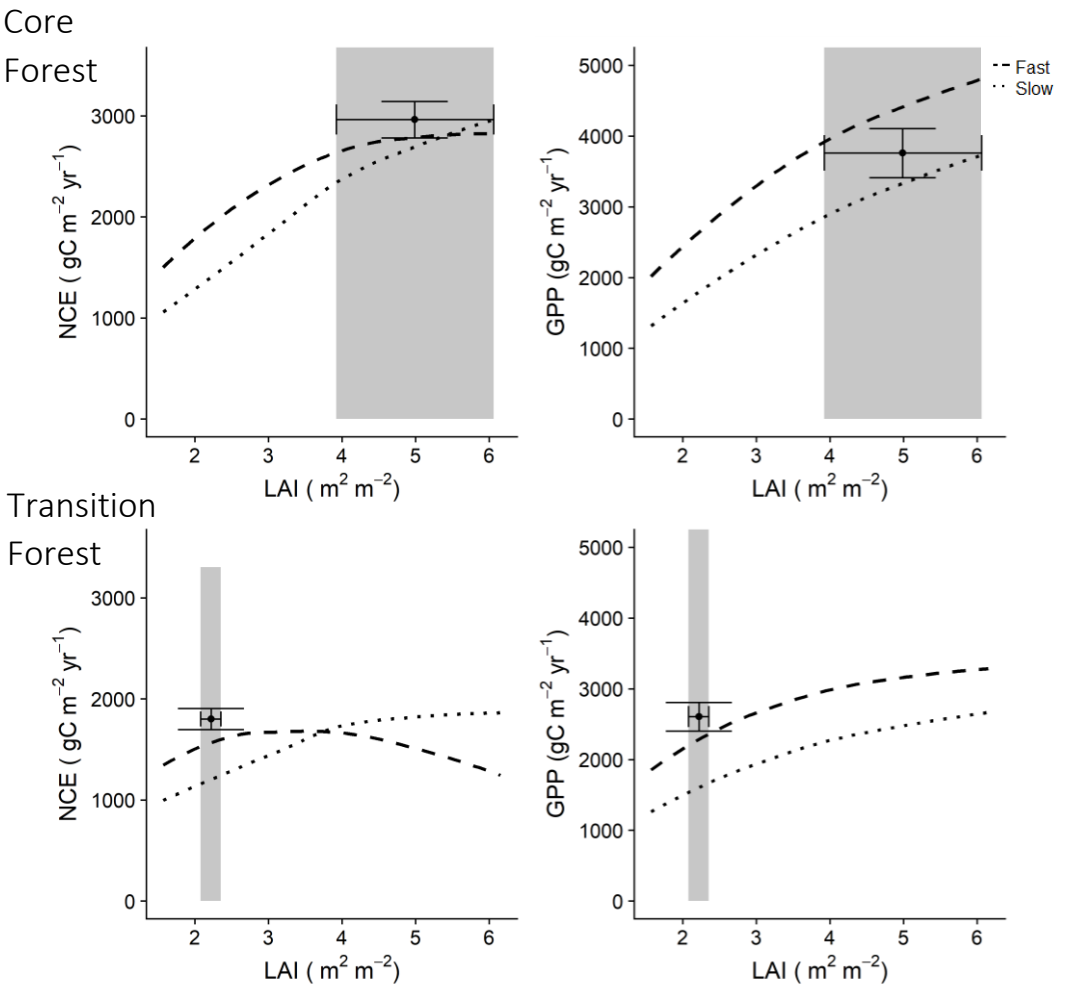

Figure 4.6. Predicted NCE and GPP for a typical core (CAX04) and transitional (KEN02) Amazon forest, across a range of simulated LAI strategies under fast and slow leaf traits. Fast traits are observed values at transitional plots and slow at core plots. Fluxes are SPA derived estimates. LAI time-series were alternated at each plot, whilst maintaining the observed meteorology, soil and vegetation structure. Shaded areas represents field estimated LAI standard error. Data points are estimated GPP and NCE (summed fine root, coarse root and wood NPP and respiration), derived from field measurements together with error bars showing propagated flux error and LAI standard error.

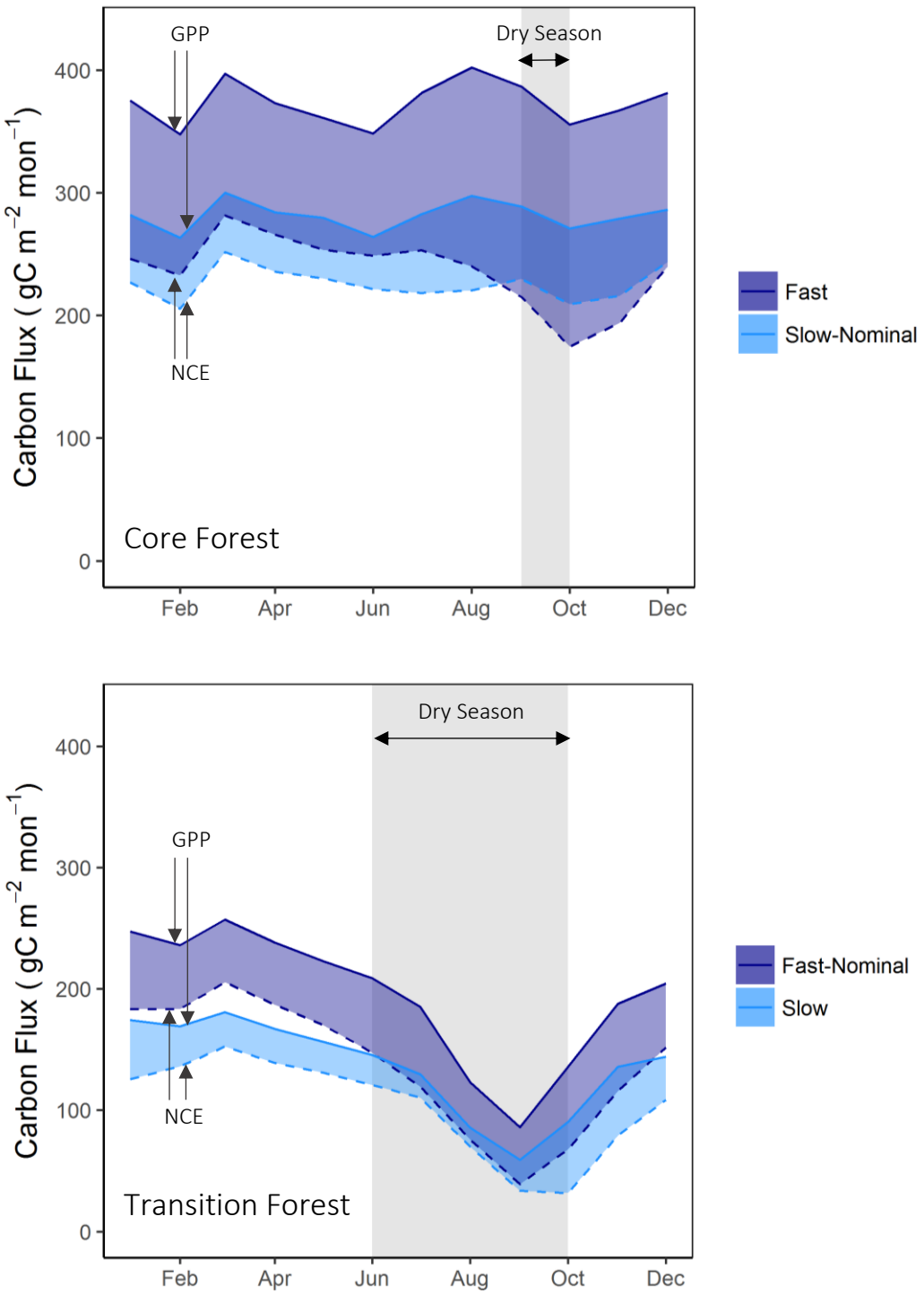

Figure 4.7. SPA simulated GPP (solid line) and NCE (dashed line) for a typical core (CAX04) and transitional (KEN02) Amazon forest, under fast (purple) and slow (blue) leaf trait strategies. Shaded areas between GPP and NCE lines represents the carbon costs of leaf growth and maintenance for the given trait strategy. Carbon fluxes are SPA estimates derived from leaf traits alternations maintaining local meteorology, soil, vegetation structure and LAI. The grey shaded area represents the dry season, where monthly rainfall was below 100mm. The fast trait strategy is the collective plot mean leaf traits from KEN02 and the slow trait strategy that of the CAX04.

4.5 Discussion

Our results show that maximisation of net canopy carbon export (NCE) explains LAI trends across an Amazon precipitation gradient. We further demonstrate the determinate effects of carbon cycle feedbacks and leaf traits on LAI optimality. Our findings were achieved by making comprehensive estimates of leaf carbon fluxes and water transport in direct response to climate drivers. Results were validated by comparing SPA estimates of NCE under local LAI to independent field estimates from the GEM network. This research offer new insights into how together, both leaf area and leaf traits shape forest photosynthetic responses to water availability. Consequently, leaf trait distributions may be more important than previously thought, in predicting the effect of shifts in precipitation patterns on the future Amazon carbon balance.

4.5.1 Maximisation of NCE Drives LAI across the Precipitation Gradient

We show that a canopy optimality approach can be used to successfully predict increases in LAI with precipitation across Amazon forests (field estimated LAI versus that at predicted NCE maxima R^2=0.39, p=0.099, RMSE=0.88 m^2m^{-2}). Our findings corroborate with other studies which have applied optimal response models to simulate LAI, consistent with field observations (Franklin, 2007; Mäkelä *et al*., 2008; McMurtrie and Dewar, 2011; McMurtrie and Dewar, 2013). However previous work has largely focused on carbon-nitrogen economics, whilst water use has received less attention (McMurtrie *et al*., 2008). Furthermore, optimality approaches have typically been validated for mono-species stands or experimental plots within a single location. This study builds on previous efforts, and demonstrates that the mechanisms shaping LAI operate under similar principles for water use, and are consistent across large spatial gradients. Addressing the regulatory role of allometry in constraining leaf biomass (Niklas and Enquist, 2002), we highlight that the amplitude of seasonal swings in LAI suggest that branching would be sufficient to support higher mean annual leaf area (LAI at Kenia plots can exceed the annual mean by over 1.5 m^2m^{-2}). Furthermore, spatial covariance between LAI and water indices on a global scale (Iio *et al*., 2014), together with evidence of short and long-term changes in leaf area in response to water availability (Brando *et al*., 2008; Hilker *et al*., 2014; Meir *et al*., 2009), disproportionate to changes in woody biomass, suggest that LAI is shaped by carbon-water economics, and not allometric constraints alone (McCarthy and Enquist, 2007). We therefore propose that optimal response approaches offer a powerful tool to predict canopy leaf area, and reduce uncertainty around changes in modelled carbon

assimilation, under projected shifts in precipitation patterns across the Amazon basin (Meir *et al*., 2015a). However, we highlight that optimality approaches marginally overestimate predicted NCE (nominal model simulated NCE were 5.8% lower; field estimated NCE were 12.2% lower), and it is unclear whether the disparity between optimal and nominal NCE is driven by uncertainty in field estimates or an alternative mechanism.

4.5.2 Carbon Cycle Feedbacks Shape LAI at Low Precipitation

Carbon cycle feedbacks had little effect when water availability was high, but had a determinate effect on NCE when water was limited (transitional forest NCE 9.2% or 111.4 gC m^{-2} yr^{-1} lower under carbon cycle feedbacks, core forest 1.9% or 35.9 gC m^{-2} yr^{-1} lower). For core forests, reduced NCE under high LAI caused a decline in fine root NPP. Lower belowground investment constrained LSC and consequently photosynthesis. A trade-off between plant organs to maximise modelled carbon gains under limited resources has similarly been reported elsewhere. Dewar *et al*. (2009) show that nitrogen availability shapes the trade-off between NPP allocated to roots and wood. Higher root NPP at lower available N allowed an increase in carbon assimilation. However feedback effects of the resultant increase in total NPP on future assimilation potential had not previously been quantified. Together with existing evidence around plant trade-offs (Franklin *et al*., 2012; Poorter and Nagel, 2000), our results highlight the importance of carbon cycle feedbacks when resources are limited, for efforts to model optimal leaf area as part of a dynamic system. However, it is important to note that our findings are based on the assumption that the non-structural carbohydrate (NSC) pool is in steady state. If our assumption was incorrect then we would be unable to make accurate inferences on carbon cycle feedback responses to LAI change (as the NSC pool could act as a C sink or source). To date few studies have quantified NSC dynamics in tropical forests (Metcalfe *et al*., 2010; Rowland *et al*., 2015; Würth *et al*., 2005). Here, we infer NSC use, constraining estimates using modelled carbon assimilation and field measurements of carbon expenditure through NPP and respiration. We recognise the limitations of our approach, but suggest that the consistency between modelled GPP and that derived from biometric estimates indicate that the assumptions made are appropriate.

4.5.3 Leaf Traits Governs the Interaction between LAI and Precipitation

Leaf traits had a large determinate effect on the LAI-NCE interaction, affecting total NCE and shifting the LAI at which NCE was maximised (transitional forest Δ LAI at maximum NCE 3.04 m^2 m^{-2}, Δ maximum NCE 168 gC m^{-2} yr^{-1}; core forest Δ LAI at maximum NCE 0.92 m^2 m^{-2}, Δ

maximum NCE 155 gC m^{-2} yr^{-1}). Our findings are in accordance with reports from Caldararu *et al*. (2016), who suggest key leaf traits (light compensation point and leaf age) explain 70% of spatial variation in global LAI distributions. Our results further showed that for transitional forests, NCE under local LAI was maximised by fast leaf traits (high photosynthetic capacity, high respiration rate, low LMA and low leaf lifespan), whilst for core forests there was no significant difference between leaf trait strategies (Figure 4.6), reflecting in part observed spatial variance of traits across this and other precipitation gradients (Table 4.1) (Santiago *et al*., 2004; Wright *et al*., 2001). Mapping the form and thresholds of the interaction between leaf traits and canopy carbon export, allowed us to explain leaf responses to water availability through optimisation hypotheses, already demonstrated for carbon-nitrogen economies (McMurtrie and Dewar, 2011). The modelled response of GPP and NCE to leaf traits (Figure 4.7) support cost-benefit theories, whereby short leaf lifespans in low MAP forests enable maximal assimilation during the wet season, whilst longer leaf lifespans minimise leaf carbon costs throughout the year in high MAP forests (Givnish, 2002; Iio *et al*., 2014; Kikuzawa, 1991). The directional covariation of LMA, leaf lifespan and photosynthetic capacity fundamentally shaped LAI trends across the precipitation gradient through their effect on photosynthesis, and the carbon cost of leaf growth and maintenance. However, variation in leaf traits across the Amazon basin are also strongly linked with soil fertility (Fyllas *et al*., 2009). Separating the effects of precipitation and soil fertility on leaf traits is difficult due to spatial covariation (Quesada *et al*., 2012). Nonetheless, we highlight the importance of concerted efforts to collate leaf trait data, such as that by the TRY trait database (Kattge *et al*., 2011) and remote sensing approaches (Asner *et al*., 2015), to the progress of optimal response model application.

4.5.4 Modelling Approaches

Current approaches to simulating LAI within terrestrial biosphere and ecosystem models do not typically employ optimality theory and instead have a strong empirical basis. Within the Joint UK Land Environment Simulator (JULES), LAI is calculated using phenological status and seasonal maximum LAI (Clark *et al*., 2011). LAI in the Ecosystem Demography model version 2.1 (ED2) is similarly dependent on phenological status, as well as the allocation relationship between plant components (Medvigy *et al*., 2009), though does include a term allowing for leaf drop under limited soil moisture. The canopy integration scheme in the Community Land Model version 3.5 (CLM3.5) simulates carbon allocated to leaves based on relationships

between plant components, accounting for losses via litterfall to determine LAI (Oleson *et al*., 2008; Thornton and Zimmermann, 2007). In the Organizing Carbon and Hydrology in Dynamic Ecosystems (ORCHIDEE) model, tropical broadleaf leaf flush is initiated a predefined number of days after moisture availability reaches its dry season minimum, whilst leaf senescence is dependent on temperature and water stress as well as leaf age (Krinner *et al*., 2005). The approaches used constrain canopy adaptation to changes in water availability within these models. In a model-data comparison of an Amazon throughfall exclusion experiment, Powell *et al*. (2013) reported that of the models tested (CLM3.5, the Integrated BIosphere Simulator version 2.6.4 (IBIS), ED2, JULES, the Simple Biosphere model version 3 (SiB3) and SPA), all failed to capture the initial increase in litter production and only some captured LAI changes. The integration of canopy optimality into ecosystem models could provide an opportunity for more accurate simulations of forest responses to precipitation regime, improving model abilities to predict the impact of climate change on future carbon dynamics. Yet, despite the benefits offered by optimal response approaches they have not been readily adopted into more complex vegetation models, and instead efforts have focused on predicting trends in traits and biomass rather than ecosystem functioning (Franklin *et al*., 2012; King, 1993). However, more recent results from carbon-nitrogen optimality models have proved promising (Thomas and Williams, 2014; Yang *et al*., 2009).

4.5.5 Limitations

We identify a number of limitations to our results including inferred fluxes, error in field estimates, model assumptions and nutrient dynamics. With respect to inferred fluxes, simulated NCE is compared against the summation of field estimated carbon export (wood and root NPP and respiration) and not leaf level measurements, causing some uncertainty in model validation. Modelled LSC could not be compared to field estimates, but we can infer that predicted values are appropriate based on model-data congruence for other water fluxes such as soil moisture (see Chapter 3). We also take into account the uncertainty around parameters used in model calibration, which is subsequently propagated through simulations. Whilst we account for LAI standard error in our results, we fail to consider the effects of measurement error which could shift reported LAI trends, especially at higher leaf area (Bréda, 2003; Jonckheere *et al*., 2004; Weiss *et al*., 2004). However, our LAI estimates do align with destructive sampling measurements from similar Amazon forests (Caxiuanã 5.11±1.41 m^2m^{-2}, McWilliam *et al*. (1993), 5.7 ± 0.5 m^2m^{-2}). We find that across the precipitation gradient, photosynthetic capacity is lowest at Caxiuanã, but does not vary widely across other plots,

introducing some uncertainty into our inferences of how leaf traits shift with precipitation. Within model experiment photosynthetic capacity was important in driving differences in photosynthesis. However, other traits such as LMA and leaf lifespan, which are important in driving leaf growth costs, do vary directionally across the precipitation gradient. Regarding model assumptions, in examining carbon allocation feedbacks we do not account for the effects of shifts in NPP allocated to wood. As SPA does not simulate competition between individual trees, we are unable to model the carbon economics of increased investment in woody biomass. Furthermore, it is notable that allocation patterns which maximise stand productivity do not necessarily coincide with those which maximise individual tree growth (King, 1990, 1993). Whilst our focus on water and carbon cycles was suitable for the posed experiment, we recognise the importance of accounting for nutrients within optimality modelling (Franklin, 2007; Franklin *et al*., 2012; Mäkelä *et al*., 2008; McMurtrie and Dewar, 2011; McMurtrie and Dewar, 2013; McMurtrie *et al*., 2008) and aim to develop our approach to include nutrient dynamics in the future. We were unable to validate simulated sub-annual GPP against field estimates. However, aseasonal GPP dynamics at Caxiuanã are in accordance with previously measured stomatal conductance time-series (Fisher *et al*., 2007).

4.6 Conclusion

We present comprehensive predictions about carbon allocation dynamics and leaf conductance in response to climate, validated against field estimates where available. Our results show that optimisation explains both LAI and leaf trait distributions across an Amazon precipitation gradient. Our finding also suggest that leaf traits may be more important than previously thought in determining the response of forests to climate change. This research demonstrates the suitability of optimality models to predict ecosystem functioning in response to water limitation. In light of projected shifts in rainfall across the Amazon basin, the ability to simulate future carbon dynamics is of increasing importance. Optimal response models therefore offer a unique opportunity to reduce uncertainty around predicted Amazon phenology, and consequently photosynthesis. Given the role of leaf traits in shaping canopy dynamics, we further highlight the importance of mapping leaf trait distributions via databases (such as the TRY trait database) and new remote sensing approaches. Further work should

focus on the how the spatial distribution of traits interact with the allocation of NPP above and belowground to support optimal functioning.

4.7 References

Asner, G. P., Martin, R. E., Anderson, C. B., & Knapp, D. E. (2015). Quantifying forest canopy traits: Imaging spectroscopy versus field survey. Remote sensing of Environment, 158, 15-27.

Atkin, O. K., Bloomfield, K. J., Reich, P. B., Tjoelker, M. G., Asner, G. P., Bonal, D., Bönisch, G., Bradford, M. G., Cernusak, L. A., & Cosio, E. G. (2015). Global variability in leaf respiration in relation to climate, plant functional types and leaf traits. New Phytologist, 206(2), 614-636.

Baldocchi, D., Valentini, R., Running, S., Oechel, W., & Dahlman, R. (1996). Strategies for measuring and modelling carbon dioxide and water vapour fluxes over terrestrial ecosystems. Global Change Biology, 2(3), 159-168.

Barbosa, J. M., Asner, G. P., Hughes, R. F., & Johnson, M. T. (2017). Landscape-scale GPP and carbon density inform patterns and impacts of an invasive tree across wet forests of Hawaii. Ecological Applications, 27(2), 403-415.

Bloom, A. J., Chapin, F. S., & Mooney, H. A. (1985). Resource Limitation in Plants - an Economic Analogy. Annual review of Ecology and Systematics, 16, 363-392.

Bonan, G. B. (2008). Forests and climate change: forcings, feedbacks, and the climate benefits of forests. Science, 320(5882), 1444-1449.

Brando, P. M., Nepstad, D. C., Davidson, E. A., Trumbore, S. E., Ray, D., & Camargo, P. (2008). Drought effects on litterfall, wood production and belowground carbon cycling in an Amazon forest: results of a throughfall reduction experiment. Philos Trans R Soc Lond B Biol Sci, 363(1498), 1839-1848.

Bréda, N. J. J. (2003). Ground-based measurements of leaf area index: a review of methods, instruments and current controversies. Journal of experimental botany, 54(392), 2403-2417.

Caldararu, S., Palmer, P. I., & Purves, D. W. (2012). Inferring Amazon leaf demography from satellite observations of leaf area index. Biogeosciences, 9(4), 1389-1404.

Caldararu, S., Purves, D. W., & Palmer, P. I. (2014). Phenology as a strategy for carbon optimality: a global model. Biogeosciences, 11(3), 763-778.

Caldararu, S., Purves, D. W., & Smith, M. J. (2016). The effect of using the plant functional type paradigm on a data-constrained global phenology model. Biogeosciences, 13(4), 925.

Carswell, F. E., Costa, A. L., Palheta, M., Malhi, Y., Meir, P., Costa, J. D. R., Ruivo, M. D., Leal, L. D. M., Costa, J. M. N., Clement, R. J., & Grace, J. (2002). Seasonality in CO2 and H2O flux at an eastern Amazonian rain forest. Journal of Geophysical Research-Atmospheres, 107(D20).

Clark, D. B., Mercado, L. M., Sitch, S., Jones, C. D., Gedney, N., Best, M. J., Pryor, M., Rooney, G. G., Essery, R. L. H., & Blyth, E. (2011). The Joint UK Land Environment Simulator (JULES), model description–Part 2: carbon fluxes and vegetation dynamics. Geoscientific Model Development, 4(3), 701-722.

Coomes, D. A., Lines, E. R., & Allen, R. B. (2011). Moving on from Metabolic Scaling Theory: hierarchical models of tree growth and asymmetric competition for light. Journal of ecology, 99(3), 748-756.

Costa, M. H., & Foley, J. A. (2000). Combined effects of deforestation and doubled atmospheric CO2 concentrations on the climate of Amazonia. Journal of Climate, 13(1), 18-34.

De Weirdt, M., Verbeeck, H., Maignan, F., Peylin, P., Poulter, B., Bonal, D., Ciais, P., & Steppe, K. (2012). Seasonal leaf dynamics for tropical evergreen forests in a process-based global ecosystem model. Geoscientific Model Development, 5(5), 1091-1108.

Dewar, R. C., Franklin, O., Mäkelä, A., McMurtrie, R. E., & Valentine, H. T. (2009). Optimal function explains forest responses to global change. Bioscience, 59(2), 127-139.

Dickinson, R. E., & Kennedy, P. (1992). Impacts on regional climate of Amazon deforestation. Geophysical Research Letters, 19(19), 1947-1950.

Dirzo, R., & Raven, P. H. (2003). Global state of biodiversity and loss. Annual Review of Environment and Resources, 28(1), 137-167.

Doughty, C. E., Metcalfe, D. B., Girardin, C. A., Amezquita, F. F., Cabrera, D. G., Huasco, W. H., Silva-Espejo, J. E., Araujo-Murakami, A., da Costa, M. C., Rocha, W., Feldpausch, T. R., Mendoza, A. L., da Costa, A. C., Meir, P., Phillips, O. L., & Malhi, Y. (2015). Drought impact on forest carbon dynamics and fluxes in Amazonia. Nature, 519(7541), 78-82.

Fisher, R. A., Williams, M., Da Costa, A. L., Malhi, Y., Da Costa, R. F., Almeida, S., & Meir, P. (2007). The response of an Eastern Amazonian rain forest to drought stress: results and modelling analyses from a throughfall exclusion experiment. Global Change Biology, 13(11), 2361-2378.

Franklin, O. (2007). Optimal nitrogen allocation controls tree responses to elevated CO2. New Phytologist, 174(4), 811-822.

Franklin, O., Johansson, J., Dewar, R. C., Dieckmann, U., McMurtrie, R. E., Brännström, Å., & Dybzinski, R. (2012). Modeling carbon allocation in trees: a search for principles. Tree Physiology, 32(6), 648-666.

Fu, R., & Li, W. (2004). The influence of the land surface on the transition from dry to wet season in Amazonia. Theoretical and applied climatology, 78(1-3), 97-110.

Fyllas, N. M., Patino, S., Baker, T. R., Bielefeld Nardoto, G., Martinelli, L. A., Quesada, C. A., Paiva, R., Schwarz, M., Horna, V., & Mercado, L. M. (2009). Basin-wide variations in foliar properties of Amazonian forest: phylogeny, soils and climate. Biogeosciences, 6(11), 2677-2708.

Fyllas, N. M., Patino, S., Baker, T. R., Nardoto, G. B., Martinelli, L. A., Quesada, C. A., Paiva, R., Schwarz, M., Horna, V., Mercado, L. M., Santos, A., Arroyo, L., Jimenez, E. M., Luizao, F. J., Neill, D. A., Silva, N., Prieto, A., Rudas, A., Silviera, M., Vieira, I. C. G., Lopez-Gonzalez, G., Malhi, Y., Phillips, O. L., & Lloyd, J. (2009). Basin-wide variations in foliar properties of Amazonian forest: phylogeny, soils and climate. Biogeosciences, 6(11), 2677-2708.

Givnish, T. J. (2002). Adaptive significance of evergreen vs. deciduous leaves: solving the triple paradox. Silva fennica, 36(3), 703-743.

Granier, A., Loustau, D., & Bréda, N. (2000). A generic model of forest canopy conductance dependent on climate, soil water availability and leaf area index. Annals of Forest Science, 57(8), 755-765.

Grier, C. C., & Running, S. W. (1977). Leaf Area of Mature Northwestern Coniferous Forests - Relation to Site Water-Balance. Ecology, 58(4), 893-899.

Hilker, T., Lyapustin, A. I., Tucker, C. J., Hall, F. G., Myneni, R. B., Wang, Y., Bi, J., Mendes de Moura, Y., & Sellers, P. J. (2014). Vegetation dynamics and rainfall sensitivity of the Amazon. Proc Natl Acad Sci U S A, 111(45), 16041-16046.

Iio, A., Hikosaka, K., Anten, N. P. R., Nakagawa, Y., & Ito, A. (2014). Global dependence of field-observed leaf area index in woody species on climate: a systematic review. Global Ecology and Biogeography, 23(3), 274-285.

Jonckheere, I., Fleck, S., Nackaerts, K., Muys, B., Coppin, P., Weiss, M., & Baret, F. (2004). Review of methods for in situ leaf area index determination - Part I. Theories, sensors and hemispherical photography. Agricultural and Forest Meteorology, 121(1-2), 19-35.

Kattge, J., Diaz, S., Lavorel, S., Prentice, I. C., Leadley, P., Bönisch, G., Garnier, E., Westoby, M., Reich, P. B., & Wright, I. J. (2011). TRY–a global database of plant traits. Global Change Biology, 17(9), 2905-2935.

Kattge, J., Diaz, S., Lavorel, S., Prentice, I. C., Leadley, P., Bönisch, G., Garnier, E., Westoby, M., Reich, P. B., & Wright, I. J. (2011). TRY–a global database of plant traits. Global Change Biology, 17(9), 2905-2935.

Kergoat, L. (1998). A model for hydrological equilibrium of leaf area index on a global scale. Journal of hydrology, 212, 268-286.

Kergoat, L., Lafont, S., Douville, H., Berthelot, B., Dedieu, G., Planton, S., & Royer, J. F. (2002). Impact of doubled CO2 on global-scale leaf area index and evapotranspiration: Conflicting stomatal conductance and LAI responses. Journal of Geophysical Research: Atmospheres, 107(D24).

Kikuzawa, K. (1991). A cost-benefit analysis of leaf habit and leaf longevity of trees and their geographical pattern. The American Naturalist, 138(5), 1250-1263.

Kim, Y., Knox, R. G., Longo, M., Medvigy, D., Hutyra, L. R., Pyle, E. H., Wofsy, S. C., Bras, R. L., & Moorcroft, P. R. (2012). Seasonal carbon dynamics and water fluxes in an Amazon rainforest. Global Change Biology, 18(4), 1322-1334.

King, D. A. (1990). The adaptive significance of tree height. The American Naturalist, 135(6), 809-828.

King, D. A. (1993). A model analysis of the influence of root and foliage allocation on forest production and competition between trees. Tree Physiology, 12(2), 119-135.

Krinner, G., Viovy, N., de Noblet-Ducoudré, N., Ogée, J., Polcher, J., Friedlingstein, P., Ciais, P., Sitch, S., & Prentice, I. C. (2005). A dynamic global vegetation model for studies of the coupled atmosphere-biosphere system. Global Biogeochemical Cycles, 19(1).

Lacointe, A. (2000). Carbon allocation among tree organs: a review of basic processes and representation in functional-structural tree models. Annals of Forest Science, 57(5), 521-533.

Maire, V., Wright, I. J., Prentice, I. C., Batjes, N. H., Bhaskar, R., van Bodegom, P. M., Cornwell, W. K., Ellsworth, D., Niinemets, Ü., & Ordonez, A. (2015). Global effects of soil and climate on leaf photosynthetic traits and rates. Global Ecology and Biogeography, 24(6), 706-717.

Mäkelä, A., Valentine, H. T., & Helmisaari, H. S. (2008). Optimal co-allocation of carbon and nitrogen in a forest stand at steady state. New Phytologist, 180(1), 114-123.

Malhi, Y., Doughty, C. E., Goldsmith, G. R., Metcalfe, D. B., Girardin, C. A. J., Marthews, T. R., del Aguila-Pasquel, J., Aragao, L. E. O. C., Araujo-Murakami, A., Brando, P., da Costa, A. C. L., Silva-Espejo, J. E., Amezquita, F. F., Galbraith, D. R., Quesada, C. A., Rocha, W., Salinas-Revilla, N., Silverio, D., Meir, P., & Phillips, O. L. (2015). The linkages between photosynthesis, productivity, growth and biomass in lowland Amazonian forests. Global Change Biology, 21(6), 2283-2295.

Malhi, Y., Roberts, J. T., Betts, R. A., Killeen, T. J., Li, W., & Nobre, C. A. (2008). Climate change, deforestation, and the fate of the Amazon. Science, 319(5860), 169-172.

McCarthy, M. C., & Enquist, B. J. (2007). Consistency between an allometric approach and optimal partitioning theory in global patterns of plant biomass allocation. Functional ecology, 21(4), 713-720.

McMurtrie, R. E., & Dewar, R. C. (2011). Leaf-trait variation explained by the hypothesis that plants maximize their canopy carbon export over the lifespan of leaves. Tree Physiology, 31(9), 1007-1023.

McMurtrie, R. E., & Dewar, R. C. (2013). New insights into carbon allocation by trees from the hypothesis that annual wood production is maximized. New Phytologist, 199(4), 981-990.

McMurtrie, R. E., Norby, R. J., Medlyn, B. E., Dewar, R. C., Pepper, D. A., Reich, P. B., & Barton, C. V. M. (2008). Why is plant-growth response to elevated CO2 amplified when water is limiting, but reduced when nitrogen is limiting? A growth-optimisation hypothesis. Functional Plant Biology, 35(6), 521-534.

McWilliam, A. L., Roberts, J. M., Cabral, O. M. R., Leitao, M., De Costa, A. C. L., Maitelli, G. T., & Zamparoni, C. (1993). Leaf area index and above-ground biomass of terra firme rain forest and adjacent clearings in Amazonia. Functional ecology, 310-317.

Medvigy, D., Wofsy, S. C., Munger, J. W., Hollinger, D. Y., & Moorcroft, P. R. (2009). Mechanistic scaling of ecosystem function and dynamics in space and time: Ecosystem Demography model version 2. Journal of Geophysical Research: Biogeosciences, 114(G1).

Meir, P., Brando, P. M., Nepstad, D., Vasconcelos, S., Costa, A. C. L., Davidson, E., Almeida, S., Fisher, R. A., Sotta, E. D., Zarin, D., & Cardinot, G. (2009). The Effects of Drought on Amazonian Rain Forests. Amazonia and Global Change, 186, 429-449.

Meir, P., Mencuccini, M., & Dewar, R. C. (2015). Drought-related tree mortality: addressing the gaps in understanding and prediction. New Phytol, 207(1), 28-33.

Meir, P., Wood, T. E., Galbraith, D. R., Brando, P. M., Da Costa, A. C., Rowland, L., & Ferreira, L. V. (2015). Threshold Responses to Soil Moisture Deficit by Trees and Soil in Tropical Rain Forests: Insights from Field Experiments. Bioscience, 65(9), 882-892.

Metcalfe, D. B., Meir, P., Aragão, L. E. O. C., Lobo-do-Vale, R., Galbraith, D., Fisher, R. A., Chaves, M. M., Maroco, J. P., da Costa, A. C. L., & de Almeida, S. S. (2010). Shifts in plant respiration and carbon use efficiency at a large-scale drought experiment in the eastern Amazon. New Phytologist, 187(3), 608-621.

Mittermeier, R. A., Myers, N., Thomsen, J. B., Da Fonseca, G. A. B., & Olivieri, S. (1998). Biodiversity hotspots and major tropical wilderness areas: approaches to setting conservation priorities. Conservation biology, 12(3), 516-520.

Mu, Q., Heinsch, F. A., Zhao, M., & Running, S. W. (2007). Development of a global evapotranspiration algorithm based on MODIS and global meteorology data. Remote sensing of Environment, 111(4), 519-536.

Muraoka, H., Saigusa, N., Nasahara, K. N., Noda, H., Yoshino, J., Saitoh, T. M., Nagai, S., Murayama, S., & Koizumi, H. (2010). Effects of seasonal and interannual variations in leaf photosynthesis and canopy leaf area index on gross primary production of a cool-temperate deciduous broadleaf forest in Takayama, Japan. Journal of plant research, 123(4), 563-576.

Nepstad, D. C., Moutinho, P., Dias-Filho, M. B., Davidson, E., Cardinot, G., Markewitz, D., Figueiredo, R., Vianna, N., Chambers, J., & Ray, D. (2002). The effects of partial throughfall exclusion on canopy processes, aboveground production, and biogeochemistry of an Amazon forest. Journal of Geophysical Research: Atmospheres, 107(D20).

Niklas, K. J., & Enquist, B. J. (2002). Canonical rules for plant organ biomass partitioning and annual allocation. American Journal of Botany, 89(5), 812-819.

Oleson, K. W., Niu, G. Y., Yang, Z. L., Lawrence, D. M., Thornton, P. E., Lawrence, P. J., Stöckli, R., Dickinson, R. E., Bonan, G. B., & Levis, S. (2008). Improvements to the Community Land Model and their impact on the hydrological cycle. Journal of Geophysical Research: Biogeosciences, 113(G1).

Pan, Y., Birdsey, R. A., Fang, J., Houghton, R., Kauppi, P. E., Kurz, W. A., Phillips, O. L., Shvidenko, A., Lewis, S. L., & Canadell, J. G. (2011). A large and persistent carbon sink in the world's forests. Science, 333(6045), 988-993.

Pettorelli, N., Ryan, S., Mueller, T., Bunnefeld, N., Jędrzejewska, B., Lima, M., & Kausrud, K. (2011). The Normalized Difference Vegetation Index (NDVI): unforeseen successes in animal ecology. Climate research, 46(1), 15-27.

Poorter, H., & Nagel, O. (2000). The role of biomass allocation in the growth response of plants to different levels of light, CO2, nutrients and water: a quantitative review. Functional Plant Biology, 27(12), 1191-1191.

Poorter, L., & Bongers, F. (2006). Leaf traits are good predictors of plant performance across 53 rain forest species. Ecology, 87(7), 1733-1743.

Poorter, L., & Bongers, F. (2006). Leaf traits are good predictors of plant performance across 53 rain forest species. Ecology, 87(7), 1733-1743.

Powell, T. L., Galbraith, D. R., Christoffersen, B. O., Harper, A., Imbuzeiro, H. M., Rowland, L., Almeida, S., Brando, P. M., da Costa, A. C., Costa, M. H., Levine, N. M., Malhi, Y., Saleska, S. R., Sotta, E., Williams, M., Meir, P., & Moorcroft, P. R. (2013). Confronting model predictions of carbon fluxes with measurements of Amazon forests subjected to experimental drought. New Phytol, 200(2), 350-365.

Reich, P. B., Ellsworth, D. S., Walters, M. B., Vose, J. M., Gresham, C., Volin, J. C., & Bowman, W. D. (1999). Generality of leaf trait relationships: a test across six biomes. Ecology, 80(6), 1955-1969.

Reich, P. B., Uhl, C., Walters, M. B., & Ellsworth, D. S. (1991). Leaf lifespan as a determinant of leaf structure and function among 23 Amazonian tree species. Oecologia, 86(1), 16-24.

Restrepo-Coupe, N., Levine, N. M., Christoffersen, B. O., Albert, L. P., Wu, J., Costa, M. H., Galbraith, D., Imbuzeiro, H., Martins, G., & Araujo, A. C. (2017). Do dynamic global vegetation models capture the seasonality of carbon fluxes in the Amazon basin? A data-model intercomparison. Global Change Biology, 23(1), 191-208.

Rowland, L., Da Costa, A. C. L., Galbraith, D. R., Oliveira, R. S., Binks, O. J., Oliveira, A. A. R., Pullen, A. M., Doughty, C. E., Metcalfe, D. B., & Vasconcelos, S. S. (2015). Death from drought in tropical forests is triggered by hydraulics not carbon starvation. Nature, 528(7580), 119-122.

Rull, V. (2011). Neotropical biodiversity: timing and potential drivers. Trends in ecology & evolution, 26(10), 508-513.

Saatchi, S., Asefi-Najafabady, S., Malhi, Y., Aragão, L. E. O. C., Anderson, L. O., Myneni, R. B., & Nemani, R. (2013). Persistent effects of a severe drought on Amazonian forest canopy. Proceedings of the National Academy of Sciences, 110(2), 565-570.

Santiago, L. S., Kitajima, K., Wright, S. J., & Mulkey, S. S. (2004). Coordinated changes in photosynthesis, water relations and leaf nutritional traits of canopy trees along a precipitation gradient in lowland tropical forest. Oecologia, 139(4), 495-502.

Santiago, L. S., & Mulkey, S. S. (2005). Leaf productivity along a precipitation gradient in lowland Panama: patterns from leaf to ecosystem. Trees, 19(3), 349-356.

Saxton, K. E., Rawls, W. J., Romberger, J. S., & Papendick, R. I. (1986). Estimating generalized soil-water characteristics from texture 1. Soil Science Society of America Journal, 50(4), 1031-1036.

Schleppi, P., Thimonier, A., & Walthert, L. (2011). Estimating leaf area index of mature temperate forests using regressions on site and vegetation data. Forest Ecology and Management, 261(3), 601-610.

Schuldt, B., Leuschner, C., Horna, V., Moser, G., Köhler, M., Van Straaten, O., & Barus, H. (2011). Change in hydraulic properties and leaf traits in a tall rainforest tree species subjected to long-term throughfall exclusion in the perhumid tropics. Biogeosciences, 8(8), 2179.

Sellers, P. J., Dickinson, R. E., Randall, D. A., Betts, A. K., Hall, F. G., Berry, J. A., Collatz, G. J., Denning, A. S., Mooney, H. A., & Nobre, C. A. (1997). Modeling the exchanges of energy, water, and carbon between continents and the atmosphere. Science, 275(5299), 502-509.

Shukla, J., Nobre, C., & Sellers, P. (1990). Amazon deforestation and climate change. Science, 247(4948), 1322-1325.

Street, L. E., Shaver, G. R., Williams, M., & Van Wijk, M. T. (2007). What is the relationship between changes in canopy leaf area and changes in photosynthetic CO2 flux in arctic ecosystems? Journal of ecology, 95(1), 139-150.

Thomas, R. Q., & Williams, M. (2014). A model using marginal efficiency of investment to analyze carbon and nitrogen interactions in terrestrial ecosystems.

Thornton, P. E., & Zimmermann, N. E. (2007). An improved canopy integration scheme for a land surface model with prognostic canopy structure. Journal of Climate, 20(15), 3902-3923.

Verbeeck, H., Peylin, P., Bacour, C., Bonal, D., Steppe, K., & Ciais, P. (2011). Seasonal patterns of CO2 fluxes in Amazon forests: Fusion of eddy covariance data and the ORCHIDEE model. Journal of Geophysical Research: Biogeosciences, 116(G2).

Walker, A. P., Beckerman, A. P., Gu, L., Kattge, J., Cernusak, L. A., Domingues, T. F., Scales, J. C., Wohlfahrt, G., Wullschleger, S. D., & Woodward, F. I. (2014). The relationship of leaf photosynthetic traits–Vcmax and Jmax–to leaf nitrogen, leaf phosphorus, and specific leaf area: a meta-analysis and modeling study. Ecology and evolution, 4(16), 3218-3235.

Watson, F. G. R., Vertessy, R. A., & Grayson, R. B. (1999). Large-scale modelling of forest hydrological processes and their long-term effect on water yield. Hydrological processes, 13(5), 689-700.

Weiss, M., Baret, F., Smith, G. J., Jonckheere, I., & Coppin, P. (2004). Review of methods for in situ leaf area index (LAI) determination Part II. Estimation of LAI, errors and sampling. Agricultural and Forest Meteorology, 121(1-2), 37-53.

Williams, M., Malhi, Y., Nobre, A. D., Rastetter, E. B., Grace, J., & Pereira, M. G. P. (1998). Seasonal variation in net carbon exchange and evapotranspiration in a Brazilian rain forest: a modelling analysis. Plant Cell and Environment, 21(10), 953-968.

Wilson, K. B., & Baldocchi, D. D. (2000). Seasonal and interannual variability of energy fluxes over a broadleaved temperate deciduous forest in North America. Agricultural and Forest Meteorology, 100(1), 1-18.

Wright, I. J., Reich, P. B., & Westoby, M. (2001). Strategy shifts in leaf physiology, structure and nutrient content between species of high-and low-rainfall and high-and low-nutrient habitats. Functional ecology, 15(4), 423-434.

Wright, I. J., Reich, P. B., Westoby, M., Ackerly, D. D., Baruch, Z., Bongers, F., Cavender-Bares, J., Chapin, T., Cornelissen, J. H., Diemer, M., Flexas, J., Garnier, E., Groom, P. K., Gulias, J., Hikosaka, K., Lamont, B. B., Lee, T., Lee, W., Lusk, C., Midgley, J. J., Navas, M. L., Niinemets, U., Oleksyn, J., Osada, N., Poorter, H., Poot, P., Prior, L., Pyankov, V. I., Roumet, C., Thomas, S. C., Tjoelker, M. G., Veneklaas, E. J., & Villar, R. (2004). The worldwide leaf economics spectrum. Nature, 428(6985), 821-827.

Wright, I. J., & Westoby, M. (2002). Leaves at low versus high rainfall: coordination of structure, lifespan and physiology. New Phytologist, 155(3), 403-416.

Wright, J. K., Williams, M., Starr, G., McGee, J., & Mitchell, R. J. (2013). Measured and modelled leaf and stand-scale productivity across a soil moisture gradient and a severe drought. Plant Cell and Environment, 36(2), 467-483.

Würth, M. K. R., Pelaez-Riedl, S., Wright, S. J., & Körner, C. (2005). Non-structural carbohydrate pools in a tropical forest. Oecologia, 143(1), 11-24.

Xu, L., & Baldocchi, D. D. (2004). Seasonal variation in carbon dioxide exchange over a Mediterranean annual grassland in California. Agricultural and Forest Meteorology, 123(1-2), 79-96.

Yang, X., Wittig, V., Jain, A. K., & Post, W. (2009). Integration of nitrogen cycle dynamics into the Integrated Science Assessment Model for the study of terrestrial ecosystem responses to global change. Global Biogeochemical Cycles, 23(4).

Zhou, L., Tian, Y., Myneni, R. B., Ciais, P., Saatchi, S., Liu, Y. Y., Piao, S., Chen, H., Vermote, E. F., Song, C., & Hwang, T. (2014). Widespread decline of Congo rainforest greenness in the past decade. Nature, 509(7498), 86-90.

5. Leaf Traits Drive Optimal Partitioning of NPP between Leaves and Roots across an Amazon Precipitation Gradient

5.1 Abstract

The allocation of net primary productivity (NPP) between leaves and roots is a major determinant of forest carbon dynamics. Optimal partitioning theory suggests that to maximise fitness, plants actively apportion NPP between leaves and roots to increase uptake of the most limiting resource. However, evidence from some tropical forests present a divergent trend: across an Amazon rainfall gradient, leaf:root NPP increased with forest dryness (R^2=0.43, p=0.07). We ask whether (i) reported leaf:root NPP allocation can be explained by optimal partitioning; (ii) and if optimal, what drives the decline in leaf:root NPP with increasing precipitation; and finally (iii) do observed leaf and root trait distributions reflect optimal responses to water availability? The Soil Plant Atmosphere model, was calibrated to plots across an Amazon precipitation gradient (1400-2800mm yr^{-1}), and validated against detailed measurements of carbon fluxes from the Global Ecosystems Monitoring network. Carbon dynamics were simulated at each plot across a range of leaf:root NPP fractions, and under different leaf and root trait strategies. Observed leaf:root NPP allocation was successfully predicted by optimisation approaches which maximised net canopy carbon export (NCE, R^2=0.60, p=0.02). Shifts in predicted optimal leaf:root NPP (maximised NCE) across the precipitation gradient were supported by concurrent shifts in observed short to long leaf residence time and long to short root residence time with increasing precipitation. Leaf traits accounted for 48% of variation in predicted optimal leaf:root NPP, whilst root traits had a lesser but still significant effect (15%). Leaf and root trait distributions across the precipitation gradient maximised predicted NCE under observed leaf:root NPP allocation strategies. However, trait distributions could not be explained using optimality approaches when

leaf:root NPP allocation was not constrained to local estimates. Our findings demonstrate that both leaf:root NPP allocation and leaf traits can be successfully predicted using optimality approaches, and that the response to water availability is effected indirectly through covariation between precipitation, leaf and root traits.

5.2 Introduction

The conversion of photosynthates into leaf, root and woody biomass underpins ecosystem carbon dynamics. We expect resource availability to determine the partitioning of net primary productivity (NPP) between plant organs, for example between light harvesting or water harvesting tissues. Together with tissue residence time, NPP allocation shapes organ biomass distributions. However, for major biomes such as rainforests we remain unable to evaluate allocation patterns, because of very limited measurements on the response of NPP partitioning to resource availability in the field (Cleveland *et al*., 2015). Yet, understanding the effect of resource availability on NPP allocation is critical to understanding the impact of climate change on future carbon cycle dynamics. Tropical rainforests are an integral part of the global carbon cycle, accounting for around one-third of terrestrial NPP (Field *et al*., 1998). Across the Amazon basin, projected declines in dry season precipitation and increases in drought are expected to have a significant impact on rainforest carbon cycle dynamics (Malhi *et al*., 2008; Metcalfe *et al*., 2010). However, there is little agreement between biosphere models as to the impact of climate change on carbon cycling, a large part of which is due to uncertainty surrounding NPP allocation between plant organs (Ise *et al*., 2010; Negrón-Juárez *et al*., 2015; Purves and Pacala, 2008). A better understanding of NPP allocation would be invaluable to the development of mechanistic partitioning in process based models, and help reduce uncertainty around predicted carbon cycle dynamics under increased moisture stress (Medlyn *et al*., 2015).

Theories proposed to explain the allocation of NPP between plant organs span structural, transport and optimality based approaches. Structural approaches suggest that NPP allocation is driven by ontogenetic drift or proportionality between biomass fractions (Coleman and McConnaughay, 1995; Müller *et al*., 2000; Niklas and Enquist, 2002; Reich, 2002). Conversely, Lacointe (2000) outlines a transport-based approach, modelling the movement of assimilates from source to sink dependent on the respective distance and the uptake ability of the sink.

The optimal partitioning approach reflects plant goals to maximise fitness, and suggests plants allocate growth to the organ that acquires the most limiting resource (Bloom *et al*., 1985; Charles-Edwards, 1976; Hilbert and Reynolds, 1991; Johnson and Thornley, 1987; Luo *et al*., 1994; McMurtrie and Dewar, 2013; Reynolds and Thornley, 1982; Thornley, 1972; Thornley, 1995). Plant fitness is defined as the capacity to grow, reproduce and survive (Geber and Griffen, 2003; Violle *et al*., 2007). The maximisation of plant fitness is captured using proxies such as total photosynthesis, NPP, and net canopy carbon export (NCE, photosynthesis minus the cost of leaf growth and maintenance). A key advantage of the approach is that it allows models to respond to differences in resource availability, furthermore, it can be easily integrated into current process based models, with low computational cost.

Despite widespread recognition of optimal partitioning approaches, they remain relatively underused (Dewar *et al*., 2009), with models typically employing allometry or fixed NPP allocation fractions between leaves, roots and woody biomass (JULES, Clark *et al*. (2011); ED2, Medvigy *et al*. (2009); SPA, Williams *et al*. (2005)). A lack of plasticity in this regard constrains the ability of models to actively respond to changes in resources through NPP allocation. However, before optimal partitioning can be successfully integrated into current models, a number of issues must be resolved including: (i) fitness proxy choice, (ii) resource availability, particularly projecting into the future, and (iii) limited validation. Optimal partitioning models typically aim to maximise a fitness proxy such as total photosynthesis, net primary production, wood growth or net canopy carbon export (Franklin *et al*., 2009; McMurtrie and Dewar, 2011; McMurtrie *et al*., 2008), but it is unclear which of these is most consistent both in theory and in practice (Dewar *et al*., 2009), and whether they capture all aspects of plant fitness. A comprehensive comparison of fitness proxy performance is therefore needed within and across model frameworks. Uncertainty around future resource availability also remains a key issue (Reich, 2002). Optimal partitioning models rely on either the current or past availability of resources to inform predictions of NPP allocation. Drought events therefore pose a major challenge in understanding the timescales over which optimal partitioning approaches should operate (Meir *et al*., 2018; Meir *et al*., 2015). More widely, the validation of optimal partitioning models against field data has largely focused on mid to high latitude forests (Franklin *et al*., 2009; Mäkelä *et al*., 2008; McMurtrie and Dewar, 2011, 2013), whilst tropical forests have received less attention (Meir *et al*., 2015). Validating optimal partitioning against field data from tropical forests across large resource availability gradients could therefore be instrumental in testing the universality of the approach.

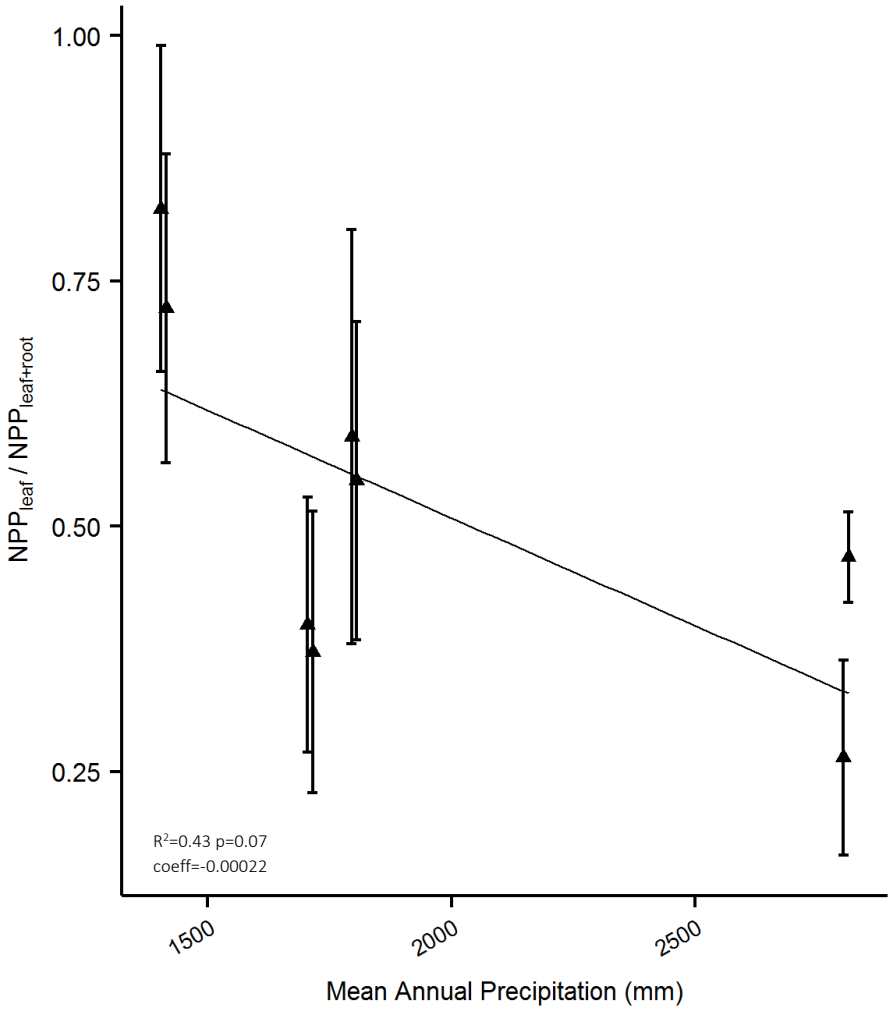

Figure 5.1. NPP fraction allocated to leaves versus that allocated to leaves and roots derived from field measurements of GEM Amazon permanent sample plots. Error bars represent field measurement propagated standard error. Precipitation estimates are marginally offset to allow clarity around the distribution of error bars for plots at the same location.

Field estimates of NPP allocation present contrasting evidence for optimal partitioning in response to resource availability. Hertel *et al*. (2013) found that in temperate forests, both root production and the ratio of above to belowground allocation increased as precipitation declined. In tropical systems, Jiménez *et al*. (2009) reported higher belowground allocation on nutrient poor soils. However, the response to water availability did not parallel the response to nutrients, and a substantial decline in fine root production was recorded during the 2005 Amazon drought. Conversely, a water and nutrient manipulation experiment in Amazon regrowth forest found that whilst declines in soil moisture led to an increase in root growth, the effects of reduced nutrient availability were limited (Lima *et al*., 2010). Similarly, Aragão

et al., (2009) found that belowground allocation increased with sand content and by proxy plant available water. Some studies report no directional variation between NPP allocation patterns and water or nutrient availability (Malhi *et al*., 2011), whilst others report trends opposing the expected response. Doughty *et al*. (2015) recorded a shift in NPP allocation away from roots in favour of the canopy following the 2010 Amazon drought. The disparity between findings suggests that NPP allocation between plant organs is not determined solely by maximisation of the most limiting resource. Emerging evidence suggests that tissue residence time could play a key role. Aragão *et al*. (2009) found that higher root biomass in nutrient poor forests was coincident with a simultaneous increase in root residence time, offsetting lower belowground allocation. Moore *et al*. (2017) suggest that residence time was the principal driver of spatial variation in leaf, root and wood biomass for forests in West Africa. Leaf and root traits such as residence time could therefore interact with NPP allocation to support optimal biomass ratios.

Table 5.1. The coefficient of determination, whether the correlation was positive or negative (denoted in brackets), and root mean square error (RMSE) for the interaction between field derived estimates of leaf, fine root and aboveground wood NPP, carbon stock and residence time at 8 plots with local mean annual precipitation (correct for 2009-2010). Values in bold indicate a significant interaction ($p<0.05$).

	Leaf			Root			Stem		
	R^2		RMSE	R^2		RMSE	R^2		RMSE
NPP (gC m^{-2} yr^{-1})	0.34	(-)	92.8	**0.49**	(+)	**72.8**	0.10	(-)	25.2
Stock (gC m^{-2})	0.29	(+)	62.9	0.63*	(-)	104.4	**0.81**	(+)	**2429**
Residence time (years)	**0.60**	(+)	**0.27**	0.46	(-)	1.40	**0.75**	(+)	**15.2**

*excludes Tanguro plots due to root stocks being estimated at these plots

Field studies alone cannot yet quantify the effects of NPP allocation strategies and leaf and root residence time on plant performance, and process based models are needed to identify if local dynamics are optimal (i.e. maximise a fitness proxy). The Soil-Plant-Atmosphere model (SPA), offers the opportunity to investigate plant economies, using a mass balance approach to link leaf and root traits to ecosystem processes. Furthermore, model approaches allow the calculation of fitness proxies such as NCE, which are not measured directly, but are consistent with field estimates of component C fluxes (NCE field estimates are calculated as the sum of wood, coarse root and fine root NPP and respiration). Across an Amazon mean annual precipitation gradient (1400-2800mm yr^{-1}) field estimates show that fine root NPP decreased significantly with increased moisture stress, whilst leaf NPP increased, though not significantly

(Table 5.1; Figure 5.1; NPP_{leaf} ~ $NPP_{leaf+root}$ R^2=0.43, p=0.07). Leaf biomass increased and fine root biomass decreased with precipitation. Leaf residence time increased significantly with precipitation, whilst root residence time decreased. High leaf or root biomass concurrent with low NPP allocation may therefore be supported by longer residence times and vice versa. Biomass ratios did not appear to be driven by allometry. Whilst leaf biomass was proportional to aboveground woody biomass (log(leaf)~ stem, R^2=0.58, p=0.02, coef=$8.1e^{-5}$), aboveground woody biomass was inversely proportional to fine root biomass (log(root)~wood, R^2=0.59, p=0.07, coef=$-4.2e^{-5}$). Forests across the precipitation gradient are mature, suggesting ontogeny does not drive NPP allocation patterns. We investigate whether optimal partitioning can explain the shift in leaf:root NPP across the precipitation gradient. We use SPA to ask three novel science questions:

1. Is observed leaf:root NPP allocation economically optimal across Amazon forests (i.e. does it maximise plant fitness), and what is the best fitness proxy?
2. What drives the observed decline in optimal leaf:root NPP with increasing precipitation?
3. Do leaf and root trait distributions across the precipitation gradient maximise plant fitness (with respect to a fitness proxy)?

For question one, we hypothesise that leaf:root NPP allocation across the precipitation gradient is optimal. We expect field estimates of leaf:root NPP allocation to maximises plant fitness under model simulations. We compare total photosynthesis, NPP and NCE as fitness proxies, and predict that NCE will perform best, as it accounts for carbon investment costs and marginal returns (McMurtrie and Dewar, 2011).

For question two, we hypothesise that leaf and root traits drive the decline in optimal leaf:root NPP with increasing precipitation. The term traits here refers to the following model parameters: photosynthetic capacity, leaf mass per area (LMA), metabolic rate and residence time. We expect the direct effects of climate on optimal leaf:root NPP to be minimal, and instead the response of NPP allocation to precipitation is predicted to be driven indirectly through the covariation of precipitation with leaf and root traits. We predict that long leaf residence times explain low leaf:root NPP allocation, and vice versa, with the opposite being true for roots. Long leaf residence times are linked to a cohort of slow leaf traits with low photosynthetic capacitance, low metabolic rate, low nitrogen content, and high LMA, whilst long root residence times are linked to slow root traits with a low metabolic rate, and vice versa for fast traits. Optimal leaf:root NPP allocation (maximises plant fitness) is thus

predicted to decline as leaf traits shift from fast to slow, and root traits shift from slow to fast, with increasing precipitation. Alternatively, leaf:root NPP allocation may be optimal independent of traits, and instead driven by climate, and the diminishing returns of increased investment in the acquisition of a finite resource.

For question three, we hypothesise that fast leaf traits and slow root traits will maximise plant fitness in low rainfall zones, whilst slow leaf traits and fast root traits will maximise fitness in high rainfall zones, reflecting observed trait distributions along the precipitation gradient. We predict that slow leaf traits promote continued uptake of light for core forests, whilst fast leaf traits exploit abundant light for transitional forests, during periods when water limitation is minimal. Slow root traits are expected to support continued uptake of water for transitional forests, whilst fast root traits are predicted to increase water uptake when light limitation in minimal.

As far as we are aware this is the first research to validate optimal partitioning theory against detailed measurements of C dynamics from tropical rainforest sites. We compare the relative performance of different fitness proxies in predicting observed leaf:root NPP partitioning. We then use the best performing fitness proxy to quantify the drivers of optimal leaf:root NPP across a precipitation gradient, and test the optimality of observed leaf and root trait distributions. We suggest that the use of a simple proxy to predict leaf:root NPP allocation is a powerful tool for process based models to estimate NPP allocation ratios. Furthermore, by explaining trends in leaf:root NPP and leaf and root traits in response to water availability, we offer new insights into the direct and indirect role of climate in shaping forest productivity.

5.3 Methods

We calibrated and validated the ecosystem model SPA to eight permanent sample plots (located at Caxiuanã, Tambopata, Kenia and Tanguro) across an Amazon mean annual precipitation gradient (1400-2800mm yr^{-1}) with detailed time-series measurements of C fluxes (Doughty *et al.*, 2015; Malhi *et al.*, 2015). We then undertook a series of model experiments to: (i) determine if observed leaf:root NPP allocation was optimal; (ii) quantify the drivers of optimal leaf:root NPP and precipitation covariance; and (iii) explore the optimality of leaf and root trait distributions across the precipitation gradient. A description of site characteristics, the SPA model, and data used in model calibration and validation are given in Chapter 2. Here

we detail model structural changes (canopy dynamics), model calibration, (reviewing soil moisture, and wood and root turnover calibration presented in full in Chapter 3), model validation and the model experiments conducted.

5.3.1 Model Canopy Dynamics

The model experiments posed necessitated structural changes to the representation of canopy dynamics in SPA. Phenology was not constrained by field estimated LAI (as in previous chapters), and was instead a function of leaf growth and litterfall parameters. For each timestep, the fraction of total NPP allocated to leaves was partitioned between foliar C stocks (direct), and the labile C pool, to be later redirected (indirect) (see Chapter 2, Figure 2.2). Leaf NPP for each timestep was then the sum of NPP allocated to leaves directly, and that redirected from the labile C pool. The labile C pool supported leaf NPP only. Therefore, over annual timescales total leaf NPP equated to NPP allocated to foliar C stocks directly, summed with that allocated to the labile C pool. The redirection of labile C to foliar C stocks was modelled as a function of the size of the labile C pool, the day of leaf out and leaf growth period. Leaf litterfall was modelled as a constant turnover rate.

5.3.2 Model Calibration and Validation

SPA was calibrated and validated for each plot prior to conducting model experiments. SPA was parameterised using field estimates of soil texture, initial soil C stock, leaf N content, LMA, photosynthetic capacity, the fraction of NPP allocated to leaves, fine roots and wood, root depth, root distribution, initial foliar, wood and fine root C stocks, and wood and root respiration coefficients, then driven using local hourly meteorological data. SPA was calibrated for each plot against field estimates of soil moisture (detailed in full in Chapter 3), LAI, leaf litterfall, wood turnover, root turnover and leaf traits for one year (2009). Initial investigations comparing modelled soil moisture to monthly field estimates highlighted an overestimation by SPA. The empirical model used in SPA to relate soil texture to water retention (Saxton *et al.*, 1986)(eqn.10) was then calibrated by adjusting the slope of the interaction to better represent soil moisture across tropical soils. Leaf growth parameters (day of leaf out and leaf growth period) were calibrated to reflect local LAI seasonality. Leaf turnover rate was calibrated against field estimates of leaf litterfall:

$$leaf\ turnover\ rate \propto \frac{leaf\ litterfall}{foliar\ C\ stock}$$

Table 5.2. Leaf trait field estimates, associated standard error of leaf N content and LMA estimates, and 95% confidence interval of κ_c and κ_j estimates, together with adjusted SPA model input for Amazon permanent sample plots. SPA inputs were adjusted within the standard error or 95% confidence interval of field-derived estimates to more accurately represent measured fluxes.

		Field Estimate	Standard Error/ 95% Confidence Interval	SPA Input
CAX04	leaf N content (g m-2)	1.82	0.43	2.08
	κ_c (µmol C gN^{-1} s^{-1})	32	14-74	16
	κ_j (µmol C gN^{-1} s^{-1})	57	28-115	31
	LMA (g m-2)	93	17	93
CAX06	leaf N content (g m-2)	2.12	0.70	1.916
	κ_c (µmol C gN^{-1} s^{-1})	30	13-69	14
	κ_j (µmol C gN^{-1} s^{-1})	53	26-107	27
	LMA (g m-2)	87	54	87
TAM05	leaf N content (g m-2)	2.38	0.56	2.79
	κ_c (µmol C gN^{-1} s^{-1})	29	13-67	19
	κ_j (µmol C gN^{-1} s^{-1})	50	25-102	34
	LMA (g m-2)	101	24	101
TAM06	leaf N content (g m-2)	2.51	0.64	2.26
	κ_c (µmol C gN^{-1} s^{-1})	28	12-66	15
	κ_j (µmol C gN^{-1} s^{-1})	49	24-99	28
	LMA (g m-2)	96	21	96
KEN01	leaf N content (g m-2)	2.12	0.25	2.37
	κ_c (µmol C gN^{-1} s^{-1})	29	13-67	67
	κ_j (µmol C gN^{-1} s^{-1})	52	26-104	103
	LMA (g m-2)	53	13	53
KEN02	leaf N content (g m-2)	2.31	0.31	2.43
	κ_c (µmol C gN^{-1} s^{-1})	29	13-67	53
	κ_j (µmol C gN^{-1} s^{-1})	50	25-102	84
	LMA (g m-2)	42	13	42
TAN05	leaf N content (g m-2)	2.01	0.52	2.53
	κ_c (µmol C gN^{-1} s^{-1})	30	13-69	26
	κ_j (µmol C gN^{-1} s^{-1})	53	26-107	46
	LMA (g m-2)	64	13	64
TAN06	leaf N content (g m-2)	2.01	0.52	2.53
	κ_c (µmol C gN^{-1} s^{-1})	30	13-68	35
	κ_j (µmol C gN^{-1} s^{-1})	53	26-106	57
	LMA (g m-2)	61	10	61

Wood and fine root turnover were calibrated using field estimates of component NPP and C stock, assuming ecosystems are at steady state:

$$turnover\ rate \propto \frac{NPP}{C\ stock}$$

With respect to leaf traits, we explored the standard error of field estimated leaf nitrogen content, and propagated model error (95% confidence interval) of κ_c and κ_j estimates (V_{cmax} and J_{max} normalised by nitrogen content), to calibrate SPA GPP to within the propagated sample error of field estimated GPP (Table 5.2). Whilst we recognise that the confidence intervals around photosynthetic capacity estimates are large, the calibration of leaf traits allowed us to better capture observed shifts in NPP allocation across the precipitation gradient. Field measurements of photosynthetic capacitance were available for CAX04 only, and to maintain consistency across plots, only estimates derived from leaf N content were used. SPA was validated against field estimates of LAI, NPP and respiration for a second year (2010). We constructed linear regression models to compare modelled and field estimated GPP, autotrophic respiration and total NPP in the calibration (2009) and validation (2010) year. A comprehensive comparison of model and field estimates of component NPP, respiration, C stocks and residence times was also made. We investigated the interaction between precipitation, carbon stocks, fluxes and traits to address the science questions.

5.3.3 Model Experiments

Optimal Leaf:Root NPP Allocation

To address question one, we tested whether leaf:root NPP was optimal (maximised plant fitness), and compared the performance of GPP, NPP and NCE as fitness proxies. Carbon and water dynamics were simulated for each plot across a range of leaf:root NPP allocation fractions to determine the ratio that maximised fitness proxies. NPP allocated to leaves relative to the sum of leaf and root NPP was simulated across the range 0-1 at 0.1 intervals, with the NPP remaining being allocated to roots (11 leaf:root NPP allocation fractions × 8 plots). The fraction of NPP allocated to above and belowground wood was held constant at local field estimates throughout. To assess the performance of potential fitness proxies, we retrieved the leaf:root NPP allocation fraction which maximised simulated GPP, NPP, and NCE for each plot. A linear regression model was applied to the interaction between leaf:root NPP allocation at simulated maxima and field estimated leaf:root NPP allocation (n=8, repeated for GPP, NPP and NCE). To provide further evidence of the suitability of the best performing

fitness proxy, a linear regression model was applied to the interaction between simulated maximum fitness and field estimated fitness, (n=8).

Leaf:Root NPP Allocation Drivers across the Precipitation Gradient

To address questions two, we quantified the effect of leaf traits, root traits and meteorology on the response of optimal leaf:root NPP allocation fractions (maximised fitness) across the precipitation gradient. Leaf:root NPP allocation fractions (as detailed above) were varied simultaneously with alternations in leaf traits, root traits and meteorology at each plot, reflecting values of all other plots (11 leaf:root NPP allocation fractions × 4 meteorology alternations × 8 leaf trait cohorts × 8 plots + 11 leaf:root NPP allocation fractions × 4 meteorology alternations × 8 root trait cohorts × 8 plots). Leaf and root traits were varied as a cohort to respect trait covariation. The leaf trait cohort included leaf photosynthetic capacity, nitrogen content, metabolic rate, LMA and residence time, whilst the root trait cohort included root metabolic rate and residence time. We retrieved the leaf:root NPP fraction which maximised fitness for each trait and meteorology combination (n=512; 4 meteorology alternations × 8 leaf trait cohorts × 8 plots + 4 meteorology alternations × 8 root trait cohorts × 8 plots). Combinations failing to achieve a sustainable carbon cycle were identified and then excluded from the analysis. A factorial ANOVA was then used to apportion variance in optimal leaf:root NPP allocation (that which maximised fitness) to leaf traits, root traits and meteorology (n=350). We calculated the proportion of variation in optimal leaf:root NPP allocation explained by leaf traits, root traits and meteorology as the conditional sum of square divided by the total sum of squares.

Optimal Leaf and Root Trait Distributions

To address question three, C fluxes were simulated at each plot under fast and slow leaf and root trait strategies to determine whether observed trait distributions maximised plant fitness. Fast leaf traits were defined as leaves with a high photosynthetic capacity, high metabolic rate, high N content, low LMA and a short leaf residence time, whilst fast root traits were defined as roots with high metabolic rate and short residence time (the opposite being true for slow traits). Carbon fluxes were simulated for each plot under fast leaf traits (observed TAN05 trait cohort), slow leaf traits (observed CAX04 trait cohort), fast root traits (observed TAN06 trait cohort), and slow root traits (observed CAX06 trait cohort). Trait alternations were ran until steady state (300 yrs) under both observed leaf:root NPP allocation and under optimal leaf:root NPP allocation (that which maximises fitness) for the given trait combination. The

difference between fitness under fast and slow leaf traits, and fast and slow root traits was calculated for observed and optimal leaf:root NPP allocation at each plot. A linear regression model was then applied to assess the relationship between mean annual precipitation and the difference in fitness under fast and slow leaf and root traits (n=32, Δ fitness under fast and slow leaf traits × 8 plots, plus Δ fitness under fast and slow root traits × 8 plots, repeated for observed and optimal leaf:root NPP allocation).

5.4 Results

5.4.1 Model Calibration

SPA simulated soil moisture, phenology, leaf litterfall and leaf traits were calibrated using field estimates. Simulated soil moisture seasonality corresponded well to field measurements from the GEM network (soil moisture range of GEM measurements and SPA simulations R^2=0.44, p=0.10, RMSE=5.1 %; timing of soil moisture peak R^2=0.97, p<0.001, RMSE=1.2 months), and modelled mean annual soil moisture estimates were within one standard error estimates for all plots. However, in transitional forest plots SPA simulated peak soil water was in some instances 46% lower than field estimates (KEN02), with the magnitude of seasonal variation up to 39% lower (see Chapter 3, Figure 3.2).

Simulated mean annual LAI correlated significantly with field estimates in the calibration year, however LAI seasonality (annual range) was poorly captured by SPA simulations (Table 5.3; R^2=0.03, p=0.659, RMSE = 1.39m^2 m^{-2}). For a number of plots (CAX06, KEN01, KEN02, TAN05 and TAN06) the magnitude of LAI peaks and troughs exceeded that of field estimates, reaching differences of up to 3.3 m^2m^{-2} (TAN06) (Figure 5.2). Because field estimates are indirect and did not determine measurement error, we cannot fully assess the degree of model mismatch. However, further analysis into the impact of higher LAI seasonality showed <2% difference in annual GPP compared to that simulated under observed values (see Chapter 3).

SPA simulated annual leaf litterfall for the calibration year significantly correlated with field estimates, and RMSE was low (Table 5.3; R^2=0.96, p=0.022, RMSE = 21.8 gC m^{-2} yr^{-1}). Calibration performance focused only on plots CAX04, CAX06, TAM05 and TAM06, as field estimates of leaf litterfall for the calibration year were absent for other plots. Leaf traits calibrations against field estimates of GPP, resulted in the SPA simulations successfully

capturing observed spatial variation of GPP. Modelled GPP was significantly correlated with biometric estimates in the calibration year (Table 5.3; GPP R^2=0.80, p<0.01, RMSE=168.0 gC m^{-2} yr^{-1}). Due to the effect of calibrated GPP on modelled NPP and autotrophic respiration, we present calibration results for all C fluxes. Modelled NPP and autotrophic respiration totals, and component specific estimates, correlated significantly with field measurements (Table 5.3).

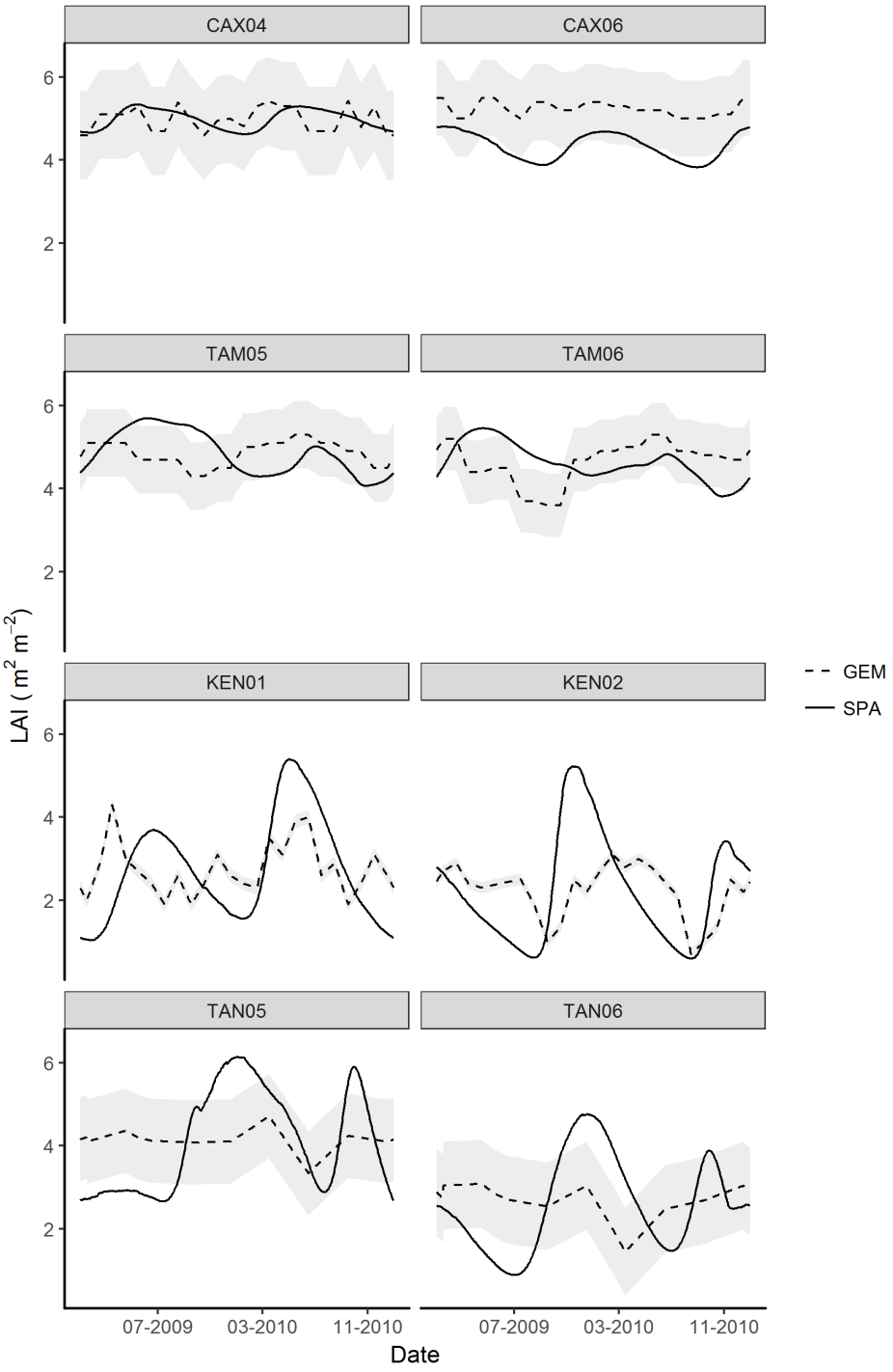

Figure 5.2. Field measured (GEM) LAI estimates from hemispherical photographs, and model simulated LAI estimates (SPA) for eight Amazon permanent sample plots. Grey shading represents field measurement standard error. Phenology in SPA was driven by modelled leaf growth and turnover, which were calibrated against field LAI and leaf litterfall estimates.

Table 5.3. A comparison of modelled C fluxes and LAI against biometric estimates (GEM network), for a calibration and validation year across eight Amazon permanent sample plots. We present the coefficient of determination, p value and root mean square error (RMSE) of constructed linear regression models. Values in bold indicate a significant interaction ($p<0.05$).

	R^2	p	RMSE
GPP (gC m^{-2} yr^{-1})			
calibration year (2009)	0.80	**0.003**	168.0
validation year (2010)	0.92	**<0.001**	121.2
NPP (gC m^{-2} yr^{-1})			
calibration year (2009)	0.53	**0.042**	72.1
validation year (2010)	0.68	**0.012**	65.7
Autotrophic Respiration (gC m^{-2} yr^{-1})			
calibration year (2009)	0.95	**<0.001**	84.8
validation year (2010)	0.96	**<0.001**	73.7
NPP by component (gC m^{-2} yr^{-1})			
wood			
calibration year (2009)	0.63	**0.018**	25.8
validation year (2010)	0.05	0.602	31.1
fine roots			
calibration year (2009)	0.83	**0.002**	47.5
validation year (2010)	0.84	**0.001**	45.8
leaf litterfall			
calibration year (2009) *	0.96	**0.022**	21.8
validation year (2010)	0.85	**0.001**	50.3
Respiration by component (gC m^{-2} yr^{-1})			
leaf			
calibration year (2009)	0.90	**<0.001**	52.7
validation year (2010)	0.83	**0.002**	61.3
wood			
calibration year (2009)	0.97	**<0.001**	39.3
validation year (2010)	0.98	**<0.001**	30.4
fine roots			
calibration year (2009)	0.91	**<0.001**	71.4
validation year (2010)	0.96	**<0.001**	50.6
LAI (m^2 m^{-2})			
mean			
calibration year (2009)	0.84	**0.001**	0.48
validation year (2010)	0.87	**0.001**	0.34
Range			
calibration year (2009)	0.03	0.659	1.39
validation year (2010)	0.85	**0.001**	0.56

*excludes KEN01, KEN02, TAN05 and TAN06 as no data available

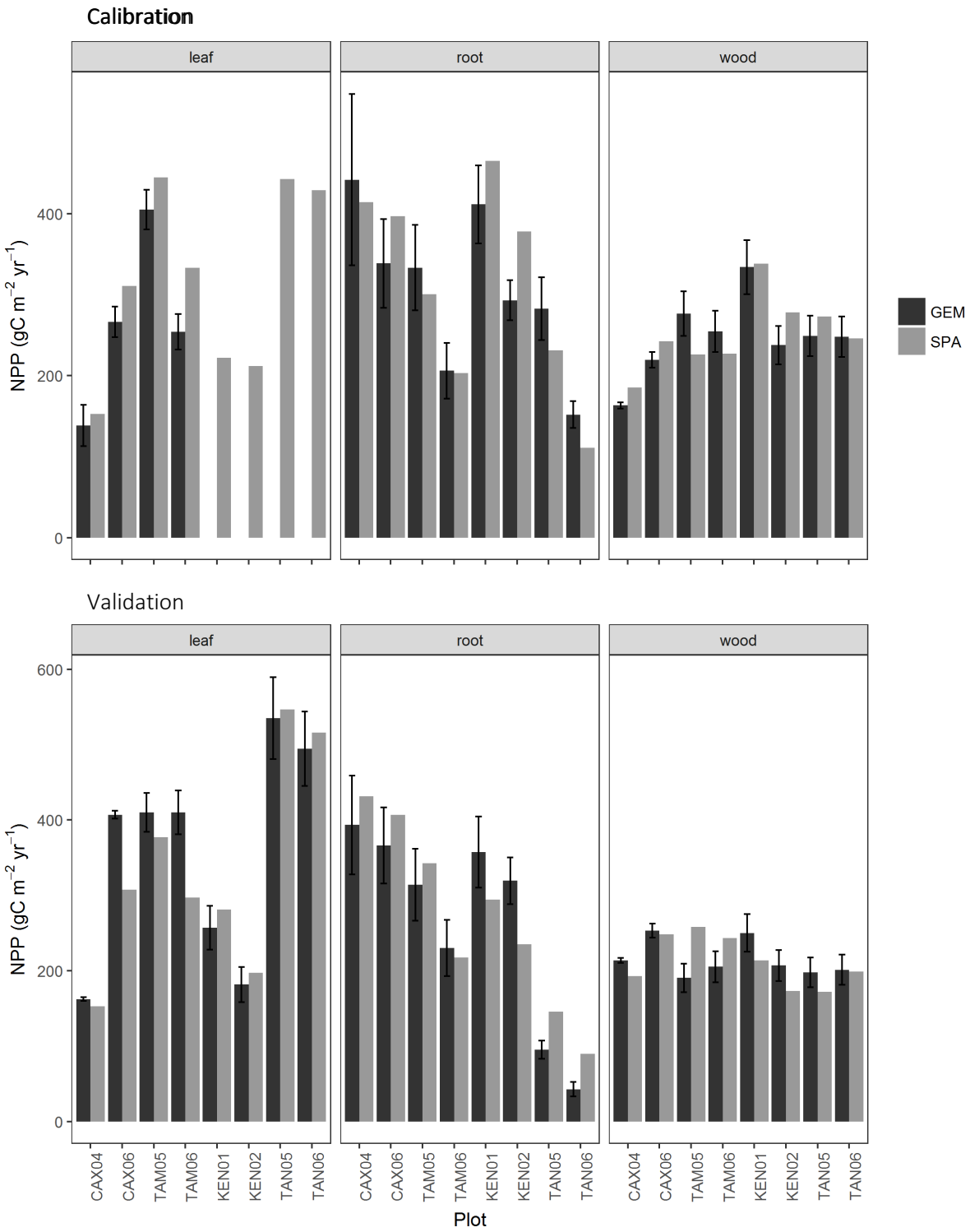

Figure 5.3. Field (GEM) and model (SPA) estimates of mean annual component NPP for Amazon permanent sample plots for the calibration (2009) and validation year(2010). Field measured leaf litterfall was used here as a proxy for leaf NPP. Error bars represents field estimate standard error. Plots are ordered from high MAP (CAX) to low MAP (TAN). Leaf litterfall data was unavailable for Kenia and Tanguro plots for the calibration year.

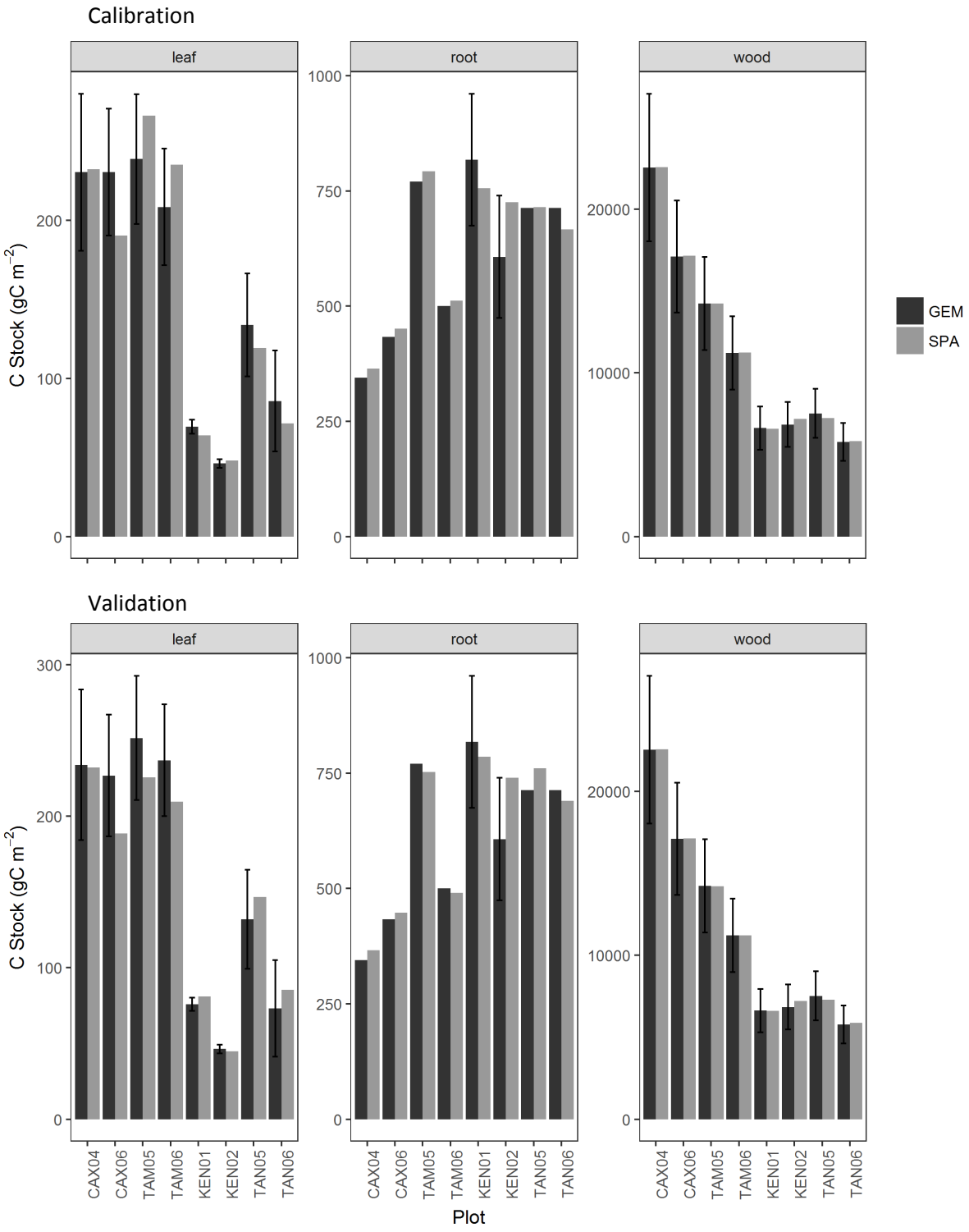

Figure 5.4. Field (GEM) and model (SPA) estimates of component carbon stocks for Amazon permanent sample plots for the calibration (2009) and validation year(2010). Error bars represents field estimate standard error, which was absent for root stock estimates at Caxiuanã and Tambopata. Measurements of root carbon stocks were absent at Tanguro, so were estimated as the Kenia mean, it being the most similar in hydroclimate and functioning. Plots are ordered from high MAP (CAX) to low MAP (TAN).

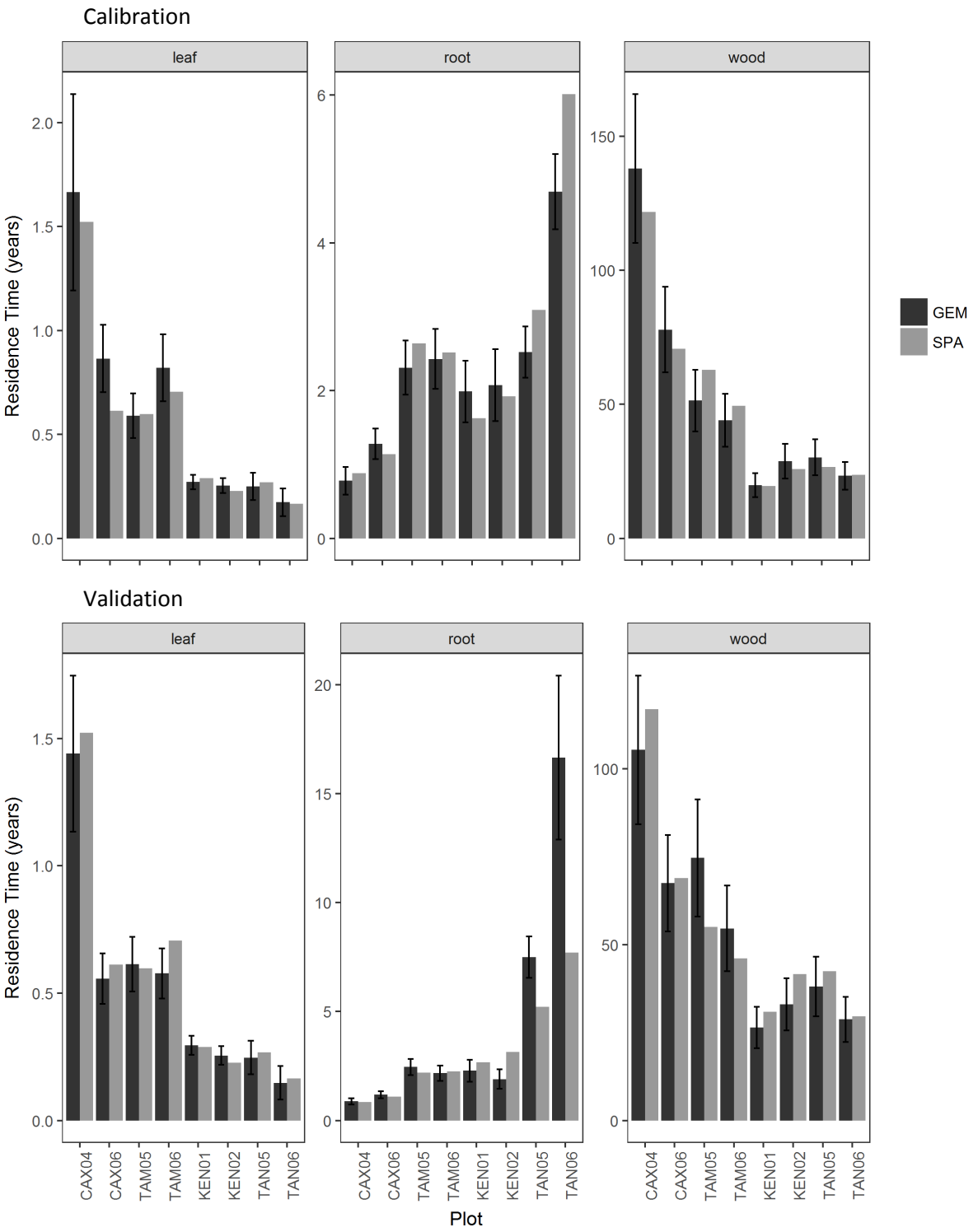

Figure 5.5. Field (GEM) and model (SPA) estimates of component residence time for Amazon permanent sample plots for the calibration (2009) and validation year(2010). Error bars represents propagated field estimate standard error. Error estimates presented for root residence times do not take into account root carbon stock standard error where data was unavailable. Plots are ordered from high MAP (CAX) to low MAP (TAN)

5.4.2 Model Validation

SPA was validated against biometric estimates of GPP, NPP and autotrophic respiration for a separate year and the spatial distribution of field derived leaf trait estimates explored (validation year, 2010). Simulated GPP, NPP and autotrophic respiration totals correlated significantly with biometric estimates for the validation year (GPP R^2=0.92, p<0.001, RMSE=121.2 gC m^{-2} yr^{-1}; NPP R^2=0.68, p=0.012, RMSE= 65.7 gC m^{-2} yr^{-1}; Respiration R^2=0.96, p<0.001, RMSE=73.7 gC m^{-2} yr^{-1}), with calculated coefficient of determination and RMSE similar to the calibration year (NPP R^2=0.53, p=0.042, RMSE=72.1 gC m^{-2} yr^{-1}; Respiration R^2=0.95, p<0.001, RMSE=84.8 gC m^{-2} yr^{-1}). Spatial variation in wood NPP was poorly captured by SPA in the validation year, however RMSE was still low (calibration year RMSE=39.3 gC m^{-2} yr^{-1}; validation year RMSE=30.4 gC m^{-2} yr^{-1}). The disparity was caused by the narrow range of wood NPP estimates across plots (biometric wood NPP estimate range ~190-250 gC m^{-2} yr^{-1}; SPA wood NPP estimate range ~ 170-260 gC m^{-2} yr^{-1}). Modelled fine root NPP and leaf litterfall also correlated significantly with biometric estimates for the validation year, as did simulated mean annual LAI and annual LAI range (Table 5.3). We further present plot specific comparisons of component NPP, residence times, and C stock estimates, across the experiment period (calibration and validation years). Interestingly, modelled NPP in the validation year captured leaf NPP best at transitional plots and root NPP best at core forest plots (Figure 5.3). Modelled leaf, root and wood carbon stocks were typically within one standard error of field estimates (Figure 5.4) as were modelled residence times (Figure 5.5), though a notable exception was root residence time at TAN06, field estimates of which increased three fold from the calibration year .

Plant traits co-varied directionally across the precipitation gradient reflecting reported trait economic spectrums. A significant positive correlation existed between modelled leaf residence time and field estimates of LMA (R^2=0.68 p=0.01), as expected from the leaf economic spectrum (Wright *et al*., 2004). Field estimated LMA also correlated negatively with photosynthetic capacity estimates derived from measured leaf N content (R^2=0.74 p=0.006). Belowground, calibrated model estimates of root turnover and root respiration rate were positively correlated, (R^2=0.57 p=0.029), though this was skewed by CAX04 and on removal the interaction was no longer significant (R^2=0.012 p=0.82). Modelled leaf and root turnover rates were negatively correlated (R^2=0.55 p=0.036), the effect of which was manifested in residence time trends, which are consistent across model and field estimates (Figure 5.5).

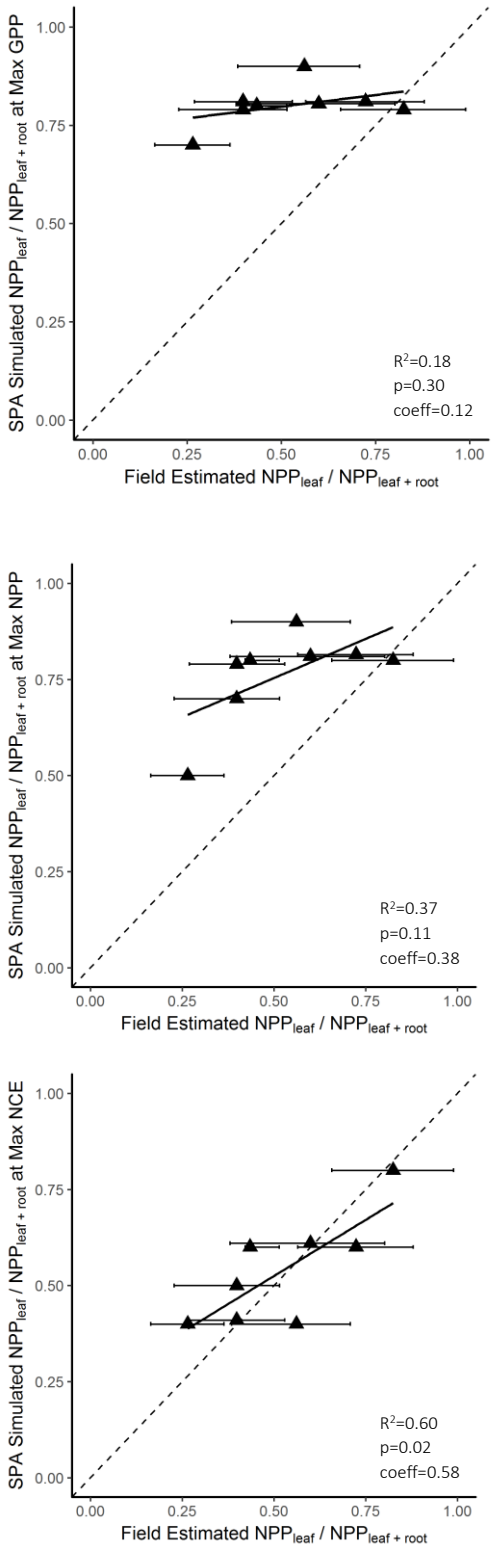

Figure 5.6. Field measured leaf NPP as a fraction of total leaf and root NPP versus SPA simulated leaf NPP as a fraction of total leaf and root NPP at maximum potential GPP, NPP, and net canopy carbon export (NCE) for eight permanent sample plots across an Amazon precipitation gradient. Points are marginally offset around the nearest 0.1 SPA simulated $NPP_{leaf}/NPP_{leaf+root}$ to allow clarity around the distribution of error bars. Solid lines represent the modelled linear fit, whilst dashed lines show the 1:1 line.

5.4.3 Model Experiments

Optimal Leaf:Root NPP Allocation

Observed leaf:root NPP allocation was optimal with respect to modelled NCE maximisation (Figure 5.6). Leaf:root NPP allocation at simulated maximum NCE was significantly correlated to field estimates of leaf:root NPP allocation (R^2=0.60, p=0.02, RMSE=0.11, coeff=0.58). However, leaf:root NPP allocation at simulated maximum GPP was a poor predictor of field estimates (R^2=0.18, p=0.30, RMSE=0.32, coeff=0.12), as was that at maximum NPP (R^2=0.37, p=0.11, RMSE=0.27, coeff=0.38). Simulated GPP and NPP typically increased with leaf:root NPP allocation, supported by higher foliar carbon stocks. However, the rate of increase in photosynthesis slowed with increasing leaf:root NPP. For transitional forest plots water constraints to stomatal conductance limited CO_2 supply, whilst for core forest plots self-shading ensued. Leaf growth and maintenance C costs also increased with leaf:root NPP allocation. Diminishing returns of increased canopy investment therefore caused NCE to decline at lower leaf:root NPP fractions than that at simulated maximum GPP or NPP.

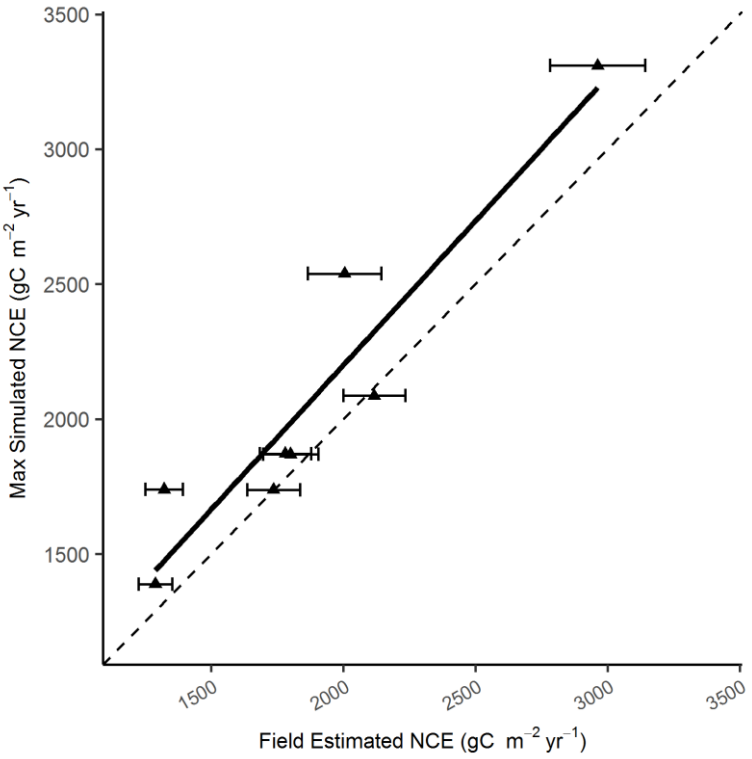

Figure 5.7. Field estimated NCE in comparison to SPA simulated maximum potential net canopy carbon export (NCE) for eight permanent sample plots across an Amazon precipitation gradient. Error bars represent field estimated standard error. Solid lines represent the modelled linear fit, whilst dashed lines show the 1:1 line.

While generally effective, using NCE optimality to predict observed leaf:root NPP allocation resulted in overestimation at low observed leaf:root NPP allocation and underestimation at high observed leaf:root NPP allocation (Figure 5.6). Simulated maximum NCE was significantly correlated to field estimates of NCE (R^2=0.88, p<0.001, RMSE=194.4, coeff=1.07, Figure 5.7). Maximum simulated NCE was also typically 8.9% higher than SPA simulated NCE under observed leaf:root NPP and 10.6% higher than field estimates of NCE (Figure 5.7). However, models using NCE as a fitness proxy to predict leaf:root NPP allocation and NCE were a good fit, supporting the use of optimality driven approaches to simulating carbon fluxes.

Table 5.4. The percentage of variation in optimal leaf:root NPP allocation (maximised NCE) across eight GEM lowland Amazonian permanent sample plots explained by sampling multiply individual drivers and driver combinations in SPA. Optimal leaf:root NPP was obtained from simulations under which leaf traits, root traits and precipitation were varied at each plot. Proportion of variance explained was calculated as Condition Sum of squares/Total Sum of Squares. Drivers listed are model inputs and are either fixed values or time series. Values in bold indicate a significant interaction (p<0.05) (n=350).

	Percentage of Variation in NCE Explained
Leaf traits	**47.9**
Root traits	**15.4**
Meteorology	**2.6**
Leaf traits* Root traits	2.9
Meteorology * Leaf traits	1.1
Meteorology * Root traits	0.8
Meteorology * Leaf traits * Root traits	2.9
Residual	26.4

Leaf:Root NPP Allocation Drivers across the Precipitation Gradient

Leaf traits were the principal drivers of variation in optimal leaf:root NPP allocation (maximises NCE) across the precipitation gradient, followed by root traits (Table 5.4). Fast leaf traits increased optimal leaf:root NPP allocation, whilst slow leaf traits decreased optimal leaf:root NPP allocation (Figure 5.8). Conversely, root traits had the opposite effect, and fast root traits reduced optimal leaf:root NPP allocation, whilst slow root traits increased optimal leaf:root NPP allocation. The effect of traits was largely driven by differences in leaf and root residence time, which necessitated shifts in leaf:root NPP allocation to maintain optimal biomass ratios. In contrast, meteorology had surprisingly little direct effect on optimal leaf:root NPP allocation. Instead, the effect of meteorology on optimal leaf:root NPP allocation was indirect, and was manifested through spatial covariation of leaf and root traits with precipitation. Drier plots had a lower range of sustainable leaf:root NPP fractions, skewed towards higher leaf

NPP, below which leaf carbon stocks were unable to support plant growth and maintenance needs (lowest MAP-Tanguro mean leaf:root NPP allocation range under local traits 0.65-0.9; highest MAP-Caxiuanã mean leaf:root NPP allocation range under local traits 0.4-0.9). The shift from fast to slow leaf traits and from slow to fast root traits therefore drives the observed decline in leaf:root NPP allocation with increasing precipitation, rather than the direct effect of meteorology.

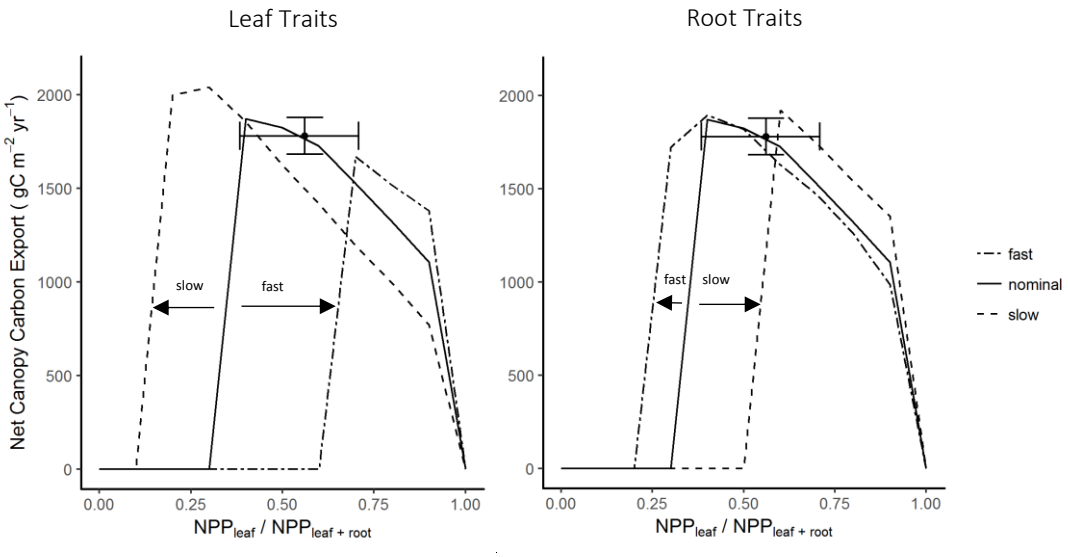

Figure 5.8. SPA simulated effect of leaf NPP as a fraction of total leaf and root NPP on net canopy carbon export (NCE) under fast and slow leaf and root traits for an Amazon permanent sample plot. Leaf and root NPP fractions (model inputs) were alternated, together with leaf and root traits to simulate carbon dynamics under the given ratio. For each alternation the model was ran to steady state; where NCE is zero the model could not stabilise under the given model inputs. Points identify field estimated allocation fractions and NCE with error bars showing associated standard error.

Optimal Leaf and Root Trait Distributions

Fast leaf traits and slow root traits maximised NCE at transitional plots, whilst slow leaf traits and fast root traits maximised NCE at core forest plots (Figure 5.9a). The difference between NCE under fast and slow leaf traits at observed leaf:root NPP allocation decreased significantly with increasing precipitation (R^2=0.85, p<0.001, RMSE=565), whilst the difference between NCE under fast and slow root traits increased, though not significantly (R^2=0.33, p=0.14, RMSE=1232). The effect of root traits on NCE was more variable than that of leaves. Whilst we account for differences in root metabolic rate and residence time, we do not account for differences in root nutrient uptake capacity, which is assumed higher for fast root traits.

Consequently, the advantage of fast root traits in SPA is limited to minimising the metabolic costs of roots through lower belowground biomass.

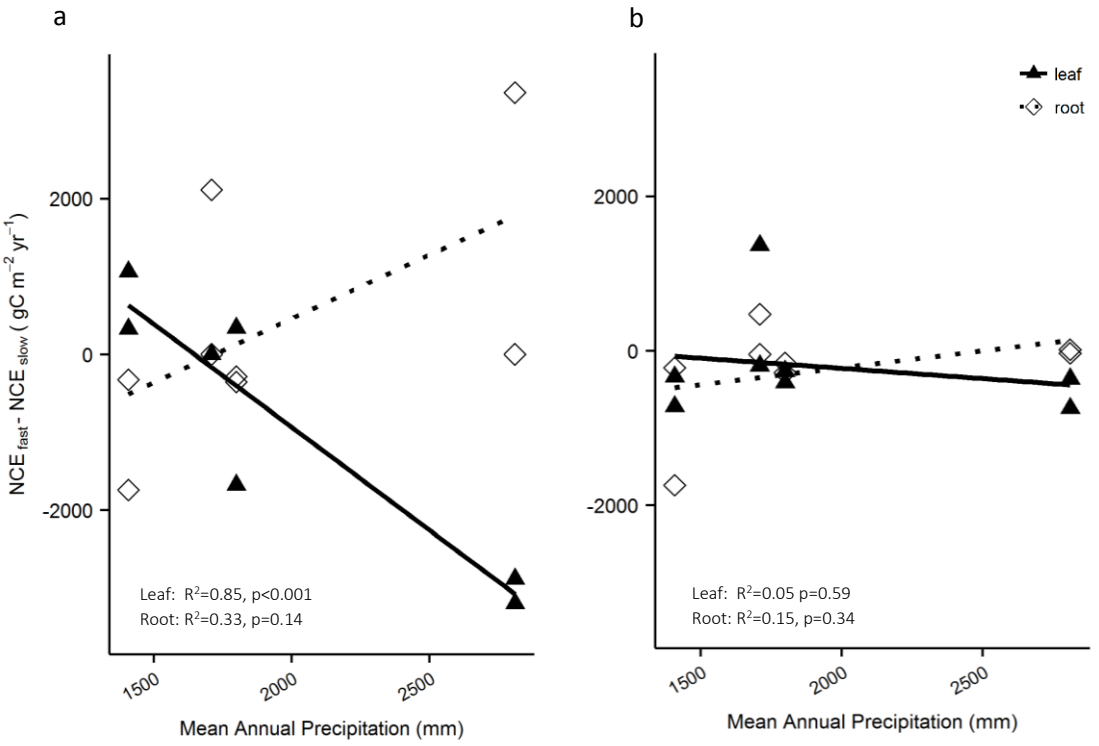

Figure 5.9. The difference between SPA simulated net canopy carbon export (NCE) under fast and slow leaf and root traits at (a) local and (b) optimal leaf:root NPP allocation for eight permanent sample plots across an Amazon precipitation gradient. Fast and slow leaf and root traits were alternated at each plot and resultant NCE retrieved. Trait used in alternations are local to the following plots: fast leaf traits TAN05, slow leaf traits CAX04, fast root traits TAN06, slow root traits CAX06. For each alternation the model was ran to steady state. Points identify SPA simulated NCE relative to local mean annual precipitation. Lines represent linear regression model fits.

The optimal distribution of leaf and root traits (maximised NCE) across the precipitation gradient is dependent on leaf:root NPP. For a given trait combination, when leaf:root NPP allocation is optimal (maximises NCE) the effect of leaf and root traits across the precipitation gradient is weakened (Figure 5.9b), in comparison to that under observed leaf:root NPP. There is little correlation between mean annual precipitation and the difference in simulated NCE for fast and slow leaf and root traits (leaves R^2=0.05 p=0.59, RMSE=607; roots R^2=0.15, p=0.34, RMSE=557), as shifts in allocation mediate NCE responses to traits. In other words, prior knowledge of the leaf:root NPP allocation ratio is required to predict trait distributions within

this optimality framework. Therefore whilst we have demonstrated our ability to predict leaf:root NPP allocation and leaf and root traits using optimality approaches, we are unable to explain the direction of the interaction across the precipitation gradient.

5.5 Discussion

Our goal was to (i) establish whether observed leaf:root NPP allocation ratios were optimal (with respect to a fitness proxy), (ii) quantify the drivers of optimal leaf:root NPP (traits vs climate), and (iii) investigate whether leaf and root trait distributions across the precipitation gradient reflect optimal strategies. We used the Soil Plant Atmosphere model (SPA) to simulate carbon cycle dynamics at each plot under a range of leaf:root NPP allocation ratios. Net canopy carbon export (NCE) was the best fitness proxy, and the maximisation of NCE successfully predicted observed leaf:root NPP allocation (Figure 5.6, R^2=0.60, p=0.02). Observed declines in optimal leaf:root NPP with increasing precipitation were explained in the model by concurrent shifts from short to long leaf residence time and long to short root residence time (Figure 5.8). Together leaf and root traits accounted for 63% of variation in optimal leaf:root NPP (Table 5.4). Under observed leaf:root NPP allocation, the distribution of leaf traits across the precipitation gradient reflected optimal strategies. However, optimality approaches could not explain observed trait distributions when leaf:root NPP allocation was not constrained to local estimates (Figure 5.9).

5.5.1 Optimal Leaf:Root NPP Allocation

Optimality approaches require a fitness proxy, however a consensus is yet to be reached on which proxy performs best. Our results demonstrated that observed leaf:root NPP allocation was optimal with respect to the maximisation of NCE, which was the best performing of the three fitness proxies (Figure 5.6). GPP and NPP maximisation proved poor predictors of observed leaf:root NPP allocation across the precipitation gradient. The performance of GPP as a fitness proxy (McMurtrie *et al*., 2008) was limited, as it overlooked relative increases in leaf respiratory costs and decreases in marginal returns on investment. As a fitness proxy, NPP (Mäkelä *et al*., 2008) combines the maximisation of carbon assimilation with the regulatory effect of carbon use efficiency. However, the maximisation of NPP does not account for returns on investment in leaf growth, which we suggest is the reason it poorly predicted leaf:root NPP allocation. The use of wood NPP as a fitness proxy, overcomes issues around

returns on leaf growth, and represents trees' competitive advantage for light acquisition and consequently survival and reproductive success (McMurtrie and Dewar, 2013). In the context of the posed experiment, we were unable to evaluate the performance of wood NPP as a fitness proxy, given the fraction of NPP allocated to wood was kept constant throughout simulations (reflecting observed values). However, the use of NCE as a fitness proxy (McMurtrie and Dewar, 2011) does in part capture the maximisation of wood NPP. NCE balances maximised carbon assimilation, with the marginal returns of canopy investment, and minimises excessive accumulation of respiring biomass, which can leave trees at risk in adverse conditions. Further work is needed to establish if the performance of NCE as a fitness proxy is consistent in different biomes and across different resource availability gradients.

Modelling ecosystem responses to changes in climate and resource availability could be improved by integrating an optimality approach. The use of fixed allocation ratios between leaves, roots and wood (as in CABLE, EALCO, GDAY and SPA; Comins and McMurtrie (1993); Wang *et al*. (2007); Wang *et al*. (2010); Williams *et al*. (2005)), precludes shifts in modelled NPP allocation in response to changes in resource availability. De Kauwe *et al*. (2014) report that ecosystem changes in response to elevated CO_2 were poorly captured by models with fixed NPP allocation ratios, and found that models with allocation schemes based on functional relationships, which varied with resource availability, performed best. However, optimisation approaches which were not constrained by structural limitations to biomass allocation proved unsuccessful in the study. The application of alternative optimisation models to FACE sites have proved successful in simulating NPP allocation (Dewar *et al*., 2009; Mäkelä *et al*., 2008), and have offered new insights into the role of nitrogen availability in plant responses to elevated CO_2 (Franklin *et al*., 2009). Our results show that the potential of optimal partitioning approaches stretch further to include water availability. We demonstrate that optimal partitioning can be used to successfully predict NPP allocation dynamics across a water availability gradient. Importantly, by using NCE as a fitness proxy, we were able to capture trade-offs between water uptake and light harvesting, via effects on modelled leaf and root biomass. Given global change in the availabilities of CO_2, water and nitrogen (Ciais, 2013), optimal partitioning approaches are a valuable tool to improve predictions of biogeochemical cycles.

5.5.2 Leaf:Root NPP Allocation Drivers across the Precipitation Gradient

Trait responses to climate, and the effect of traits on biomass, productivity and ecosystem functioning are well documented (Comas *et al*., 2013; Enquist *et al*., 2007; Freschet *et al*., 2015; Lavorel and Garnier, 2002; Poorter and Bongers, 2006; Reich, 2012; Wright *et al*., 2004). More recent studies have gone further, suggesting that spatial variation in productivity could be explained by ecosystem structure and plant traits alone. Michaletz *et al*. (2018) argue that NPP is best predicted by indirect effects of climate on stand biomass, age and size structure and growing season length, rather than direct effects of climate on plant metabolism. Fyllas *et al*. (2017) show that along a tropical elevation gradient, trait distributions are linked to variation in temperature, so that the inclusion of temperature (at least to a cooler limit of about 20^{o}C), is not required to accurately predict spatial variation in productivity. Whilst empirical evidence for the determination of NPP allocation by traits, spans edaphic and elevation gradients, as well as continents (Aragão *et al*., 2009; Girardin *et al*., 2010; Moore *et al*., 2017), until now the mechanism had not been identified. Our results show that as well as being able to explain variation in total NPP, plant trait distributions explain variation in NPP allocation between leaves and roots within an optimality framework. We show that leaf traits account for 48% of variation in optimal leaf:root NPP allocation (maximises NCE) across the Amazon precipitation gradient, with short leaf residence times supporting higher leaf:root NPP and longer leaf leaf residence times supporting shorter leaf:root NPP (Figure 5.8). The effect of root traits on optimal leaf:root NPP (15%) did not match that of leaves, whilst the direct effects of climate where minimal (<3%). The effect of climate on NPP allocation is therefore indirect, through covariation with trait distributions, and not through direct physiology-climate interactions.

5.5.3 Optimal Leaf and Root Trait Distributions

The distribution of leaf traits across the precipitation gradient were optimal (maximise NCE) (Figure 5.9). Our findings are in accordance with results from McMurtrie and Dewar (2011) which demonstrate the ability of NCE maximisation to explain spatial variation in leaf traits for an individual species. Root trait distributions were less well predicted, likely due to SPA not accounting for differences in nutrient cycling. Whilst optimality approaches appear able to explain the coupling between leaf traits and NPP allocation, it is unclear whether traits vary in response to NPP allocation, NPP allocation varies in response to traits or whether the interaction is biologically iterative. Evidence of temporal variation in both NPP allocation and

plant traits in response to resource availability offers little resolution (Chaves *et al*., 2003; David *et al*., 1998; Hamann *et al*., 2017; Huasco *et al*., 2014; Kho *et al*., 2013; Ludlow and Ng, 1974; Metcalfe *et al*., 2010; Schuldt *et al*., 2011), and it remains unknown which should be used to constrain models, and which should be assumed plastic (Mäkelä, 2012). Interestingly, optimality approaches failed to describe observed trait distributions when leaf:root NPP was not constrained to local estimates, as plasticity in leaf:root NPP allocation permitted optimal NCE independent of trait combination. Without separating the interdependence of traits and NPP allocation, we remain unable to explain the determination of their observed distributions across the precipitation gradient. Further work is therefore needed to understand how traits and NPP allocation are coordinated across resource availability gradients and across timescales.

5.5.4 Limitations

We recognise limitations of the model-data approach used including: uncertainty in biometric C flux estimates used in model calibration and validation; model assumptions around the use of labile C; fixed NPP allocated to wood within model experiments; and the absence of nutrient cycles. Model fitting of leaf traits, within the measurement standard error (or 95% confidence interval), to simulate observed carbon assimilation within one standard error, was necessitated by the aim to capture trends in field data, but error in biometric estimates of C fluxes was then propagated into model simulations. We identify leaf NPP estimates derived from litterfall and LAI measurements, and root NPP measurements using root cores, as key sources of uncertainty in our results (Clark *et al*., 2001). The accuracy and spatial validity of LAI estimates derived from indirect field measurements has been questioned (Bréda, 2003; Jonckheere *et al*., 2004; Weiss *et al*., 2004), however, our estimates align with reports from destructive harvests (see Chapter 3). Further uncertainty exists due to the time resolution of LAI and leaf litterfall measurements, which are typically 1-2 times per month. A comparison of measurement approaches for root and leaf NPP would also help reduce the uncertainty in our interpretation of NPP allocation responses to water availability (Metcalfe *et al*., 2007).

Underlying model and field estimates of NCE is an assumption of stable labile carbon dynamics, supported in part by evidence of limited year-to-year variation (Gough *et al*., 2009; Richardson *et al*., 2013). However, in response to temporal changes in water availability, Metcalfe *et al*. (2010) report that for an Amazon throughfall exclusion experiment, forest C usage exceeds total photosynthesis. More data is therefore needed to investigate inter-annual

variability in non-structural carbon stores, and to assess how the use of labile carbon supports NCE maximisation.

The fraction of NPP allocated to wood is constrained to local estimates throughout the model experiments presented. Within SPA, the constraint to wood dynamics had little effect on simulated fluxes beyond influencing wood maintenance respiration costs. We would expect that shifts in wood NPP could effect changes in light capture through stem competition. Furthermore, SPA does not account for variation in nutrient availability, which decreased with increasing precipitation across plots (Malhi *et al*., 2015). The model therefore does not capture the effect of differences in root diameter on nutrient uptake capacity, with root traits used only including root metabolic rate and root residence time. In the absence of field measurements, a lack of clarity around root trait trade-offs meant root diameter and nutrient uptake capacity could not be estimated from known interactions with other root traits (Comas and Eissenstat, 2009; Westoby and Wright, 2006). We expect that the inclusion of nutrient cycles and a broader range of root traits would strengthen reported root trait effects on optimal leaf:root NPP, through higher returns of fast root traits (with expected higher nutrient uptake rates; Roumet *et al*. (2006), Richardson *et al*. (2009)) at high MAP plots where nutrient availability is lowest.

5.6 Conclusion

This work offers new insights into the mechanisms shaping NPP allocation and trait distributions in response to water availability. We validated the optimal partitioning approach in determining leaf:root NPP allocation, against detailed field measurements, along a tropical precipitation gradient. We perform a comprehensive comparison of fitness proxies, and show that leaf:root NPP allocation is best predicted by maximisation of NCE, and not GPP or NPP. The observed distribution of leaf and root traits explained the shift in optimal leaf:root NPP across forests. Trait distributions captured the indirect effects of climate on leaf:root NPP allocation, whilst direct effects were largely absent. Leaf trait distributions were optimal across the precipitation gradient but only if leaf:root NPP was constrained to observed fractions. Our results highlight the importance of integrating NPP allocation responses to resource availability in model predictions of future carbon dynamics. However, whilst the coupling between traits and NPP allocation can be explained by optimal response theory, it remains

unclear how they interact to determine their observed distributions across the precipitation gradient (i.e. which is dependent on the other?). Here we have focused on a climate gradient to explore optimality, but alternate approaches could include similar analyses for chronosequences, and manipulation experiments. Further work is also needed to quantify the role of the labile C pool nutrients in modelled responses to water availability.

5.7 References

Aragao, L. E. O. C., Malhi, Y., Metcalfe, D. B., Silva-Espejo, J. E., Jimenez, E., Navarrete, D., Almeida, S., Costa, A. C. L., Salinas, N., Phillips, O. L., Anderson, L. O., Alvarez, E., Baker, T. R., Goncalvez, P. H., Huaman-Ovalle, J., Mamani-Solorzano, M., Meir, P., Monteagudo, A., Patino, S., Penuela, M. C., Prieto, A., Quesada, C. A., Rozas-Davila, A., Rudas, A., Silva, J. A., & Vasquez, R. (2009). Above- and below-ground net primary productivity across ten Amazonian forests on contrasting soils. Biogeosciences, 6(12), 2759-2778.

Bloom, A. J., Chapin, F. S., & Mooney, H. A. (1985). Resource Limitation in Plants - an Economic Analogy. Annual review of Ecology and Systematics, 16, 363-392.

Bréda, N. J. J. (2003). Ground-based measurements of leaf area index: a review of methods, instruments and current controversies. Journal of experimental botany, 54(392), 2403-2417.

Charles-Edwards, D. A. (1976). Shoot and root activities during steady-state plant growth. Annals of Botany, 40(4), 767-772.

Chaves, M. M., Maroco, J. P., & Pereira, J. S. (2003). Understanding plant responses to drought—from genes to the whole plant. Functional Plant Biology, 30(3), 239-264.

Ciais, P. (2013). Carbon and other biogeochemical cycles Climate Change 2013: The Physical Science Basis ed TF Stocker et al: Cambridge: Cambridge University Press.

Clark, D. A., Brown, S., Kicklighter, D. W., Chambers, J. Q., Thomlinson, J. R., & Ni, J. (2001). Measuring net primary production in forests: concepts and field methods. Ecological Applications, 11(2), 356-370.

Clark, D. B., Mercado, L. M., Sitch, S., Jones, C. D., Gedney, N., Best, M. J., Pryor, M., Rooney, G. G., Essery, R. L. H., & Blyth, E. (2011). The Joint UK Land Environment Simulator (JULES), model description–Part 2: carbon fluxes and vegetation dynamics. Geoscientific Model Development, 4(3), 701-722.

Cleveland, C. C., Taylor, P., Chadwick, K. D., Dahlin, K., Doughty, C. E., Malhi, Y., Smith, W. K., Sullivan, B. W., Wieder, W. R., & Townsend, A. R. (2015). A comparison of plot-based satellite and Earth system model estimates of tropical forest net primary production. Global Biogeochemical Cycles, 29(5), 626-644.

Coleman, J. S., & McConnaughay, K. D. M. (1995). A non-functional interpretation of a classical optimal-partitioning example: JSTOR.

Comas, L., Becker, S., Cruz, V. M. V., Byrne, P. F., & Dierig, D. A. (2013). Root traits contributing to plant productivity under drought. Frontiers in plant science, 4, 442.

Comas, L. H., & Eissenstat, D. M. (2009). Patterns in root trait variation among 25 co-existing North American forest species. New Phytologist, 182(4), 919-928.

Comins, H. N., & McMurtrie, R. E. (1993). Long-Term Response of Nutrient-Limited Forests to CO" 2 Enrichment; Equilibrium Behavior of Plant-Soil Models. Ecological Applications, 3(4), 666-681.

David, M. M., Coelho, D., Barrote, I., & Correia, M. J. (1998). Leaf age effects on photosynthetic activity and sugar accumulation in droughted and rewatered Lupinus albus plants. Functional Plant Biology, 25(3), 299-306.

De Kauwe, M. G., Medlyn, B. E., Zaehle, S., Walker, A. P., Dietze, M. C., Wang, Y. P., Luo, Y., Jain, A. K., El-Masri, B., & Hickler, T. (2014). Where does the carbon go? A model–data intercomparison of vegetation carbon allocation and turnover processes at two temperate forest free-air CO2 enrichment sites. New Phytologist, 203(3), 883-899.

Dewar, R. C., Franklin, O., Mäkelä, A., McMurtrie, R. E., & Valentine, H. T. (2009). Optimal function explains forest responses to global change. Bioscience, 59(2), 127-139.

Doughty, C. E., Metcalfe, D. B., Girardin, C. A., Amezquita, F. F., Cabrera, D. G., Huasco, W. H., Silva-Espejo, J. E., Araujo-Murakami, A., da Costa, M. C., Rocha, W., Feldpausch, T. R., Mendoza, A. L., da Costa, A. C., Meir, P., Phillips, O. L., & Malhi, Y. (2015). Drought impact on forest carbon dynamics and fluxes in Amazonia. Nature, 519(7541), 78-82.

Enquist, B. J., Kerkhoff, A. J., Stark, S. C., Swenson, N. G., McCarthy, M. C., & Price, C. A. (2007). A general integrative model for scaling plant growth, carbon flux, and functional trait spectra. Nature, 449(7159), 218.

Field, C. B., Behrenfeld, M. J., Randerson, J. T., & Falkowski, P. (1998). Primary production of the biosphere: integrating terrestrial and oceanic components. Science, 281(5374), 237-240.

Franklin, O., McMurtrie, R., Iversen, C. M., Crous, K. Y., Finzi, A. C., Tissue, D. T., Ellsworth, D. S., Oren, R. A. M., & Norby, R. J. (2009). Forest fine-root production and nitrogen use under

elevated CO2: contrasting responses in evergreen and deciduous trees explained by a common principle. Global Change Biology, 15(1), 132-144.

Freschet, G. T., Kichenin, E., & Wardle, D. A. (2015). Explaining within-community variation in plant biomass allocation: a balance between organ biomass and morphology above vs below ground? Journal of Vegetation Science, 26(3), 431-440.

Fyllas, N. M., Bentley, L. P., Shenkin, A., Asner, G. P., Atkin, O. K., Diaz, S., Enquist, B. J., Farfan-Rios, W., Gloor, E., Guerrieri, R., Huasco, W. H., Ishida, Y., Martin, R. E., Meir, P., Phillips, O., Salinas, N., Silman, M., Weerasinghe, L. K., Zaragoza-Castells, J., & Malhi, Y. (2017). Solar radiation and functional traits explain the decline of forest primary productivity along a tropical elevation gradient. Ecol Lett, 20(6), 730-740.

Geber, M. A., & Griffen, L. R. (2003). Inheritance and natural selection on functional traits. International Journal of Plant Sciences, 164(S3), S21-S42.

Girardin, C. A. J., Malhi, Y., Aragao, L., Mamani, M., Huaraca Huasco, W., Durand, L., Feeley, K. J., Rapp, J., Silva-Espejo, J. E., & Silman, M. (2010). Net primary productivity allocation and cycling of carbon along a tropical forest elevational transect in the Peruvian Andes. Global Change Biology, 16(12), 3176-3192.

Gough, C. M., Flower, C. E., Vogel, C. S., Dragoni, D., & Curtis, P. S. (2009). Whole-ecosystem labile carbon production in a north temperate deciduous forest. Agricultural and Forest Meteorology, 149(9), 1531-1540.

Hamann, E., Kesselring, H., & Stöcklin, J. (2017). Plant responses to simulated warming and drought: a comparative study of functional plasticity between congeneric mid and high elevation species. Journal of Plant Ecology.

Hertel, D., Strecker, T., Müller-Haubold, H., & Leuschner, C. (2013). Fine root biomass and dynamics in beech forests across a precipitation gradient–is optimal resource partitioning theory applicable to water-limited mature trees? Journal of ecology, 101(5), 1183-1200.

Hilbert, D. W., & Reynolds, J. F. (1991). A model allocating growth among leaf proteins, shoot structure, and root biomass to produce balanced activity. Annals of Botany, 68(5), 417-425.

Huasco, W. H., Girardin, C. A. J., Doughty, C. E., Metcalfe, D. B., Baca, L. D., Silva-Espejo, J. E., Cabrera, D. G., Aragão, L. E. O. C., Davila, A. R., & Marthews, T. R. (2014). Seasonal

production, allocation and cycling of carbon in two mid-elevation tropical montane forest plots in the Peruvian Andes. Plant Ecology & Diversity, 7(1-2), 125-142.

Ise, T., Litton, C. M., Giardina, C. P., & Ito, A. (2010). Comparison of modeling approaches for carbon partitioning: impact on estimates of global net primary production and equilibrium biomass of woody vegetation from MODIS GPP. Journal of Geophysical Research: Biogeosciences, 115(G4).

Jiménez, E. M., Moreno, F. H., Peñuel, M. C., Patino, S., & Lloyd, J. (2009). Fine root dynamics for forests on contrasting soils in the Colombian Amazon. Biogeosciences, 6, 2809-2827.

Johnson, I. R. t., & Thornley, J. H. M. (1987). A model of shoot: root partitioning with optimal growth. Annals of Botany, 60(2), 133-142.

Jonckheere, I., Fleck, S., Nackaerts, K., Muys, B., Coppin, P., Weiss, M., & Baret, F. (2004). Review of methods for in situ leaf area index determination - Part I. Theories, sensors and hemispherical photography. Agricultural and Forest Meteorology, 121(1-2), 19-35.

Kho, L. K., Malhi, Y., & Tan, S. K. S. (2013). Annual budget and seasonal variation of aboveground and belowground net primary productivity in a lowland dipterocarp forest in Borneo. Journal of Geophysical Research: Biogeosciences, 118(3), 1282-1296.

Lacointe, A. (2000). Carbon allocation among tree organs: a review of basic processes and representation in functional-structural tree models. Annals of Forest Science, 57(5), 521-533.

Lavorel, S., & Garnier, É. (2002). Predicting changes in community composition and ecosystem functioning from plant traits: revisiting the Holy Grail. Functional ecology, 16(5), 545-556.

Lima, T. T. S., Miranda, I. S., & Vasconcelos, S. S. (2010). Effects of water and nutrient availability on fine root growth in eastern Amazonian forest regrowth, Brazil. New Phytologist, 187(3), 622-630.

Ludlow, M. M., & Ng, T. T. (1974). Water stress suspends leaf ageing. Plant science letters, 3(4), 235-240.

Luo, Y., Field, C. B., & Mooney, H. A. (1994). Predicting responses of photosynthesis and root fraction to elevated [CO2] a: interactions among carbon, nitrogen, and growth. Plant, Cell & Environment, 17(11), 1195-1204.

Mäkelä, A. (2012). On guiding principles for carbon allocation in eco-physiological growth models. Tree Physiology, 32(6), 644-647.

Mäkelä, A., Valentine, H. T., & Helmisaari, H. S. (2008). Optimal co-allocation of carbon and nitrogen in a forest stand at steady state. New Phytologist, 180(1), 114-123.

Malhi, Y., Doughty, C., & Galbraith, D. (2011). The allocation of ecosystem net primary productivity in tropical forests. Phil. Trans. R. Soc. B, 366(1582), 3225-3245.

Malhi, Y., Doughty, C. E., Goldsmith, G. R., Metcalfe, D. B., Girardin, C. A. J., Marthews, T. R., del Aguila-Pasquel, J., Aragao, L. E. O. C., Araujo-Murakami, A., Brando, P., da Costa, A. C. L., Silva-Espejo, J. E., Amezquita, F. F., Galbraith, D. R., Quesada, C. A., Rocha, W., Salinas-Revilla, N., Silverio, D., Meir, P., & Phillips, O. L. (2015). The linkages between photosynthesis, productivity, growth and biomass in lowland Amazonian forests. Global Change Biology, 21(6), 2283-2295.

Malhi, Y., Roberts, J. T., Betts, R. A., Killeen, T. J., Li, W., & Nobre, C. A. (2008). Climate change, deforestation, and the fate of the Amazon. Science, 319(5860), 169-172.

McMurtrie, R. E., & Dewar, R. C. (2011). Leaf-trait variation explained by the hypothesis that plants maximize their canopy carbon export over the lifespan of leaves. Tree Physiology, 31(9), 1007-1023.

McMurtrie, R. E., & Dewar, R. C. (2013). New insights into carbon allocation by trees from the hypothesis that annual wood production is maximized. New Phytologist, 199(4), 981-990.

McMurtrie, R. E., Norby, R. J., Medlyn, B. E., Dewar, R. C., Pepper, D. A., Reich, P. B., & Barton, C. V. M. (2008). Why is plant-growth response to elevated CO2 amplified when water is limiting, but reduced when nitrogen is limiting? A growth-optimisation hypothesis. Functional Plant Biology, 35(6), 521-534.

Medlyn, B. E., Zaehle, S., De Kauwe, M. G., Walker, A. P., Dietze, M. C., Hanson, P. J., Hickler, T., Jain, A. K., Luo, Y., & Parton, W. (2015). Using ecosystem experiments to improve vegetation models. Nature Climate Change, 5(6), 528.

Medvigy, D., Wofsy, S. C., Munger, J. W., Hollinger, D. Y., & Moorcroft, P. R. (2009). Mechanistic scaling of ecosystem function and dynamics in space and time: Ecosystem Demography model version 2. Journal of Geophysical Research: Biogeosciences, 114(G1).

Meir, P., Mencuccini, M., Binks, O., Da Costa, A. C. L., Ferreira, L. V., & Rowland, L. (2018). Short-term effects of drought on tropical forest do not fully predict impacts of repeated or

long-term drought: gas exchange vs growth. Philosophical Transactions of the Royal Society B: Biological Sciences.

Meir, P., Mencuccini, M., & Dewar, R. C. (2015). Drought-related tree mortality: addressing the gaps in understanding and prediction. New Phytol, 207(1), 28-33.

Metcalfe, D. B., Meir, P., Aragao, L., Malhi, Y., Da Costa, A. C. L., Braga, A., Gonçalves, P. H. L., de Athaydes, J., De Almeida, S. S., & Williams, M. (2007). Factors controlling spatio-temporal variation in carbon dioxide efflux from surface litter, roots, and soil organic matter at four rain forest sites in the eastern Amazon. Journal of Geophysical Research: Biogeosciences, 112(G4).

Metcalfe, D. B., Meir, P., Aragão, L. E. O. C., Lobo-do-Vale, R., Galbraith, D., Fisher, R. A., Chaves, M. M., Maroco, J. P., da Costa, A. C. L., & de Almeida, S. S. (2010). Shifts in plant respiration and carbon use efficiency at a large-scale drought experiment in the eastern Amazon. New Phytologist, 187(3), 608-621.

Michaletz, S. T., Kerkhoff, A. J., & Enquist, B. J. (2018). Drivers of terrestrial plant production across broad geographical gradients. Global Ecology and Biogeography, 27(2), 166-174.

Moore, S., Adu-Bredu, S., Duah-Gyamfi, A., Addo-Danso, S. D., Ibrahim, F., Mbou, A. T., Grandcourt, A., Valentini, R., Nicolini, G., & Djagbletey, G. (2017). Forest biomass, productivity and carbon cycling along a rainfall gradient in West Africa. Global Change Biology.

Müller, I., Schmid, B., & Weiner, J. (2000). The effect of nutrient availability on biomass allocation patterns in 27 species of herbaceous plants. Perspectives in plant ecology, evolution and systematics, 3(2), 115-127.

Negrón-Juárez, R. I., Koven, C. D., Riley, W. J., Knox, R. G., & Chambers, J. Q. (2015). Observed allocations of productivity and biomass, and turnover times in tropical forests are not accurately represented in CMIP5 Earth system models. Environmental Research Letters, 10(6), 064017.

Niklas, K. J., & Enquist, B. J. (2002). Canonical rules for plant organ biomass partitioning and annual allocation. American Journal of Botany, 89(5), 812-819.

Poorter, L., & Bongers, F. (2006). Leaf traits are good predictors of plant performance across 53 rain forest species. Ecology, 87(7), 1733-1743.

Purves, D., & Pacala, S. (2008). Predictive models of forest dynamics. Science, 320(5882), 1452-1453.

Reich, P. B. (2002). Root-shoot relations: optimality in acclimation and adaptation or the 'Emperor, s new clothes. Plant roots: the hidden half, 205-220.

Reich, P. B. (2012). Key canopy traits drive forest productivity. Proceedings of the Royal Society of London B: Biological Sciences, rspb20112270.

Reynolds, J. F., & Thornley, J. H. M. (1982). A shoot: root partitioning model. Annals of Botany, 49(5), 585-597.

Richardson, A. D., Carbone, M. S., Keenan, T. F., Czimczik, C. I., Hollinger, D. Y., Murakami, P., Schaberg, P. G., & Xu, X. (2013). Seasonal dynamics and age of stemwood nonstructural carbohydrates in temperate forest trees. New Phytologist, 197(3), 850-861.

Richardson, A. E., Barea, J.-M., McNeill, A. M., & Prigent-Combaret, C. (2009). Acquisition of phosphorus and nitrogen in the rhizosphere and plant growth promotion by microorganisms. Plant and Soil, 321(1-2), 305-339.

Roumet, C., Urcelay, C., & Díaz, S. (2006). Suites of root traits differ between annual and perennial species growing in the field. New Phytologist, 170(2), 357-368.

Saxton, K. E., Rawls, W. J., Romberger, J. S., & Papendick, R. I. (1986). Estimating generalized soil-water characteristics from texture 1. Soil Science Society of America Journal, 50(4), 1031-1036.

Schuldt, B., Leuschner, C., Horna, V., Moser, G., Köhler, M., Van Straaten, O., & Barus, H. (2011). Change in hydraulic properties and leaf traits in a tall rainforest tree species subjected to long-term throughfall exclusion in the perhumid tropics. Biogeosciences, 8(8), 2179.

Thornley, J. H. M. (1972). A model to describe the partitioning of photosynthate during vegetative plant growth. Annals of Botany, 36(2), 419-430.

Thornley, J. H. M. (1995). Shoot: root allocation with respect to C, N and P: an investigation and comparison of resistance and teleonomic models. Annals of Botany, 75(4), 391-405.

Violle, C., Navas, M. L., Vile, D., Kazakou, E., Fortunel, C., Hummel, I., & Garnier, E. (2007). Let the concept of trait be functional! Oikos, 116(5), 882-892.

Wang, S., Trishchenko, A. P., & Sun, X. (2007). Simulation of canopy radiation transfer and surface albedo in the EALCO model. Climate Dynamics, 29(6), 615-632.

Wang, Y. P., Law, R. M., & Pak, B. (2010). A global model of carbon, nitrogen and phosphorus cycles for the terrestrial biosphere. Biogeosciences, 7(7), 2261-2282.

Weiss, M., Baret, F., Smith, G. J., Jonckheere, I., & Coppin, P. (2004). Review of methods for in situ leaf area index (LAI) determination Part II. Estimation of LAI, errors and sampling. Agricultural and Forest Meteorology, 121(1-2), 37-53.

Westoby, M., & Wright, I. J. (2006). Land-plant ecology on the basis of functional traits. Trends in ecology & evolution, 21(5), 261-268.

Williams, M., Schwarz, P. A., Law, B. E., Irvine, J., & Kurpius, M. R. (2005). An improved analysis of forest carbon dynamics using data assimilation. Global Change Biology, 11(1), 89-105.

Wright, I. J., Reich, P. B., Westoby, M., Ackerly, D. D., Baruch, Z., Bongers, F., Cavender-Bares, J., Chapin, T., Cornelissen, J. H., Diemer, M., Flexas, J., Garnier, E., Groom, P. K., Gulias, J., Hikosaka, K., Lamont, B. B., Lee, T., Lee, W., Lusk, C., Midgley, J. J., Navas, M. L., Niinemets, U., Oleksyn, J., Osada, N., Poorter, H., Poot, P., Prior, L., Pyankov, V. I., Roumet, C., Thomas, S. C., Tjoelker, M. G., Veneklaas, E. J., & Villar, R. (2004). The worldwide leaf economics spectrum. Nature, 428(6985), 821-827.

6. Discussion

In light of projected climate change induced shifts in precipitation, understanding the effect of water availability on ecosystem functioning is critical to predicting the future Amazon carbon balance. Our goal was to better understand the coupling between precipitation and carbon dynamics, by separating direct physiology-climate interactions, from indirect effects through forest structure, traits and carbon cycle feedbacks. We used detailed measurements of carbon fluxes and plant traits from eight permanent sample plots along an Amazon precipitation gradient, to calibrate and validate the Soil Plant Atmosphere (SPA) model. We then used SPA to undertake a series of modelling experiments to; (i) quantify the drivers of variation in photosynthesis across the precipitation gradient, (ii) explain the covariation between LAI and precipitation underpinning changes in photosynthesis, and (iii) understand carbon dynamics and plant traits supporting shifts in leaf and root biomass with precipitation. Our results demonstrate new understanding around the role of direct and indirect effects of climate in shaping spatial variation in photosynthesis, the applicability of optimality approaches to predict carbon dynamics under changes in resource availability, and how plant traits capture the effects of climate on ecosystem functioning across Amazon forests. Here we review and collate these findings. We then highlight key gaps in our knowledge around the role of the non-structural carbohydrate (NSC) pool, uncertainty in biometric data used in model calibration and validation, root traits, nutrient cycling, the representation of wood and fine root respiration within SPA and the timescale over which shifts in NPP allocation and traits in response to resource availability occur. We outline suggested future work to resolve the knowledge gaps presented, using both model and field-based approaches.

6.1 LAI Drives Photosynthesis across Amazon Forests

LAI was the principal driver of spatial variation in photosynthesis along the Amazon precipitation gradient. Together, the indirect effects of climate (LAI and leaf traits accounted for 56% of observed variance) exceeded direct effects (physiology-climate interactions accounted for 12%) in explaining photosynthesis trends, reflecting reports across other climatic gradients and biomes (Fyllas *et al*., 2017; Hui *et al*., 2003; Richardson *et al*., 2007). The relative sensitivity of photosynthesis to direct and indirect climate forcings shifted with water availability, demand and acquisition potential, whereby forests with a bigger evaporative demand (high LAI) relative to water supply were most sensitive to differences in climate and rooting depth, whilst forests occupying the highest rainfall zone where most sensitive to changes in LAI and leaf traits. The divergence in sensitivities highlighted the importance of considering water demand versus supply when investigating the resilience of Amazon forests to changes in precipitation (Malhi *et al*., 2008; Phillips *et al*., 2009). Across sub-annual timescales, the direct effects of climate on photosynthesis were more important than indirect effects via LAI. The relative importance of solar radiation and VPD in driving sub-annual photosynthesis increased and decreased with precipitation respectively (solar radiation R^2 = 0.64, p=0.017; VPD R^2= 0.32, p=0.14). We reason that the importance of LAI and leaf traits in determining spatial variation in photosynthesis, reflects the timescales over which acclimation and adaptation to resource availability occur (via emergent canopy properties and shifts in species composition), and that variation in climate relative to LAI and leaf traits, drives stronger determination of photosynthesis across sub-annual timescales (Richardson *et al*., 2007). Given the role of LAI in driving photosynthesis across the precipitation gradient, understanding how water availability shapes canopy dynamics is critical to discerning the impact of future precipitation change on Amazon forests.

6.2 Maximisation of NCE explains LAI trends

Tropical forest canopy dynamics operate in accordance with their hydraulic environment. Maximisation of net canopy carbon export (NCE) explained the increase in LAI with precipitation (observed LAI versus that at predicted NCE maxima R^2=0.39, p=0.099, RMSE=0.88 m^2m^{-2}), corroborating with results from optimality studies in mid to high latitude

forests (Franklin, 2007; Mäkelä *et al*., 2008; McMurtrie and Dewar, 2011, 2013). Carbon cycle feedbacks (whereby declines in NCE, as a result of non-optimal LAI, caused declines in root biomass, water acquisition, carbon assimilation and consequently NCE) strengthened the interaction between NCE and LAI for forests in the lowest precipitation zone, highlighting the importance of representing the all autotrophic pools in the carbon cycle when modelling optimal leaf area (with respect to NCE maximisation). Leaf traits proved most important in shaping optimal LAI across the precipitation gradient (Caldararu *et al*., 2016). For transitional forests 'fast' leaf trait strategies maximised photosynthesis during the wet season and minimised carbon losses during the dry season. For core forests, 'slow' leaf traits lower photosynthesis was offset by lower carbon costs of leaf construction and maintenance throughout the year. The observed distribution of leaf traits across the precipitation gradient therefore supported cost-benefit theories (Givnish, 2002; Iio *et al*., 2014; Kikuzawa, 1991). Our results demonstrated the value of optimality approaches in modelling LAI and the importance of leaf traits. However, the increase in LAI with MAP (R^2=0.42, p=0.08) was not coincident with increases in leaf NPP, prompting us to ask what drives NPP allocation across Amazon forests?

6.3 Leaf Traits Drive Optimal Leaf:Root NPP Allocation

Across Amazon forests the decline in leaf:root NPP with increasing precipitation (R^2=0.43, p=0.07), appeared to oppose optimal partitioning theory, which suggests plant maximise fitness by actively apportioning NPP between organs to increase uptake of the most limiting resource (Bloom *et al*., 1985; Charles-Edwards, 1976; Hilbert and Reynolds, 1991; Johnson and Thornley, 1987; Luo *et al*., 1994; McMurtrie and Dewar, 2013; Reynolds and Thornley, 1982; Thornley, 1972; Thornley, 1995). Yet, the distribution of organ biomass was as predicted, and leaf biomass increased and root biomass decreased with increasing precipitation (leaves R^2=0.29, p=0.165; roots R^2= 0.63, p=0.059). However, leaf:root NPP trends proved optimal with respect to the maximisation of NCE (observed leaf:root NPP allocation versus that at predicted NCE maxima R^2=0.60, p=0.02). Our finding corroborate with other reports which use optimality approaches to predict NPP allocation in response to resource availability (Dewar *et al*., 2009; Franklin *et al*., 2009; Mäkelä *et al*., 2008). Opposing NPP and biomass trends were supported by shifts in plant traits along the precipitation gradient. Leaf residence time increased with increasing precipitation, whilst root residence time decreased (leaves R^2=0.60,

p=0.03; roots R^2= 0.46, p=0.06). Leaf traits accounted for 48% of variation in optimal leaf:root NPP (with respect to maximum NCE), whilst root traits accounted for 15%. Our results are therefore in accordance with empirical studies, which suggest biomass distributions are driven by differences in residence times rather than NPP allocation (Moore *et al*., 2017). Whilst indirect effect of climate explained much of the variation in optimal leaf:root NPP (via determination of plant trait distributions), direct effects (via physiology-climate interactions) were minimal (<3%). The distribution of leaf traits across the precipitation gradient maximised NCE, but optimality approaches failed to explain spatial variation in root traits. Furthermore, neither leaf nor root trait distributions could be explained using optimality approaches when leaf:root NPP allocation was not constrained to observed leaf:root NPP, highlighting an interdependency of plant traits and NPP allocation. It therefore remains unclear from a modelling perspective which should be constrained and which should be assumed plastic (Mäkelä, 2012) and further work is needed to successfully integrate optimality approaches into ecosystem models. Despite the uncertainty around the effect of root traits and interdependency of traits and NPP allocation, it is clear that the previously unquantified role of leaf traits is important in shaping optimal NPP allocation responses to water availability.

6.4 Coupling Between Precipitation and Carbon Dynamics

Collectively, our results demonstrate that photosynthesis trends across the Amazon precipitation gradient are principally driven by LAI, that LAI is shaped by an optimal response to water availability, and underpinning changes in LAI is optimal partitioning of NPP allocation, which is largely dependent of leaf trait distributions (see Chapter 1, Figure 1.1). We show that variation in LAI, NPP allocation and leaf traits can be successfully predicted using an optimality approach. Importantly, our results highlight the potential to use optimality approaches to reduce uncertainty in the predicted response of Amazon forests to long-term changes in precipitation. We further show that the indirect effects of climate, via a determinate effect on leaf traits, proves more important in driving NPP allocation, LAI, and ultimately photosynthesis, than the direct effects of physiology-climate interactions. Given the role of leaf traits in underpinning ecosystem functioning, we suggest that the response of Amazon forests to changes in precipitation will largely be dependent on the current spatial distribution

of leaf traits, their plasticity and the likelihood of future shifts in floristic and functional trait composition.

6.5 Optimality Approaches

Given global change in the availabilities of CO_2, water and nitrogen (Ciais, 2013), capturing the response of ecosystem dynamics to changes in resource availability remains a key challenge. Across tropical forests, shifts in LAI have been reported in response to both long and short term changes in precipitation (Barbosa and Asner, 2017; Hilker *et al*., 2014; Saatchi *et al*., 2013; Zhou *et al*., 2014), together with shifts in NPP allocation (Doughty *et al*., 2014; Doughty *et al*., 2015) and leaf traits (Fauset *et al*., 2012). Yet these processes are poorly represented in current land-surface and ecosystem models (Negrón-Juárez *et al*., 2015). Phenology is typically modelled using empirical relationships between phenological status, moisture availability and temperature (Clark *et al*., 2011; Jolly *et al*., 2005; Krinner *et al*., 2005; Medvigy *et al*., 2009). The representation of NPP allocation often follows allometry or fixed allocation ratios, whilst plant traits can also be fixed parameters (Clark *et al*., 2011; Medvigy *et al*., 2009; Williams *et al*., 1998; Williams *et al.,* 1996*)*. The fixed nature of ecosystem dynamics in many modelling approaches, limits their ability to represent ecosystem responses to changing resource availabilities. Representing ecosystem dynamics that vary with resource availability can be achieved using an optimality approach. Optimality models have been used to successfully predict stomatal conductance, LAI, carbon allocation and leaf traits (Caldararu *et al*., 2014; McMurtrie and Dewar, 2011, 2013; Medlyn *et al*., 2011; Sugiura and Tateno, 2011; Xu *et al*., 2017). We show that the performance of an optimality model (using NCE as a fitness proxy) is consistent across a tropical precipitation gradient and can explain variation in LAI, NPP allocation and leaf traits in response to water availability. Optimality approaches therefore offer a unique opportunity to reduce uncertainty around predicted Amazon carbon dynamics in response to future climate change (Meir *et al*., 2015).

6.6 Traits Capture the Effects of Climate on Ecosystem Functioning

It is widely recognised that forest structure and traits can predict ecosystem dynamics such as carbon storage, biomass partitioning, and productivity (Duursma and Falster, 2016; Finegan *et al*., 2015; Garnier *et al*., 2004; Mercado *et al*., 2011; Poorter and Bongers, 2006; Poorter *et*

al., 2017). Emerging evidence suggests that the explanatory power of forest structure and plant traits in predicting ecosystem dynamics outweighs and captures climate and edaphic effects through indirect pathways (Fyllas *et al*., 2017; Michaletz *et al*., 2014; Michaletz *et al*., 2015; Poorter *et al*., 2017; Richardson *et al*., 2007; Van Bodegom *et al*., 2012). Under the response-effect trait framework, abiotic variation filters community traits (trait response), and the selected traits then influence productivity (trait effect). The indirect effect of nutrient availability on productivity through trait response and effects are well documented (Lavorel and Garnier, 2002). However, Griffin-Nolan *et al*. (2018) highlight that whilst for nutrients there is a clear overlap between response traits and effect traits, the same is not necessarily true for precipitation. Li *et al*. (2015) suggest that the leaf economic spectrum, associated with light capture and carbon economics, is separate from the hydraulic spectrum associated with water transport. Yet, our results show that plant traits do capture the indirect effects of precipitation on variation in LAI, NPP allocation, and ultimately variation in photosynthesis. Our findings develop on previous work drawing correlates between ecosystem process drivers, by mechanistically demonstrating trait effects (Michaletz *et al*., 2014; Poorter *et al*., 2017; Sande *et al*., 2017; van der Sande *et al*., 2018). However, we do not quantify the trait responses to precipitation beyond presenting observed spatial distributions. Given the importance of traits in determining ecosystem processes, efforts to collate field estimates such as the TRY trait database (Kattge *et al*., 2011), and efforts to map local and regional scale variation in leaf traits using new techniques in airborne spectroscopy (Asner *et al*., 2015; Asner *et al*., 2017) are increasingly important.

6.7 Limitations

We recognise key limitations to our interpretation of the effects of water availability on ecosystem functioning including: the role of the NSC pool, uncertainty in biometric data used in model calibration and validation, root traits, nutrient cycling and the representation of wood and fine root respiration within SPA. Inferred NSC dynamics were constrained to an extent by model-simulated photosynthesis and the validation of modelled NPP and respiration against field estimates. However, we were unable to validate simulated NSC dynamics directly, causing uncertainty in our interpretation of optimal LAI and NPP allocation, which assumed a mass balance approach.

Uncertainty associated with field data used in model calibration and validation was propagated into model simulations. Notably, fine roots are notoriously difficult to measure,

and the sampling effort required to capture standing crop root mass is large (Metcalfe *et al*., 2007), causing uncertainty in the validation of belowground dynamics. Aboveground, whilst we account for the standard error of field estimated LAI in our results, we fail to consider the effects of measurement error, which could shift reported LAI trends. The accuracy of LAI estimates from hemispherical photographs has been questioned, especially at higher leaf areas (Bréda, 2003; Jonckheere *et al*., 2004; Weiss *et al*., 2004). However, Asner *et al*. (2003) report no systematic difference between LAI estimates from different methods, and field estimates used in the presented study were in line with destructive sampling measurements from similar Amazon forests (McWilliam *et al*., 1993).

A lack of root trait field estimates, limited understanding around root trait trade-offs and the poor representation of root multi-functionality in ecosystem models (Bardgett *et al*., 2014; Kramer-Walter *et al*., 2016), limited our interpretation of leaf:root NPP allocation in response to water availability. Root traits proved less important than leaf traits in shaping optimal NPP allocation, which could reflect the role of light limitation in tropical rainforests, but could also result from our inability to capture root trait variation. Furthermore, nutrient cycling was not accounted for within the SPA model framework. As such, we were unable to quantify the impact of soil nutrients, which decreased with increasing precipitation (Malhi *et al*., 2015), on ecosystem functioning beyond its manifestation in leaf traits. We expect the inclusion of nutrient cycling within analyses would constrain LAI and leaf:root NPP optimality estimates, dependent on local nutrient availability and uptake capacity.

Modelling autotrophic respiration poses numerous difficulties including systematic differences in respiration rates between plant tissues (leaves, stems, and roots) (Reich *et al*., 2008), and their sensitivity to temperature (Atkin *et al*., 2005; Tjoelker *et al*., 2001), water (Metcalfe *et al*., 2010) and respiratory substrate availability (Atkin and Tjoelker, 2003). Leaf respiration in SPA was modelled using field estimates of leaf N content and the equation presented in Reich *et al*. (2008), validated against biometric estimates. Wood and fine root respiration was modelled using a coefficient derived from field estimates as a function of organ biomass. Wood and fine root respiration dynamics under non-observed conditions were therefore less robust.

6.8 Further Work

We recommend further work to address both the limitations highlighted above, and knowledge gaps around the timescale over which shifts in NPP allocation and traits in response to resource availability occur. Whilst able to report overall NSC trends, restrictions to current NSC data available from tropical forests, limit the opportunities to quantify the pool in the context of other plant C fluxes such as photosynthesis, NPP and respiration (Rowland *et al*., 2015; Würth *et al*., 2005). As a consequence of our limited understanding, NSC dynamics are poorly represented in ecosystem models (Dietze *et al*., 2014). Further efforts in field data collection and model development are required to resolve NSC pools, fluxes and responses to abiotic variation. Field approaches should aim to measure the whole plant NSC pool over time, in conjunction with biometric and eddy covariance tower flux estimates. Modelling approaches can then be used to collate C flux estimates, constrain NSC dynamics, and test and validate new theories around NSC usage.

To address uncertainty around field estimates used in model calibration and validation, more data from different sources is needed. By combining biometric, flux and satellite products C flux estimates can be better constrained (Cleveland *et al*., 2015). In particular, modelling effort should utilise current and upcoming satellite missions such as FLEX, GEDI and Sentinel, to constrain canopy dynamics, using new data on changes in leaves in-situ, vertical canopy structure, and temporal variability via repeat measurements (Asner *et al*., 2015; Drusch *et al*., 2017; Morton, 2016; Pettorelli *et al*., 2018). Efforts to map trait distributions will also prove important (Asner *et al*., 2015; Kattge *et al*., 2011) given the role of traits in shaping ecosystem functioning presented in this thesis.

At present data on root traits in tropical forests is limited (Metcalfe *et al*., 2008), and the linkages between root traits remain unclear (Mommer and Weemstra, 2012; Roumet *et al*., 2016). To improve understanding of carbon (and nutrient) dynamics, the quantification of root traits across Amazon forests is needed. Mapping root trait distributions such as nutrient uptake capacity, root N content and specific root length could then help modelling efforts to accurately represent belowground dynamics, and separate nutrient and climate effects within the global change framework. Efforts to collect nutrient cycling data should focus on organ specific measurements as demonstrated in Inagawa *et al*. (*in prep.*). Such measurements would enable modelling teams to improve the representation of nutrient usage within the plant.

We were unable to utilise the N content based wood and fine root respiration equations presented in Reich *et al*. (2008), due to a lack of plot based N content estimates, and the use of literature based estimates proving unsuccessful. The disparity between N content derived respiration and biometric estimates may have been caused by tropical rainforest species being underrepresented in the data used to derive the equations. Furthermore excepting one study (Pruyn *et al*., 2005), stems used by Reich *et al*. (2008) to derive respiration equations are not thought to exceed 25cm in diameter (25cm was the maximum diameter noted, though often diameter details were not given, this assumption is based on other reported details such as the stem being a sapling or leaf bearing). A mechanistic understanding of wood respiration (especially for larger trees) and fine root respiration is needed, and would be invaluable to predicting changes in autotrophic respiration in response to water availability (Doughty *et al*., 2015), not currently captured by ecosystem models.

In addition to the limitations highlighted, we identify the interdependency of NPP allocation and traits as a key gap in our current understanding. Evidence of temporal variation in both NPP allocation and plant traits in response to resource availability are typically in isolation, and are therefore insufficient to separate the interaction (Chaves *et al*., 2003; David *et al*., 1998; Hamann *et al*., 2017; Huasco *et al*., 2014; Kho *et al*., 2013; Ludlow and Ng, 1974; Metcalfe *et al*., 2010; Schuldt *et al*., 2011). From a modelling perspective, it is unclear whether NPP allocation or traits should be assumed plastic, and which should be constrained (Mäkelä, 2012). Opportunities to understand how traits and NPP allocation decision making is coordinated, could include chronosequences, large scale plot based experiments such as the new Amazon FACE (Norbey *et al*., 2016), or laboratory based approaches.

6.9 References

Asner, G. P., Martin, R. E., Anderson, C. B., & Knapp, D. E. (2015). Quantifying forest canopy traits: Imaging spectroscopy versus field survey. Remote sensing of Environment, 158, 15-27.

Asner, G. P., Martin, R. E., Knapp, D. E., Tupayachi, R., Anderson, C. B., Sinca, F., Vaughn, N. R., & Llactayo, W. (2017). Airborne laser-guided imaging spectroscopy to map forest trait diversity and guide conservation. Science, 355(6323), 385-389.

Asner, G. P., Scurlock, J. M. O., & Hicke, J. A. (2003). Global synthesis of leaf area index observations: implications for ecological and remote sensing studies. Global Ecology and Biogeography, 12(3), 191-205.

Atkin, O. K., Bruhn, D., Hurry, V. M., & Tjoelker, M. G. (2005). Evans Review No. 2: The hot and the cold: unravelling the variable response of plant respiration to temperature. Functional Plant Biology, 32(2), 87-105.

Atkin, O. K., & Tjoelker, M. G. (2003). Thermal acclimation and the dynamic response of plant respiration to temperature. Trends in plant science, 8(7), 343-351.

Barbosa, J. M., & Asner, G. P. (2017). Prioritizing landscapes for restoration based on spatial patterns of ecosystem controls and plant–plant interactions. Journal of Applied Ecology, 54(5), 1459-1468.

Bardgett, R. D., Mommer, L., & De Vries, F. T. (2014). Going underground: root traits as drivers of ecosystem processes. Trends in ecology & evolution, 29(12), 692-699.

Bloom, A. J., Chapin, F. S., & Mooney, H. A. (1985). Resource Limitation in Plants - an Economic Analogy. Annual review of Ecology and Systematics, 16, 363-392.

Bréda, N. J. J. (2003). Ground-based measurements of leaf area index: a review of methods, instruments and current controversies. Journal of experimental botany, 54(392), 2403-2417.

Caldararu, S., Purves, D. W., & Palmer, P. I. (2014). Phenology as a strategy for carbon optimality: a global model. Biogeosciences, 11(3), 763-778.

Caldararu, S., Purves, D. W., & Smith, M. J. (2016). The effect of using the plant functional type paradigm on a data-constrained global phenology model. Biogeosciences, 13(4), 925.

Charles-Edwards, D. A. (1976). Shoot and root activities during steady-state plant growth. Annals of Botany, 40(4), 767-772.

Chaves, M. M., Maroco, J. P., & Pereira, J. S. (2003). Understanding plant responses to drought—from genes to the whole plant. Functional Plant Biology, 30(3), 239-264.

Ciais, P. (2013). Carbon and other biogeochemical cycles Climate Change 2013: The Physical Science Basis ed TF Stocker et al: Cambridge: Cambridge University Press.

Clark, D. B., Mercado, L. M., Sitch, S., Jones, C. D., Gedney, N., Best, M. J., Pryor, M., Rooney, G. G., Essery, R. L. H., & Blyth, E. (2011). The Joint UK Land Environment Simulator (JULES),

model description–Part 2: carbon fluxes and vegetation dynamics. Geoscientific Model Development, 4(3), 701-722.

Cleveland, C. C., Taylor, P., Chadwick, K. D., Dahlin, K., Doughty, C. E., Malhi, Y., Smith, W. K., Sullivan, B. W., Wieder, W. R., & Townsend, A. R. (2015). A comparison of plot-based satellite and Earth system model estimates of tropical forest net primary production. Global Biogeochemical Cycles, 29(5), 626-644.

David, M. M., Coelho, D., Barrote, I., & Correia, M. J. (1998). Leaf age effects on photosynthetic activity and sugar accumulation in droughted and rewatered Lupinus albus plants. Functional Plant Biology, 25(3), 299-306.

Dewar, R. C., Franklin, O., Mäkelä, A., McMurtrie, R. E., & Valentine, H. T. (2009). Optimal function explains forest responses to global change. Bioscience, 59(2), 127-139.

Dietze, M. C., Sala, A., Carbone, M. S., Czimczik, C. I., Mantooth, J. A., Richardson, A. D., & Vargas, R. (2014). Nonstructural carbon in woody plants. Annu Rev Plant Biol, 65, 667-687.

Doughty, C. E., Malhi, Y., Araujo-Murakami, A., Metcalfe, D. B., Silva-Espejo, J. E., Arroyo, L., Heredia, J. P., Pardo-Toledo, E., Mendizabal, L. M., & Rojas-Landivar, V. D. (2014). Allocation trade-offs dominate the response of tropical forest growth to seasonal and interannual drought. Ecology, 95(8), 2192-2201.

Doughty, C. E., Metcalfe, D. B., Girardin, C. A., Amezquita, F. F., Cabrera, D. G., Huasco, W. H., Silva-Espejo, J. E., Araujo-Murakami, A., da Costa, M. C., Rocha, W., Feldpausch, T. R., Mendoza, A. L., da Costa, A. C., Meir, P., Phillips, O. L., & Malhi, Y. (2015). Drought impact on forest carbon dynamics and fluxes in Amazonia. Nature, 519(7541), 78-82.

Drusch, M., Moreno, J., Del Bello, U., Franco, R., Goulas, Y., Huth, A., Kraft, S., Middleton, E. M., Miglietta, F., & Mohammed, G. (2017). The FLuorescence EXplorer Mission Concept—ESA's Earth Explorer 8. IEEE Transactions on Geoscience and Remote Sensing, 55(3), 1273-1284.

Duursma, R. A., & Falster, D. S. (2016). Leaf mass per area, not total leaf area, drives differences in above-ground biomass distribution among woody plant functional types. New Phytologist, 212(2), 368-376.

Fauset, S., Baker, T. R., Lewis, S. L., Feldpausch, T. R., Affum-Baffoe, K., Foli, E. G., Hamer, K. C., & Swaine, M. D. (2012). Drought-induced shifts in the floristic and functional composition of tropical forests in Ghana. Ecol Lett, 15(10), 1120-1129.

Finegan, B., Peña-Claros, M., de Oliveira, A., Ascarrunz, N., Bret-Harte, M. S., Carreño-Rocabado, G., Casanoves, F., Díaz, S., Velepucha, P. E., & Fernandez, F. (2015). Does functional trait diversity predict above-ground biomass and productivity of tropical forests? Testing three alternative hypotheses. Journal of ecology, 103(1), 191-201.

Franklin, O. (2007). Optimal nitrogen allocation controls tree responses to elevated CO2. New Phytologist, 174(4), 811-822.

Franklin, O., McMurtrie, R., Iversen, C. M., Crous, K. Y., Finzi, A. C., Tissue, D. T., Ellsworth, D. S., Oren, R. A. M., & Norby, R. J. (2009). Forest fine-root production and nitrogen use under

elevated CO2: contrasting responses in evergreen and deciduous trees explained by a common principle. Global Change Biology, 15(1), 132-144.

Fyllas, N. M., Bentley, L. P., Shenkin, A., Asner, G. P., Atkin, O. K., Diaz, S., Enquist, B. J., Farfan-Rios, W., Gloor, E., Guerrieri, R., Huasco, W. H., Ishida, Y., Martin, R. E., Meir, P., Phillips, O., Salinas, N., Silman, M., Weerasinghe, L. K., Zaragoza-Castells, J., & Malhi, Y. (2017). Solar radiation and functional traits explain the decline of forest primary productivity along a tropical elevation gradient. Ecol Lett, 20(6), 730-740.

Garnier, E., Cortez, J., Billès, G., Navas, M.-L., Roumet, C., Debussche, M., Laurent, G., Blanchard, A., Aubry, D., & Bellmann, A. (2004). Plant functional markers capture ecosystem properties during secondary succession. Ecology, 85(9), 2630-2637.

Givnish, T. J. (2002). Adaptive significance of evergreen vs. deciduous leaves: solving the triple paradox. Silva fennica, 36(3), 703-743.

Griffin-Nolan, R. J., Bushey, J. A., Carroll, C. J. W., Challis, A., Chieppa, J., Garbowski, M., Hoffman, A. M., Post, A. K., Slette, I. J., & Spitzer, D. (2018). Trait selection and community weighting are key to understanding ecosystem responses to changing precipitation regimes. Functional ecology.

Hamann, E., Kesselring, H., & Stöcklin, J. (2017). Plant responses to simulated warming and drought: a comparative study of functional plasticity between congeneric mid and high elevation species. Journal of Plant Ecology.

Hilbert, D. W., & Reynolds, J. F. (1991). A model allocating growth among leaf proteins, shoot structure, and root biomass to produce balanced activity. Annals of Botany, 68(5), 417-425.

Hilker, T., Lyapustin, A. I., Tucker, C. J., Hall, F. G., Myneni, R. B., Wang, Y., Bi, J., Mendes de Moura, Y., & Sellers, P. J. (2014). Vegetation dynamics and rainfall sensitivity of the Amazon. Proc Natl Acad Sci U S A, 111(45), 16041-16046.

Huasco, W. H., Girardin, C. A. J., Doughty, C. E., Metcalfe, D. B., Baca, L. D., Silva-Espejo, J. E., Cabrera, D. G., Aragão, L. E. O. C., Davila, A. R., & Marthews, T. R. (2014). Seasonal production, allocation and cycling of carbon in two mid-elevation tropical montane forest plots in the Peruvian Andes. Plant Ecology & Diversity, 7(1-2), 125-142.

Hui, D., Luo, Y., & Katul, G. (2003). Partitioning interannual variability in net ecosystem exchange between climatic variability and functional change. Tree Physiology, 23(7), 433-442.

Iio, A., Hikosaka, K., Anten, N. P. R., Nakagawa, Y., & Ito, A. (2014). Global dependence of field-observed leaf area index in woody species on climate: a systematic review. Global Ecology and Biogeography, 23(3), 274-285.

Inagawa, T., Riutta, T., Kho, L. K., Majalap-Lee, N., & Malhi, Y. (in prep.). Nutrient uptake, use efficiency, resorption and allocation along a disturbance gradient in Bornean tropical forests.

Johnson, I. R. t., & Thornley, J. H. M. (1987). A model of shoot: root partitioning with optimal growth. Annals of Botany, 60(2), 133-142.

Jolly, W. M., Nemani, R., & Running, S. W. (2005). A generalized, bioclimatic index to predict foliar phenology in response to climate. Global Change Biology, 11(4), 619-632.

Jonckheere, I., Fleck, S., Nackaerts, K., Muys, B., Coppin, P., Weiss, M., & Baret, F. (2004). Review of methods for in situ leaf area index determination - Part I. Theories, sensors and hemispherical photography. Agricultural and Forest Meteorology, 121(1-2), 19-35.

Kattge, J., Diaz, S., Lavorel, S., Prentice, I. C., Leadley, P., Bönisch, G., Garnier, E., Westoby, M., Reich, P. B., & Wright, I. J. (2011). TRY–a global database of plant traits. Global Change Biology, 17(9), 2905-2935.

Kho, L. K., Malhi, Y., & Tan, S. K. S. (2013). Annual budget and seasonal variation of aboveground and belowground net primary productivity in a lowland dipterocarp forest in Borneo. Journal of Geophysical Research: Biogeosciences, 118(3), 1282-1296.

Kikuzawa, K. (1991). A cost-benefit analysis of leaf habit and leaf longevity of trees and their geographical pattern. The American Naturalist, 138(5), 1250-1263.

Kramer-Walter, K. R., Bellingham, P. J., Millar, T. R., Smissen, R. D., Richardson, S. J., & Laughlin, D. C. (2016). Root traits are multidimensional: specific root length is independent from root tissue density and the plant economic spectrum. Journal of ecology, 104(5), 1299-1310.

Krinner, G., Viovy, N., de Noblet-Ducoudré, N., Ogée, J., Polcher, J., Friedlingstein, P., Ciais, P., Sitch, S., & Prentice, I. C. (2005). A dynamic global vegetation model for studies of the coupled atmosphere-biosphere system. Global Biogeochemical Cycles, 19(1).

Lavorel, S., & Garnier, É. (2002). Predicting changes in community composition and ecosystem functioning from plant traits: revisiting the Holy Grail. Functional ecology, 16(5), 545-556.

Li, L., McCormack, M. L., Ma, C., Kong, D., Zhang, Q., Chen, X., Zeng, H., Niinemets, Ü., & Guo, D. (2015). Leaf economics and hydraulic traits are decoupled in five species-rich tropical-subtropical forests. Ecology letters, 18(9), 899-906.

Ludlow, M. M., & Ng, T. T. (1974). Water stress suspends leaf ageing. Plant science letters, 3(4), 235-240.

Luo, Y., Field, C. B., & Mooney, H. A. (1994). Predicting responses of photosynthesis and root fraction to elevated [CO2] a: interactions among carbon, nitrogen, and growth. Plant, Cell & Environment, 17(11), 1195-1204.

Mäkelä, A. (2012). On guiding principles for carbon allocation in eco-physiological growth models. Tree Physiology, 32(6), 644-647.

Mäkelä, A., Valentine, H. T., & Helmisaari, H. S. (2008). Optimal co-allocation of carbon and nitrogen in a forest stand at steady state. New Phytologist, 180(1), 114-123.

Malhi, Y., Doughty, C. E., Goldsmith, G. R., Metcalfe, D. B., Girardin, C. A. J., Marthews, T. R., del Aguila-Pasquel, J., Aragao, L. E. O. C., Araujo-Murakami, A., Brando, P., da Costa, A. C. L., Silva-Espejo, J. E., Amezquita, F. F., Galbraith, D. R., Quesada, C. A., Rocha, W., Salinas-Revilla, N., Silverio, D., Meir, P., & Phillips, O. L. (2015). The linkages between photosynthesis,

productivity, growth and biomass in lowland Amazonian forests. Global Change Biology, 21(6), 2283-2295.

Malhi, Y., Roberts, J. T., Betts, R. A., Killeen, T. J., Li, W., & Nobre, C. A. (2008). Climate change, deforestation, and the fate of the Amazon. Science, 319(5860), 169-172.

McMurtrie, R. E., & Dewar, R. C. (2011). Leaf-trait variation explained by the hypothesis that plants maximize their canopy carbon export over the lifespan of leaves. Tree Physiology, 31(9), 1007-1023.

McMurtrie, R. E., & Dewar, R. C. (2013). New insights into carbon allocation by trees from the hypothesis that annual wood production is maximized. New Phytologist, 199(4), 981-990.

McWilliam, A. L., Roberts, J. M., Cabral, O. M. R., Leitao, M., De Costa, A. C. L., Maitelli, G. T., & Zamparoni, C. (1993). Leaf area index and above-ground biomass of terra firme rain forest and adjacent clearings in Amazonia. Functional ecology, 310-317.

Medlyn, B. E., Duursma, R. A., Eamus, D., Ellsworth, D. S., Prentice, I. C., Barton, C. V. M., Crous, K. Y., De Angelis, P., Freeman, M., & Wingate, L. (2011). Reconciling the optimal and empirical approaches to modelling stomatal conductance. Global Change Biology, 17(6), 2134-2144.

Medvigy, D., Wofsy, S. C., Munger, J. W., Hollinger, D. Y., & Moorcroft, P. R. (2009). Mechanistic scaling of ecosystem function and dynamics in space and time: Ecosystem Demography model version 2. Journal of Geophysical Research: Biogeosciences, 114(G1).

Meir, P., Mencuccini, M., & Dewar, R. C. (2015). Drought-related tree mortality: addressing the gaps in understanding and prediction. New Phytol, 207(1), 28-33.

Mercado, L. M., Patino, S., Domingues, T. F., Fyllas, N. M., Weedon, G. P., Sitch, S., Quesada, C. A., Phillips, O. L., Aragao, L. E., Malhi, Y., Dolman, A. J., Restrepo-Coupe, N., Saleska, S. R., Baker, T. R., Almeida, S., Higuchi, N., & Lloyd, J. (2011). Variations in Amazon forest productivity correlated with foliar nutrients and modelled rates of photosynthetic carbon supply. Philos Trans R Soc Lond B Biol Sci, 366(1582), 3316-3329.

Metcalfe, D. B., Meir, P., Aragao, L., Malhi, Y., Da Costa, A. C. L., Braga, A., Gonçalves, P. H. L., de Athaydes, J., De Almeida, S. S., & Williams, M. (2007). Factors controlling spatio-temporal variation in carbon dioxide efflux from surface litter, roots, and soil organic matter at four rain forest sites in the eastern Amazon. Journal of Geophysical Research: Biogeosciences, 112(G4).

Metcalfe, D. B., Meir, P., Aragao, L. E. O. C., da Costa, A. C. L., Braga, A. P., Goncalves, P. H. L., Silva, J. D., de Almeida, S. S., Dawson, L. A., Malhi, Y., & Williams, M. (2008). The effects of water availability on root growth and morphology in an Amazon rainforest. Plant and Soil, 311(1-2), 189-199.

Metcalfe, D. B., Meir, P., Aragão, L. E. O. C., Lobo-do-Vale, R., Galbraith, D., Fisher, R. A., Chaves, M. M., Maroco, J. P., da Costa, A. C. L., & de Almeida, S. S. (2010). Shifts in plant respiration and carbon use efficiency at a large-scale drought experiment in the eastern Amazon. New Phytologist, 187(3), 608-621.

Michaletz, S. T., Cheng, D., Kerkhoff, A. J., & Enquist, B. J. (2014). Convergence of terrestrial plant production across global climate gradients. Nature, 512(7512), 39.

Michaletz, S. T., Weiser, M. D., Zhou, J., Kaspari, M., Helliker, B. R., & Enquist, B. J. (2015). Plant thermoregulation: energetics, trait–environment interactions, and carbon economics. Trends in ecology & evolution, 30(12), 714-724.

Mommer, L., & Weemstra, M. (2012). The role of roots in the resource economics spectrum. New Phytologist, 195(4), 725-727.

Moore, S., Adu-Bredu, S., Duah-Gyamfi, A., Addo-Danso, S. D., Ibrahim, F., Mbou, A. T., Grandcourt, A., Valentini, R., Nicolini, G., & Djagbletey, G. (2017). Forest biomass, productivity and carbon cycling along a rainfall gradient in West Africa. Global Change Biology.

Morton, D. C. (2016). FOREST CARBON FLUXES A satellite perspective. Nature Climate Change, 6(4), 346-348.

Negrón-Juárez, R. I., Koven, C. D., Riley, W. J., Knox, R. G., & Chambers, J. Q. (2015). Observed allocations of productivity and biomass, and turnover times in tropical forests are not accurately represented in CMIP5 Earth system models. Environmental Research Letters, 10(6), 064017.

Pettorelli, N., Buhne, H. S. T., Tulloch, A., Dubois, G., Macinnis-Ng, C., Queiros, A. M., Keith, D. A., Wegmann, M., Schrodt, F., Stellmes, M., Sonnenschein, R., Geller, G. N., Roy, S., Somers, B., Murray, N., Bland, L., Geijzendorffer, I., Kerr, J. T., Broszeit, S., Leitao, P. J., Duncan, C., El Serafy, G., He, K. S., Blanchard, J. L., Lucas, R., Mairota, P., Webb, T. J., & Nicholson, E. (2018). Satellite remote sensing of ecosystem functions: opportunities, challenges and way forward. Remote Sensing in Ecology and Conservation, 4(2), 71-93.

Phillips, O. L., Aragao, L. E., Lewis, S. L., Fisher, J. B., Lloyd, J., Lopez-Gonzalez, G., Malhi, Y., Monteagudo, A., Peacock, J., Quesada, C. A., van der Heijden, G., Almeida, S., Amaral, I., Arroyo, L., Aymard, G., Baker, T. R., Banki, O., Blanc, L., Bonal, D., Brando, P., Chave, J., de Oliveira, A. C., Cardozo, N. D., Czimczik, C. I., Feldpausch, T. R., Freitas, M. A., Gloor, E., Higuchi, N., Jimenez, E., Lloyd, G., Meir, P., Mendoza, C., Morel, A., Neill, D. A., Nepstad, D., Patino, S., Penuela, M. C., Prieto, A., Ramirez, F., Schwarz, M., Silva, J., Silveira, M., Thomas, A. S., Steege, H. T., Stropp, J., Vasquez, R., Zelazowski, P., Alvarez Davila, E., Andelman, S., Andrade, A., Chao, K. J., Erwin, T., Di Fiore, A., Honorio, C. E., Keeling, H., Killeen, T. J., Laurance, W. F., Pena Cruz, A., Pitman, N. C., Nunez Vargas, P., Ramirez-Angulo, H., Rudas, A., Salamao, R., Silva, N., Terborgh, J., & Torres-Lezama, A. (2009). Drought sensitivity of the Amazon rainforest. Science, 323(5919), 1344-1347.

Poorter, L., & Bongers, F. (2006). Leaf traits are good predictors of plant performance across 53 rain forest species. Ecology, 87(7), 1733-1743.

Poorter, L., van der Sande, M. T., Arets, E. J. M. M., Ascarrunz, N., Enquist, B. J., Finegan, B., Licona, J. C., Martínez-Ramos, M., Mazzei, L., & Meave, J. A. (2017). Biodiversity and climate determine the functioning of Neotropical forests. Global Ecology and Biogeography, 26(12), 1423-1434.

Pruyn, M. L., Gartner, B. L., & Harmon, M. E. (2005). Storage versus substrate limitation to bole respiratory potential in two coniferous tree species of contrasting sapwood width. Journal of experimental botany, 56(420), 2637-2649.

Reich, P. B., Tjoelker, M. G., Pregitzer, K. S., Wright, I. J., Oleksyn, J., & Machado, J. L. (2008). Scaling of respiration to nitrogen in leaves, stems and roots of higher land plants. Ecol Lett, 11(8), 793-801.

Reich, P. B., Tjoelker, M. G., Pregitzer, K. S., Wright, I. J., Oleksyn, J., & Machado, J. L. (2008). Scaling of respiration to nitrogen in leaves, stems and roots of higher land plants. Ecology letters, 11(8), 793-801.

Reynolds, J. F., & Thornley, J. H. M. (1982). A shoot: root partitioning model. Annals of Botany, 49(5), 585-597.

Richardson, A. D., Hollinger, D. Y., Aber, J. D., Ollinger, S. V., & Braswell, B. H. (2007). Environmental variation is directly responsible for short-but not long-term variation in forest-atmosphere carbon exchange. Global Change Biology, 13(4), 788-803.

Roumet, C., Birouste, M., Picon-Cochard, C., Ghestem, M., Osman, N., Vrignon-Brenas, S., Cao, K. f., & Stokes, A. (2016). Root structure–function relationships in 74 species: evidence of a root economics spectrum related to carbon economy. New Phytologist, 210(3), 815-826.

Rowland, L., Da Costa, A. C. L., Galbraith, D. R., Oliveira, R. S., Binks, O. J., Oliveira, A. A. R., Pullen, A. M., Doughty, C. E., Metcalfe, D. B., & Vasconcelos, S. S. (2015). Death from drought in tropical forests is triggered by hydraulics not carbon starvation. Nature, 528(7580), 119-122.

Saatchi, S., Asefi-Najafabady, S., Malhi, Y., Aragão, L. E. O. C., Anderson, L. O., Myneni, R. B., & Nemani, R. (2013). Persistent effects of a severe drought on Amazonian forest canopy. Proceedings of the National Academy of Sciences, 110(2), 565-570.

Sande, M. T., Peña-Claros, M., Ascarrunz, N., Arets, E. J. M. M., Licona, J. C., Toledo, M., & Poorter, L. (2017). Abiotic and biotic drivers of biomass change in a Neotropical forest. Journal of ecology, 105(5), 1223-1234.

Schuldt, B., Leuschner, C., Horna, V., Moser, G., Köhler, M., Van Straaten, O., & Barus, H. (2011). Change in hydraulic properties and leaf traits in a tall rainforest tree species subjected to long-term throughfall exclusion in the perhumid tropics. Biogeosciences, 8(8), 2179.

Sugiura, D., & Tateno, M. (2011). Optimal leaf-to-root ratio and leaf nitrogen content determined by light and nitrogen availabilities. PloS one, 6(7), e22236.

Thornley, J. H. M. (1972). A model to describe the partitioning of photosynthate during vegetative plant growth. Annals of Botany, 36(2), 419-430.

Thornley, J. H. M. (1995). Shoot: root allocation with respect to C, N and P: an investigation and comparison of resistance and teleonomic models. Annals of Botany, 75(4), 391-405.

Tjoelker, M. G., Oleksyn, J., & Reich, P. B. (2001). Modelling respiration of vegetation: evidence for a general temperature-dependent Q10. Global Change Biology, 7(2), 223-230.

Van Bodegom, P. M., Douma, J. C., Witte, J. P. M., Ordonez, J. C., Bartholomeus, R. P., & Aerts, R. (2012). Going beyond limitations of plant functional types when predicting global ecosystem–atmosphere fluxes: exploring the merits of traits-based approaches. Global Ecology and Biogeography, 21(6), 625-636.

van der Sande, M. T., Arets, E. J. M. M., Peña-Claros, M., Hoosbeek, M. R., Cáceres-Siani, Y., van der Hout, P., & Poorter, L. (2018). Soil fertility and species traits, but not diversity, drive productivity and biomass stocks in a Guyanese tropical rainforest. Functional ecology, 32(2), 461-474.

Weiss, M., Baret, F., Smith, G. J., Jonckheere, I., & Coppin, P. (2004). Review of methods for in situ leaf area index (LAI) determination Part II. Estimation of LAI, errors and sampling. Agricultural and Forest Meteorology, 121(1-2), 37-53.

Williams, M., Malhi, Y., Nobre, A. D., Rastetter, E. B., Grace, J., & Pereira, M. G. P. (1998). Seasonal variation in net carbon exchange and evapotranspiration in a Brazilian rain forest: a modelling analysis. Plant Cell and Environment, 21(10), 953-968.

Williams, M., Rastetter, E. B., Fernandes, D. N., Goulden, M. L., Wofsy, S. C., Shaver, G. R., Melillo, J. M., Munger, J. W., Fan, S. M., & Nadelhoffer, K. J. (1996). Modelling the soil-plant-atmosphere continuum in a Quercus–Acer stand at Harvard Forest: the regulation of stomatal conductance by light, nitrogen and soil/plant hydraulic properties. Plant, Cell & Environment, 19(8), 911-927.

Würth, M. K. R., Pelaez-Riedl, S., Wright, S. J., & Körner, C. (2005). Non-structural carbohydrate pools in a tropical forest. Oecologia, 143(1), 11-24.

Xu, X., Medvigy, D., Joseph Wright, S., Kitajima, K., Wu, J., Albert, L. P., Martins, G. A., Saleska, S. R., & Pacala, S. W. (2017). Variations of leaf longevity in tropical moist forests predicted by a trait-driven carbon optimality model. Ecology letters, 20(9), 1097-1106.

Zhou, L., Tian, Y., Myneni, R. B., Ciais, P., Saatchi, S., Liu, Y. Y., Piao, S., Chen, H., Vermote, E. F., Song, C., & Hwang, T. (2014). Widespread decline of Congo rainforest greenness in the past decade. Nature, 509(7498), 86-90.

7. Concluding Remarks

We go beyond the physiological-stomatal limitations to photosynthesis, to understand how forests respond to water availability through canopy dynamics and leaf traits. We explicitly quantify the effect of leaf traits on carbon economics, and demonstrate how LAI, NPP allocation and leaf traits can be predicted through optimality approaches that maximise plant fitness. Finally, we show how spatial variation in leaf traits capture the effects of climate on NPP allocation, LAI and ultimately photosynthesis. Our findings bring new understanding of the mechanisms shaping plant responses to resource availability, which is critical to predicting future carbon dynamics under anticipated global change in biogeochemical cycles.